

VOLUME 34

OCTOBER 1956

NUMBER 10

Canadian Journal of Chemistry

Editor: LÉO MARION

Associate Editors:

HERBERT C. BROWN, *Purdue University*
A. R. GORDON, *University of Toronto*
C. B. PURVES, *McGill University*
Sir ERIC RIDEAL, *Imperial College, University of London*
J. W. T. SPINKS, *University of Saskatchewan*
E. W. R. STEACIE, *National Research Council of Canada*
H. G. THODE, *McMaster University*
A. E. VAN ARKEL, *University of Leiden*

Published by THE NATIONAL RESEARCH COUNCIL
OTTAWA **CANADA**

CANADIAN JOURNAL OF CHEMISTRY

(Formerly Section B, Canadian Journal of Research)

Under the authority of the Chairman of the Committee of the Privy Council on Scientific and Industrial Research, the National Research Council issues THE CANADIAN JOURNAL OF CHEMISTRY and six other journals devoted to the publication, in English or French, of the results of original scientific research. Matters of general policy concerning these journals are the responsibility of a joint Editorial Board consisting of: members representing the National Research Council of Canada; the Editors of the Journals; and members representing the Royal Society of Canada and four other scientific societies.

The Chemical Institute of Canada has chosen the Canadian Journal of Chemistry and the Canadian Journal of Technology as its medium of publication for scientific papers.

EDITORIAL BOARD

Representatives of the National Research Council

A. N. Campbell, *University of Manitoba* H. G. Thode, *McMaster University*
G. E. Hall, *University of Western Ontario* D. L. Thomson, *McGill University*
W. H. Watson (Chairman), *University of Toronto*

Editors of the Journals

D. L. Bailey, *University of Toronto* G. A. Ledingham, *National Research Council*
T. W. M. Cameron, *Macdonald College* Léo Marion, *National Research Council*
J. B. Collip, *University of Western Ontario* R. G. E. Murray, *University of Western Ontario*
G. M. Volkoff, *University of British Columbia*

Representatives of Societies

D. L. Bailey, *University of Toronto* R. G. E. Murray, *University of Western Ontario*
Royal Society of Canada Canadian Society of Microbiologists
T. W. M. Cameron, *Macdonald College* H. G. Thode, *McMaster University*
Royal Society of Canada Chemical Institute of Canada
J. B. Collip, *University of Western Ontario* T. Thorvaldson, *University of Saskatchewan*
Canadian Physiological Society Royal Society of Canada
G. M. Volkoff, *University of British Columbia*
Royal Society of Canada; Canadian Association of Physicists

Ex officio

Léo Marion (Editor-in-Chief), *National Research Council*
F. T. Rosser, Director, Division of Administration, *National Research Council*

Manuscripts for publication should be submitted to Dr. Léo Marion, Editor-in-Chief, Canadian Journal of Chemistry, National Research Council, Ottawa 2, Canada.
(For instructions on preparation of copy, see **Notes to Contributors** (inside back cover).)

Proof, correspondence concerning proof, and orders for reprints should be sent to the Manager, Editorial Office (Research Journals), Division of Administration, National Research Council, Ottawa 2, Canada.

Subscriptions, renewals, requests for single or back numbers, and all remittances should be sent to Division of Administration, National Research Council, Ottawa 2, Canada. Remittances should be made payable to the Receiver General of Canada, credit National Research Council.

The journals published, frequency of publication, and prices are:

Canadian Journal of Biochemistry and Physiology	Bimonthly	\$3.00 a year
Canadian Journal of Botany	Bimonthly	\$4.00 a year
Canadian Journal of Chemistry	Monthly	\$5.00 a year
Canadian Journal of Microbiology	Bimonthly	\$3.00 a year
Canadian Journal of Physics	Monthly	\$4.00 a year
Canadian Journal of Technology	Bimonthly	\$3.00 a year
Canadian Journal of Zoology	Bimonthly	\$3.00 a year

The price of single numbers of all journals is 75 cents.

"Reprinted in entirety by photo-offset from the original issue"

Canadian Journal of Chemistry

Issued by THE NATIONAL RESEARCH COUNCIL OF CANADA

VOLUME 34

OCTOBER 1956

NUMBER 10

PREPARATIVE PARTITION CHROMATOGRAPHY OF CARBOHYDRATES ON CELITE COLUMNS¹

BY R. U. LEMIEUX, C. T. BISHOP, AND G. E. PELLETIER

ABSTRACT

Partition on Celite columns, using both elution and extrusion techniques, was found to be a convenient and satisfactory chromatographic method for preparative or analytical work involving carbohydrates and their derivatives. The method is superior to other chromatographic procedures for carbohydrates in resolution of mixtures; cost, ease, and speed of operation; yield and purity of products; and range of applicability. To illustrate these advantages a number of specific examples are given involving partially methylated derivatives of D-glucose and D-xylose and isolation of products from reaction mixtures.

The use of Celite* to support the static phase in partition chromatography was reported soon after the discovery of this technique (19). This use for the material gained rapid and widespread application in the field of organic chemistry, for example, to resolve fatty acids (24), hydroxy acids (15), fermentation products (22, 23, 25), and alkaloids (2). Although Neish (21, 22, 23) has used silica gel and Celite interchangeably in the separation of such fermentation products as glycerol and 2,3-butanediol, the only other applications made in the field of carbohydrates to our knowledge are those of Baker (12) and of Lemieux and Cipera (16). Our experience in these laboratories has convinced us that columns supported by Celite for partition chromatography provide the most convenient and satisfactory chromatographic method presently available to carbohydrate chemists for preparative and analytical work. This communication describes in some detail the basis for this conclusion.

Mixtures of sugars and their derivatives have been separated by adsorption chromatography using a wide variety of adsorbents, for example, magnesol (18), alumina (11), clays (17), charcoal (26), and silicic acid (10). Certain of these methods possess virtues which ensure their continued use, especially for the separation of such closely related compounds as anomers and certain diastereoisomers. Nevertheless, these methods are subject to the unpredictability of adsorption chromatography and are difficult, expensive, and time-consuming. To avoid these difficulties most workers have favored methods of

¹Manuscript received June 13, 1956.

Contribution from the Department of Chemistry, University of Ottawa, and the Division of Applied Biology, National Research Council, Ottawa, Canada. Issued as N.R.C. No. 4042.

*A brand of diatomaceous earth manufactured by the Johns-Manville Company, New York.

partition chromatography, especially the one in which the static phase is supported by cellulose either in the form of columns (4, 6, 7, 8) or large sheets (3). It is to this method, because of its widespread use and resemblance in applicability, that the use of Celite columns is best compared. The comparison is based on resolution of mixtures; cost, ease, and speed of operation; yield and purity of product; and range of applicability. The Celite technique is believed superior in all respects.

Our experience indicates that the resolving power of Celite columns is at least equal to that of cellulose sheets and better than that of cellulose columns under comparable conditions of operation. The data given in Table I are typical of those which form the basis for this conclusion.

TABLE I
SEPARATION OF D-XYLOSE AND ITS METHYL ETHERS ON A CELITE COLUMN

Fraction number (2 ml. each)	D-Xylose derivative	Yield (mgm.)	$[\alpha]_D^{26}$ ($c = 1$ in water)	Reported $[\alpha]_D$
70-120	2,3,4-Tri- <i>O</i> -methyl	76.9	+19.0°	+18.0°
130-161	2,3-Di- <i>O</i> -methyl	67.0	+22.0°	+23.0°
162-191	2,4-Di- <i>O</i> -methyl	15.7	+22.0°	+22.0°
250-305	3- <i>O</i> -Methyl	51.6	+18.6°	+17.0°
A further 400 ml.	D-Xylose	86.8	+17.3°	+18.8°
Recovery		298.0 (96.1%)		

A measure of the relative mobilities of materials on Celite No. 535 columns is given by the following dimensionless term:

$$[1] \quad R_V = d\tau^2/V \text{ (mm.}^3 \times \text{ml.}^{-1}\text{)}.$$

In this expression d is the distance from the top of the column to the center of the band of material, τ is the radius of the column, and V is the volume of developing phase used to obtain the chromatogram. The R_V term is of value because it was found to bear a rough but useful relationship to the R_f term of paper chromatography. For example, using the operating conditions described here and the *n*-butanol: water solvent system, the following relationship held true with useful accuracy (see Fig. 1):

$$[2] \quad R_V = 300 R_f + 15.$$

It was found empirically that 1 cc. of packed column contains about 0.29 gm. of Celite and that the approximate optimum load for a chromatogram is 10 mgm. of each component per cm.² of column cross-sectional area. We have found it useful to apply this knowledge together with expressions [1] and [2] for predicting the conditions required to obtain a given separation. The approximate relationship between R_V and R_f values has also been used to locate compounds on an extruded Celite column when the compounds were insensitive to the spray reagents that could be used.

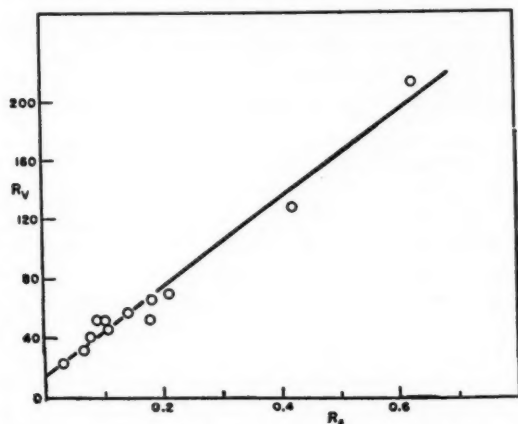


FIG. 1. The relationship obtained between the R_V (Celite column) and R_f (Whatman No. 1 paper) values using the *n*-butanol-water systems in each case.

Celite No. 535 is a low-cost, inert material that can be reclaimed repeatedly; consequently chromatographic separations can be made at a small fraction of the cost of the material and equipment required in using cellulose sheets. Because of its unique physical properties and structure, uniform Celite columns are easily and quickly constructed using the slurry technique (22). With a little practice only 15 to 30 min. are required for the preparation of a column which will extrude easily and perfectly from a tapered tube. In contrast, the construction (7) of cellulose columns is a slow laborious process and the developed columns cannot be extruded. It is important to note in this respect that extrusion chromatography using Celite columns eliminates the need for a fraction collector.

Celite allows ready passage of the developing phase. Primarily because the gravity flow rate through Celite columns is about 10 times that of cellulose columns, separations requiring 12 to 14 days on cellulose columns have been accomplished in only one to two days on Celite columns. The extrusion technique allows the separation of many closely related compounds in only two to three hours and the products are recovered in much more concentrated solution. In comparison, the preparation of preparative paper chromatograms together with location and elution of the separated products is very time-consuming.

Sugars or their derivatives which have been separated by partition on cellulose are always contaminated by material which is often difficult to remove. The impurities are either present in the cellulose to begin with or arise from a slow breakdown of the cellulose under the conditions used. The chemical nature of this material has been studied by Smith *et al.* (9). Although recoveries of sugars from cellulose columns are nearly quantitative, the use of paper sheets can result in severe losses of material. Acid-washed Celite has none of these disadvantages since the chemically inert material is essentially

non-adsorbing. Minute particles of Celite which sometimes pass into the eluate can be quantitatively removed by filtration through a fine filter such as a bacterial filter plate. The absence of contaminants promises to be of great value in the identification of separated compounds by infrared absorption spectroscopy.

Although we report only the use of the *n*-butanol: water system, a wide variety of solvent systems can be used for partition chromatography on Celite (12, 15, 22, 24) and also a succession of different solvents can be used in the course of a given separation (15, 23). The fact that Celite can be used to support buffered solutions (2) is of practical importance; for example, addition of ammonia to the *n*-butanol: water system was of considerable assistance in separating uronic acids from sugars (1). The method can be used to advantage for removing salts, mineral acids, and mineral bases from carbohydrate materials; for example, D-gulose from its complex with calcium chloride, D-glucose diethyl thioacetal from a mercaptolysis reaction mixture, and D-glucose from a sodium borohydride reduction of D-gluconolactone.

EXPERIMENTAL

The columns are constructed as described in detail by Neish (22). The use of acid-washed Celite No. 535 is recommended because recoveries are improved (22). We found no advantage in drying the material at 500° C. over drying at 110° C. The practice of using a 1:1 volume to weight ratio of stationary phase to Celite provided optimum conditions. The technique of Lemieux and Charanduk (15) is believed most convenient for adding the sample to the top of the column. An approximately 10% solution of the sample (preferably in the developing phase) is absorbed on dry Celite No. 535 (1 ml./gm.) and the resulting powder is packed to the top of a packed Celite column which is just filled with developing phase. The developing phase is then percolated through the column either by gravity or under pressure. The high porosity of Celite columns permits a wide range of flow rates. Our experience indicates that a flow rate of about 0.1 ml./min./cm.² of column cross-sectional area is desirable. However, four to five times this rate can often be used. A sample size of about 10 mgm. of each component per cm.² of column cross-sectional area appears about optimum for preparative work. Of course the width of the band increases as it travels down the column. It is of great practical importance to realize that much larger samples (by a factor as large as 10) can be used when the R_F values of the components differ substantially. For example, 3,5-di-*O*-methyl-D-glucose was separated from about 4% of 3-*O*-methyl-D-glucose by passing 5.4 gm. of the mixture through a 500 gm. Celite column having a radius of 37.5 mm.

The following specific examples were chosen to illustrate the various features of the method.

Separation of Methylated D-Xyloses

A mixture (310 mgm.) of *O*-methyl ethers of D-xylose, obtained by hydrolysis of a methylated polysaccharide, was resolved on a Celite column (3.75 × 34 cm.,

80.0 gm. Celite) using water-saturated butanol. The eluate was fractionated into 2-ml. portions by an automatic collector which changed the receiver every 72 sec. Distribution of components among the receivers was determined by qualitative paper chromatographic examination of every fifth fraction. Portions of eluate were combined to give solutions of each individual sugar. The solutions were evaporated to dryness and the residues were redissolved in water. These solutions were then clarified by filtration and evaporated to dryness in weighed flasks. Table I shows the results of the separation. The spontaneous crystallization of 2,3,4-tri-*O*-methyl- and 2,4-di-*O*-methyl-D-xylose was a further indication of the purity of the separated components. The remaining fractions were crystallized eventually or yielded crystalline derivatives. After the monomethyl derivative had all been eluted the column was removed from the automatic collector and the eluate was collected in 100-ml. portions until all the D-xylose was removed as shown by a negative test with aniline oxalate spray (5).

Separation of Partially Methylated D-Glucoses

(a) Elution

The hydrolyzate, 300 mgm., of a water-soluble methyl cellulose (13) was resolved into five distinct fractions on a 35 mm. (diam.) column of Celite, 72 gm., as shown by colorimetric assay of successive aliquots of the eluate using the anthrone reagent (20). Inspection of the fractions by paper chromatography showed the first band (200 to 460 ml. of eluate) to be 2,3,6-tri-*O*-methyl-D-glucose (crystallized), the second (490-565 ml.) and third (580-670 ml.) bands to be two different di-*O*-methyl-D-glucoses (one of which crystallized spontaneously from a sirup), the fourth band (930-1320 ml.) to be a mixture of mono-*O*-methyl-D-glucoses, and the fifth band to be D-glucose. This last band was removed from the column by changing the developing phase to water.

(b) Extrusion

The hydrolyzate, 147 mgm., was chromatographed on a 35 mm. (diam.) column of Celite, 40 gm., using 170 ml. of developing phase. The extruded column was sprayed through a mask (14) with alkaline permanganate (18). The four separate bands which developed were cut out and the contents washed out with water. The materials were shown to be 2,3,6-tri-*O*-methyl-D-glucose ($R_F = 228$), 41 mgm., a mixture of di-*O*-methyl-D-glucoses ($R_F = 122$), 38.4 mgm., a mixture of mono-*O*-methyl-D-glucoses ($R_F = 69$), 42 mgm., and D-glucose ($R_F = 39$), 15.4 mgm., which was slightly contaminated with mono-*O*-methyl-D-glucoses. The per cent recovery was 92.5.

Separation of Product from Sodium Borohydride Reduction

D-Glucono- δ -lactone (205.7 mgm.) in water (1.3 ml.) at 0° C. was reduced by sodium borohydride (33.0 mgm.) in water (0.7 ml.) according to the method of Wolfrom and Wood (28) for reduction of sugar lactones to aldoses. Excess sodium borohydride was decomposed by addition of 0.5 *N* sulphuric acid and the resulting clear solution (3.5 ml.) was added to dry, acid-washed Celite

(3.5 gm.) which was then placed on the top of a Celite column (80 gm., 38×340 mm.). Water-saturated butanol was passed through the column and the eluate was collected in 7-ml. portions by an automatic fraction collector which changed the receiver every five minutes. Every fifth fraction was tested for aldose content by the aniline oxalate spray reagent (5). Positive tests were given by fractions 225–374 inclusive. These fractions were combined and evaporated to a sirup which was redissolved in water (20 ml.). This solution was passed through a medium porosity sintered glass funnel and the filtrate was evaporated to a colorless sirup which was dried to constant weight over phosphorus pentoxide at 0.02 mm. The product (192 mgm., 92.4%) had $[\alpha]_D^{25} = +48.2^\circ$ ($c = 3.84$ in water) and was crystallized from methanol–isopropyl alcohol to yield α -D-glucose (104 mgm.), m.p. and mixed m.p. 145.5–147° C., $[\alpha]_D^{25} = +76^\circ$ after one-half hour falling to $+52.6^\circ$ in 24 hr. ($c = 1.16$ in water). The mother liquors from this crystallization yielded a further 66 mgm. of the same product.

Mercaptolysis of D-Glucose

Wolf from and Karabinos (27) have shown that diethyl thioacetals are useful derivatives for the characterization of sugars. For this reason and the fact that thioacetals and related compounds have proved extremely valuable in determinations of structures of natural products, it was decided to test the value of the present chromatographic technique for the isolation of the product formed in a mercaptolysis. D-Glucose diethyl thioacetal was readily isolated in an extremely high state of purity from the reaction of micro amounts of glucose with ethyl mercaptan and concentrated hydrochloric acid in the usual manner. The reaction mixture could be added directly to the column or neutralized with sodium carbonate before chromatography. The thioacetal possessed the high R_F value of 254 which rendered its separation from D-glucose extremely easy.

Separation of D-Glucose, D-Fructose, and Sucrose

A mixture of D-glucose, D-fructose, and sucrose (100 mgm. of each) was dissolved in water (1 ml.), taken up on Celite (1 gm.), and added to the top of a column of Celite (80 gm., 35×380 mm.). The chromatogram was developed with 1500 ml. of water-saturated *n*-butanol and the column was then extruded. The alkaline permanganate spray reagent (18), applied through a mask (14), revealed two bands 260–295 mm. and 320–380 mm. from the top of the column. These two portions of the column were sectioned out and eluted with water. Evaporation of the eluate from the band nearer the top of the column yielded sucrose (81 mgm., 81%), $[\alpha]_D^{20} = +65^\circ \pm 2^\circ$ ($c = 1.8\%$ in water). By the same procedure, the band at the bottom of the column yielded D-glucose (100 mgm., 100%), $[\alpha]_D^{25} = +54^\circ \pm 2^\circ$ ($c = 2\%$ in water). No other band could be found on the column, so the solvent used to develop the chromatogram was evaporated and yielded D-fructose (74 mgm., 74%), $[\alpha]_D^{20} = -92^\circ \pm 1.5^\circ$ ($c = 1.5\%$ in water). The three separated sugars were examined by paper strip chromatography using *n*-butanol saturated with water as the irrigating solvent. Both sucrose and D-fructose were chromatographically

pure and the D-glucose contained only a slight trace of D-fructose, obviously very little since the specific rotation of the D-glucose was not affected. There is little doubt that D-glucose, D-fructose, and sucrose could be separated completely by using a longer column or the elution technique.

Miscellaneous Experiments

The general usefulness of the technique has been further illustrated by application in these laboratories to the separation of partially esterified sugars, anhydro sugars from their parent compounds, and uronic acids from sugars.

ACKNOWLEDGMENT

The authors wish to thank Canadian Industries Limited for a scholarship held by one of them (G.E.P.) during the course of this work. The technical assistance of D. Torley is gratefully acknowledged.

REFERENCES

1. ADAMS, G. A. Private communication.
2. CULVENOR, C. C. J., DRUMMOND, L. J., and PRICE, J. R. *Australian J. Chem.* 7: 277. 1954.
3. FLOOD, A. E., HIRST, E. L., and JONES, J. K. N. *Nature*, 160: 86. 1947.
4. GEERDES, J. D., LEWIS, B. A., MONTGOMERY, R., and SMITH, F. *Anal. Chem.* 26: 264. 1954.
5. HORROCKS, R. H. and MANNING, G. B. *Lancet*, 256: 1042. 1949.
6. HOUGH, L., JONES, J. K. N., and WADMAN, W. H. *Nature*, 162: 448. 1948.
7. HOUGH, L., JONES, J. K. N., and WADMAN, W. H. *J. Chem. Soc.* 2511. 1949.
8. HOUGH, L., JONES, J. K. N., and WADMAN, W. H. *J. Chem. Soc.* 1702. 1950.
9. HUFFMAN, G. W., REBERS, P. A., SPRIESTERSBACH, D. R., and SMITH, F. *Nature*, 175: 990. 1955.
10. JEANLOZ, R. W. Abstracts of Papers, 128th Meeting of the American Chemical Society, 2D. 1955.
11. JONES, J. K. N. *J. Chem. Soc.* 333. 1944.
12. KISSMAN, H. M., PIDACKS, C., and BAKER, B. R. *J. Am. Chem. Soc.* 77: 18. 1955.
13. LEMIEUX, R. U. and BAUER, H. F. *Can. J. Chem.* 31: 814. 1953.
14. LEMIEUX, R. U. and BAUER, H. F. *Can. J. Chem.* 32: 340. 1954.
15. LEMIEUX, R. U. and CHARANDUK, R. *Can. J. Chem.* 29: 759. 1951.
16. LEMIEUX, R. U. and CIPERA, J. D. T. *Can. J. Chem.* 34: 906. 1956.
17. LEW, B. W., WOLFROTH, M. L., and GOEPP, R. M. *J. Am. Chem. Soc.* 67: 1865. 1945.
18. MCNEELY, W. H., BINKLEY, W. W., and WOLFROTH, M. L. *J. Am. Chem. Soc.* 67: 527. 1945.
19. MARTIN, A. J. P. and SYNGE, R. L. M. *Biochem. J.* 35: 1358. 1941.
20. MORRIS, D. L. *Science*, 107: 254. 1948.
21. NEISH, A. C. *Can. J. Research, B*, 27: 6. 1949.
22. NEISH, A. C. *Can. J. Research, B*, 28: 535. 1950.
23. NEISH, A. C. Analytical methods for bacterial fermentations. Rept. No. 46-8-3. National Research Council of Canada. 1952.
24. PETERSON, M. H. and JOHNSON, M. J. *J. Biol. Chem.* 174: 775. 1948.
25. THORN, J. A. and JOHNSON, M. J. *J. Am. Chem. Soc.* 72: 2052. 1950.
26. WHISTLER, R. L. and DURSO, D. F. *J. Am. Chem. Soc.* 72: 677. 1950.
27. WOLFROTH, M. L. and KARABINOS, J. V. *J. Am. Chem. Soc.* 67: 500. 1945.
28. WOLFROTH, M. L. and WOOD, H. B. *J. Am. Chem. Soc.* 73: 2933. 1951.

EFFECTS OF COMPLEXING ON THE HOMOGENEOUS REDUCTION OF MERCURIC SALTS IN AQUEOUS SOLUTION BY MOLECULAR HYDROGEN¹

BY G. J. KORINEK² AND J. HALPERN³

ABSTRACT

The effects of various complexing agents on the homogeneous reduction of mercuric salts by molecular hydrogen in aqueous solution were determined. In all cases the kinetics suggest that the rate-determining step is a bimolecular reaction between a mercuric ion or complex and a hydrogen molecule, probably leading to the formation of an intermediate mercury atom. The reactivity of various mercuric complexes was found to decrease in the following order: $\text{HgSO}_4 > \text{Hg}^{++} > \text{HgAc}_2, \text{HgPr}_2 > \text{HgCl}_2 > \text{HgBr}_2 > \text{Hg(EDA)}_2^{++}$. Addition of anions such as OH^- , CO_3^{--} , Ac^- , Pr^- , and Cl^- , in excess of the amounts required to form stable mercuric complexes, was found to increase the rate. An interpretation of these effects is given.

INTRODUCTION

Mercuric salts are reduced homogeneously by molecular hydrogen in aqueous solution to mercurous salts or, under certain conditions, to metallic mercury. A detailed kinetic study of this reaction has been made in the case of mercuric perchlorate (7) and some preliminary results have also been reported for mercuric acetate (4). In view of the marked differences in kinetics which were observed (the rate of reduction of mercuric acetate was much lower than that of the perchlorate) it seemed of interest to study the acetate system in greater detail and also to determine the effects on the reaction of other organic and inorganic complexing agents. The results of these studies are described in the present paper. A related investigation of the effects of complexing on the homogeneous catalytic activation of hydrogen by cupric salts has also been described recently (10).

EXPERIMENTAL

Ethylenediamine (EDA) and ethylenediaminetetraacetic acid (EDTA) were Eastman white label products. The perchlorate salts were obtained from G. F. Smith Chemical Co. All other chemicals were Baker and Adamson reagent grade. Hydrogen and nitrogen gases were supplied by Canadian Liquid Air Co. Distilled water was used in the preparation of all solutions.

The solutions were analyzed for Hg(I) by potentiometric titration with KMnO_4 . In most cases the total Hg concentration was determined by titration with KCNS using a ferric indicator, following acidification and oxidation with KMnO_4 where necessary. With solutions containing chloride or bromide, Hg(II) determinations were made by the iodide method (6). An excess of KI

¹Manuscript received June 4, 1956.

²Contribution from the Department of Mining and Metallurgy, University of British Columbia, Vancouver, B.C., with financial assistance from the Consolidated Mining and Smelting Co. and the National Research Council of Canada.

³Holder of the Cominco Fellowship, 1955-56.

⁴Present address: Department of Chemistry, University of British Columbia, Vancouver, B.C.

(beyond that necessary to convert all the Hg(II) to the stable HgI_4^- complex) was added, and back-titrated with HgCl_2 to the first appearance of a red precipitate of HgI_2 .

The experiments were conducted in a stainless steel autoclave which has been described previously (2). When corrosive solutions (such as those containing chloride or bromide) were used, a titanium liner was placed in the autoclave and the stainless steel stirrer, thermocouple well, and sampling tube were replaced by titanium counterparts. Three liters of solution, of desired composition, was placed in the autoclave, which was then sealed, flushed with nitrogen, and heated to the desired reaction temperature, maintained to within $\pm 0.3^\circ\text{C}$. throughout the experiment with a Micromax recording controller. In each experiment, it was ascertained that the solutions were stable at the reaction temperature in the absence of hydrogen. Where any reduction of Hg(II) (i.e. as a result of side reactions with the metal autoclave or with organic complexing agents) was detected, its rate was determined and subtracted from the subsequently measured rate of reduction in the presence of hydrogen. It can be seen from the rate plots that this correction was generally small. After the hydrogen was introduced (taken as zero reaction time) its partial pressure above the solution was held constant throughout the experiment. To follow the reaction, the solution was sampled periodically and analyzed for Hg(I) and Hg(II) as described earlier.

The concentration of hydrogen in solution, $[\text{H}_2]$, was estimated from the measured partial pressure using available data for the solubility of H_2 in water (11, 13). It was ascertained that the stirring (provided by an impeller of 2.5 in. diameter, rotating at 950 r.p.m.) was adequate to keep the solution saturated with hydrogen throughout the reaction.

RESULTS AND DISCUSSION

It is convenient to divide the systems studied into three categories depending on whether the reduction product is (i) a soluble mercurous salt, (ii) an insoluble mercurous salt, or (iii) metallic mercury. Each of these categories is characterized by different stoichiometric and kinetic patterns which are described in Table I.

Reactions in the first category are distinguished by the fact that H_2 is activated by interaction, not only with the mercuric salt but also with the mercurous ions which result from its reduction. The resulting kinetics, and the methods used to evaluate the rate constants k_1 and k_2 , have been described in connection with an earlier study of the reduction of mercuric perchlorate (7).

In the reactions of the other two categories, only the mercuric salts contribute to the activation of H_2 , in each case apparently through a bimolecular rate-determining step (characterized by the rate constant k_1) involving a dissolved mercuric ion or complex and an H_2 molecule. Since the concentration of H_2 is kept constant throughout the reaction, the resulting kinetics are of first order (i.e. in the Hg(II) concentration).

Values of k_1 were estimated from the slopes of linear kinetic plots, using the appropriate rate equations. In order to facilitate kinetic comparison of different

TABLE I
CLASSIFICATION OF REACTIONS

Systems	Category		
	I	II	III
	Perchlorate, nitrate, sulphate	Acetate,* propionate,* chloride, bromide	EDA and EDTA complexes in basic soln.
Reaction stoichiometry	$2\text{Hg(II)} + \text{H}_2 \rightarrow 2\text{Hg(I)}(\text{soluble})$	$2\text{Hg(II)} + \text{H}_2 \rightarrow 2\text{Hg(I)}(\text{ppt.})$	$\text{Hg(II)} + \text{H}_2 \rightarrow \text{Hg}$
Rate-determining steps	$\text{Hg(II)} + \text{H}_2 \xrightarrow{k_1}$ $\text{Hg(I)}_2 + \text{H}_2 \xrightarrow{k_2}$	$\text{Hg(II)} + \text{H}_2 \xrightarrow{k_1}$	$\text{Hg(II)} + \text{H}_2 \xrightarrow{k_1}$
Rate law	$-d[\text{Hg(II)}]/dt = 2k_1[\text{Hg(II)}][\text{H}_2] + k_2[\text{Hg(I)}][\text{H}_2]$	$-d[\text{Hg(II)}]/dt = 2k_1[\text{Hg(II)}][\text{H}_2]$	$-d[\text{Hg(II)}]/dt = k_1[\text{Hg(II)}][\text{H}_2]$
Integrated rate equation	$\log \left(\frac{2k_1/(2k_1 - k_2)[\text{Hg(II)}]_0}{[\text{Hg(II)}] + [k_2/(2k_1 - k_2)][\text{Hg(II)}]_0} \right)$ $= \frac{(2k_1 - k_2)[\text{H}_2]t}{2.3}$	$\log \frac{[\text{Hg(II)}]_0}{[\text{Hg(II)}]} = \frac{2k_1[\text{H}_2]t}{2.3}$	$\log \frac{[\text{Hg(II)}]_0}{[\text{Hg(II)}]} = \frac{k_1[\text{H}_2]t}{2.3}$

* Although mercurous acetate and propionate are appreciably soluble, they do not contribute to the activation of H_2 . Hence the kinetics conform to those of category II.

† This equation is derived in Ref. 7.

systems (since the activation of H_2 is rate-limiting in all cases) the rate laws defining k_1 are uniformly expressed in terms of the equivalent rate of reaction of H_2 ($-d[H_2]/dt$). The latter could be calculated from the measured rate of reduction of $Hg(II)$ and the known stoichiometry of the reaction. All forms of $Hg(II)$ were found to contribute to the activation of H_2 , although with varying rates. Hence with solutions containing more than one mercuric species the apparent value of k_1 , determined in this way, obviously represents a weighted average of the rate constants for all the species present.

The investigations of the individual systems, the results of which are described below, generally involved the determination of (i) the products and stoichiometry of the reaction, (ii) the kinetic dependence on the $Hg(II)$ and H_2 concentrations, and (iii) the effects of varying the solution composition, pH, concentrations of complexing agents, etc.

Nitrate

The kinetics of the reduction of $Hg(II)$ to $Hg(I)$ in nitrate solution were found to be identical with those for perchlorate (7). The rate was unaffected by variations in solution composition, in the range 0.05–0.75 M HNO_3 and 0–1 M $NaNO_3$. The extent of complexing in this system (i.e. between Hg^{++} and NO_3^-) is apparently slight (5) and, as in the perchlorate system, H_2 is activated by interaction with simple Hg^{++} and Hg_2^{++} ions. At 86°, the measured value of k_1 , 0.397 liter mole⁻¹ sec.⁻¹, was in good agreement with that determined earlier for perchlorate solutions (7).

Sulphate

Although the form of the kinetics remained substantially unchanged, the addition of sodium sulphate to a solution of mercuric perchlorate was found to increase the rate of reduction of $Hg(II)$ to $Hg(I)$ (reflected in an increased value of k_1) as shown in Figs. 1 and 2. This is attributed* to complexing

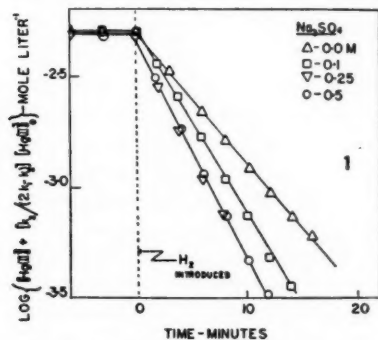


FIG. 1. Rate plots showing the effect of sulphate on the reduction of $Hg(II)$ at 86°, 4 atm. H_2 , in solutions containing initially 0.005 M $Hg(ClO_4)_2$, 0.02 M $HClO_4$.

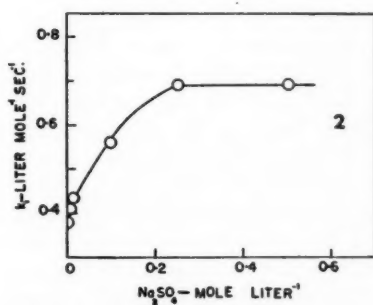


FIG. 2. Effect of sulphate on k_1 (same conditions as in Fig. 1).

*Since the addition of sodium perchlorate was always found to be without effect on the rate, it seems reasonable to attribute the effects obtained with other sodium salts to the respective anions.

between Hg^{++} and SO_4^{--} (5) and, by analogy with similar observations in the cupric system (10), it seems reasonable to conclude that the constant value of k_1 ($0.69 \text{ liter mole}^{-1} \text{ sec}^{-1}$ at 86°), attained at SO_4^{--} concentrations above $0.25 M$, represents the rate constant for the activation of H_2 by the undissociated HgSO_4 molecules. Its reactivity is about 80% higher than that of the uncomplexed Hg^{++} ion.

Acetate

A preliminary study of the reduction of mercuric acetate by hydrogen was described earlier (4). The product of the reaction is mercurous acetate, which has only a limited solubility (ranging from $0.003 M$ at room temperature to about $0.04 M$ at 100°) and starts to precipitate from the solution before the reaction is complete.

Some rate plots depicting the reduction of mercuric acetate are shown in Fig. 3. As in the perchlorate system, the reaction is characterized by two

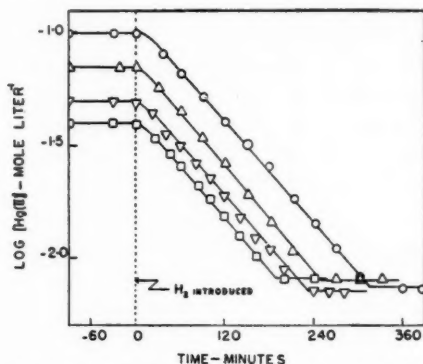


FIG. 3. Rate plots for the reduction of mercuric acetate at 90.2° , 4 atm. H_2 .

distinct kinetic regions. The initial first order region (the rate here is also first order in H_2) corresponds to the reduction of Hg(II) to Hg(I) , referred to earlier. As this reaction proceeds, the $\text{Hg(II)}-\text{Hg(I)}$ potential is lowered (as a result of the decreasing Hg(II) concentration) and ultimately reaches the point where the reduction of Hg(I) to metallic Hg becomes preferred thermodynamically. The horizontal portion of the rate plot apparently represents a region in which only the latter reaction is occurring. The concentration of Hg(I) retains a constant value in this region (determined by the solubility of mercurous acetate) and hence no further Hg(II) reacts until all the precipitated mercurous acetate has been reduced to metallic mercury. Consistent with this interpretation, it was found that the limiting Hg(II) concentration ($\approx 0.007 M$ at 90°) is essentially independent of the initial Hg(II) concentration and of the H_2 partial pressure, but that it increases slightly with the temperature (presumably reflecting the increasing solubility of mercurous acetate). Although its solubility at the reaction temperatures is appreciable,

it seems fairly clear from the kinetics that the mercurous acetate product (in contrast to the uncomplexed Hg_2^{++} ion (7)) does not contribute significantly to the activation of H_2 in this system.

Rate measurements over the temperature range 69° to 115° yielded a good Arrhenius plot, which is fitted by the equation: $k_1 = 1.3 \times 10^{10} \exp[-19,400/RT]$ liter mole $^{-1}$ sec. $^{-1}$. The activation energy is about 1300 cal./mole higher than that for mercuric perchlorate (consistent with the lower rate) and the frequency factor is normal for a simple bimolecular reaction in solution. It seems likely that the above expression for k_1 represents the rate constant for the bimolecular activation of H_2 by the HgAc_2 molecule, the extent of whose dissociation in aqueous solution is known to be small (8). At 90.2° , the value of k_1 (0.021 liter mole $^{-1}$ sec. $^{-1}$) is about 25 times smaller than that for the uncomplexed Hg_2^{++} ion. This is in marked contrast to the results reported for the activation of H_2 by cupric salts, where the acetate complex is about 120 times more reactive than the simple Cu^{++} ion (9).

Addition of sodium acetate to a solution of mercuric acetate was found to increase the rate as shown in Fig. 4. The increase is linear in the acetate concentration and may reflect the formation of higher mercuric acetate complexes such as HgAc_3^- and HgAc_4^{2-} which are more reactive than HgAc_2 , or alternatively it may be a purely kinetic effect, the possible significance of which will be discussed later.

Propionate

The results of a few experiments on the reduction of Hg(II) in propionate solution were analogous to those for the acetate system. The reduction product is a precipitate of mercurous propionate. At 90.2° , the value of k_1 (0.021 liter mole $^{-1}$ sec. $^{-1}$) is close to that for mercurous acetate. The linear increase in the rate with increasing sodium propionate concentration (Fig. 4), although slightly greater, parallels the effect observed in the acetate system.

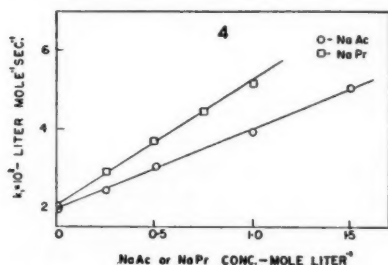


FIG. 4. Effect of excess acetate and propionate, respectively, on the rates of reduction of mercuric acetate and propionate at 90.2° .

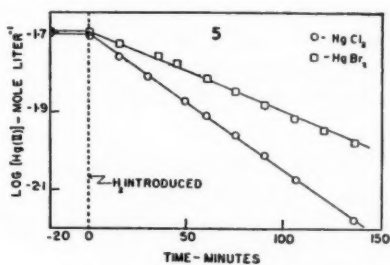


FIG. 5. Rate plots for the reduction of mercuric chloride and mercuric bromide at 123° , 10 atm. H_2 .

Chloride

In chloride-containing solutions, the reduction of Hg(II) yields a precipitate of mercurous chloride, whose solubility is negligible. When the ratio of the

initial concentration of Cl^- to that of Hg(II) in the solution was 2 or greater, the kinetics of the reaction were consistently first order in Hg(II) (see Fig. 5) and in H_2 . At 123° and a Cl^- to Hg(II) ratio of 2, k_1 was found to have a value of $0.0075 \text{ liter mole}^{-1} \text{ sec}^{-1}$. Since complexing in this system is probably complete (12), this presumably represents the rate constant for the bimolecular reaction between H_2 and the HgCl_2 molecule and is about 400 times smaller than the corresponding value for the uncomplexed Hg^{++} ion.

With further addition of sodium chloride the rate increased slightly (see Fig. 6) approaching a constant value for ratios of Cl^- to Hg(II) greater than about 4.5. The value of k_1 in this region, which presumably represents the rate constant for the reaction of H_2 with HgCl_4^{2-} , is about 30% higher than for HgCl_2 .

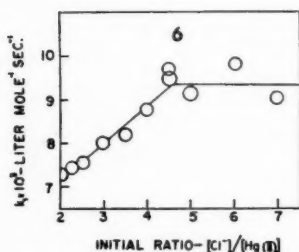


FIG. 6. Effect of excess chloride concentration on the rate of reduction of mercuric chloride at 123° . Initial HgCl_2 concentration, 0.02 M .

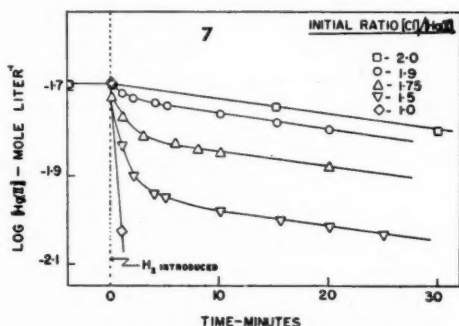


FIG. 7. Rate plots for the reduction of Hg(II) in solutions with various initial $\text{Cl}^-/\text{Hg(II)}$ ratios at 123° , 10 atm. H_2 .

With initial Cl^- to Hg(II) ratios below 2, the kinetics were more complicated, as shown by the rate plots in Fig. 7. The high initial rate is presumably due to the reaction of H_2 with incompletely complexed Hg(II) species such as Hg^{++} and HgCl^+ . As the reaction proceeds, the ratio of Cl^- to Hg(II) in the solution increases until it reaches a value of 2. Beyond this point, the first order rate plots are, as expected, linear and parallel.

Bromide

The results in bromide-containing solutions parallel those for the chloride system. Hg(II) is reduced to an insoluble precipitate of mercurous bromide. The value of k_1 for HgBr_2 ($0.005 \text{ liter mole}^{-1} \text{ sec}^{-1}$ at 123°) is about 30% lower than that for HgCl_2 .

Ethylenediamine

The effect of EDA on the reduction of Hg(II) was examined in basic solutions where the Hg(EDA)_2^{2+} complex is stable. Mercurous salts disproportionate under these conditions so that metallic mercury is the only product of the reaction. The rate of reduction was found to be first order in Hg(II)

(see Fig. 8), first order in H_2 , and independent of the ratio of EDA to $Hg(II)$ in the solution, provided the latter exceeds 2. At 123° and low OH^- concentrations, k_1 was found to be about $0.003 \text{ liter mole}^{-1} \text{ sec}^{-1}$. It seems reasonable to conclude that this value (which is about 1000 times smaller than that for the Hg^{++} ion) represents the rate constant for the bimolecular reaction between H_2 and $Hg(EDA)_2^{++}$.

It was found, even when an excess of EDA was present, that the rate increased on the addition to the solution of salts of certain anions such as OH^- , Ac^- , Pr^- , and CO_3^{--} , as shown in Figs. 8 and 9. The effects resemble those

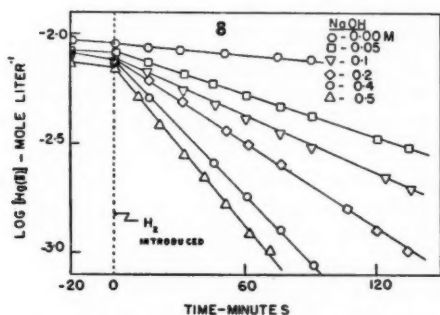


FIG. 8. Rate plots for the reduction of $Hg(II)$ at 123° , 5 atm. H_2 , in solutions containing initially $0.01 \text{ M } Hg(ClO_4)_2$, 0.05 M EDA , and various concentrations of $NaOH$.

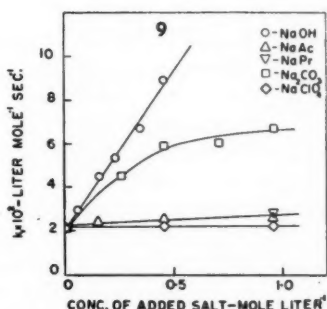


FIG. 9. Effect of various added bases and salts on the rate of reduction of $Hg(II)$ at 123° , in solutions containing initially $0.01 \text{ M } Hg(ClO_4)_2$, 0.05 M EDA , and 0.05 M NaOH (in addition to concentration of $NaOH$ or salt shown).

which were observed in the acetate, chloride, and propionate systems on increasing the concentration of the anion (X^-) beyond that required to convert all the $Hg(II)$ to the stable complex HgX_2 . In those systems the increased rate seemed attributable to the formation of higher complexes, i.e. HgX_3^- and HgX_4^{--} . However such an interpretation does not fit the present case, since the solution already contains an excess of EDA and all the $Hg(II)$ is presumably present as the very stable $Hg(EDA)_2^{++}$ complex. Further complexing with anions such as OH^- , CO_3^{--} , or Ac^- (except possibly for the formation of weak ionic complexes of the type $Hg(EDA)_2X^+$) seems unlikely, and it is more probable that the increase in rate, caused by these anions, is due to a kinetic effect.

Ethylenediaminetetraacetic Acid

A few experiments were made under similar conditions to those above, using EDTA instead of EDA to complex the Hg^{++} . The resulting rate of reaction between $Hg(II)$ and H_2 could not be measured accurately (because of the competing reduction of $Hg(II)$ by EDTA) but was apparently of the same order as that of the EDA complex.

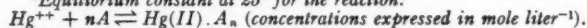
CONCLUSIONS

The data obtained in these studies have been used to compile Table II, in which the various mercuric complexes, for which values of k_1 have been determined, are arranged in order of decreasing reactivity toward H_2 (that of the uncomplexed Hg^{++} ion being taken as unity). In each case the probable formula of the reactive complex and its stability constant (where known) are given. The listed values of the relative reactivities are only approximate since they are based on rate measurements at different temperatures (ranging from 90° to 123°) and of varying precision.

TABLE II
RELATIVE REACTIVITIES AND STABILITY CONSTANTS OF
VARIOUS MERCURIC COMPLEXES

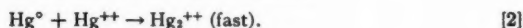
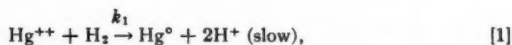
Complex	Stability constant*	Reactivity†
$HgSO_4$	22 (5)	1.8
Hg^{++}		1
$HgAc_2$	2.7×10^8 (8)	4×10^{-2}
$HgPr_2$		4×10^{-2}
$HgCl_2$	1.7×10^{12} (12)	2.5×10^{-3}
$HgBr_2$	1.2×10^{12} (12)	1.7×10^{-3}
$Hg(EDA)_2^{++}$	2.6×10^{22} (1)	1×10^{-3}

*Equilibrium constant at 25° for the reaction:



†Value of k_1 relative to that for Hg^{++} .

In the case of the simple Hg^{++} ion, it has been proposed, on the basis of kinetic and energetic considerations (3, 7), that the reaction proceeds through the following mechanism, involving the intermediate formation of a free Hg° atom, i.e.



In view of their similar kinetic pattern, it seems likely that the other mercuric complexes react by the same mechanism. Since the rate-determining step presumably involves the transfer of electrons from H_2 to $Hg(II)$, it would be expected to be influenced by the following considerations:

1. The unfilled low-lying electronic orbitals of Hg^{++} , on which this electron transfer depends, may be used up to varying degrees in forming covalent bonds with complexing ligands, with a resulting decrease in the electron affinity of the $Hg(II)$ species and, hence, in its reactivity toward H_2 . The inverse correlation, apparent in Table II, between the stability of the complexes and their reactivity, is consistent with this interpretation. The $HgSO_4$ complex, which is more reactive than the simple Hg^{++} ion, is relatively unstable and is probably of the ionic type. This is also the case for the various cupric complexes (e.g. $CuSO_4$, $CuAc_2$, $CuPr_2$, $CuCl_4^{2-}$) whose reactivities toward H_2 are greater than that of the simple Cu^{++} ion and which are also much less stable than the corresponding mercuric complexes (10).

2. Apart from the above consideration, the reaction should be favored by the presence of reagents of high basicity, capable of stabilizing the H^+ ions which are released in the rate-determining step. It is probable that this explains the general promoting influence of basic anions on the reaction under conditions such that $Hg(II)$ is already complexed to the point where any additional reduction of its electron affinity, through further complexing, is unlikely. This is probably the case for the chloride, acetate, and propionate systems, when the ratio of the concentration of complexing anion to that of $Hg(II)$ is greater than 2, and for the EDA system where the promoting influence on the reaction of various anions was found to follow the same order as their basicities, i.e. $OH^- > CO_3^{2-} > Pr^-, Ac^- > ClO_4^-$. To be effective in this way, the anion may participate in the reaction either as a separate kinetic entity or by complexing with $Hg(II)$. In the former case, the rate would increase linearly with the anion concentration, while in the latter case a saturation effect might be expected. Both types of behavior have been observed.

An alternative interpretation, not readily distinguishable from that just given, has been proposed to explain the catalytic influence which certain anions (e.g. OH^- and Cl^-) exert in other electron transfer reactions such as the exchange between isotopic metal ions of different valence. It has been suggested that the anion forms a polarizable bridge between the two reacting species, thereby lowering the electrostatic repulsion barrier to their mutual approach and facilitating electron transfer between them (14). It is possible that some of the anion influences observed in the present reaction should also be regarded in this light.

REFERENCES

1. BJERRUM, J. *Chem. Revs.* 46: 381. 1950.
2. DAKERS, R. G. and HALPERN, J. *Can. J. Chem.* 32: 969. 1954.
3. HALPERN, J. *Proc. Intern. Congr. Catalysis, Philadelphia.* 1956. In press.
4. HALPERN, J., KORINEK, G. J., and PETERS, E. *Research (London)*, 7: 61s. 1954.
5. INFELDT, G. and SILLÉN, L. G. *Svensk Kem. Tidskr.* 57: 104. 1946.
6. KOLTHOFF, I. M. and STENGER, V. A. *Volumetric analysis. Vol. 2.* Interscience Publishers, Inc., New York. 1947. p. 205.
7. KORINEK, G. J. and HALPERN, J. *J. Phys. Chem.* 60: 285. 1956.
8. MAHAPATRA, P., ADITYA, S., and PRASAD, B. *J. Indian Chem. Soc.* 30: 509. 1953.
9. PETERS, E. and HALPERN, J. *Can. J. Chem.* 33: 356. 1955; *J. Phys. Chem.* 59: 793. 1955.
10. PETERS, E. and HALPERN, J. *Can. J. Chem.* 34: 554. 1956.
11. PRAY, H. E., SCHWEICKERT, C. E., and MINNICH, B. H. *Ind. Eng. Chem.* 44: 1146. 1952.
12. SILLÉN, L. G. *Acta Chem. Scand.* 3: 539. 1949.
13. WIEBE, R. and GADDY, V. L. *J. Am. Chem. Soc.* 56: 76. 1934.
14. ZWOLINSKI, B., MARCUS, R. J., and EYRING, H. *Chem. Revs.* 55: 157. 1955.

THE INFRARED ABSORPTION SPECTRA OF DEUTERATED ESTERS

I. METHYL ACETATE¹

BY B. NOLIN² AND R. NORMAN JONES

ABSTRACT

By comparison of the infrared absorption spectrum of methyl acetate with the spectra of three deuterium substitution products, it has been possible to assign the bands in the 3100–2800 cm^{-1} and 1500–1300 cm^{-1} regions of methyl acetate to vibrations localized in the individual methyl groups. Bands characteristic of the individual trideuteromethyl groups are also identified between 2300 and 2000 cm^{-1} . The C=O stretching frequency is observed to shift to lower frequency with increasing deuteration. The spectra in the range 1300–700 cm^{-1} are also reported.

INTRODUCTION

The use of deuterium substitution as an aid in the interpretation of the infrared spectra of organic compounds of low symmetry has been demonstrated in previous publications from this laboratory (4, 6, 9). In an endeavor to gain more information concerning the nature of the absorption bands characteristic of alkyl esters, a series of deuterated analogues of methyl acetate and ethyl acetate have been synthesized, and their infrared spectra compared. This paper is concerned only with the spectra of methyl acetate (I) and the three deuterated analogues II–IV; the ethyl acetate spectra will be dealt with separately (10). More recently, deuterated analogues of methyl laurate have been synthesized by Dr. L. C. Leitch and their spectra will be discussed in a later publication.

- I. $\text{CH}_3\text{CO.O.CH}_3$
- II. $\text{CD}_3\text{CO.O.CH}_3$
- III. $\text{CH}_3\text{CO.O.CD}_3$
- IV. $\text{CD}_3\text{CO.O.CD}_3$

EXPERIMENTAL

The preparation and chemical and physical characterization of the deuterium substituted methyl acetates have been described elsewhere (8). Their isotopic purity was at least 99.0 at. % deuterium. The spectra were measured quantitatively in carbon tetrachloride solution between 4000 and 1300 cm^{-1} and in carbon disulphide solution below 1300 cm^{-1} . A Perkin-Elmer Model 12C single-beam spectrometer was employed with a full range of prisms. A control solvent spectrum was recorded on each chart and duplicate determinations were made for each compound. The absorption intensities were computed

¹Manuscript received June 15, 1956.

Contribution from the Division of Pure Chemistry, National Research Council, Ottawa, Canada. Issued as N.R.C. No. 4049.

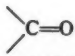
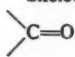
²National Research Council Postdoctorate Fellow. Present address: Carothers Research Laboratory, E. I. du Pont de Nemours, Wilmington, Del., U.S.A.

and plotted as apparent molecular extinction coefficients (7, pp. 276, 287).³ The computed spectral slit widths (7, p. 274) were approximately 3 cm.⁻¹ between 3200 and 2800 cm.⁻¹ (with LiF prism); 2 cm.⁻¹ between 2400 and 2000 cm.⁻¹ (with LiF prism); 3 cm.⁻¹ between 1800 and 1300 cm.⁻¹ (with CaF₂ prism); and 4 cm.⁻¹ at 1300 cm.⁻¹ diminishing to 3 cm.⁻¹ at 750 cm.⁻¹ (with NaCl prism).

RESULTS AND DISCUSSION

It is observed that several of the bands present in the spectrum of the normal compound disappear on deuteration. The missing bands are associated with vibrations localized in the groups which have been deuterated; by inference the bands that remain unchanged on deuteration are attributed to vibrations centered in other parts of the molecule. The absorption spectrum of the fully deuterated analogue IV has also been described by Corval and Lecomte (1), but the infrared spectra of the partly deuterated analogues have not been previously investigated. Our analyses of the spectra of the light and fully deuterated compounds are summarized in Table I, and the individual bands in all the analogues are considered separately below.

TABLE I
GROUP FREQUENCY ASSIGNMENTS IN CH₃CO.O.CH₃ AND CD₃CO.O.CD₃

ν_{\max} , cm. ⁻¹	Group	Type of vibration
CH ₃ CO.O.CH ₃		
3460		Overtone of carbonyl stretching vibration
3026, 2999	—O.CH ₃	Combination bands
2957	—O.CH ₃	Asymmetrical C—H stretching vibration
2905	—O.CH ₃	Combination band
2846	—O.CH ₃	Symmetrical C—H stretching vibration
2080	Skeletal	Overtone of 1047 cm. ⁻¹ band
1748		Carbonyl stretching vibration
1487, 1480	—	—
1456	—O.CH ₃	Asymmetrical C—H bending vibration
1435	—O.CH ₃	Symmetrical C—H bending vibration
(1401)*	—	See footnote *
1369	CH ₃ CO—	Symmetrical C—H bending vibration
1312	—	—
1279	—	Methyl bending vibration (?)
1243	Skeletal	See text
1047	Skeletal	See text
980	—	Methyl bending vibration (?)
844	Skeletal (?)	See text

³The apparent molecular extinction coefficient ($\epsilon_p(\nu)$) at the wave number ν is given by the expression:

$$\epsilon_p(\nu) = (1/cl) \log_{10}(T_0/T),$$

where c is the concentration of the solute in moles per liter of solution, l the cell length in cm., and $\log_{10}(T_0/T)$, the apparent optical density when the spectrometer is set to the wave number ν .

TABLE I (Concluded)

ν_{\max} , cm^{-1}	Group	Type of vibration
$\text{CD}_3\text{CO.O.CD}_3$		
3460	>C=O	Overtone of carbonyl stretching vibration
2272, 2254	—O.CD_3	Combination bands
2196	—O.CD_3	Asymmetrical C—D stretching vibration
2128	—O.CD_3	Combination band
2082	—O.CD_3	Symmetrical C—D stretching vibration
2016	—	Combination band
1740	>C=O	Carbonyl stretching vibration
1275	Skeletal	See text
1190	$\text{CD}_3\text{CO—}$	—
1092	Skeletal	See text
1053	—	—
1034†	—	—
970	$\text{CD}_3\text{CO— (?)}$	—
920	$\text{CD}_3\text{CO— (?)}$	—
744	Skeletal (?)	—

*This band is observed in $\text{CH}_3\text{CO.O.CD}_3$ but not in $\text{CH}_3\text{CO.O.CH}_3$ where it may be overlapped by the much stronger absorption at 1435 cm^{-1} . The bands at 1430 and 1401 cm^{-1} are alternatives for the asymmetrical C—H bending vibration in the $\text{CH}_3\text{CO—}$ group; the 1430 cm^{-1} assignment is supported by comparison with the spectrum of $\text{CH}_3\text{CO.O.CD}_2\text{CD}_3$ (10).

†Inflection.

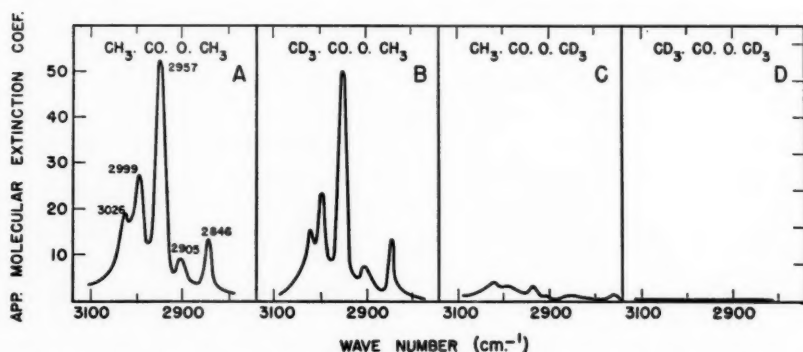


FIG. 1. Infrared spectra. Region of C—H stretching vibrations. (Carbon tetrachloride solution.)

C—H Stretching Vibrations ($3050\text{--}2800\text{ cm}^{-1}$)

In methyl acetate (I) we observe bands at 3026 , 2999 , 2957 , 2905 , and 2846 cm^{-1} (Fig. 1A). This spectrum is almost identical with that recorded by Francis (3) who noted the same five maxima. He employed a high resolution grating spectrometer and the extinction coefficients of the two most prominent bands, after interpolation from his curve and conversion to our intensity units, were 42 and 26 respectively (cf. our values of 52 and 26 respectively).

The association of all five of these bands with C—H vibrations is sub-

stantiated by the fact that they are all absent from the spectrum of the fully deuterated analogue (IV), which shows no measurable absorption in this region of the spectrum (Fig. 1D). Under the experimental conditions employed any bands with $\epsilon_{\max}^{(a)} > 0.5$ would have been detected.

The spectra of the partly deuterated analogues II and III are shown in Figs. 1B and 1C. They are of unusual interest, as they demonstrate that the significant absorption of the non-deuterated compound in this region of the spectrum is all associated with the ester methoxyl group, since the spectrum of II is almost identical with that of I, whereas in the spectrum of III the C—H stretching bands are weaker by a factor of 10. This spectrum is reproduced in Fig. 2 with an expanded ordinate scale. This observation conforms with

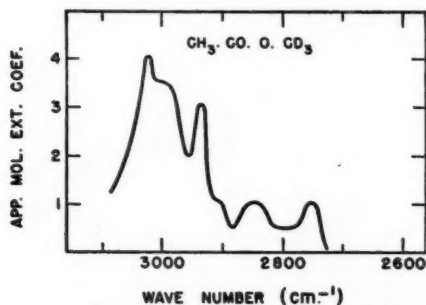


FIG. 2. Infrared spectrum of $\text{CH}_3\text{CO.O.CD}_3$ in same spectral region as Fig. 1, but with 10-fold expansion of intensity scale. (Carbon tetrachloride solution.)

Francis's conclusion (3) that the integrated absorption intensity in this region of the spectrum associated with the $-\text{CO.OCH}_3$ group is much greater than that associated with the $\text{CH}_3\text{CO.O}-$ structure. It is also consistent with the behavior of the C—D stretching bands of these compounds (see below) and with our observations on deuterated ethyl acetates (10).

Vibrational theory allows for only two fundamental C—H stretching vibrations for an isolated methyl group. Comparison with the spectra of *n*-paraffin hydrocarbons (7, pp. 339–342) suggests that the bands at 2957 and 2846 cm^{-1} are probably to be assigned respectively to the asymmetrical and symmetrical C—H stretching vibrations of the ester methoxyl group, and the other three bands to combination tones associated with the same structure.

All our samples of methyl and ethyl acetates, both deuterated and non-deuterated, exhibited a weak band near 3460 cm^{-1} ($\epsilon_{\max}^{(a)}$ 3–5) which was noted also by Corval and Lecomte (1). These authors attributed this band to a trace of methanol impurity, but it is more probably an overtone of the C=O stretching vibration, the fundamental of which occurs near 1745 cm^{-1} .

Between 2800 and 2300 cm^{-1} weak bands ($\epsilon_{\max}^{(a)} < 2$), probably due to overtones, are noted as follows: $\text{CH}_3\text{CO.O.CH}_3$ (2595, 2475 cm^{-1}); $\text{CD}_3\text{CO.O.CH}_3$ (2605, 2510 cm^{-1}); $\text{CH}_3\text{CO.O.CD}_3$ (2755, 2515 cm^{-1}); $\text{CD}_3\text{CO.O.CD}_3$ (2565 cm^{-1}).

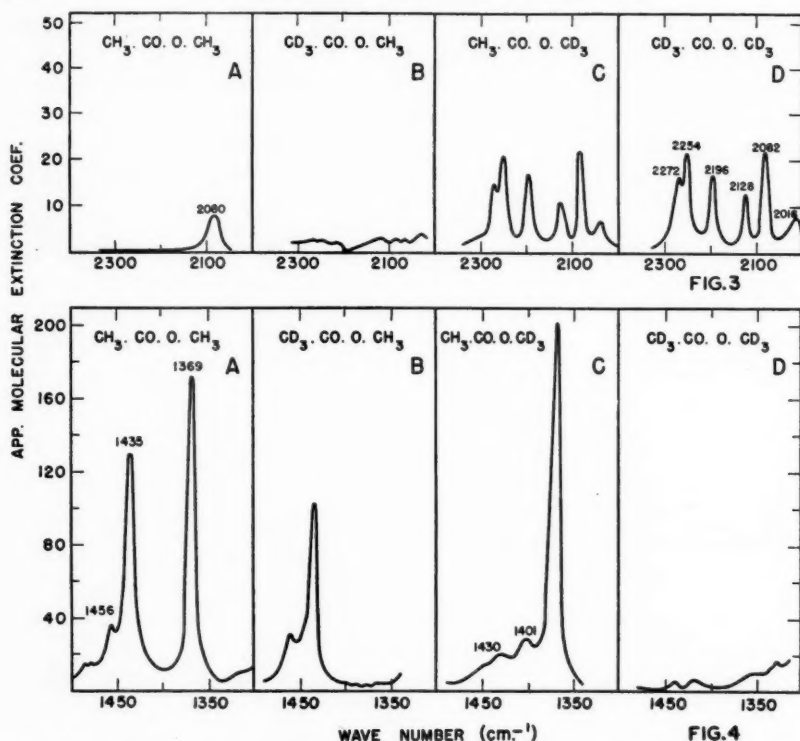


FIG. 3. (Upper figure) Infrared spectra. Region of C—D stretching vibrations. (Carbon tetrachloride solution.)

FIG. 4. (Lower figure) Infrared spectra. Region of the most characteristic C—H deformation vibrations. (Carbon tetrachloride solution.)

C—D Stretching Vibrations (2300–2050 cm^{-1})

Methyl acetate (I) exhibits a single weak band in this region at 2080 cm^{-1} ($\epsilon_{\text{max}}^{(a)} 7$) (Fig. 3A). This is possibly an overtone of the strong band at 1047 cm^{-1} (Fig. 5A). The fully deuterated analogue gives bands at 2272, 2254, 2196, 2128, 2082, and 2016 cm^{-1} (Fig. 3D). Five of these are probably analogues of the C—H vibrations described above and the sixth may be an overtone of the strong skeletal vibration at 1093 cm^{-1} by analogy with the 2080 cm^{-1} of methyl acetate. As the spectra of $\text{CH}_3\text{COOCD}_3$ and $\text{CD}_3\text{COOCD}_3$ are almost identical in this region (Figs. 3C, 3D) it is evident that only the $-\text{OCD}_3$ trideuteromethyl group is involved in this absorption. Comparison with Figs. 1A and 1B would suggest that the bands at 2196 and 2082 cm^{-1} may be asymmetrical and symmetrical C—D stretching vibrations of the trideuteromethoxy group, and the remaining bands combination tones. However the relative intensities of these bands do not correspond with those of the analogous C—H absorption; there may be mixing of the vibrations and a redistribution of intensity through coupling with the overtone of the skeletal band near 1090 cm^{-1} .

Carbonyl Stretching Vibrations (1748–1740 cm.⁻¹)

The carbonyl stretching vibration of methyl acetate in carbon tetrachloride solution occurs at 1748 cm.⁻¹. The position of the band in the various deuterated esters is given in Table II, from which it will be seen that there is a progressive shift to lower frequency with increasing deuteration, amounting to 8 cm.⁻¹ for the fully exchanged compound. Both of the trideuteromethyl groups contribute about equally to the shift and their effect is cumulative. This is similar to the deuteration displacements on the C=O frequency in diethyl ketone (9) and would seem to be a simple mass effect (7, p. 473).

C—H Bending Vibrations (1490–1300 cm.⁻¹)

Methyl acetate exhibits prominent bands at 1456, 1435, and 1369 cm.⁻¹ and two much weaker bands at 1487 and 1480 cm.⁻¹ (Fig. 4A). Francis observed the same spectrum (3); his molecular extinction coefficients for the two principal peaks, as interpolated from his curve, are 165 and 123 in our units, and these compare well with our values of 174 and 130 units.

In compounds of this type it is reasonable to assume *a priori* that the more prominent bands in this region of the spectrum involve C—H deformation vibrations; this is confirmed by the fact that the spectrum of the fully deuterated compound shows negligible absorption (Fig. 4D). Comparison with the spectra of the partly deuterated compounds shown in Figs. 4B and 4C shows clearly that both the 1456 and the 1435 cm.⁻¹ bands involve vibrations of the ester methoxyl group, while the 1369 cm.⁻¹ band is associated with the ester acetoxy group. This is consistent with earlier observations on more complex acetates and trideuteroacetates from which absorption near 1365 cm.⁻¹ was attributed to the acetate methyl group (4). The weak 1430 cm.⁻¹ band of CH₃CO.O.CD₃ could also be present in the spectrum of the light ester where it would be obscured by the much stronger 1435 cm.⁻¹ band.

From vibration theory we would expect altogether four C—H deformation vibrations associated with each isolated methyl group, and two of these would normally be observed in this region; the others (methyl "rocking" vibrations) occur at lower frequencies. In the *n*-paraffin hydrocarbons the asymmetrical and symmetrical methyl bending vibrations occur at 1460 and 1379 cm.⁻¹ (7, pp. 347–349). In methyl acetate we may tentatively assign the bands at 1456 and 1436 cm.⁻¹ respectively to the asymmetrical and symmetrical C—H bending vibrations of the ester methoxy group. The 1369 cm.⁻¹ band is almost certainly associated with the symmetrical C—H bending vibration of the acetoxy methyl group. Doubt remains as to the assignment of the asymmetrical C—H bending vibration of the acetoxy methyl; this could be one of the weak bands at 1430 or 1401 cm.⁻¹ observed only in CH₃CO.O.CD₃; comparison with the spectrum of the ethyl acetate derivatives (10) would suggest that the 1430 cm.⁻¹ band is more likely, as a band is also observed at 1430 cm.⁻¹ in CH₃CO.O.CD₂.CD₃.

It is also to be noted that whereas the intensities of the C—H stretching bands of the acetoxy methyl group are depressed by the vicinal carbonyl group, the symmetrical C—H bending band at 1369 cm.⁻¹ is much intensified. The maximal extinction coefficient of this band in methyl acetate is 174, while

TABLE II
DISPLACEMENT OF C=O STRETCHING AND SKELETAL
FREQUENCIES WITH DEUTERATION

	C=O stretching bands,* cm. ⁻¹	Skeletal bands,† cm. ⁻¹	
CH ₃ .CO.O.CH ₃	1748	1243	1047
CD ₃ .CO.O.CH ₃	1743	1256	1077
CH ₃ .CO.O.CD ₃	1744	1264	1089
CD ₃ .CO.O.CD ₃	1740	1275	1092

*Carbon tetrachloride solution.

†Carbon disulphide solution.

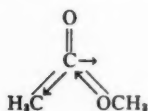
in short chain *n*-paraffin hydrocarbons values of about 20 per methyl group are observed (7, pp. 347-349). This agrees with the conclusions of Francis (3) based on integrated absorption intensity measurements.

Absorption Below 1300 cm.⁻¹

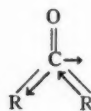
The absorption of the four compounds in the 1300-700 cm.⁻¹ region is shown in Figs. 5A-5D. In these spectra we can observe changes characteristic of the deuteration of the specific methyl groups, but we cannot at present assign these to vibrational modes.

In methyl acetate (I) there are two prominent bands, at 1243 cm.⁻¹ and 1046 cm.⁻¹, which are observed also in more complex acetates (5). Bands clearly corresponding with these are seen in the spectra of the deuterated methyl acetates and they shift progressively to higher frequency with increasing deuteration, as is shown in Table II. In more complex acetates (5) it has been shown that displacement of the 1243 cm.⁻¹ band to higher frequency is associated with a lowering of the C=O stretching frequency, and this is seen to hold true also in the deuterated methyl acetates.

The 1243 cm.⁻¹ band in methyl acetate has been identified with the skeletal vibration V (3) by analogy with VI which is a normal mode of vibration in aliphatic ketones. Aliphatic ethers also possess a strong band between 1150 and 1070 cm.⁻¹ associated with the asymmetrical stretching vibration VII, and it is possible that the 1243 and 1047 cm.⁻¹ bands of methyl acetate result from coupling of V and VII.



V



VI



VII

The band at 844 cm.⁻¹ in methyl acetate is strong enough to suggest a skeletal motion involving the significant participation of at least one of the more polar atoms, presumably the carbonyl carbon atom or the methoxy oxygen atom. In the vapor phase spectrum of dimethyl ether there is a band at 940 cm.⁻¹ assigned to the symmetrical motion VIII, which might couple

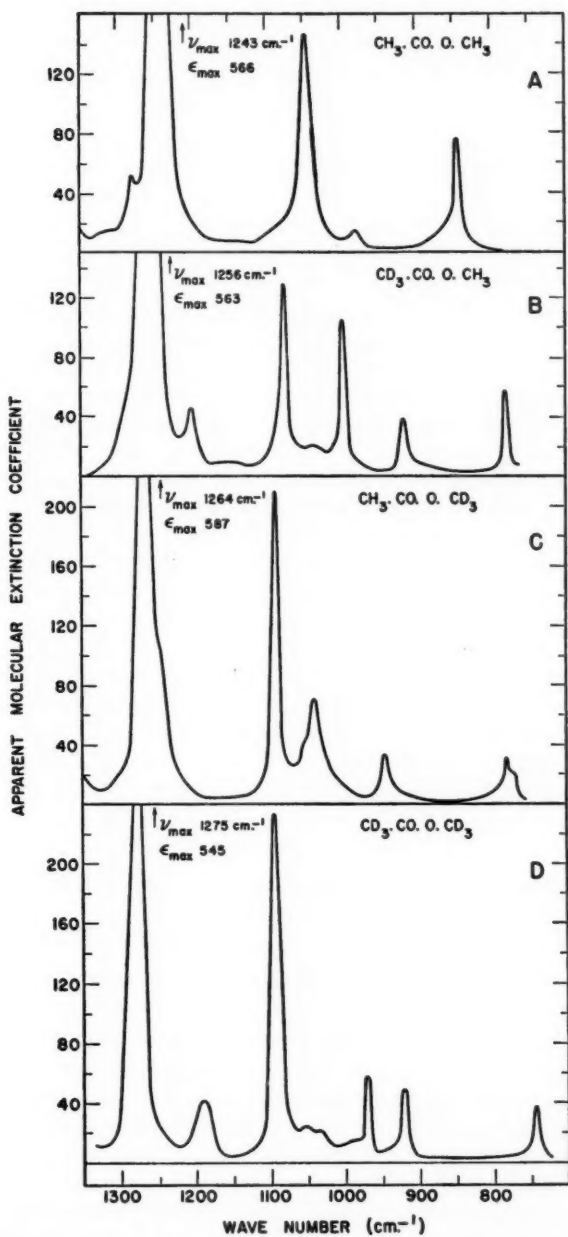
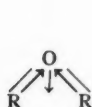
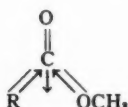


FIG. 5. Infrared spectra. "Fingerprint region". (Carbon disulphide solution.)

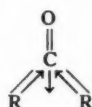
with a symmetrical motion IX of the acetoxy group. Vibration IX would be an analogue of the ketone vibration X which is assigned to a band at 790 cm^{-1} in the infrared spectrum of acetone. In the spectra of the deuterated methyl



VIII



IX



X

acetates (Figs. 5B-5D) this band is either lost, or displaced into the $780\text{--}730\text{ cm}^{-1}$ range. The weak bands in the methyl acetate spectrum at 1279 and 980 cm^{-1} may be combination tones or methyl rocking vibrations.

In the deuterated compounds additional absorption will be introduced from the C—D deformation vibrations of the trideuteromethyl groups. In $\text{CD}_3\text{COOCH}_3$ bands appear at 1200 cm^{-1} , 998 cm^{-1} , and 916 cm^{-1} which may correspond with bands at 1192 , 970 , and 920 cm^{-1} in $\text{CD}_3\text{COOCd}_3$. These can be assigned tentatively to motions localized in the $\text{CD}_3\text{CO—}$ group and one of the lower two may be the symmetrical C—D bending vibration displaced from 1368 cm^{-1} in the hydrogen compound. The 998 and 970 cm^{-1} bands would fit better for a calculated frequency shift by a factor of $1/\sqrt{2}$, but a larger displacement could occur if appreciable mixing with other vibrations is involved.

Characteristic structure appears in the spectrum of $\text{CH}_3\text{COOCd}_3$ at 1038 and 944 cm^{-1} but analogous bands are not recognizable in the spectrum of the fully deuterated compound. All the deuterated compounds show at least one band between 780 and 740 cm^{-1} which may be the analogue of the 844 cm^{-1} band of methyl acetate discussed above.

CONCLUDING REMARKS

These comparative studies demonstrate that at frequencies above 1300 cm^{-1} all the major absorption bands of methyl acetate can be treated in good approximation as associated with vibrations localized within the $\text{CH}_3\text{CO—}$, —O—CH_3 , or >C=O groups. They also serve to emphasize the complexity of the C—H stretching absorption. The simple nature of the spectra of aliphatic and alicyclic hydrocarbons between 3100 and 2800 cm^{-1} , which was first demonstrated by Fox and Martin (2), suggested that this region of the spectrum might prove to be very helpful for the interpretation of the molecular structure of more complex compounds. These observations on methyl acetate substantiate the conclusions of Francis (3) and of Pozefsky and Coggeshall (11), as well as earlier work from this laboratory (9), in showing that the C—H stretching absorption is particularly sensitive to the introduction of heteroatoms, in respect to both the band intensities and the prevalence of strong combination bands.

ACKNOWLEDGMENTS

We are very grateful to Mr. Armand Nadeau for technical assistance with the measurement of the spectra.

REFERENCES

1. CORVAL, M. and LECOMTE, J. *Mikrochim. Acta*, **25**. 1955.
2. FOX, J. J. and MARTIN, A. E. *Proc. Roy. Soc. (London)*, **A**, **167**: 257. 1938; **175**: 208. 1940.
3. FRANCIS, S. A. *J. Phys. Chem.* **19**: 942. 1951.
4. JONES, R. N., COLE, A. R. H., and NOLIN, B. *J. Am. Chem. Soc.* **74**: 5662. 1952.
5. JONES, R. N. and HERLING, F. *J. Am. Chem. Soc.* **78**: 1152. 1956.
6. JONES, R. N., NOLIN, B., and ROBERTS, G. *J. Am. Chem. Soc.* **77**: 6331. 1955.
7. JONES, R. N. and SANDORFY, C. The application of infrared and Raman spectrometry to the elucidation of molecular structure. *In* *Technique of organic chemistry IX*. Edited by A. Weissberger. Interscience Publishers, Inc., New York, London. 1956.
8. NOLIN, B. *Can. J. Chem.* **32**: 1. 1954.
9. NOLIN, B. and JONES, R. N. *J. Am. Chem. Soc.* **75**: 5626. 1953.
10. NOLIN, B. and JONES, R. N. *Can. J. Chem.* **34**: 1392. 1956.
11. POZEFSKY, A. and COGGESHALL, N. P. *Anal. Chem.* **23**: 1611. 1951.

THE INFRARED ABSORPTION SPECTRA OF DEUTERATED ESTERS

I. ETHYL ACETATE¹

BY B. NOLIN² AND R. NORMAN JONES

ABSTRACT

The infrared absorption spectrum of ethyl acetate has been compared with the spectra of seven derivatives deuterated in the methyl and methylene groups. In the region 3500–1300 cm^{-1} most of the bands can be assigned to vibrations localized in the individual groups. Absorption characteristic of the trideutero-methyl and dideuteromethylene groups can be recognized between 2300 and 2000 cm^{-1} . The C=O stretching vibration shows progressive displacement to lower frequency with increasing deuteration. The spectra in the range 1300–700 cm^{-1} are also reported.

INTRODUCTION

This paper is concerned with a comparison of the infrared spectra of ethyl acetate (I) and seven derivatives (II–VIII) in which deuterium has been introduced selectively into the methyl and methylene groups. This investigation parallels studies of diethyl ketone (4) and methyl acetate (5) which have been reported elsewhere.

- | | |
|---|--|
| I. $\text{CH}_3\text{CO.O.CH}_2\text{CH}_3$ | V. $\text{CH}_3\text{CO.O.CD}_2\text{CD}_3$ |
| II. $\text{CH}_3\text{CO.O.CD}_2\text{CH}_3$ | VI. $\text{CD}_3\text{CO.O.CD}_2\text{CH}_3$ |
| III. $\text{CH}_3\text{CO.O.CH}_2\text{CD}_3$ | VII. $\text{CD}_3\text{CO.O.CH}_2\text{CD}_3$ |
| IV. $\text{CD}_3\text{CO.O.CH}_2\text{CH}_3$ | VIII. $\text{CD}_3\text{CO.O.CD}_2\text{CD}_3$ |

The preparation of the deuterated esters and their physical and chemical characterization have been described previously (3). In all compounds the isotopic purity was of the order of 99.0 at. % deuterium. These spectra were measured under the same conditions as were the methyl acetate spectra (5).

RESULTS AND DISCUSSION

C—H Stretching Vibrations (3000–2850 cm^{-1})

The spectra are shown in Figs. 1A–1H. Light ethyl acetate (I) exhibits four distinct bands at 2982, 2939, 2906, and 2873 cm^{-1} with an additional inflection at 2962 cm^{-1} (Fig. 1A).

These bands are all associated with C—H vibrations, as the spectrum of

¹Manuscript received June 15, 1956.

Contribution from the Division of Pure Chemistry, National Research Council, Ottawa, Canada. Issued as N.R.C. No. 4050.

²National Research Council Postdoctorate Fellow. Present address: Carothers Research Laboratory, E. I. du Pont de Nemours, Wilmington, Del., U.S.A.

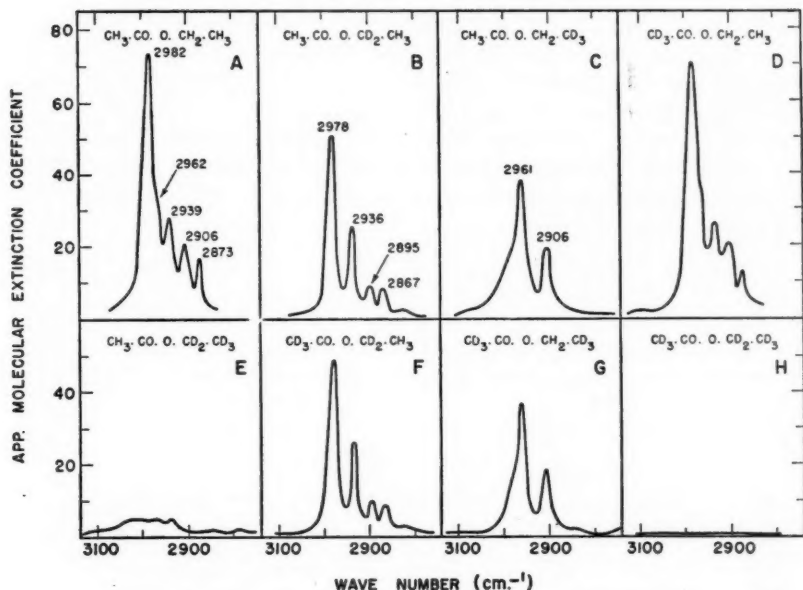


FIG. 1. Infrared spectra. Region of C—H stretching vibrations. (Carbon tetrachloride solution.)

the fully deuterated compound (VIII) shows no absorption in this region (Fig. 1H). The significant absorption is further restricted to the $-\text{CH}_2\text{CH}_3$ group, as the spectrum of $\text{CH}_2\text{CO.O.CD}_2\text{CD}_3$ is extremely weak (Fig. 1E). Conversely the spectrum of $\text{CD}_3\text{CO.O.CH}_2\text{CH}_3$ in this region (Fig. 1D) resembles that of the non-deuterated compound. The weak band system in $\text{CH}_3\text{CO.O.CD}_2\text{CD}_3$ is shown more clearly in Fig. 2, where the ordinate scale

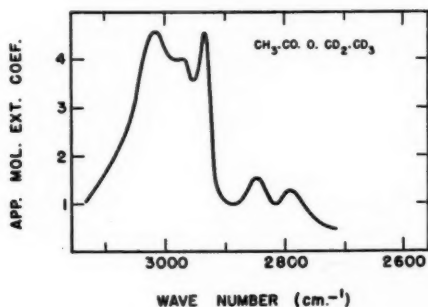


FIG. 2. Infrared spectrum of $\text{CH}_3\text{CO.O.CD}_2\text{CD}_3$ in same spectral region as Fig. 1, but with 10-fold expansion of intensity scale. (Carbon tetrachloride solution.)

is expanded by a factor of 10. Although weak, this absorption would appear to be characteristic for the CH_3COO —structure, and closely resembles that observed in the spectrum of the related deuterated methyl acetate ($\text{CH}_3\text{COOCD}_3$) shown in Fig. 2 of Reference 5.

A more detailed comparison among these spectra suggests that some of the observed bands are composite; the bands are considered individually below and the tentative assignments for the light and the fully deuterated compounds are summarized in Table I.

TABLE I
GROUP FREQUENCY ASSIGNMENTS IN $\text{CH}_3\text{COOCH}_2\text{CH}_3$ AND $\text{CD}_3\text{COOCD}_2\text{CD}_2$

ν_{max} , cm^{-1}	Group	Type of vibration
A. $\text{CH}_3\text{COOCH}_2\text{CH}_3$		
3460	>C=O	Overtone of carbonyl stretching vibration
2982	$-\text{CH}_2-\text{CH}_3$	Asymmetrical C—H stretching vibration of methyl group superimposed on weak methylene absorption
2962*	$-\text{CH}_2-$	Asymmetrical C—H stretching vibration
2939	$-\text{CH}_3$ of ethoxy group	Combination band (see 2873 cm^{-1} band)
2906	$-\text{CH}_2-\text{CH}_3$	Primarily a symmetrical C—H stretching vibration of the methylene group superimposed on weaker methyl absorption
2873	$-\text{CH}_3$ of ethoxy group	Symmetrical C—H stretching vibration (this might be reversed with the 2939 cm^{-1} band)
1741	>C=O	Carbonyl stretching vibration
1475	$-\text{CH}_2-\text{CH}_3$	See text
1464	$-\text{CH}_2-\text{CH}_3$	An overlapping doublet, one component of which is probably the scissoring C—H deformation vibration of the methylene group
1446	$-\text{CH}_2$ of ethoxy group	Asymmetrical C—H bending vibration
1430*	$\text{CH}_3-\text{CO}-$	Asymmetrical C—H bending vibration
1393	$-\text{CH}_2\text{CH}_3$	Primarily a symmetrical C—H bending vibration of the methyl group, perturbed from 1380 cm^{-1} by interaction with a methylene vibration and further displaced by interaction with the 1373 cm^{-1} vibration of the acetoxy methyl group (cf. 1359 cm^{-1} band)
1373	$\text{CH}_3\text{CO}-$	Symmetrical C—H bending vibration
1359	$-\text{CH}_2\text{CH}_3$	Primarily a (wagging?) vibration of the methylene group, perturbed from 1382 cm^{-1} by interaction with a methyl vibration and further displaced by interaction with the 1373 cm^{-1} vibration of the acetoxy methyl group (cf. 1393 cm^{-1} band)
1300	—	—
1264	—	—
1238	Skeletal	See Reference 5
1115*	—	—
1097	—	—
1046	Skeletal	See Reference 5
1000	—	—
938	—	—
915	—	—
806	—	—
784	$-\text{CH}_2\text{CH}_3$	—

TABLE I (Concluded)

ν_{\max} , cm. ⁻¹	Group	Type of vibration
B. CD ₃ .CO.O.CD ₂ .CD ₃		
3460	\diagup C=O	Overtone of carbonyl stretching vibration
2242	—CD ₂ .CD ₃	Principally a —CD ₂ vibration with some contribution from —CD ₃ —
2230	—CD ₂ .CD ₃	Principally a —CD ₂ — vibration with some contribution from —CD ₃
2186	—CD ₂ .CD ₃	Principally a —CD ₂ — vibration but may be combined with an overtone of a skeletal band
2151	—CD ₂ —	—
2120	—	See text
2074	—CD ₃ of ethoxy group	Symmetrical C—D stretching vibration (?)
1737	\diagup C=O	Carbonyl stretching vibration
1194	—CD ₂ .CD ₃	—
1178	—CD ₂ .CD ₃	—
1097	—CD ₂ .CD ₃	—
1082	CD ₃ .CO—	—
1059	—CD ₂ .CD ₃	—
1047	—CD ₂ .CD ₃	—
988	—	—
958	—	—
917	CD ₃ .CO—	—
815	—	—
780	—	—
718	—	—

*Inflection.

(a) *The 2982 cm.⁻¹ band.*—This band occurs in light ethyl acetate with $\epsilon_{\max}^{(a)}$ 74 and in CD₃.CO.O.CH₂.CH₃ with $\epsilon_{\max}^{(a)}$ 71 (Figs. 1A, 1D). It also occurs in CH₃.CO.O.CD₂.CH₃ with $\epsilon_{\max}^{(a)}$ 54 and in CD₃.CO.O.CD₂.CH₃ with $\epsilon_{\max}^{(a)}$ 48 (Figs. 1B, 1F). It therefore appears that the CH₃ group of the ethoxy radical is mainly responsible for this absorption, but the intensity is enhanced in the —CH₂.CH₃ compounds. It will be shown later that this probably results from the superposition of an underlying —CH₂— band.

(b) *The 2962 cm.⁻¹ inflection.*—This can be assigned to the methylene group, since it remains in CH₃.CO.O.CH₂.CD₃ and CD₃.CO.O.CH₂.CD₃ (Figs. 1C, 1G). In these spectra the 2962 cm.⁻¹ band exhibits asymmetry on the high frequency side, suggestive of an additional band. It is this component that enhances the intensity of the 2982 cm.⁻¹ band discussed in section (a) above.

(c) *The 2939 cm.⁻¹ band.*—This band is absent from CH₃.CO.O.CH₂.CD₃ and CD₃.CO.O.CH₂.CD₃ (Figs. 1C, 1G), and is therefore associated with the methyl group of the ethoxy radical. This is confirmed by comparison among Figs. 1B, 1D, 1E, and 1F.

(d) *The 2906 cm.⁻¹ band.*—This band is probably composite, with a weaker component on the low frequency side. In light ethyl acetate it occurs with $\epsilon_{\max}^{(a)}$ 20 (Fig. 1A); it remains in CH₃.CO.O.CH₂.CD₃ and CD₃.CO.O.CH₂.CD₃ with $\epsilon_{\max}^{(a)}$ 18 (Figs. 1C, 1G) and is therefore associated primarily with the methylene group. In CH₃.CO.O.CD₂.CH₃ and CD₃.CO.O.CD₂.CH₃ (Figs. 1B,

1F) the major component at 2906 cm^{-1} is removed and the weaker band appears at 2895 cm^{-1} with $\epsilon_{\text{max}}^{(a)}$ 9. This must be associated with the methyl group of the ethoxy radical.

(e) *The 2873 cm^{-1} band.*—This band must also be assigned to the methyl group of the ethoxy radical as it is missing from the spectra of $\text{CH}_3\text{COOCH}_2\text{CD}_3$ and $\text{CD}_3\text{COOCH}_2\text{CD}_3$ (Figs. 1C, 1G).

The more specific assignment of these bands to particular modes of vibration is difficult, although by analogy with the spectra of *n*-paraffin hydrocarbons (2) the primary component of the 2982 cm^{-1} band, and the 2873 cm^{-1} band, can probably be assigned respectively to the asymmetrical and symmetrical C—H stretching vibrations of the methyl group of the ethoxy radical. The 2906 cm^{-1} band shows analogy with the band at 2902 cm^{-1} in diethyl ketone (4) which has been assigned to the symmetrical C—H stretching vibration of the methylene group. This leaves the asymmetrical methylene C—H stretch for consideration, and this may account for the 2962 cm^{-1} inflection. The other absorption (notably the 2939 cm^{-1} band) would then be assigned to combination bands.

In these arguments it has been tacitly assumed that both the fundamental and the combination bands can be treated as localized in the individual methyl and methylene groups, and that they are not appreciably perturbed by deuteration at other centers in the molecule. This is substantiated by the summation spectra shown in Figs. 3A and 3B. By addition of the spectra of

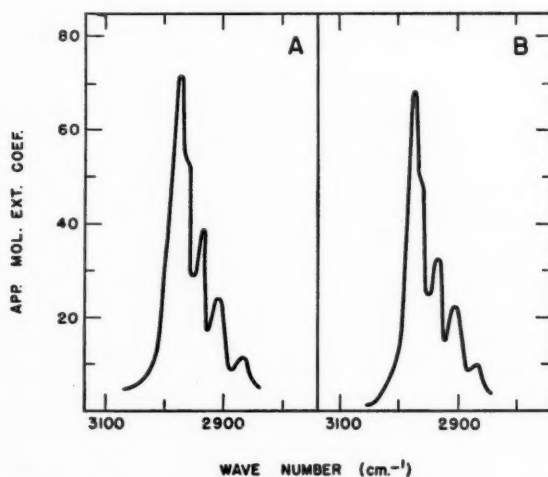


FIG. 3. Summation spectra.

A. $\text{CH}_3\text{COOCD}_2\text{CD}_3 + \text{CD}_3\text{COOCH}_2\text{CD}_3 + \text{CH}_3\text{COOCD}_2\text{CD}_3$
 B. $\text{CD}_3\text{COOCH}_2\text{CD}_3 + \text{CD}_3\text{COOCD}_2\text{CH}_3$

$\text{CH}_3\text{COOCD}_2\text{CD}_3$, $\text{CD}_3\text{COOCH}_2\text{CD}_3$, and $\text{CD}_3\text{COOCD}_2\text{CH}_3$ the curve shown in Fig. 3A is obtained; this represents the composite absorption of the isolated methylene and two methyl groups, and it does in fact simulate the curve observed for light ethyl acetate (Fig. 1A), both qualitatively and

quantitatively. The combination of the curves for $\text{CD}_3\text{CO.O.CH}_2\text{CD}_3$ and $\text{CD}_3\text{CO.O.CD}_2\text{CH}_3$ likewise simulates the spectrum of $\text{CD}_3\text{CO.O.CH}_2\text{CH}_3$ (cf. Figs. 3B and 1D).

Absorption Between 2850 and 2250 cm^{-1}

In the spectra of the partly deuterated compounds a few weak bands ($\epsilon_{\text{max}}^{(a)} < 2$) are observed in this region as follows: $\text{CH}_3\text{CO.O.CD}_2\text{CH}_3$ (2510 cm^{-1}); $\text{CH}_3\text{CO.O.CH}_2\text{CD}_3$ (2725, 2600, 2470 cm^{-1}); $\text{CD}_3\text{CO.O.CH}_2\text{CH}_3$ (2620, 2470 cm^{-1}); $\text{CH}_3\text{CO.O.CD}_2\text{CD}_3$ (2510 cm^{-1}); $\text{CD}_3\text{CO.O.CD}_2\text{CH}_3$ (2545 cm^{-1}); $\text{CD}_3\text{CO.O.CH}_2\text{CD}_3$ (2740, 2600, 2495 cm^{-1}). These are probably overtones of skeletal vibrations, but it is curious that similar bands were not observed in the spectra of the light or the fully deuterated compound.

C—D Stretching Vibrations (2250–2050 cm^{-1})

Light ethyl acetate is transparent in this region (Fig. 4A) and does not exhibit any absorption near 2080 cm^{-1} comparable with the band in light methyl acetate which has been attributed to a skeletal overtone vibration (5). The fully deuterated ester (VIII) exhibits six bands at 2242, 2230, 2186, 2151, 2120, and 2074 cm^{-1} (Fig. 4H). As would be anticipated, this spectrum is

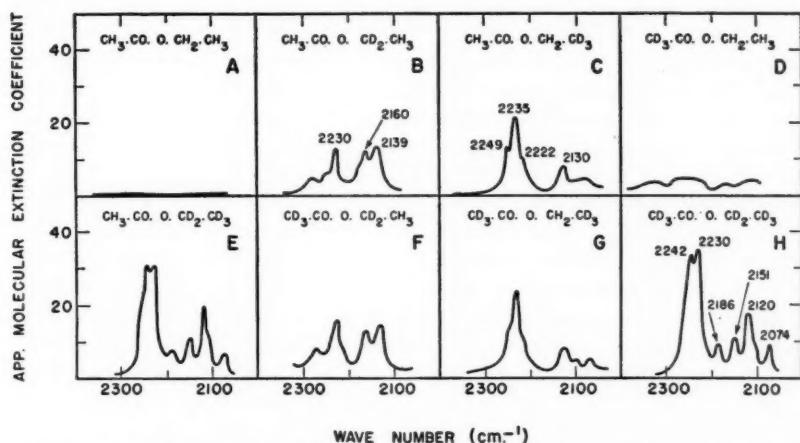


FIG. 4. Infrared spectra. Region of C—D stretching vibrations. (Carbon tetrachloride solution.)

almost identical with that of $\text{CH}_3\text{CO.O.CD}_2\text{CD}_3$ (Fig. 4E); the $\text{CD}_3\text{CO.O—}$ group therefore absorbs extremely weakly in this region. These bands are discussed individually below, and tentative assignments for the light compound and the fully deuterated compound are summarized in Table I. In general the assignments for the C—D stretching vibrations are less satisfactory than those for the C—H stretching vibrations and they seem less localized and more susceptible to perturbation effects of neighboring groups. This is indicated by the summation spectrum for $\text{CD}_3\text{CO.O.CH}_2\text{CH}_3 + \text{CH}_3\text{CO.O.CD}_2\text{CH}_3 + \text{CH}_3\text{CO.O.CH}_2\text{CD}_3$ which does not conform well with the spectrum observed for $\text{CD}_3\text{CO.O.CD}_2\text{CD}_3$ (Fig. 5).

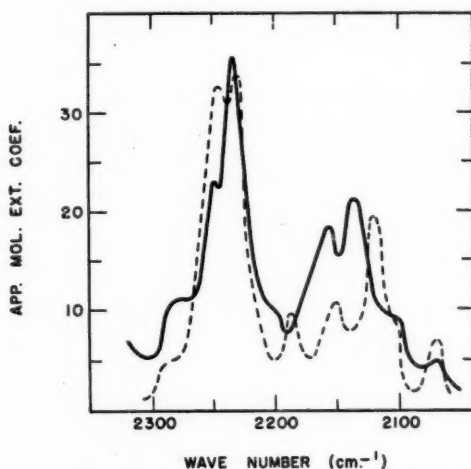


FIG. 5. — Summation spectrum of $\text{CD}_3\text{CO.O.CH}_2\text{CH}_3 + \text{CH}_3\text{CO.O.CD}_2\text{CH}_3 + \text{CH}_3\text{CO.O.CH}_2\text{CD}_3$.
 - - - Observed spectrum of $\text{CD}_3\text{CO.O.CD}_2\text{CD}_3$.

(a) *The 2242–2230 cm^{-1} region.*—The absorption in this region is composite. The compounds containing $-\text{O.CD}_2\text{CD}_3$ exhibit two peaks at 2242 and 2230 cm^{-1} both with extinction coefficients of about 30 units (Figs. 4E, 4H). In $\text{CH}_3\text{CO.O.CH}_2\text{CD}_3$ and $\text{CD}_3\text{CO.O.CH}_2\text{CD}_3$ (Figs. 4C, 4G), there is a weaker triplet at 2249, 2235, and 2222 cm^{-1} , and in $\text{CH}_3\text{CO.O.CD}_2\text{CH}_3$ and $\text{CD}_3\text{CO.O.CD}_2\text{CH}_3$ (Figs. 4B, 4F) there is a single peak at 2230 cm^{-1} ($\epsilon_{\text{max}}^{(a)}$ 13–15). We may therefore regard the 2230 cm^{-1} band as coming principally from the dideuteromethylene group and the 2242 cm^{-1} band from the trideuteromethyl group, but there is appreciable overlap; possibly some mixing of the vibrations is also indicated by comparison with the summation spectrum in Fig. 5.

(b) *The 2186 cm^{-1} band.*—This appears only in molecules containing the $-\text{CD}_2\text{CD}_3$ structure (Figs. 4E, 4H), but $\text{CH}_3\text{CO.O.CD}_2\text{CH}_3$ shows a weak inflection at 2177 cm^{-1} (Fig. 4B) which is also observable in the summation spectrum in Fig. 5 and this may contribute to the 2186 cm^{-1} band envelope.

(c) *The 2151 cm^{-1} band.*—This is probably a dideuteromethylene vibration; it is observed at this position only in $\text{CH}_3\text{CO.O.CD}_2\text{CD}_3$ and $\text{CD}_3\text{CO.O.CD}_2\text{CD}_3$ (Figs. 4E, 4H), but is probably similar to the bands at 2160 cm^{-1} in $\text{CH}_3\text{CO.O.CD}_2\text{CH}_3$ and at 2163 cm^{-1} in $\text{CD}_3\text{CO.O.CD}_2\text{CH}_3$ (Figs. 4B, 4F).

(d) *The 2140–2120 cm^{-1} absorption.*—All the deuterated ethyl acetates exhibit a band in this region; the position and intensity depends on the type of deuterium substitution in the ethoxy group, as shown in Table II. It does not seem possible to characterize these bands further at the present time.

TABLE II
 ABSORPTION AT 2140-2120 cm^{-1} IN DEUTERATED ETHYL ACETATES*

	ν_{max} , cm^{-1}	$\epsilon_{\text{max}}^{(a)}$
$\text{CH}_3\text{CO.O.CD}_2\text{CD}_3$	2120	20
$\text{CD}_3\text{CO.O.CD}_2\text{CD}_3$	2120	18
$\text{CH}_3\text{CO.O.CD}_2\text{CH}_3$	2139	13
$\text{CD}_3\text{CO.O.CD}_2\text{CH}_3$	2134	13
$\text{CH}_3\text{CO.O.CH}_2\text{CD}_3$	2130	7
$\text{CD}_3\text{CO.O.CH}_2\text{CD}_3$	2130	8

*Carbon tetrachloride solution.

(e) The 2074 cm^{-1} band.—This weak band is absent from the spectra of $\text{CH}_3\text{CO.O.CD}_2\text{CH}_3$ and $\text{CD}_3\text{CO.O.CD}_2\text{CH}_3$ (Figs. 4B, 4F) but present in all compounds containing a trideuteromethyl group in the ethoxy radical and it is obviously associated with the latter group (Figs. 4C, 4E, 4G, 4H).

C=O Stretching Vibrations (1742-1737 cm^{-1})

In light ethyl acetate the carbonyl stretching band occurs at 1742 cm^{-1} in carbon tetrachloride solution. The effect of increasing deuteration is shown in Table III. In general deuteration shifts the band to lower frequency, with the

 TABLE III
 DISPLACEMENT OF THE C=O STRETCHING AND THE PRINCIPAL SKELETAL FREQUENCY WITH DEUTERATION

	C=O stretching band,* cm^{-1}	Skeletal band,† cm^{-1}
$\text{CH}_3\text{CO.O.CH}_2\text{CH}_3$	1742	1235
$\text{CH}_3\text{CO.O.CH}_2\text{CD}_3$	1742	1238
$\text{CH}_3\text{CO.O.CD}_2\text{CH}_3$	1742	1263
$\text{CD}_3\text{CO.O.CH}_2\text{CH}_3$	1739	1254
$\text{CH}_3\text{CO.O.CD}_2\text{CD}_3$	1739	1264
$\text{CD}_3\text{CO.O.CH}_2\text{CD}_3$	1738	1251
$\text{CD}_3\text{CO.O.CD}_2\text{CH}_3$	1738	1277
$\text{CD}_3\text{CO.O.CD}_2\text{CD}_3$	1737	1275

*Carbon tetrachloride solution.

†Carbon disulphide solution.

fully deuterated compound absorbing at 1737 cm^{-1} . Deuteration in the acetoxy group appears to have a greater effect than deuteration in the ethoxy group.

All the compounds exhibit a weak band near 3460 cm^{-1} ($\epsilon_{\text{max}}^{(a)}$ 3-5) which is most probably the first overtone of this carbonyl band.

C-H Bending Vibrations (1500-1300 cm^{-1})

In this region light ethyl acetate exhibits six absorption bands (Fig. 6A); there is an additional inflection at 1430 cm^{-1} which only appears clearly when adjacent bands are eliminated by deuteration (Figs. 6C, 6E). These bands are

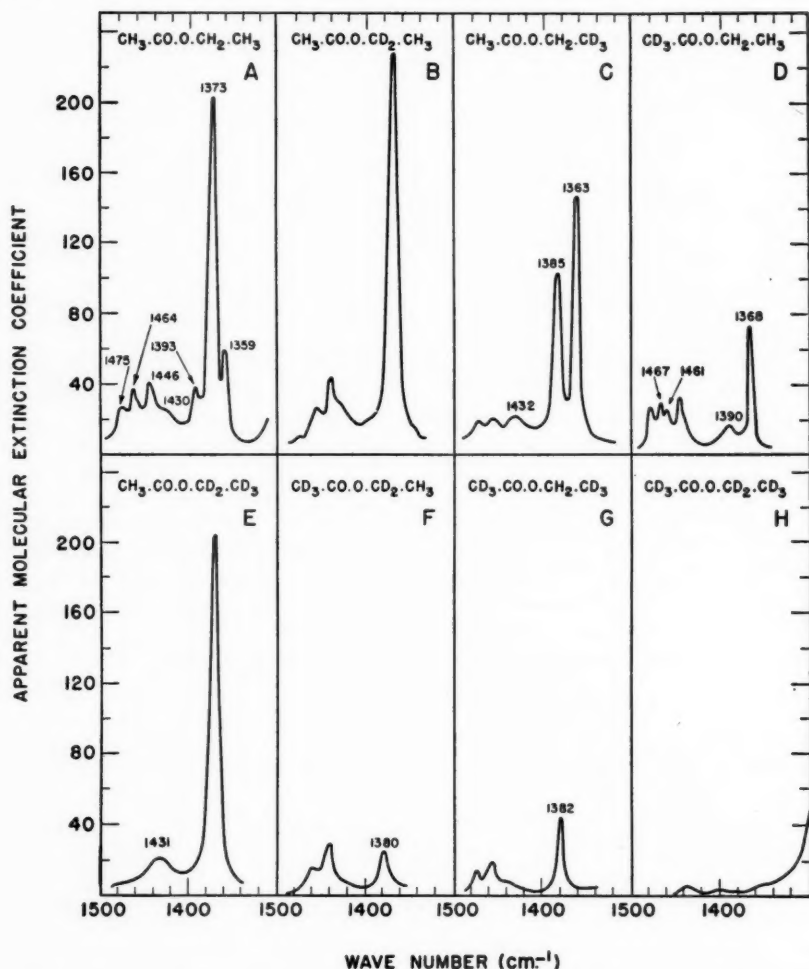


FIG. 6. Infrared spectra. Region of the most characteristic C—H deformation vibrations. (Carbon tetrachloride solution.)

all associated with C—H bending vibrations, as the spectrum of the fully deuterated compound shows no significant absorption in this region (Fig. 6H).

The assignments of these bands are summarized in Table I and they are considered individually below.

(a) *The 1475 cm^{-1} band.*—This is observed in the spectra of all molecules that contain the methylene group and it must therefore be assigned primarily to a $-\text{CH}_2-$ vibration. However the band is appreciably stronger ($\epsilon_{\text{max}}^{(a)} 26$) in compounds containing $-\text{CH}_2\text{CH}_3$ (Figs. 6A, 6D) than in those containing

$-\text{CH}_2\text{CD}_3$ (Figs. 6C, 6G), for which $\epsilon_{\text{max}}^{(a)}$ is 14–18. There must therefore be a weak contribution from the ethoxy methyl group. This is substantiated by the spectrum of $\text{CH}_3\text{COOCD}_2\text{CH}_3$ which exhibits a band with $\epsilon_{\text{max}}^{(a)}$ 10 at this position. No similar band, however, is observed in the spectrum of $\text{CD}_3\text{COOCD}_2\text{CH}_3$.

(b) *The 1464 cm^{-1} band.*—In the light ester this band exhibits asymmetry on the low frequency side and it separates into a clear doublet at 1467 and 1461 cm^{-1} in $\text{CD}_3\text{COOCH}_2\text{CH}_3$ (Fig. 6D). It is missing from the spectrum of $\text{CH}_3\text{COOCD}_2\text{CD}_3$ (Fig. 6E) and would appear to involve superimposed absorption associated with the $-\text{CH}_2-$ and $-\text{CH}_3$ groups of the ethoxy radical. In compounds containing $-\text{CH}_2\text{CD}_3$ and $-\text{CD}_2\text{CH}_3$ the band is displaced down to 1458 cm^{-1} (Figs. 6B, 6C, 6F, 6G).

(c) *The 1446 cm^{-1} band.*—This band is clearly associated with the methyl group of the ethoxy radical. It is present in the spectra of $\text{CH}_3\text{COOCD}_2\text{CH}_3$, $\text{CD}_3\text{COOCH}_2\text{CH}_3$, and $\text{CD}_3\text{COOCD}_2\text{CH}_3$ (Figs. 6B, 6D, 6F), and absent from the spectra of $\text{CH}_3\text{COOCH}_2\text{CD}_3$, $\text{CH}_3\text{COOCD}_2\text{CD}_3$, and $\text{CD}_3\text{COOCH}_2\text{CD}_3$ (Figs. 6C, 6E, 6G).

(d) *The 1430 cm^{-1} inflection.*—This band can be assigned to the methyl group of the acetoxy radical. It is present in the spectra of $\text{CH}_3\text{COOCD}_2\text{CH}_3$, $\text{CH}_3\text{COOCH}_2\text{CD}_3$, and $\text{CH}_3\text{COOCD}_2\text{CD}_3$ (Figs. 6B, 6C, 6E), and absent from the spectra of $\text{CD}_3\text{COOCH}_2\text{CH}_3$, $\text{CD}_3\text{COOCD}_2\text{CH}_3$, and $\text{CD}_3\text{COOCH}_2\text{CD}_3$ (Figs. 6D, 6F, 6G). It is clearly resolved in the spectra of the compounds that lack the overlapping 1446 cm^{-1} band (Figs. 6C, 6E).

The 1400–1350 cm^{-1} Absorption

The light compound exhibits three bands in this region; an intense band at 1373 cm^{-1} ($\epsilon_{\text{max}}^{(a)}$ 203) with weaker satellites at 1393 and 1359 cm^{-1} .

The strong 1373 cm^{-1} band can be attributed to the $\text{CH}_3\text{CO}-$ group, as it is present with comparable intensity in $\text{CH}_3\text{COOCD}_2\text{CD}_3$ (Fig. 6E), and with enhanced intensity ($\epsilon_{\text{max}}^{(a)}$ 222) in $\text{CH}_3\text{COOCD}_2\text{CH}_3$ (Fig. 6B). The satellite bands must be associated with the ethoxy group, as they are absent from the spectrum of $\text{CH}_3\text{COOCD}_2\text{CD}_3$ (Fig. 6E). However, the relationship is not a simple one, and a satisfactory rationalization is possible only if an appreciable wandering of these bands is recognized in the spectra of the various partly deuterated compounds.

In $\text{CD}_3\text{COOCD}_2\text{CH}_3$ (Fig. 6F) there is a band at 1380 cm^{-1} assignable to the methyl group of the ethoxy radical and in $\text{CD}_3\text{COOCH}_2\text{CD}_3$ (Fig. 6G) a somewhat stronger band at 1382 cm^{-1} which must be assigned to the methylene group. $\text{CD}_3\text{COOCH}_2\text{CH}_3$ exhibits two bands at 1390 and 1368 cm^{-1} (Fig. 6D). These are suggestive of a Fermi resonance interaction between the 1380 and 1382 cm^{-1} bands observed for the "isolated" methyl and methylene groups with increase in frequency separation and redistribution of intensity. In the spectrum of $\text{CH}_3\text{COOCD}_2\text{CH}_3$ (Fig. 6B) the intensity of the 1370 cm^{-1} band is increased, and it seems reasonable to presume that this results from the superposition of the 1373 cm^{-1} acetoxy methyl band on the ethoxy methyl band, with the latter displaced down by about 10 cm^{-1} from

its position at 1380 cm^{-1} in $\text{CD}_3\text{CO.O.CD}_2\text{CH}_3$ (Fig. 6F). There still remains the spectrum of $\text{CH}_3\text{CO.O.CH}_2\text{CD}_3$ to be explained. Here there are two bands of medium intensity at 1385 and 1363 cm^{-1} (Fig. 6C) and to account for these we must presume interaction between the 1382 cm^{-1} methylene band and the 1370 cm^{-1} acetoxy methyl band, in the course of which the separation increases and the higher frequency band (predominantly methylene) gains intensity at the expense of the lower frequency (predominantly methyl) band.

These spectra are considerably more complex than those of methyl acetate discussed previously (5). This is probably because the symmetrical C—H bending vibration of the $-\text{O.CH}_3$ group in methyl acetate is displaced up to 1435 cm^{-1} where it does not perturb the corresponding vibration of the acetoxy methyl group at 1369 cm^{-1} .

The more detailed assignment of these ethyl acetate bands to specific modes of vibration within the alkyl groups is difficult, and must be treated very circumspectly. From analogy with the *n*-paraffin hydrocarbons we would expect to find two C—H bending vibrations associated with each methyl group, and one (scissoring) C—H bending vibration of the methylene group. The situation is comparatively clear with respect to the acetoxy methyl group for which we can assign the asymmetrical C—H bending vibration to the 1430 cm^{-1} band and the symmetrical vibration to the 1373 cm^{-1} band. The methylene scissoring vibration probably provides the $-\text{CH}_2-$ component of the 1463 cm^{-1} band. The 1446 cm^{-1} band would likely be the asymmetrical C—H bending vibration in the ethoxy methyl group while the corresponding symmetrical vibration mixes with a methylene C—H vibration to give the 1393 , 1359 cm^{-1} doublet. This methylene vibration could be the wagging mode displaced up from its position near 1307 cm^{-1} in *n*-paraffin hydrocarbons by a vicinal effect of the oxygen atom. The remaining bands must perforce be assigned to combination bands.

Absorption Below 1300 cm^{-1}

The spectra in the range 1300 – 700 cm^{-1} are shown in Figs. 7A–7H for solutions in carbon disulphide. As with the methyl acetates, it is possible to recognize systematic changes in these spectra on selective deuteration. Most prominent is the strong skeletal band that occurs at 1238 cm^{-1} in the spectrum of the light compound. As in methyl acetate, this shifts upwards on deuteration, but the displacements do not in all cases correlate with the decrease in the C=O stretching frequency (Table III) the principal exceptions being $\text{CH}_3\text{CO.O.CD}_2\text{CH}_3$ and $\text{CD}_3\text{CO.O.CH}_2\text{CD}_3$.

The second strongest band, at 1046 cm^{-1} , in light ethyl acetate (Fig. 7A) obviously parallels the band at 1047 cm^{-1} in light methyl acetate, but is more sensitive to perturbation on deuteration. It is clearly present at 1034 cm^{-1} in the spectrum of $\text{CH}_3\text{CO.O.CH}_2\text{CD}_3$ (Fig. 7C), but is not obviously recognizable in the other deuterated analogues. It might be tentatively identified with the band at 1124 cm^{-1} in $\text{CH}_3\text{CO.O.CD}_2\text{CH}_3$ and $\text{CD}_3\text{CO.O.CD}_2\text{CH}_3$ (Figs. 7B, 7F), which is accompanied by weaker bands at 1164 and 1144 cm^{-1} , forming a triplet characteristic of the $-\text{O.CD}_2\text{CH}_3$ system.

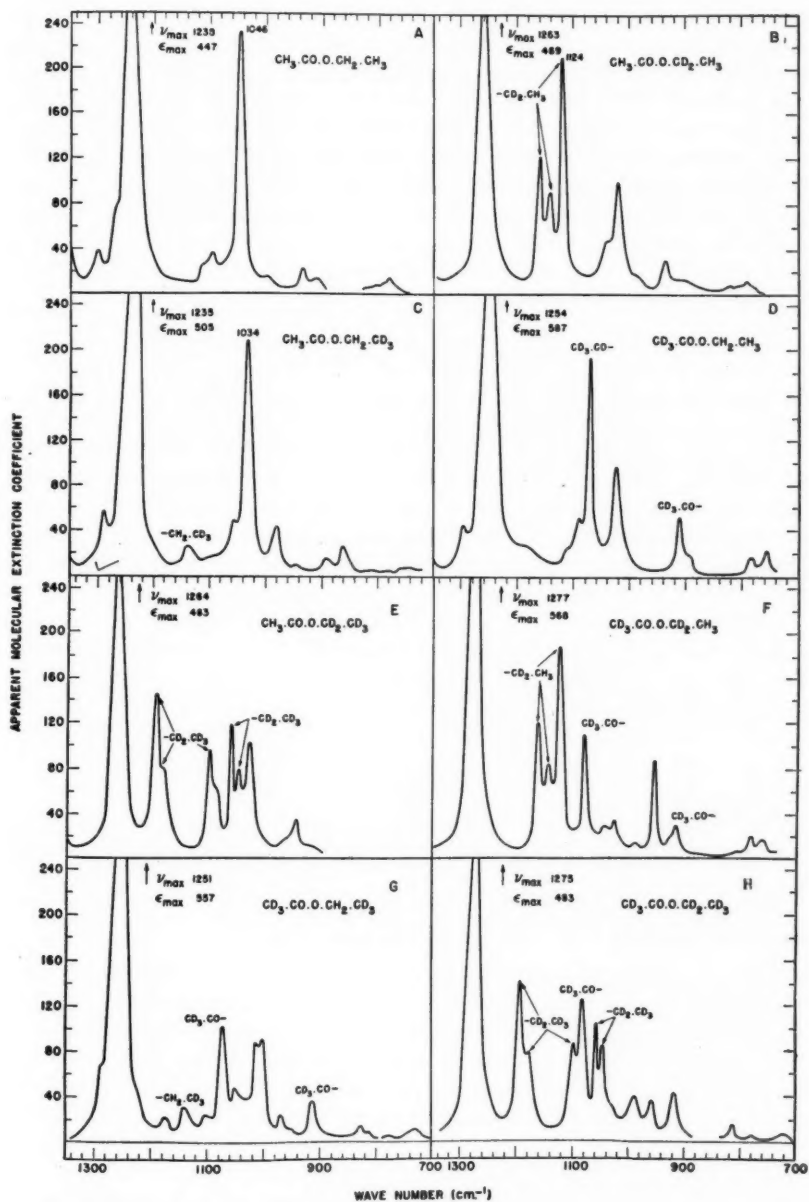


FIG. 7. Infrared spectra. "Fingerprint region". (Carbon disulphide solution.)

A comparison among the spectra reveals several other bands characteristic of the various deuterated and partly deuterated alkyl groups. These are summarized in Table I and indicated on the curves in Figs. 7B-7G. In most cases these bands are too intense to be attributed to pure C—D deformation vibrations displaced down from the 1500–1300 cm^{-1} region; the majority of them also occur between 1200 and 1000 cm^{-1} whereas the simple $\sqrt{2}$ displacement factor would place such bands in the 1050–900 cm^{-1} range. It is probable that they arise mainly from the interaction of C—D deformation modes with skeletal vibrations. This adds support to the generalization that in such deuteration studies it is relatively easy to observe the disappearance of bands associated with C—H vibrations, but only rarely can the corresponding C—D vibration be identified with certainty.

CONCLUDING REMARKS

In the course of a study of the intensities of some characteristic bands in ketones and esters, Francis (1) assigned a few of the bands in light ethyl acetate. These assignments, which were limited to the 2982, 2939, 1393, 1373, and 1359 cm^{-1} bands, agree with ours, although Francis from the spectrum of the light acetate alone was not in a position to recognize the perturbations associated with the 1393–1359 cm^{-1} absorption. To our knowledge the partly deuterated ethyl acetates have not been prepared previously and the spectra are recorded here for the first time.

ACKNOWLEDGMENTS

We are very grateful to Mr. Armand Nadeau for technical assistance with the measurement of the spectra.

REFERENCES

1. FRANCIS, S. A. *J. Phys. Chem.* 19: 942. 1951.
2. JONES, R. N. and SANDORFY, C. The application of infrared and Raman spectrometry to the elucidation of molecular structure. In *Technique of organic chemistry IX. Edited by A. Weissberger.* Interscience Publishers, Inc., New York, London. 1956. pp. 347–349.
3. NOLIN, B. *Can. J. Chem.* 31: 1257. 1953.
4. NOLIN, B. and JONES, R. N. *J. Am. Chem. Soc.* 75: 5626. 1953.
5. NOLIN, B. and JONES, R. N. *Can. J. Chem.* 34: 1382. 1956

THE SYSTEM $\text{LiNO}_3\text{-C}_2\text{H}_5\text{OH-H}_2\text{O}$ AT 25°C .¹

BY A. N. CAMPBELL AND E. M. KARTZMARK

ABSTRACT

Lithium nitrate does not form solid alcoholates at 25°C . The hydrate consisting of one molecule of nitrate to half a molecule of water, which is claimed to exist by Donnan and Burt, appears not to exist. Not only does this half hydrate not appear on the 25° isotherm but it cannot be detected dilatometrically at any temperature.

The work of Campbell and Debus on the conductances of lithium nitrate solutions in alcohol-water mixtures (1) has led us to suppose that at a concentration of alcohol lying between 30 and 70% by weight of alcohol, the solvation of the lithium ion changes from a water solvation to an alcohol solvation. Since lithium nitrate forms a hydrate, $\text{LiNO}_3 \cdot 3\text{H}_2\text{O}$, it seemed an obvious course to investigate whether this salt also forms one or more solid alcoholates, by investigating the equilibrium diagram of the system $\text{LiNO}_3\text{-C}_2\text{H}_5\text{OH-H}_2\text{O}$ at 25°C .

No solid alcoholate was found. It does not by any means follow that the lithium ion is not alcoholated. It is sufficient to say that, if a solid compound of lithium nitrate and alcohol does exist, its melting point is below 25°C ., and, if the chemical nature of the alcohol molecule is compared with that of the water molecule, this is inherently probable.

We were surprised to find that, though trihydrate and anhydrous lithium nitrate appeared as solid phases on our diagram, there was never any indication of the half hydrate, claimed by Donnan and Burt (2), as a solid phase. After many attempts to obtain this hydrate and use it as an inoculant, we finally concluded that it does not exist. Donnan and Burt base their claim for the existence of this hydrate on the doubtful procedure of crystallizing at 40° (above the transition temperature of the trihydrate), filtering, and analyzing the solid. Their solubility curve shows a slight break at their assumed transition temperature of 61°C . In addition they claim a change in dilatometer expansion about this temperature.

EXPERIMENTAL

Schreinemakers' "wet rest" method was used for the investigation of the solubility isotherm. Alcohol was determined by distillation, dilution of distillate to a fixed volume of 100 ml., and determination of the density. Reference to standard tables for the density of ethyl alcohol-water mixtures then gave the alcohol content. Lithium nitrate was determined by evaporation of the residue from the distillation to dryness, followed by melting of the solid to drive off the last traces of water.

In order to investigate the claim of Donnan and Burt that the change from the half hydrate to the anhydrous form, at 61°C ., can be detected dilato-

¹Manuscript received June 22, 1956.

Contribution from the Department of Chemistry, University of Manitoba, Winnipeg, Manitoba.

metrically, we made up a mixture of the stoichiometric composition of the half hydrate and placed some 50 gm. of this mixture in the bulb of a dilatometer, using *m*-xylene as indicator fluid; the temperature was then raised slowly and the height of the xylene column followed with a cathetometer. The change of the trihydrate (to half hydrate or anhydrous salt) is readily observed about 30°C., since it is accompanied by a large increase in volume. On further heating to 75°, however, no trace of discontinuity could be detected on the height vs. temperature curve. Our dilatometer was a very delicate one and it is impossible that any expansion or contraction, however slight, could have escaped us. It is possible that the half hydrate continued to exist metastably above its transition temperature but this is most unlikely.

RESULTS

Our solubility results are contained in Table I.

TABLE I
COMPOSITIONS OF SATURATED SOLUTIONS AND "WET RESTS" AT 25.0°C.

Solution, % by wt.		"Wet rest", % by wt.		Nature of solid phase
C ₂ H ₅ OH	LiNO ₃	C ₂ H ₅ OH	LiNO ₃	
—	47.8	—	55.4	LiNO ₃ ·3H ₂ O
0.9	47.3	Trace	55.3	"
5.0	47.0	0.7	56.4	"
11.6	47.8	1.4	56.5	"
13.5	49.2	2.8	55.2	"
14.1	51.9	6.8	54.0	"
11.2	53.5	2.5	55.7	"
6.9	58.0	2.7	66.9	LiNO ₃ ·3H ₂ O + LiNO ₃
6.6	58.4	1.8	90.2	LiNO ₃
10.3	55.7	Trace	97.7	"
16.9	53.2	4.0	90.4	"
35.8	44.5	9.0	85.6	"
60.0	32.8	12.2	86.2	"
72.9	26.3	10.7	89.2	"

NOTE: The results are expressed graphically in Fig. 1.

DISCUSSION

It is apparent from Fig. 1 that no alcoholate appears as solid phase at 25.0°.

The isotherm gives no indication of the hydrate, LiNO₃·½H₂O, claimed to exist by Donnan and Burt (2). The dilatometric experiments also show no indication of a phase change in the region claimed by Donnan and Burt for the change: LiNO₃·½H₂O = LiNO₃ + ½H₂O. It is also significant, in our opinion, that the composition of the peritectic point, on the equilibrium diagram of Donnan and Burt, is very far removed from the composition of the half hydrate.

The form of the solubility curve of the trihydrate on the 25° isotherm is what would be expected, bearing in mind that the trihydrate melts congruently at about 29°C. The form of this re-entrant curve means, as the figures of

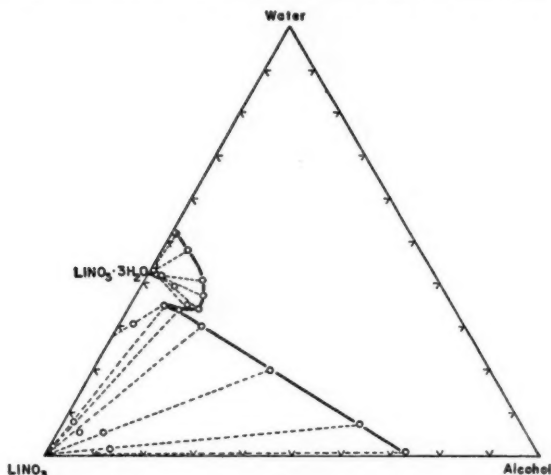


FIG. 1. The system $\text{LiNO}_3\text{-C}_2\text{H}_5\text{OH-H}_2\text{O}$; 25° isotherm.

Table I show, that the solubility of lithium nitrate in water is increased to a maximum by the addition of alcohol (from 47.8% in pure water to 58.0% for 6.9% alcohol).

The single isothermal invariant point occurring on the diagram, corresponding to the coexistence of lithium nitrate trihydrate and anhydrous lithium nitrate, has a concentration of 6.9% alcohol and 58.0% lithium nitrate.

REFERENCES

1. CAMPBELL, A. N. and DEBUS, G. Can. J. Chem. 34: 1232. 1956.
2. DONNAN, F. G. and BURT, B. C. J. Chem. Soc. 83: 335. 1903.

DIPHENYLCYANAMIDE DERIVATIVES

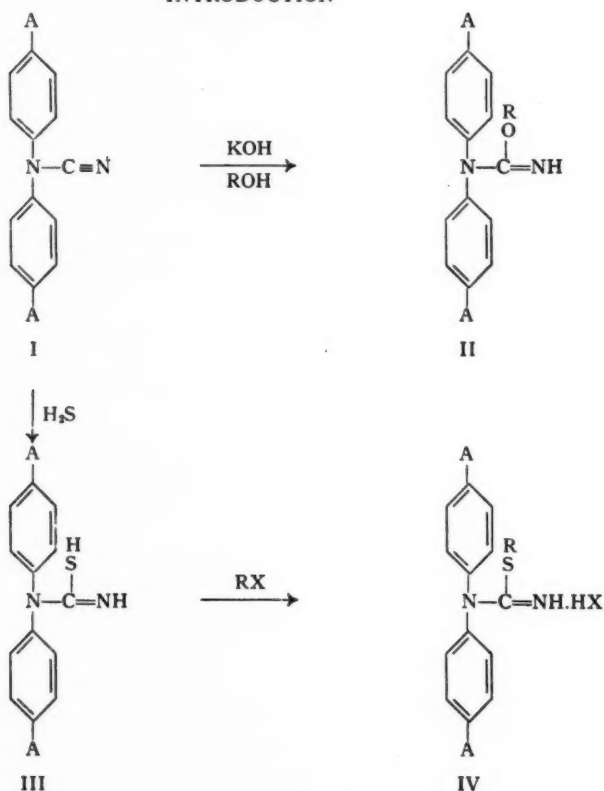
III. 2-THIOPSEUDOUREAS^{1,2}

BY RONALD E. BEALS³ AND WILLIAM H. BROWN⁴

ABSTRACT

Diphenylalkylthiopseudourea hydrohalides and dichlorodiphenylalkylthiopseudourea hydrohalides are formed when the corresponding thiourea is treated with an alkyl halide. The thiourea is prepared by the addition of hydrogen sulphide to the corresponding cyanamide compound. The hydrohalides are unstable in the presence of alkali.

INTRODUCTION



¹Manuscript received May 29, 1956.

Contribution from the Department of Chemistry, Ontario Agricultural College, Guelph, Ontario.
²The terms "isourea" and "isothiurea" are no longer used by Chemical Abstracts. The names "pseudoureas" and "2-thiopseudoureas" are used. The compounds are numbered according to the scheme: $\text{HN}=\text{C}(\text{OR})-\text{NH}_2$.

³Holder of a C.I.L. Fellowship 1954-55. Present address: Canadian Industries (1954) Limited, Toronto, Ontario.

⁴Associate Professor of Chemistry, Ontario Agricultural College, Guelph, Ontario.

When diphenylcyanamide (I: A = H) is hydrolyzed in the presence of hydroxylated solvents, of the type ROH, stable pseudoureas (II: A = H) are formed (10). Similarly, di-*p*-chlorophenylcyanamide (I: A = Cl) yields the chlorinated pseudourea (II: A = Cl). These latter compounds (II: A = Cl, R = Me or Et) have been shown to be physiologically active (2).

Since thioureas and thiopseudoureas have shown promise as organic fungicides (1, 3, 6), it was of interest to prepare the sulphur analogues of II.

DISCUSSION

Various methods for the preparation of 3,3-diphenyl-2-thiourea (III: A = H) have been previously employed (4, 9, 11). In particular, Kurzer (8) has prepared the compound by the addition of hydrogen sulphide to diphenylcyanamide in ethanol solution in the presence of ammonia.

In the present investigation it has been found that hydrogen sulphide adds to diphenylcyanamide (I: A = H) in the presence of dimethylamine and sodium ethoxide to form 3,3-diphenyl-2-thiourea (III: A = H). Also, 3,3-di-*p*-chlorophenyl-2-thiourea (III: A = Cl) is formed when di-*p*-chlorophenylcyanamide (I: A = Cl), prepared by the method of Robinson and Brown (10), is treated with hydrogen sulphide under the same conditions.

When 3,3-diphenyl-2-thiourea (III: A = H) is treated with ethyl iodide, the product is 3,3-diphenyl-2-ethyl-2-thiopseudourea hydroiodide (IV: A = H, R = Et, X = I). In the same manner 3,3-diphenyl-2-ethyl-2-thiopseudourea hydrobromide (IV: A = H, R = Et, X = Br) and 3,3-diphenyl-2-methyl-2-thiopseudourea hydroiodide (IV: A = H, R = Me, X = I) were produced from the corresponding alkyl halides. No product is obtained if the alkyl halide used is a chloride or a branched chain alkyl bromide.

Similarly, when 3,3-di-*p*-chlorophenyl-2-thiourea (III: A = Cl) is treated with an alkyl halide the product is the corresponding 2-alkyl-2-thiopseudourea hydrohalide (IV: A = Cl).

In all cases, alkaline decomposition of IV yields the corresponding alkane-thiol and the corresponding diphenylcyanamide.

Treatment of either the 3,3-diphenyl-2-alkyl-2-thiopseudourea hydrohalide (IV: A = H) or the 3,3-di-*p*-chlorophenyl-2-alkyl-2-thiopseudourea hydrohalide (IV: A = Cl) in ethanol with aqueous picric acid solution results in the formation of the corresponding stable picrate.

In Table I are listed the 2-thiopseudourea hydrohalides and picrates prepared as well as their properties.

For fungicidal evaluation tests refer to the work of Kempton (5).

EXPERIMENTAL

All melting points have been corrected against reliable standards. Molecular weights were determined by the Rast method. A typical preparative method is given for a 2-thiopseudourea hydrohalide. All the others listed in Table I may be obtained by a similar procedure.

TABLE I
2-THIOPSEUDOURA HYDROHALIDES AND PICRATES

Compound IV	M.P.	Yield, %	Stability (stable below)	Mol. formula	Analysis	
					Calculated	Found
A = H, R = Me, X = I	159.5-160.0°	67	5°	C ₁₀ H ₁₀ N ₂ S	I, 34.2; mol. wt., 369	I, 34.2; mol. wt., 368
A = H, R = Et, X = I	85.0-86.0°	99	5°	C ₁₂ H ₁₂ N ₂ S	I, 32.8; mol. wt., 384	I, 32.1; mol. wt., 394
A = H, R = Et, X = Br	169.5-170.0°	81	25°	C ₁₂ H ₁₀ BrN ₂ S	Br, 23.6; mol. wt., 337	Br, 22.7; mol. wt., 350
A = H, R = Me, X = Pic.	166.0-166.5°	72	25°	C ₁₂ H ₁₀ N ₂ O ₂ S	N, 14.9	N, 14.1
A = Cl, R = Me, X = I	200°	90	25°			
A = Cl, R = Et, X = I	133.0-134.5°	90	5°			

3,3-Diphenyl-2-thiourea (III: A = H)

A solution of 0.90 gm. (0.020 mole) of anhydrous dimethylamine (E.K. 601) and 0.46 gm. (0.020 mole) of sodium in 100 ml. of absolute ethanol was cooled to -8°C . and saturated with hydrogen sulphide gas at this temperature. The solution was treated with 5.0 gm. (0.026 mole) of diphenylcyanamide, prepared according to the procedure of Kurzer (7). Hydrogen sulphide was again passed into the mixture for 10 min. The mixture was placed in a Pyrex bottle as found in a Parr low-pressure hydrogenation apparatus and securely stoppered. The mixture was heated to $80-90^{\circ}\text{C}$. with occasional shaking. The pressure varied between 60–80 p.s.i.g. After four hours, the ethanol was removed by evaporation. The solid brown residue was crystallized from ethanol yielding 3.0 gm. (35%) of white needles, m.p. 218°C . The compound is insoluble in water, sodium hydroxide, and hydrochloric acid and soluble in acetone, ethanol, and chloroform. A mixture melting point with a sample of 3,3-diphenyl-2-thiourea, prepared by the method of Passing (9), showed no depression.

3,3-Di-p-chlorophenyl-2-thiourea (III: A = Cl)

A solution of 0.10 gm. (0.004 mole) of sodium and 0.50 gm. (0.011 mole) of anhydrous dimethylamine in 25 ml. of absolute ethanol in a "Coca-Cola" bottle was cooled to -5.0°C . and saturated with hydrogen sulphide gas. To this solution was added 1.0 gm. (0.0038 mole) of di-*p*-chlorophenylcyanamide prepared according to the procedure of Robinson and Brown (10). The bottle was then capped and placed in a water bath at $80-86^{\circ}\text{C}$. for four hours. After cooling there remained in the bottle a heavy yellow precipitate. The mixture was filtered and the residue washed with cold ethanol. Crystallization from ethanol gave 0.99 gm. (86%) of fine white needles, m.p. 195.5°C . Qualitative analysis gave positive tests for nitrogen, halogen, and sulphur. The compound is insoluble in water, sodium hydroxide, and hydrochloric acid. It is soluble in ethanol, ether, and chloroform. Anal. Calc. for $\text{C}_{13}\text{H}_{10}\text{Cl}_2\text{N}_2\text{S}$: Cl, 23.9; N, 9.44; mol. wt., 297. Found: Cl, 23.9; N, 9.46; mol. wt., 294.

3,3-Diphenyl-2-methyl-2-thiopseudourea Hydroiodide (IV: A = H, R = Me, X = I)

A solution of 0.50 gm. (0.002 mole) of 3,3-diphenyl-2-thiourea in 30 ml. of benzene was treated with 2.3 gm. (0.016 mole) of methyl iodide. The solution was refluxed for 23 hr. and when cooled, a precipitate formed which weighed 0.55 gm. (67%). The solid, after being washed with benzene, melted at $159.5-160.0^{\circ}\text{C}$. Qualitative analysis showed the presence of halogen, sulphur, and nitrogen. The compound is soluble in water, hydrochloric acid, and ethanol. It decomposes in ether and sodium hydroxide and is unstable unless stored at temperatures below 5°C . Anal. Calc. for $\text{C}_{14}\text{H}_{15}\text{IN}_2\text{S}$: I, 34.2; mol. wt., 369. Found: I, 34.2; mol. wt., 368.

Alkaline Decomposition of 3,3-Diphenyl-2-methyl-2-thiopseudourea Hydroiodide (IV: A = H, R = Me, X = I) to Yield Methanethiol and Diphenylcyanamide

A solution of 0.20 gm. of IV: A = H, R = Me, X = I in 10 ml. of ethanol was treated with 10 ml. of a 5% aqueous sodium hydroxide solution. A precipi-

tate formed immediately. It weighed 0.10 gm. and was shown to be diphenylcyanamide by mixture melting point. To the filtrate was added 1.0 gm. of 2,4-dinitrochlorobenzene in ethanol and the mixture was refluxed for five minutes. On cooling a fluffy yellow precipitate formed. The precipitate, after being crystallized twice from ethanol, melted at 128° C. A mixture melting point with authentic 2,4-dinitrophenyl-methyl-sulphide showed no depression.

ACKNOWLEDGMENTS

We are grateful to Canadian Industries (1954) Limited for financial assistance to one of us (R.E.B.). Generous samples of diphenylamine were provided by Naugatuck Chemicals.

REFERENCES

1. BANDELIN, F. J. and TUSCHHOFF, J. V. *J. Am. Chem. Soc.* 74: 4271. 1952.
2. BROWN, W. H., MINSHALL, W. H., ROBINSON, J. R., and WAYWELL, C. G. *Can. J. Agr. Sci.* 33: 622. 1953.
3. DEWAR, M. J. S. *J. Chem. Soc.* 534. 1944.
4. DIXON, A. E. and TAYLOR, J. *J. Chem. Soc.* 93: 690. 1908.
5. KEMPTON, A. G. M.S.A. Thesis, University of Toronto, Toronto, Ont. 1956. pp. 38, 40, 41.
6. KLOPPING, H. L. and VAN DER KERK, G. J. M. *Rec. trav. chim.* 70: 917. 1951.
7. KURZER, F. *J. Chem. Soc.* 3035. 1949.
8. KURZER, F. *J. Chem. Soc.* 3274. 1950.
9. PASSING, H. *J. prakt. Chem.* 153 (2): 1. 1939.
10. ROBINSON, J. R. and BROWN, W. H. *Can. J. Chem.* 29: 1069. 1951.
11. SUMIKI, Y., YAMAMOTO, K., and SATAKE, K. *J. Agr. Chem. Soc. Japan*, 25: 178. 1951-52. *Chem. Abstr.* 47: 10643. 1953.

PERIODATE-PERMANGANATE OXIDATIONS

V. OXIDATION OF LIPIDS IN MEDIA CONTAINING ORGANIC SOLVENTS¹

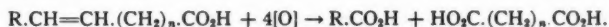
BY E. VON RUDLOFF

ABSTRACT

The periodate-permanganate reaction with methyl oleate and triolein has been studied in media containing a variety of organic solvents. The oxidation proceeded favorably in media containing tertiary butanol or pyridine and conditions have been found which permit the quantitative analysis of unsaturated lipids.

INTRODUCTION

The quantitative oxidation of unsaturated fatty acids to specific and easily identifiable end products was described previously (8). It was shown that the periodate-permanganate oxidation of such acids adheres strictly to the reaction scheme



Erucic acid, methyl esters, and triglycerides were not soluble in the weakly alkaline, dilute aqueous reaction mixture (5) and did not give satisfactory results. The solubility of these lipids was increased by using a modified reagent (7) containing pyridine, and quantitative results could be obtained in the oxidation of erucic acid and methyl linoleate. Methyl oleate and triolein, however, were incompletely oxidized under these conditions (8).

Conditions have now been found which permit the quantitative oxidation of these latter unreactive compounds. Thus when methyl oleate was shaken in media containing 20 to 50% pyridine and a small amount of potassium carbonate, oxidant equivalent to the theoretical value of four oxygen atoms was consumed in three to six hours' reaction time (Table I), and this value was not appreciably exceeded during three days' reaction time. Chromatographic analysis of the saponified oxidation products gave pelargonic and azelaic acids in 96 and 98% ($\pm 1\%$) of the theoretical yield respectively. The quantitative oxidation of triolein in media containing pyridine was not possible, mainly because of the very low rate of reaction (Table I). Increasing the rate of oxidation by employing higher temperatures, pH, or concentrations of permanganate (5) was not feasible because of overoxidation after correspondingly shorter reaction times. Virtually theoretical results, however, were obtained with triolein, as well as with methyl oleate, by using tertiary butanol - water as solvent (Table I), and 98 to 99% of the calculated amount of azelaic acid was isolated after four to eight hours' reaction time.

Oleodistearin reacted to completion in media containing 60% tertiary butanol (Table I), and sunflower-seed oil and linseed oil, i.e. triglycerides

¹Manuscript received in original form March 7, 1956, and as revised, June 22, 1956.

Contribution from the National Research Council of Canada, Prairie Regional Laboratory, Saskatoon, Saskatchewan. Issued as Paper No. 228 on the Uses of Plant Products and as N.R.C. No. 4056.

TABLE I

RATE OF REACTION OF LIPIDS (EXPRESSED AS AMOUNT OF OXIDANT CONSUMED IN PER CENT OF THE CALCULATED THEORETICAL AMOUNT) IN MEDIA CONTAINING PYRIDINE OR TERTIARY BUTANOL

	Reaction time, hr.						pH at start*
	$\frac{1}{2}$	1	3	6	24	48	
Methyl oleate in:							
10% pyridine soln.	—	4	10	18	58	—	7.5
20% " " "	—	38	80	96	100	102	8.0
30% " " "	—	68	90	100	101	100	8.2
40% " " "	—	83	99	100	100	100	8.3
50% " " "	—	80	96	100	99	102	8.3
20% <i>tert</i> -butanol soln.	5	10	26	—	—	—	7.2
30% " " "	85	100	100	—	103	—	7.6
40% " " "	90	100	100	—	107	—	8.1
60% " " "	40	68	93	—	107	—	8.4
Triolein in:							
40% pyridine soln.	—	—	4	8	25	—	8.5
40% <i>tert</i> -butanol soln.	—	12	22	27	48	63	8.1
50% " " "	10	21	73	98	98	104	8.2
60% " " "	16	37	86	100	102	106	8.4
70% " " "	12	27	65	83	98	104	8.4
Oleodistearin in:							
60% <i>tert</i> -butanol soln.	—	40	75	83	95	96	8.3

*At the end of the reaction the pH had dropped by 0.3 to 0.5 units.

containing polyunsaturated acids, reacted at about the same rate in media containing either tertiary butanol or pyridine. It, therefore, appears possible to oxidize quantitatively both reactive and unreactive unsaturated lipids, including fatty acids, their methyl esters and triglycerides, by using either an aqueous solution of the periodate-permanganate reagent, or solutions containing various amounts of tertiary butanol or pyridine. These methods may also provide an accurate and convenient means for determining the amount of saturated lipids in mixtures containing unsaturated ones.

Acetone (1) and pyridine (2, 3, 6, 9) have frequently been employed as solvents in permanganate oxidations, and glycol cleavage has been effected by periodate in a variety of solvents, including alcohols, esters, and acids (4). These and other solvents were examined for suitability with the combined periodate-permanganate reagent, and tertiary butanol and pyridine were found to be most satisfactory for the oxidation of lipids. Tertiary butanol gave results which were in many respects superior to those obtained with the latter solvent, but overoxidation occurred after shorter reaction times (Table I). The oxidation of methyl oleate proceeded less favorably in media containing dimethyl formamide, butyrolactone, or acetone and was very much slower when methyl acetate, ethyl acetate, 2-methoxy ethanol acetate, and dioxane were used. The oxidation was rapid in media containing alcohols, but methanol,

ethanol, isopropanol, and 2-methoxy ethanol were themselves oxidized at a comparatively high rate. Tetrahydrofuran and formamide were degraded extensively by the reagent.

Pyridine and tertiary butanol consumed oxidant at a low rate even after repeated purification, and this blank consumption decreased with a decrease in initial concentration of oxidant. Hence, a correction was necessary to account for the higher concentration of oxidant in blank determinations than was present in corresponding solutions containing the compound to be oxidized, once the latter had consumed oxidant. This correction was negligibly small in reaction times of less than six hours, but became increasingly more important after longer periods of reaction. Because an exact correction was not possible, the margin of error increased from about 1% to 3% and more. The amount of oxidant consumed in blank determinations increased slightly with increasing concentrations of tertiary butanol, but was practically constant with 10 to 50% pyridine.

To prevent a drop of the pH to below 6 by the formation of acidic end products, sufficient potassium carbonate was added to neutralize these acids (5, 8). When potassium carbonate was present in blank determinations with tertiary butanol the amount of oxidant consumed increased slightly. A very marked increase, however, was found when pyridine was used, e.g. using 10% pyridine and potassium carbonate (15 mgm. per aliquot of 10 ml.) the reaction mixture decolorized after six hours' reaction time with the consumption of more than 10% of oxidant. With increasing concentrations of pyridine this effect decreased noticeably and was no longer apparent when 40% pyridine was present. Also, although an initial increase in the concentration of potassium carbonate resulted in an increase in the rate of oxidation of pyridine, no further change was observed when more than 15 mgm. per aliquot (up to 30 mgm.) was added. The increase of the rate of oxidation cannot be explained solely as a pH effect (5), and appears to be due to catalysis, and may merit further study.

In the presence of potassium carbonate the oxidant precipitated partially when 50% or more tertiary butanol or pyridine was used and this precipitate did not react readily with arsenite solution in the cold. Heating on a steam bath for about one hour gave complete reduction, and thus reproducible results, when tertiary butanol was present, and this solvent could be employed advantageously in concentrations up to 70%. When more than 50% pyridine was used the results were not consistent. The degree of oxidation of methyl oleate and triolein in such media was, therefore, determined by the amount of azelaic acid obtained. The results showed that the rate of oxidation decreased when more than 50% pyridine was present and it was concluded that the most favorable range of pyridine concentration for the oxidation of lipids was from 30 to 50%.

The reaction mixtures described above are probably heterogeneous at the outset and the manner of addition of the compound to be oxidized is important, since rapid addition, or addition before enough solvent was present, frequently

resulted in the lipid separating in droplets. Also, in some experiments on a larger scale the rate of oxidation was lower.

Although the object of the present study was to find reaction conditions for the quantitative oxidation of unsaturated lipids, it is conceivable that the modifications of the periodate-permanganate reagent described herein may find application to other classes of compounds which are insoluble in the aqueous reagent. The fact that terpenes reacted equally well in media containing pyridine or dioxane (7) indicates that the choice of solvent need not necessarily be limited to tertiary butanol and pyridine.

EXPERIMENTAL

Analytical grade reagents were used and all solvents were fractionally distilled in a Podbielniak column. Pyridine and dioxane were purified by conventional methods. Further purification was achieved by reacting under nitrogen with 2 to 10 ml. concentrated periodate-permanganate reagent per liter of solvent. After the mixture was left at room temperature for at least six hours the excess oxidant was reduced and the solvent was distilled under nitrogen and over solid potassium hydroxide. Pyridine thus purified did not deteriorate noticeably within two weeks when stored in a brown, glass stoppered flask, and in blank determinations less oxidant was consumed than was previously reported (7).

The stock oxidant solution consisted of 20.86 gm. (97.5 mM.) sodium metaperiodate and 250 ml. 0.01 *M* (2.5 mM.) potassium permanganate per liter. The test compounds had the following iodine values:

Methyl oleate—found: 85.6; calculated: 85.61.

Triolein —found: 85.2; calculated: 85.90.

Oleodistearin —found: 26.7; calculated: 28.54; m.p. 35°–36° C.

Melting points were obtained on a hot-stage microscope and are corrected.

Standard Procedure of Oxidation

Stock oxidant solution, 2.0 ml., was placed in a 125 ml. stoppered flask and to this was added 1.0 ml. aqueous solution containing 2.5 mgm. potassium carbonate, water, and solvent to give 9.0 ml. of a solution which contained 1.0 ml. less solvent than was desired in the final reaction mixture. To this was added slowly with shaking 1.0 ml. of a solution of methyl oleate, 1.25 mM. per 100 ml. solution in the corresponding solvent, and the time of addition was noted. When triolein was oxidized 1.0 ml. of a solution containing 0.4167 mM. per 100 ml. solution was employed, and with sunflower-seed oil and linseed oil correspondingly smaller amounts were used to keep the concentration of oxidant about twice that required theoretically. The flask was stoppered and put onto a shaker for the required reaction time. A corresponding blank experiment was started at the same time. The temperature of reaction was 24° C. ($\pm 2^\circ$).

After the desired time of reaction, the oxidation was stopped by addition, with shaking, of sodium bicarbonate, 0.5 to 1 gm., followed immediately by

5.0 ml. 0.1 *N* sodium arsenite solution. A few crystals of potassium iodide were added after all permanganate color had disappeared, and the aliquots were allowed to stand at least 15 min. When 40% or less solvent was present, the aliquots were diluted with 30 to 40 ml. water, and were then titrated slowly to the starch end point with 0.015 *N* iodine solution. Duplicate determinations agreed within 0.10 ml. iodine solution when pyridine was used, and 0.20 ml. when tertiary butanol was present. The solutions containing tertiary butanol were easily overtitrated, and it was found advantageous to evaporate most of the solvent before titration. At higher concentrations of solvent the flasks containing the reduced reaction mixtures were placed on a steam bath for one-half to one hour, cooled to room temperature, and diluted and titrated as before. Duplicate determinations agreed within 0.20 to 0.30 ml. iodine solution, but when more than 50% pyridine was used, the error became larger.

Oxidation and Isolation of End Products

The same oxidation procedure as above was used, taking 10 to 20 times the amount of reactants and solvents. The reaction was stopped one to two hours after the required minimum for complete reaction by the addition of enough sodium metabisulphite to reduce all iodine to iodide. Potassium hydroxide, 1 to 2 gm., was added and the flask was put on a rotary evaporator, the temperature being kept at about 50° C. During the course of the one and one-half to two hours the organic solvent was completely evaporated whilst any ester was saponified simultaneously. The solution was acidified strongly with 10% sulphuric acid and then extracted continuously with ethyl ether for 8 to 10 hr. The ether extract was thoroughly dried over anhydrous sodium sulphate and then evaporated to dryness at 35°–40° C. The residue was weighed and then triturated with Skellysolve "F". The solution of monocarboxylic acids was reduced to about 0.5 ml. and then analyzed chromatographically by the same procedure as reported previously (8). The residual dicarboxylic acid fraction was weighed and, after the melting point and mixed melting point had been taken, analyzed chromatographically.

A typical example gave the following results: methyl oleate 74.1 mgm. (0.25 mM.) was oxidized with shaking during the course of six hours in 100 ml. solution containing 30% tertiary butanol, 25 mgm. potassium carbonate, and 20 ml. oxidant. Crude yield of saponified end products was 85.6 mgm., yielding 38.5 mgm. (97.5% of theory) monocarboxylic acid fraction and 46.7 mgm. (99% of theory) dicarboxylic acid, m.p. 104.5–106.8° C., mixed m.p. 106.2–107.3° C. with an authentic sample of azelaic acid (m.p. 106.2–107.5° C.). Chromatographic analysis gave only the bands corresponding to pelargonic and azelaic acids and their recovery was 98% ($\pm 1\%$).

ACKNOWLEDGMENTS

The author wishes to thank Dr. A. S. Perlin for helpful advice, and Dr. B. M. Craig and Mr. C. G. Youngs, who kindly supplied methyl oleate, triolein, and oleodistearin.

REFERENCES

1. ARMSTRONG, E. F. and HILDITCH, T. P. *J. Soc. Chem. Ind.* 44: 43T. 1925.
2. BRAND, K. and MATSUI, M. *Ber.* 46: 2942. 1913.
3. FUJIKAWA, F. and KOBAYASHI, T. *J. Pharm. Soc. Japan*, 64(8A):7. 1944. See also *Chem. Abstr.* 45: 8472a. 1951.
4. JACKSON, E. L. *Organic reactions*. Vol. II. John Wiley & Sons, Inc., New York. 1946. pp. 359-360.
5. LEMIEUX, R. U. and RUDLOFF, E. VON. *Can. J. Chem.* 33: 1701. 1955.
6. PUMMERER, R. and DORFMÜLLER, G. *Ber.* 46: 2386. 1913.
7. RUDLOFF, E. VON. *Can. J. Chem.* 33: 1714. 1955.
8. RUDLOFF, E. VON. *J. Am. Oil Chemists' Soc.* 33: 126. 1956.
9. SMITH, J. H. C. and SPOEHR, H. A. *J. Biol. Chem.* 86: 87. 1930.

KINETICS OF THE OXIDATION OF URANIUM(IV) BY MOLECULAR OXYGEN IN AQUEOUS PERCHLORIC ACID SOLUTION¹

BY J. HALPERN² AND J. G. SMITH

ABSTRACT

The kinetics of the oxidation of uranium(IV) by molecular oxygen in aqueous perchloric acid solution were studied. Over a considerable range of conditions, the results are fitted approximately by the rate law:

$$-d[U^{IV}]/dt = k[U^{IV}][O_2]/[H^+], \text{ where } k \approx 2 \times 10^{14} \exp[-22,000/RT] \text{ sec}^{-1}.$$

The reaction is catalyzed by Cu^{++} and inhibited by small amounts of Ag^+ and Cl^- . The results are interpreted in terms of a chain reaction mechanism involving UO_2^+ and HO_2 as chain carriers.

INTRODUCTION

In recent years considerable progress has been made toward the understanding of the kinetics and mechanisms of inorganic oxidation-reduction reactions in aqueous solution (25, 10). Among the systems which have been subjected to study are those involving elementary electron transfer reactions between metal ions (25, 1), as well as reactions between metal ions and molecular oxidizing and reducing agents such as H_2O_2 (3, 24), O_2 (7), H_2 (18, 23, 12), $HCOOH$ (2, 21, 8). The present paper reports the results of a further study of a reaction of the latter type, involving the oxidation of uranium(IV) by molecular oxygen. This reaction has been examined previously in sulphate (16) and chloride (17) solutions but the kinetics, which appeared to be fairly complex, were not fully elucidated and no conclusions were drawn concerning the reaction mechanism. The present investigation was made using perchlorate solutions, to minimize complications due to complexing between cations and anions. The question of possible intermediates in the reaction appeared to be of particular interest in view of the fact that the over-all oxidation of U^{IV} involves a net loss of two electrons while the over-all reduction of O_2 requires four electrons. A kinetic study of related interest, of the reaction between uranium(IV) and iron(III) in aqueous perchloric acid solution, has also been reported recently (4).

EXPERIMENTAL

Both Analar and Baker and Adamson perchloric acid (chloride free) were used and gave identical results. Ceric sulphate and the various perchlorate salts were obtained from G. Frederick Smith Chemical Co. All other chemicals were Baker and Adamson reagent grade. Oxygen was supplied by Canadian Liquid Air Co. Distilled water was used in the preparation of all solutions.

Solutions of uranium(IV) were prepared as follows: Hydrogen peroxide was added to a solution of uranyl nitrate (0.02 M) in aqueous perchloric acid

¹Manuscript received June 12, 1958.

Contribution from the Department of Mining and Metallurgy, University of British Columbia, Vancouver, B.C., with financial assistance from the National Research Council of Canada.

²Present address: Department of Chemistry, University of British Columbia, Vancouver, B.C.

(0.03 *M*) to precipitate uranium peroxide (this precipitation was repeated twice to ensure removal of foreign anions). The final precipitate was decomposed by boiling with dilute perchloric acid and the resulting solution of uranyl perchlorate was reduced electrolytically using a gold cathode and a platinum anode. Providing the solution was kept cold, the reduction of uranium(VI) to uranium(IV) went readily to completion.

The solutions were analyzed for uranium(IV) by titration with ceric sulphate using ferroin as indicator. To determine the total uranium content, the uranium(VI) was first reduced by passing the solution through a Jones reductor.

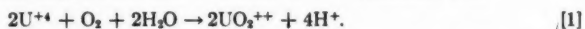
The glass reaction apparatus was completely immersed in a water bath whose temperature was controlled to $\pm 0.03^\circ \text{C}$. (most of the experiments were made at 30°C .). The oxygen gas, after saturation with water vapor, was dispersed into the reacting solution (200 ml.) through a sintered glass plate. Samples were withdrawn periodically and the concentration of unreacted uranium(IV) was measured, to determine the extent of reaction.

The oxygen partial pressure was taken as the difference between the atmospheric pressure and the vapor pressure of the solution at the reaction temperature. From the observation that the reaction rate was unaffected by variation of the oxygen flow rate in the apparatus, from 0.5 to 3 liters/min. (a flow rate of 2 liters/min. was normally used), it was concluded that the solutions were always saturated with the gas. The solution concentration of oxygen was estimated from available solubility data (19).

RESULTS AND DISCUSSION

Stoichiometry of the Reaction

With the experimental procedure that was employed, which involved passing a large excess of oxygen through the solution, there was no way of measuring the amount of oxygen which was consumed. Hence, the stoichiometry of the reaction could not be established directly. However the known chemistry of the system suggested that the only likely reaction was



The following observations support this stoichiometry: (1) the solutions were completely stable, and no oxidation of U^{IV} could be detected, in the absence of oxygen, (2) the titration demonstrated that oxygen converts U^{IV} quantitatively to U^{VI} , (3) spectrophotometric measurements indicated that U^{IV} and U^{VI} were the only uranium species present in the solution at any time during the reaction, (4) sensitive tests could not detect any H_2O_2 in the solution at any time during the reaction, and (5) when H_2O_2 was added to a solution of U^{IV} , it reacted instantaneously according to:



These observations make it appear very unlikely that any stable products other than U^{VI} and H_2O are formed in the reaction. Hence, they support the stoichiometry represented by equation [1] which was assumed in all the subsequent kinetic work.

Kinetics of the Reaction

Some typical rate plots, depicting the oxidation of U^{IV} in solutions containing different concentrations of $HClO_4$, are reproduced in Fig. 1. The O_2 partial pressure, and hence its concentration in solution, remained constant throughout each experiment. The change in rate during the reaction should thus reflect, principally, the changing concentration of U^{IV} in the solution.

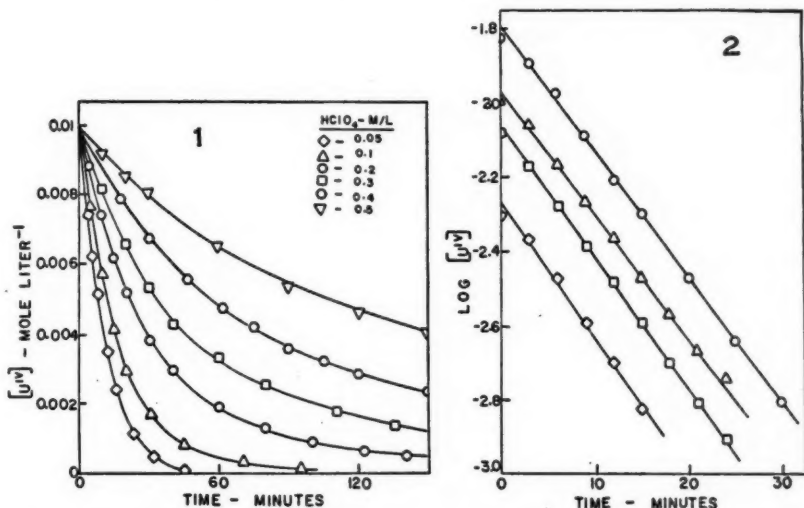


FIG. 1. Typical rate plots for the oxidation of uranium(IV) at 30° C., 0.96 atm. O_2 .
FIG. 2. First-order rate plots for the reaction in solutions containing 0.08 M $HClO_4$ at 30° C., 0.96 atm. O_2 .

At the outset it was established that the rate was unaffected by packing the reaction vessel with glass wool and by the addition of UO_2^{++} in amounts comparable to those in which it is formed during the reaction.

At relatively low $HClO_4$ concentrations (<0.2 M) the kinetic dependence on U^{IV} was consistently first order as shown by the plots in Fig. 2 which are fitted by the rate law:

$$-d[U^{IV}]/dt = k'[U^{IV}], \quad [3]$$

where the apparent first-order constant, k' , is independent of the initial U^{IV} concentration and of its changing concentration during the reaction.

At higher $HClO_4$ concentration, some departure from this rate law (i.e. from the linearity of the first-order rate plots) was observed, but usually not until the reaction had proceeded about halfway to completion. That this is due to some complication which develops during the course of the reaction and does not reflect an inherent departure from first-order kinetic dependence on U^{IV} is demonstrated by the fact that even at the highest $HClO_4$ concentration used (0.5 M), the initial slopes of the first-order rate plots (and hence the apparent

value of k') were unaffected by varying the initial U^{IV} concentration between 0.05 and 0.15 M (see Fig. 3). Equation [3] therefore represents accurately the dependence of the initial rate on the initial U^{IV} concentration even at high $HClO_4$ concentrations. In view of this, it was decided to use the value of k' so derived (i.e. from initial slope of the first-order rate plot) as the measure of the rate in all the experiments. This seemed at least as satisfactory as adopting some more arbitrary measure of the rate, such as the time required for the completion of 50% reaction. The reproducibility of the rate measurements was about $\pm 5\%$ at low $HClO_4$ concentrations and $\pm 8\%$ at high $HClO_4$ concentrations.

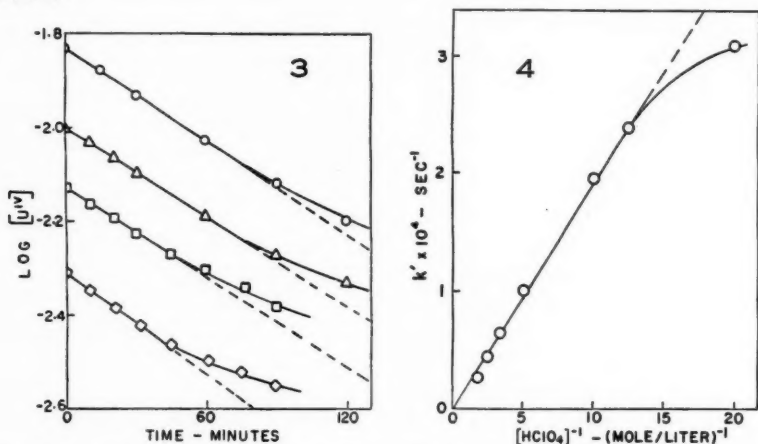


FIG. 3. Typical rate plots for the reaction in solutions containing 0.5 M $HClO_4$ at $30^\circ C.$, 0.96 atm. O_2 .

FIG. 4. Dependence of the rate on the concentration of $HClO_4$ at $30^\circ C.$, 0.96 atm. O_2 .

The reason for the apparent departure from first-order kinetics at high $HClO_4$ concentrations has not been established. It may reflect a slow secondary reaction such as hydrolysis, or the influence on the rate either of an impurity originally present in the solution or of some by-product of the reaction, which accumulates in trace concentrations as the reaction proceeds. This anomaly disappeared at higher temperatures.

The results plotted in Fig. 4 show that k' is inversely proportional to the $HClO_4$ concentration between 0.08 and 0.5 M . The simplest interpretation of this is that the U^{IV} species which takes part in the reaction is hydrolyzed. The thermodynamics of the hydrolysis reaction:



have been determined (13) and the results indicate that at 0.5 M $HClO_4$ about 10% of the U^{IV} is present as the hydrolyzed ion, UOH^{+3} . At $HClO_4$ concentrations below 0.08 M , the inverse proportionality between k' and $[HClO_4]$ no longer applies (see Fig. 4), presumably because a relatively large proportion of the U^{IV} is hydrolyzed in this region.

To determine the kinetic dependence on the oxygen concentration, parallel experiments were made in which air and oxygen, respectively, were passed through the solution. As shown in Fig. 5, the value of k' , at both low and high HClO_4 concentrations, was directly proportional to the O_2 partial pressure and, hence, to the O_2 concentration in solution. Thus over a fairly wide range of conditions, the kinetics of the reaction conform approximately to the rate law:

$$-d[\text{U}^{\text{IV}}]/dt = k[\text{U}^{\text{IV}}][\text{O}_2]/[\text{H}^+]. \quad [5]$$

Experiments at 0.08 M and 0.5 M HClO_4 were made at several temperatures ranging from 20° to 60° C. The Arrhenius plots, based on values of k calculated from the slopes of first-order rate plots by means of equation [5], are shown in

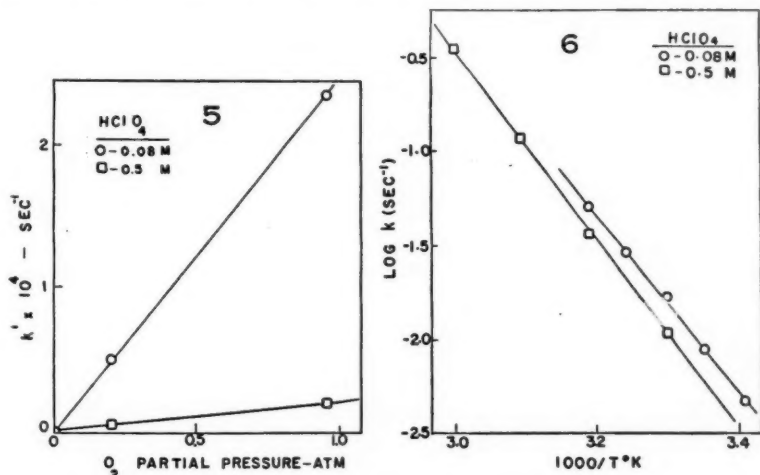


FIG. 5. Dependence of the rate on the oxygen partial pressure at 30° C.

FIG. 6. Arrhenius plots showing the dependence of the rate on temperature.

Fig. 6. The plots for the low and high acid series are seen to be displaced slightly and are fitted, respectively, by the equations:

$$k(0.08 \text{ } M \text{ } \text{HClO}_4) = 2 \times 10^{14} \exp[-21,500/RT] \text{ sec}^{-1}. \quad [6]$$

and
$$k(0.5 \text{ } M \text{ } \text{HClO}_4) = 1.6 \times 10^{14} \exp[-22,400/RT] \text{ sec}^{-1}. \quad [7]$$

The agreement between the corresponding parameters in the two equations is probably within the experimental error of the determinations. It should be noted that the apparent frequency factor in these equations is several orders of magnitude higher than would be expected for a simple bimolecular reaction, i.e. between an O_2 molecule and a hydrolyzed U^{IV} species.

Effects of Added Salts

The addition of 0.4 M Mg^{++} , 0.005 M Co^{++} , or 0.05 M Mn^{++} (all as their perchlorate salts) to solutions containing 0.5 M HClO_4 was found to be without

appreciable effect on the rate. A number of other ions, including Cl^- , Ag^+ , and Fe^{2+} , were found to inhibit the reaction, while Hg^{2+} and Cu^{2+} exerted a catalytic influence. These various effects are illustrated in Fig. 7. Those due to Cu^{2+} , Ag^+ , and Cl^- were particularly marked and were subjected to more detailed study.

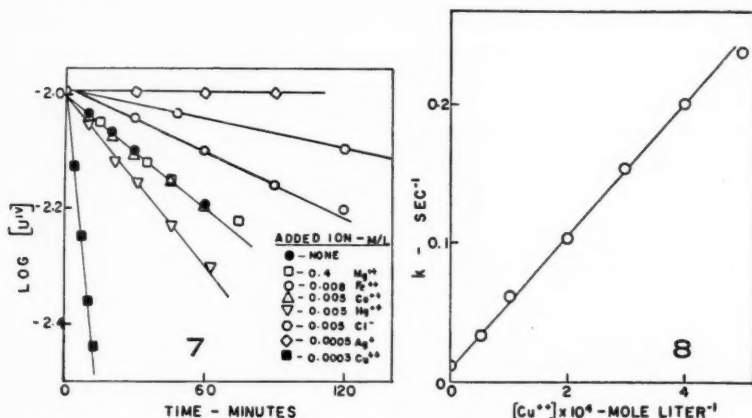


FIG. 7. Effect of various ions on the rate at 30°C , 0.96 atm. O_2 , 0.5 M HClO_4 .

FIG. 8. Dependence of the rate at 30°C . on the Cu^{2+} concentration in solutions containing 0.5 M HClO_4 .

In the presence of Cu^{2+} , the rate remained first order in U^{IV} , but the apparent value of k , calculated from the slopes of the first-order rate plots, increased linearly with the Cu^{2+} concentration as shown in Fig. 8. The plot in this figure is fitted by the equation:

$$k(\text{sec}^{-1}) = 0.011 + 480[\text{Cu}^{2+}]. \quad [8]$$

The sensitivity of the reaction to Cu^{2+} is very marked; thus the rate is tripled by the addition of only $5 \times 10^{-5} \text{ M./liter}$ of Cu^{2+} . The catalytic effect of Cu^{2+} on the auto-oxidation of U^{IV} has been reported previously (5, 17).

The inhibiting effect of Cl^- on the reaction is depicted in Fig. 9. Addition of only 0.001 M./liter of Cl^- (as the sodium salt) reduces the rate to about one-half its original value. It should be noted that this corresponds to only about 10% of the amount of U^{IV} originally present in the solution. Hence, the Cl^- cannot be inhibiting the reaction by tying up the U^{IV} in some inactive form (e.g. by complexing with it). Further addition of Cl^- had only a limited effect, and above 0.01 M Cl^- the rate levels off at a substantially constant value (corresponding to $k \approx 0.002 \text{ sec}^{-1}$) which is about one-fifth that of the uninhibited rate.

The inhibiting effect of Ag^+ on the reaction is of quite a different form. As shown in Fig. 10, the presence of very small amounts of Ag^+ ($\approx 10^{-4} \text{ M./liter}$) was found to stop the reaction almost completely for a finite period of time, the duration of which was approximately proportional to the initial Ag^+

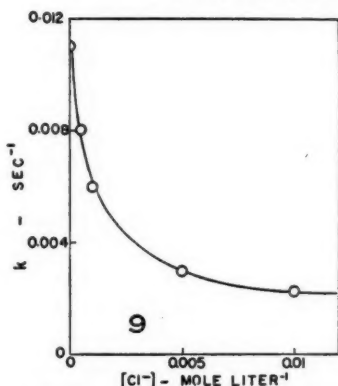


FIG. 9. Dependence of the rate at 30° C. on the Cl^- concentration in solutions containing 0.5 M HClO_4 .

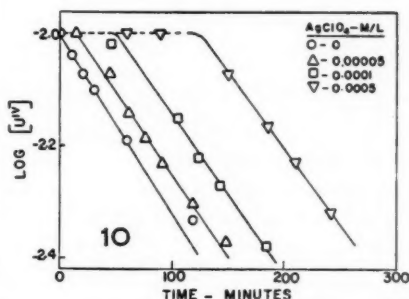


FIG. 10. Effect of Ag^+ on the reaction at 30° C. in solutions containing 0.5 M HClO_4 .

concentration. During this interval, a gray colloidal suspension, presumably of metallic silver, was observed to form in the solution. Following the induction period, the oxidation of U^{IV} proceeded at the normal (i.e. uninhibited) rate.

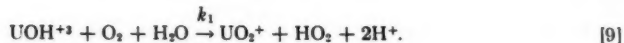
CONCLUSIONS

A number of features of the kinetics, including the anomalously high frequency factor and the marked sensitivity of the rate to catalytic and inhibitory influences by various ions, strongly suggest that the reaction proceeds by a chain mechanism. The most likely intermediates would appear to be uranium(V) (generally believed to exist in solution as the UO_2^+ ion (9, 14)) and HO_2 . A mechanism for the uncatalyzed-uninhibited reaction, involving these species as chain carriers, is proposed below:*

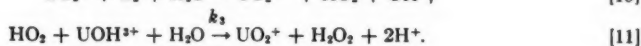
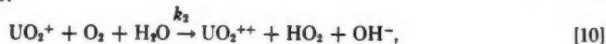
Rapid pre-equilibrium:



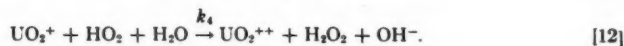
Initiation step:



Chain propagation steps:



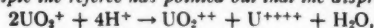
Termination step:



Fast reaction:



*The reactions included in the proposed mechanism were selected because they appear reasonable on chemical and energetic grounds and because they form a sequence which is compatible with the observed kinetics. However the available evidence does not rule out the possibility that other reactions also participate. For example the referee has pointed out that the disproportionation of UO_2^+ , i.e.



may compete with the suggested termination step, represented by equation [12], particularly at high acidities. This seems plausible in the light of available kinetic (9) and thermodynamic (15) data about this reaction.

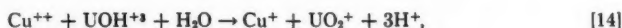
K is the equilibrium constant for the initial step, while k_1 , k_2 , k_3 , and k_4 are the respective rate constants for the initiation, propagation, and termination steps.

Using the steady-state method, the following rate law has been derived for this mechanism:

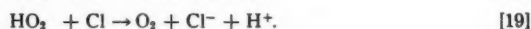
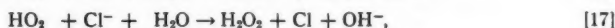
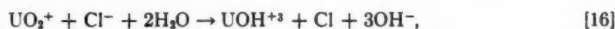
$$-d[U^{IV}]/dt = 2k_1K\{1 + (k_2k_3/k_1k_4)^{1/2}\}[U^{4+}][O_2]/[H^+]. \quad [13]$$

This has the same form as equation [5] and is thus qualitatively consistent with the experimental results.

The marked catalytic influence of Cu^{++} may be explained through the following reactions* which generate UO_2^+ and HO_2 and thus cause chain initiation:

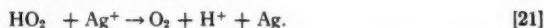


The inhibiting effect of Cl^- can be accounted for by reactions between Cl^- and the chain-carrying species, UO_2^+ and HO_2 , which result in disruption of the chain, i.e.



The last two reactions also result in the regeneration of Cl^- and, hence, in the indefinite persistence of the inhibition.

A similar explanation can be advanced for the inhibition due to Ag^+ , which can disrupt the chain through the following reactions:



However in contrast to Cl^- , the Ag^+ is apparently removed irreversibly from the solution (i.e. as metallic silver) as a result of these reactions. Hence its inhibiting effect persists only for a limited time, following which the reaction proceeds normally.

The influence of other catalysts and inhibitors (e.g. Hg^{++} and Fe^{++}), all of which are readily oxidizable or reducible ions, can be accounted for through similar reactions.

A number of other examples have been recorded of inorganic oxidation-reduction reactions which proceed through chain mechanisms, analogous to that which has been proposed for the present system, and whose rates are susceptible to similar catalytic and inhibitory influences (3, 24, 22, 11, 20, 6). Some of these reactions involve O_2 as the oxidant. However, this appears to be the first time that a chain reaction in aqueous solution, involving a uranium species as the chain carrier, has been reported.

*Reaction [15] seems plausible on energetic grounds (15), although the reverse of this reaction has also been postulated to occur (e.g. Reference 4) under certain conditions.

ACKNOWLEDGMENT

We are grateful to Dr. R. H. Betts for helpful discussion about this reaction and for making available to us his unpublished data on it.

REFERENCES

1. AMPHLETT, C. B. *Quart. Revs. (London)*, **8**: 219. 1954.
2. BAWN, C. E. H. and WHITE, A. G. *J. Chem. Soc.* 339. 1951.
3. BAXENDALE, J. H. *In Advances in catalysis*. Vol. 4. Academic Press, Inc., New York. 1952. p. 31.
4. BETTS, R. H. *Can. J. Chem.* **33**: 1780. 1955.
5. BLOCHE, E., GUÉRON, J., HERING, H., and PROVVISOR, H. *Bull. soc. chim. France*, 1150. 1948.
6. FULLER, E. C. and CRIST, R. H. *J. Am. Chem. Soc.* **63**: 1644. 1941.
7. GEORGE, P. *J. Chem. Soc.* 4349. 1954.
8. HALVORSON, H. N. and HALPERN, J. *J. Am. Chem. Soc.* In press.
9. HEAL, H. G. *Nature*, **157**: 225. 1946. *Trans. Faraday Soc.* **45**: 1. 1949.
10. HEAL, H. G. and THOMAS, J. G. N. *Trans. Faraday Soc.* **45**: 11. 1949.
11. KINETICS AND MECHANISM OF INORGANIC REACTIONS IN SOLUTION. The Chemical Society, London. 1954.
12. KING, E. L. *In Catalysis*. Vol. 2. Edited by P. H. Emmett. Reinhold Publishing Corporation, New York. 1955. pp. 425-49.
13. KORINEK, J. G. and HALPERN, J. *J. Phys. Chem.* **60**: 285. 1956.
14. KRAUS, K. A. and NELSON, F. *J. Am. Chem. Soc.* **72**: 3901. 1950; **77**: 3721. 1955.
15. KRAUS, K. A., NELSON, F., and JOHNSON, J. G. *J. Am. Chem. Soc.* **71**: 2510. 1949.
16. LATIMER, W. M. *The oxidation states of the elements and their potentials in aqueous solution*. Prentice-Hall, Inc., New York. 1952.
17. MCCOY, H. N. and BUNZEL, H. H. *J. Am. Chem. Soc.* **31**: 367. 1909.
18. NICHOLS, A. R., Jr. U.S. Atomic Energy Commission Publication MDDC-436. 1946.
19. PETERS, E. and HALPERN, J. *J. Phys. Chem.* **59**: 793. 1955; *Can. J. Chem.* **33**: 356. 1955; **34**: 554. 1956.
20. SEIDELL, A. *Solubilities of inorganic and metal organic compounds*. 3rd ed. Vol. 1. D. van Nostrand Company, Inc., New York. 1940.
21. TAUBE, H. *J. Am. Chem. Soc.* **68**: 611. 1946.
22. TOPHAM, A. R. and WHITE, A. G. *J. Chem. Soc.* 105. 1956.
23. URI, N. *Chem. Revs.* **50**: 375. 1952.
24. WEBSTER, A. H. and HALPERN, J. *J. Phys. Chem.* **60**: 280. 1956.
25. WEISS, J. H. *In Advances in catalysis*. Vol. 4. Academic Press, Inc., New York. 1952. p. 343.
26. ZWOLINSKI, B. J., MARCUS, R. J., and EYRING, H. *Chem. Revs.* **55**: 157. 1955.

THE SYSTEMS ALUMINUM-TIN AND ALUMINUM-LEAD-TIN¹

By A. N. CAMPBELL AND R. KARTZMARK²

ABSTRACT

The solubility of tin in aluminum, between 400° and 645° C., has been determined by an isothermal method. The system Al-Pb-Sn has been investigated, isothermally, at 500° and 600° C. The eutectic temperature and composition of this system have also been determined. The structure of the phases in completely solid alloys has been identified by photomicrography. The liquidus curves at 500° and 600° C. are continuous, extending across the ternary diagram from the Al-Pb system to the Al-Sn system. On neither of the two isotherms does a two-liquid region occur, despite the fact that a well-defined two-liquid region exists at temperatures above 650° C. This was found to be due to inaccuracy in the published diagram for the Al-Sn system and this led to the work mentioned above. The solubility of tin in aluminum is much less than it has been supposed and this causes the surface of solid aluminum to intrude into the solid diagram at an early stage, thus blocking out the two-liquid region. The ternary eutectic temperature is 183.0° C. and the composition, 0.08 weight per cent Al, 38.1% Pb, and 61.7% Sn. In any alloy at room temperature, the solid phases are: primary aluminum, α -lead, and β -tin. Brinell Ball and Vickers Diamond Pyramid hardness tests show that the ternary eutectic alloy is the hardest of the system. When alloys approximating to the eutectic composition are used as solders, it has been found that the alloy of ternary eutectic composition has a greater shear strength than ordinary solder.

Despite the simplicity of the three-component system, Al-Pb-Sn, it has not been studied previously in its entirety; work has been confined to the completely liquid two-layer condition. Wright (10), working between 750 and 850° C., found the critical solution to contain 64 weight per cent tin and 17% lead. Lorenz and Erbe (4) carried out a few experiments at 750° C., using a quenching technique, but their results are too crude to merit mention. Very excellent work was done by Davies (2) in 1953. He studied the region of partial miscibility at 650°, 730°, and 800° C., using the purest materials and keeping the temperature truly constant. Davies' data are shown graphically in Fig. 1. It is surprising that the numerical values were never published. We consider these data so valuable that we offer them here, with the consent of the author.

Of the component binary systems, little need be said of the systems Al-Pb and Pb-Sn, save that they are simple and have been investigated completely. The system Al-Pb gives at all temperatures above 658.5° C. two liquid layers; in the solid state there is no compound formation or appreciable solid solution (11).

The Pb-Sn system, to which the soft solders belong, exhibits a simple eutectic accompanied by considerable solid solubility of tin in lead, at the eutectic temperature of 183.3° C., but this decreases to zero at room temperature (6). The lead-rich alloys show a mysterious evolution of heat, on cooling, at about 150° C., and for this no satisfactory explanation has been offered, though the fact is beyond question.

¹Manuscript received May 28, 1956.

Contribution from the Chemistry Department, University of Manitoba, Winnipeg, Manitoba.

²Holder of the Cominco Fellowship, University of Manitoba, 1955-56.

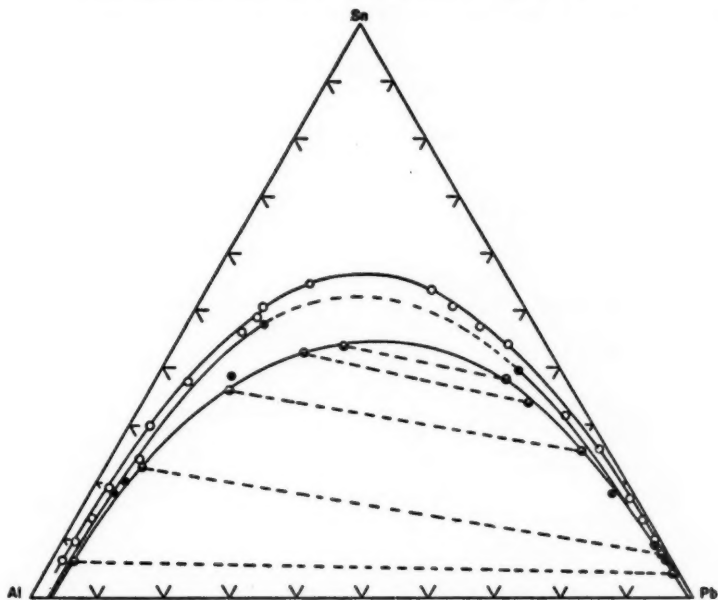


FIG. 1. The liquid immiscibility region in the aluminum-lead-tin system at 650° (O), 730° (●), and 800° C. (●). (Davies)

The remaining binary system, Al-Sn, is also simple in character (3). Some earlier claims for the existence of an intermetallic compound, AlSn , have now been given up. It is probable that the distorted (non-ideal) form of the liquidus gave rise to these claims. It was the distorted character of the liquidus which led to our redetermining it. Between 10 and 90 weight per cent aluminum, the liquidus is almost horizontal; to be exact, the equilibrium temperature changes only by about 100° over this region, i.e. about 1° per 1%. It results from this that determination of the form of the liquidus by thermal analysis, the method invariably used hitherto, is bound to give low results in respect of temperature. If the accepted curve is too low in respect of temperature, it results from this that if this curve is used to interpret a temperature in terms of composition, the aluminum content appears too high. Our work on the ternary system Al-Pb-Sn convinced us that this was the case and led to our redetermination of part of the Al-Sn liquidus by an isothermal method.

EXPERIMENTAL

It is unnecessary, in these days of pure materials, to give lengthy analyses of trace elements. Suffice it to say that the aluminum was a special research grade kindly donated to us by the Aluminum Company of America, the lead was Merck 'Reagent' grade, and the tin (so-called 'commercial', from the Vulcan Detinning Company) was actually a very pure product, containing 99.995% tin.

TABLE I
RESULTS OF M. H. DAVIES ON THE AL-PB-SN SYSTEM
Al-rich in equilibrium with Pb/Sn-rich

Al	Pb	Sn	Al	Pb	Sn
At 650° C.					
92.0	1.7	6.3	0.3	94.3	5.3
88.3	2.0	9.7	0.3	92.7	7.0
84.0	2.3	13.7	0.7	89.3	10.0
78.7	2.3	19.0	1.0	85.7	13.3
71.7	4.3	24.0	1.0	82.0	17.0
67.0	3.0	29.7	1.3	73.0	25.7
57.3	5.0	37.7	3.7	66.0	31.7
45.0	9.0	46.0	5.7	50.3	44.0
41.3	10.0	48.7	8.3	44.6	47.0
39.7	10.0	50.3	10.7	38.7	50.7
30.7	15.0	54.3	12.6	34.0	53.7
At 730° C.					
78.7	3.3	18.0	1.0	92.6	6.7
75.7	4.3	20.0	1.0	90.3	9.0
50.3	11.0	38.7	3.3	69.0	27.7
41.0	11.6	47.3	6.3	54.3	39.3
At 800° C.					
90.7	3.3	6.0	1.0	95.3	3.7
72.0	5.3	22.7	1.0	91.7	7.3
No analysis for sample			1.3	87.0	11.7
52.0	12.0	36.0	4.0	70.6	25.0
37.3	20.0	42.7	7.7	58.3	34.0
35.7	20.7	43.7	9.0	53.0	37.0

NOTE: These results are taken from the analysis of 150 samples and are adjusted to the nearest 1%. At low concentrations only the minor constituents were analyzed but at higher concentrations figures for lead, tin, and aluminum were obtained. Total errors amounting to 2% were common in the latter case and in isolated samples the total error was occasionally as high as 5%.

Because of the ready oxidation, in the furnace, of all three metals, the composition of all alloys had to be determined by chemical analysis. After trying in vain to adopt polarographic and conductometric methods, we finally used the following method which, though old-fashioned and crude, was sufficiently accurate for our purposes. Tin was determined as metastannic acid, ignited to SnO_2 . The filtrate was diluted to known volume and aliquot portions used for lead and aluminum determination. Lead was estimated as chromate, weighed on a sintered glass crucible. Aluminum was determined as hydroxy-quinolate, in the presence of lead. Determination of aluminum in lead-aluminum mixtures of known composition showed that lead did not interfere. When the alloy contained less than two per cent aluminum, the hydroxy-quinolate was dissolved in hydrochloric acid and reprecipitated.

It has been the practice of this laboratory, for some years past, to make increasing use of the isothermal method, rather than that of thermal analysis, for the determination of liquidus curves and surfaces. In effect, this amounts to taking horizontal sections of the three-dimensional model and, in our opinion, the method is often more accurate than that of thermal analysis although, of course, thermal analysis will always retain its value.

The method of keeping the furnace at constant temperature is essentially

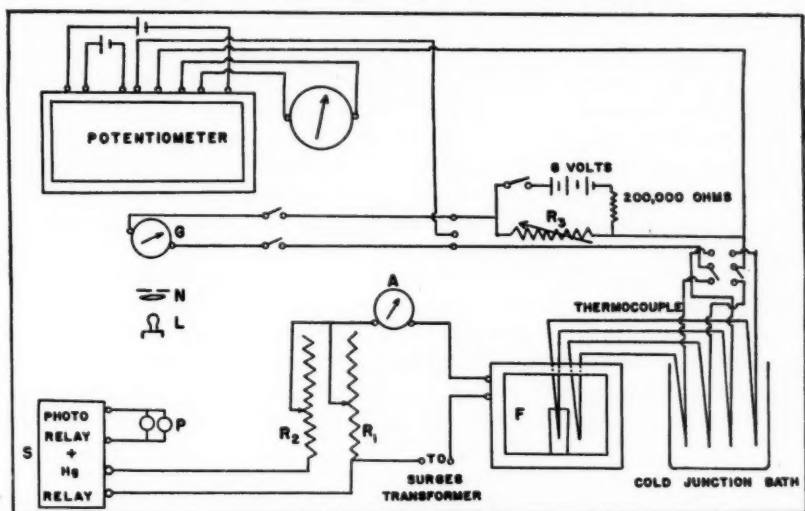


FIG. 2. Temperature control circuit.

that of Lutz and Wood (5) but the circuit is now much simplified. The essential layout is shown in Fig. 2. The furnace, *F*, contains two chromel-alumel thermocouples, one actually in the melt, the other in the air space of the furnace. Either of these thermocouples can be switched into the potentiometer circuit when it is desired to measure temperature. A constant current from the transformer to the furnace, through resistance R_1 , is sufficient to keep the furnace a few degrees below the desired temperature. A second resistance, R_2 , in parallel with R_1 , supplies additional current under control. It was found that the additional current had to be reduced to a few tenths of an ampere for good temperature control. Control is obtained by opposing the thermocouple e.m.f. by an equal e.m.f., obtained by applying a potential divider to a 6-volt storage battery. This circuit also contains a delicate galvanometer. When the thermocouple e.m.f. exceeds the opposing e.m.f., the mirror of the galvanometer moves, reflecting a spot of light onto the photocells. These cells then operate the relay, cutting out the extra heating current. Simple as the arrangement is, it operates admirably for our purposes, giving a constancy of $\pm 0.5^\circ$, at 600°C . The thermocouples were calibrated by means of pure tin, lead, zinc, and aluminum. The thermocouple in the melt gave the actual temperature of the melt, while the other served to keep the furnace under control while the former thermocouple was removed for sampling of the melt. Most alloys had a crust of solid aluminum on the top and the hole left by removal of the thermocouple case served for sampling.

Alundum ware (crucibles, sampling tubes, thermocouple case, etc.) was used throughout: glass is rapidly reduced by hot aluminum, with production of elementary silicon.

All isotherms were determined at temperatures below the freezing point of aluminum and therefore aluminum was always a solid phase. To ensure

homogeneity of the liquid phase, all alloys were heated to complete fusion with stirring, before their introduction to the furnace. The alloy was then allowed to cool in the furnace, with constant stirring with an alundum rod, until the controlled temperature was reached. The alloy was then kept at controlled temperature for from 4 to 24 hr., before a sample was withdrawn for analysis. Sampling was done by withdrawing molten alloy through a narrow ($\frac{1}{8}$ in. inside diameter) alundum tube. The alloy solidified in the tube just above furnace height. The entire sample was weighed and analyzed; this was done in case there had been segregation of the sample in the tube. We satisfied ourselves by frequent sampling of top and bottom of crucible contents that two liquid layers never occurred at the temperature of investigation.

The ternary eutectic temperature and composition in the Al-Pb-Sn system were determined by thermal analysis. Aluminum was added in very small quantities at a time to the binary eutectic mixture of the Pb-Sn system until the eutectic temperature remained constant. The eutectic alloy was then analyzed.

The techniques of polishing and of photomicrography are well known. The polishing and etching of these soft metals is, however, notoriously difficult. We used as etching reagent that of Vilella and Beregekoff (9); it consists of a mixture of glacial acetic acid, nitric acid, and glycerol. The results were extremely satisfactory, as can be seen from our photomicrographs.

Hardness was determined by means of a modified Brinell tester (load 5.5 kgm.) and by the Vickers-Armstrong tester. To test the tensile strength, the alloys were treated as solders, in the following manner: Two pieces of half-inch brass strip, six inches long, were soldered together in the form of a lap joint; the area of the lap was one-eighth of a square inch. Both pieces were 'tinned' with the solder under investigation, then fused together. Any excess of solder round the joint was removed with a file. The strength of the joint was determined with an Olsen 10,000 lb. tester. Four tests were made with each solder and the results, which agreed reasonably well, were averaged.

EXPERIMENTAL RESULTS

TABLE II

SOLUBILITY OF ALUMINUM IN TIN BETWEEN 400° AND 645° C.

Alloy No.	Temperature, ° C.	Composition by weight	
		Al	Sn
1	400	2.6	97.5
2	425	3.3	97.0
3	450	4.0	96.0
4	475	4.8	95.2
5	500	5.4	94.6
5a	500	5.7	93.9
6	525	8.3	92.1
7	550	11.8	88.3
8	575	17.1	83.0
9	600	30.8	69.1
9a	600	29.9	68.8
10	625	58.6	41.0
11	645	87.6	12.4

TABLE III

COMPOSITION OF LIQUIDUS IN EQUILIBRIUM WITH SOLID ALUMINUM
AT 500° C., IN SYSTEM AL-Pb-Sn

Alloy No.	Al, wt. %	Pb, wt. %	Sn, wt. %
2	3.5	27.5	69.1
3	4.0	16.1	80.0
4	4.9	6.2	88.8
5	5.7	0.0	93.9
5a	5.5	0.0	94.4

TABLE IV

COMPOSITION OF LIQUIDUS IN EQUILIBRIUM WITH SOLID ALUMINUM
AT 600° C. IN SYSTEM AL-Pb-Sn

Alloy No.	Composition by weight		
	Al	Pb	Sn
6	5.0	43.0	52.5
9	9.1	30.4	60.5
10	10.3	26.2	63.5
11	0.45	85.0	15.1
12	29.2	0.0	68.8
12a	30.3	0.0	68.9
13	2.7	61.3	36.5
14	5.5	40.2	54.5
15	9.4	27.7	63.1
16	15.9	12.2	70.5
17	23.8	5.2	71.4

TABLE V

COMPARISON OF Pb-Sn EUTECTIC WITH AL-Pb-Sn EUTECTIC

Eutectic	Temperature, ° C.	Composition of liquid (wt. %)		
		Al	Pb	Sn
Pb-Sn	183.3	—	38.1	61.9
Al-Pb-Sn	183.0	0.08	38.1	61.7

The results of Table II are plotted as the equilibrium diagram Fig. 3. Experiments were not carried below 400° C. because below that temperature our results were in agreement with the published results, and, in any case, the solubility is too small to be interesting. The dotted curve of Fig. 3 represents ideal behavior as calculated by Seltz' (7) thermodynamic equations. The difference between the dotted and full curves points up the very non-ideal form of the liquidus.

Fig. 4 is the equilibrium diagram of the system Al-Pb-Sn at 500° C., derived from the data of Table III; in all cases aluminum was the solid phase. The investigation was not pursued below 69% tin content, since the aluminum

TABLE VI
SOME MECHANICAL PROPERTIES OF THE PURE METALS AND CERTAIN
ALLOYS OF THE SYSTEM AL-PB-SN

Alloy	Hardness		Tensile strength as a solder, p.s.i.
	B.h.n.*	D.P.H.†	
Al	14.9	16.6	—
Sn	5.0	11.4	—
Pb	3.4	7.6	—
Pb-Sn eut.	14.2	16.4	6200
Al-Pb-Sn eut.	18.2	19.8	6450
Pb-Sn eut. + 1% Al	15.8	18.4	5900
Pb-Sn eut. + 5% Al	14.2	17.7	—

The shear strength of a soldered joint under prolonged load was determined for the Pb-Sn eutectic. This solder supported 1360 p.s.i. for 264 hr. at room temperature.

*Diameter of ball, 2.5 mm.; load, 5.5 kgm.; time of application, 30 sec.
†Load, 5.0 kgm.

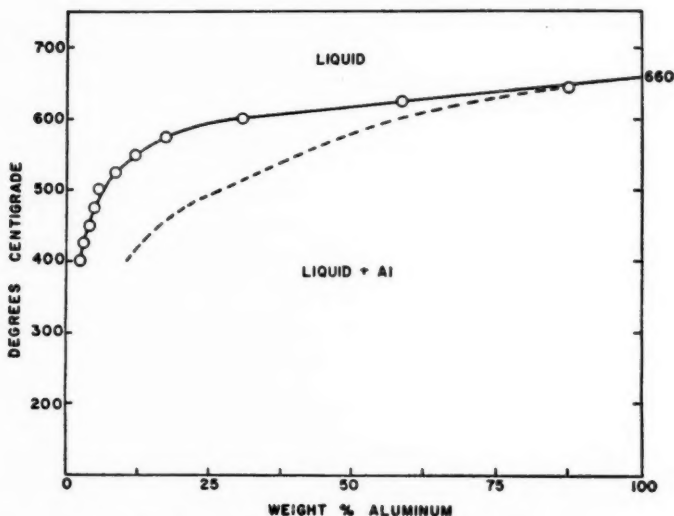


FIG. 3. System aluminum-tin. Equilibrium diagram.

content had fallen to 3.5% and since the solubility of aluminum in lead, at 500° C., is only 0.02% (1). Fig. 5 is the corresponding isotherm for 600° C. Even at 600° C., no two liquid layers were ever observed.

Figs. 6-11 are photomicrographs ($\times 500$) showing the various phases in equilibrium, in the region of the ternary eutectic.

Table VI shows the relationship between the hardness of the pure metals, the Pb-Sn eutectic, and two alloys having primary separated aluminum. Brinell Ball and Vickers Diamond Pyramid hardness numbers are given. The trend in the hardness is the same on both scales. The binary eutectic alloy was

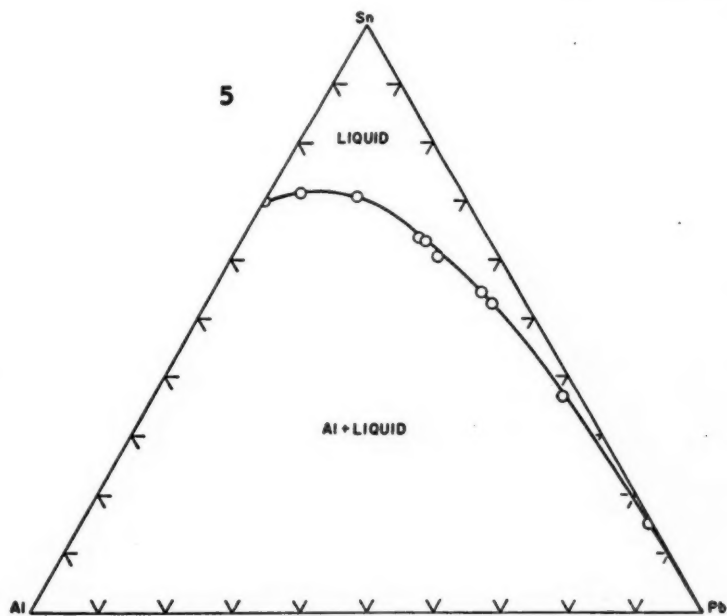
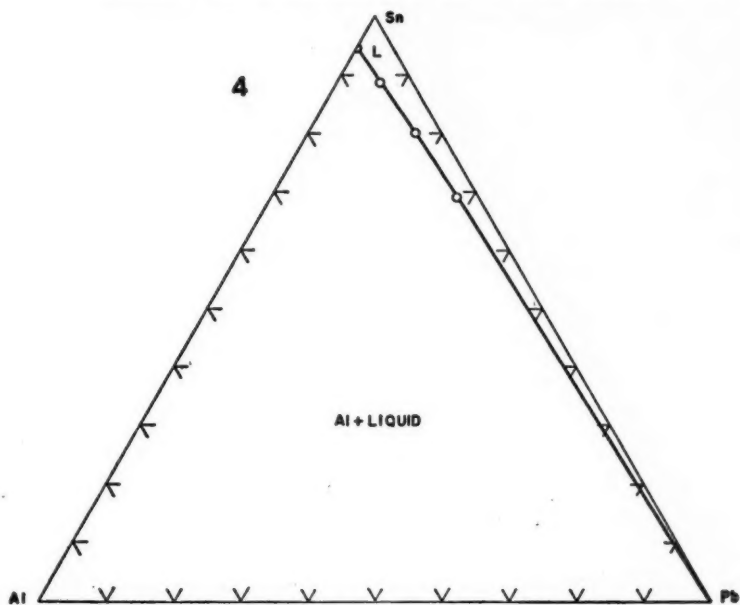


FIG. 4. 500° C. isotherm system Al-Pb-Sn.

FIG. 5. 600° C. isotherm system Al-Pb-Sn.

found to have a greater hardness than lead or tin, the two pure components. Likewise the ternary eutectic alloy had a greater hardness than both the binary Pb-Sn eutectic and aluminum, the third alloying component. The alloy made by adding 1% aluminum to the Pb-Sn eutectic, thus forming an alloy that was mainly ternary eutectic surrounding primary separated aluminum, had a hardness less than the eutectic and approaching that of pure aluminum. Aluminum occupies about 20% of the volume in the alloy containing 5 weight per cent aluminum plus the Pb-Sn eutectic composition. Consequently the hardness of this alloy was almost equal to that of pure aluminum.

The effect of aluminum on the shear strength of the Pb-Sn eutectic solder was determined. As shown in Table VI the shear strength and the hardness were greater for the ternary eutectic than for the binary. The alloy containing 1% aluminum showed a marked decrease in shear strength due to the appearance of primary aluminum. The 5% aluminum alloy could not be used as a solder owing to the large volume of aluminum present. Aluminum does not fuse at soldering temperatures.

DISCUSSION OF RESULTS

When this work was commenced it was naturally supposed that the region of solid aluminum would intrude, with falling temperature, into the region of two liquid layers, giving rise to an invariant triangle, i.e. a heterogeneous area in which solid aluminum is in equilibrium with two liquid layers of fixed composition; further addition of tin would cause solid aluminum to disappear and a region of two congruent liquids to appear, terminating in a liquid of critical composition. In fact, however, no congruent triangle or two-liquid region was observed, either at 500° or at 600° C. Phenomena as described above must exist somewhere between 600° C. and the melting point of aluminum but, since this represents an extreme range of 60°, it was not thought worth while to pursue the matter further. The interesting thing is the absence of a two-liquid region at 600° C., for the figures of Davies (2) on the two-liquid region, at and above 650° C., and the accepted equilibrium diagram of the system Al-Sn would certainly lead one to expect the existence of a two-liquid region at 600° C. We were hence forced to the conclusion that the accepted solubility figures of aluminum in tin were erroneous and this led to our re-determining part of this diagram. We have plotted our results for Al-Sn, along with those of Sully, Hardy, and Heal (8), the latest and presumably the best work, in Fig. 12; the dotted line represents the results of Sully, Hardy, and Heal. The two curves coincide between 400° and 450° C., and between 450° and 550° C. the deviation in composition is less than two per cent by weight. Above 550° C., the curve flattens out and, although the difference in temperature between the two curves is only about 10° C., in this region, the difference in composition can be as great as 20%. Sully, Hardy, and Heal used thermal analysis and this method does not yield accurate results when there is a large change in composition for a small change in temperature.

Using our new data, for the solubility of aluminum in tin, it became obvious that a two-liquid region is no longer to be expected at 600° C.; the miscibility

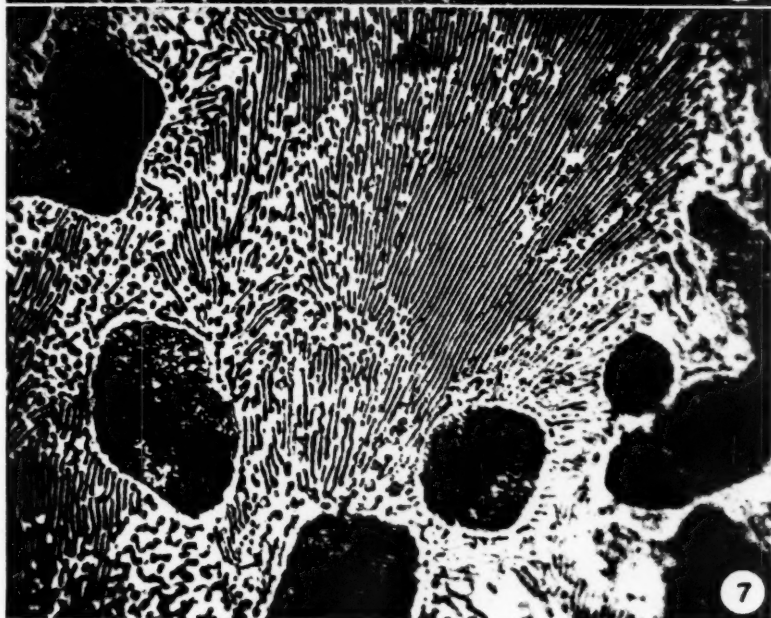
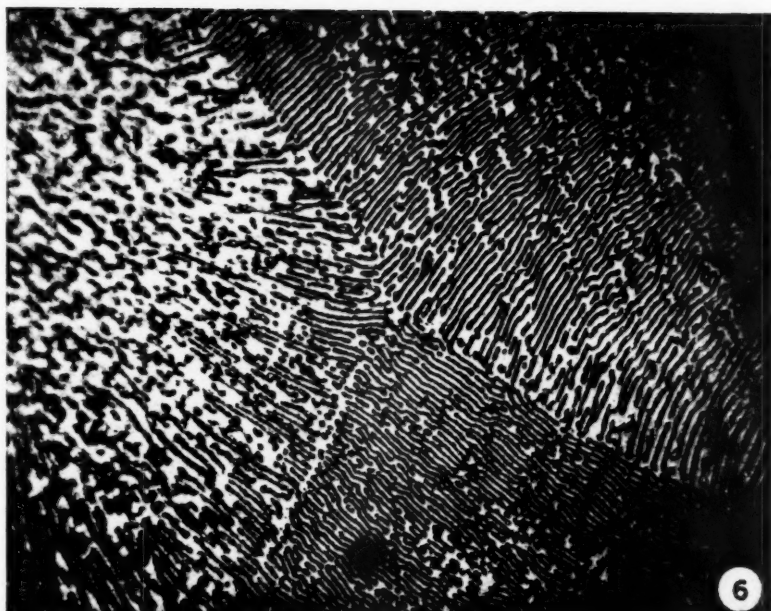


FIG. 6. Pb-Sn eutectic, $\times 500$.

FIG. 7. Alpha lead embedded in Pb-Sn eutectic matrix, $\times 500$.

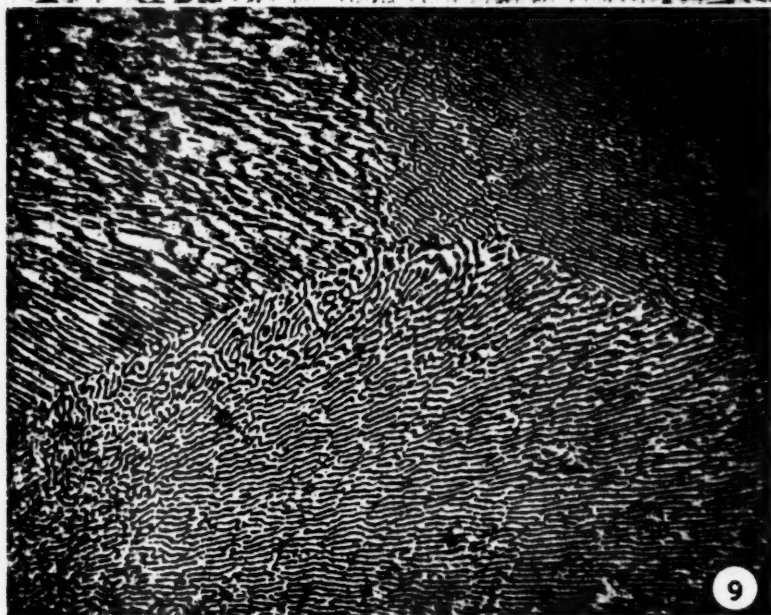


FIG. 8. Beta tin embedded in Al-Pb-Sn eutectic matrix, $\times 500$.
FIG. 9. Al-Pb-Sn eutectic, $\times 500$.

PLATE III

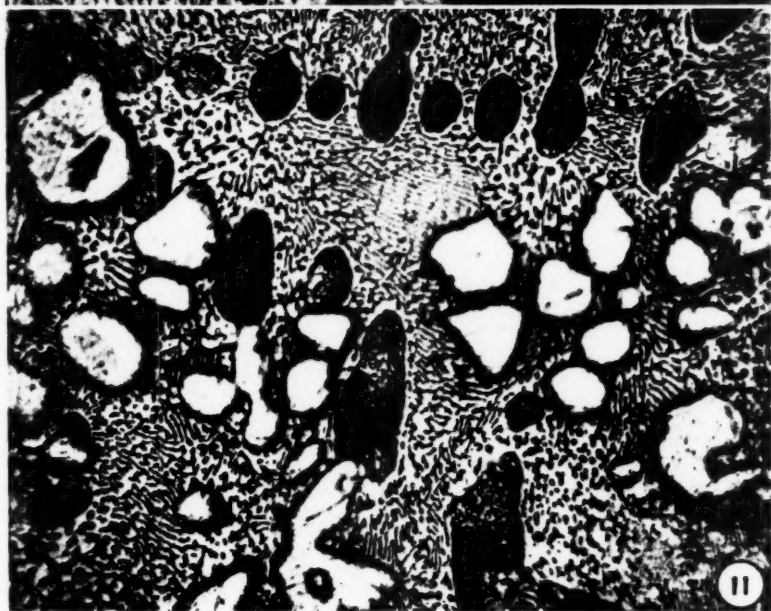


FIG. 10. Primary aluminum in Al-Pb-Sn eutectic matrix, $\times 500$.

FIG. 11. Alpha lead (dark), primary aluminum (light) in Al-Pb-Sn eutectic matrix, $\times 500$.

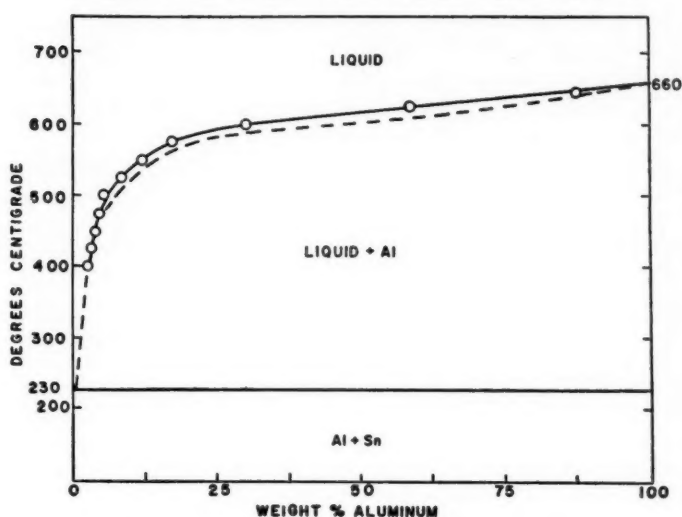


FIG. 12. System aluminum-tin. Redetermined equilibrium diagram.

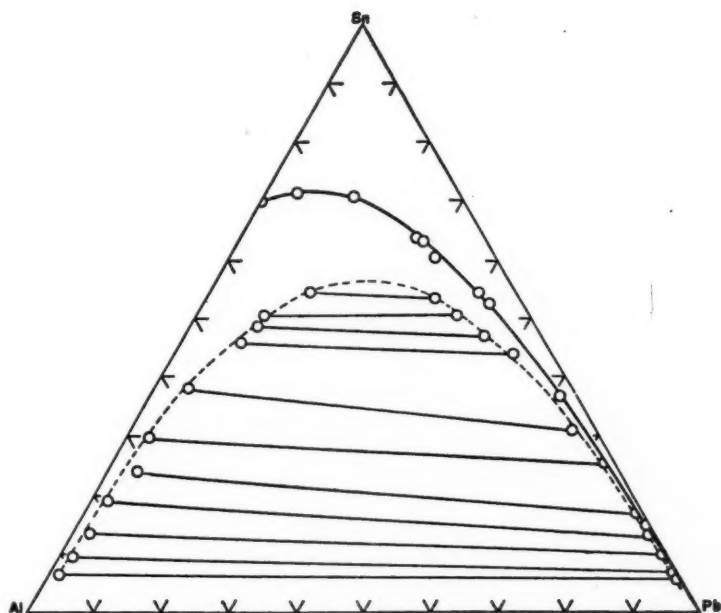


FIG. 13. System Al-Pb-Sn. ——— 600° C. isotherm. - - - - 650° C. isotherm.

gap which undoubtedly exists at 650° C. (Davies (2)) is completely intruded by solid aluminum at 600° C. This is illustrated in Fig. 13 which shows our 600° isotherm and that of Davies for 650° C. The diagram shows to what extent the region of solid aluminum has moved across the region of two liquids, when the temperature has dropped 50°.

The ternary eutectic is very near to the binary eutectic of the Pb-Sn system. The binary eutectics of the Al-Pb and the Al-Sn systems contain very little aluminum and therefore the eutectic troughs must almost coincide with the side of the diagram; in other words, the amount of aluminum in any eutectic of the system is almost vanishingly small.

The photomicrographs are almost self-explanatory and are only of interest as being unusually fine examples of photomicrographs of soft metals. Figs. 6 and 9 show the lamellar structure of the Pb-Sn and Al-Pb-Sn eutectics respectively. Fig. 7 shows α -lead embedded in Pb-Sn eutectic matrix. The solubility of tin in lead at the eutectic temperature is 19.2%, while at room temperature it is only 1½%. The α -phase exhibits a white outline and light spots, owing to the precipitation of tin in the solid phase as the temperature is lowered.

Fig. 8 is a photomicrograph of a ternary alloy that has been allowed to solidify in the furnace, then thrust into powdered dry ice for quenching. It shows β -tin embedded in eutectic matrix. Tin contains 2.5% lead in solid solution at the eutectic temperature but only a negligible amount at room temperature. The β -phase here shows lead precipitated at the grain boundaries and in the crystallographic planes. This structure is called *widmannstätten*. The central island exhibits an example of twinning through cold working.

Primary separation of aluminum in an Al-Pb-Sn matrix is shown in Fig. 10. The sample was selected so that the outside edge of the ingot formed one side of the specimen. One of the sides perpendicular to this edge was then polished and etched. This alloy contained 1% aluminum and lead and tin in the eutectic ratio and shows a primary aluminum crystal formed at the outer edge of the ingot. The phases present in an alloy containing 5% aluminum plus the Pb-Sn eutectic are shown in Fig. 11. α -Lead is the dark phase with some tin precipitated. The light polygonal-shaped crystallites are primary aluminum. Because aluminum is more resistant to the polishing abrasive, these crystallites are not in the same plane as the α -lead and eutectic matrix, and hence are slightly out of focus.

ACKNOWLEDGMENT

In this, as in all similar work, we acknowledge our deep indebtedness to Professor C. M. Hovey, of the Department of Civil Engineering, without whose patient supervision the photomicrographs would be impossible.

REFERENCES

1. CAMPBELL, A. N. and ASHLEY, R. W. *Can. J. Research*, B, 18: 281. 1940.
2. DAVIES, M. H. *J. Inst. Metals*, 81: 415. 1953.
3. HEYCOCK, C. T. and NEVILLE, F. H. *J. Chem. Soc.* 57: 376. 1890. GAUTIER, H. *Bull. soc. encour. ind. natl.* 1: 1293. 1896. GWYER, A. G. C. *Z. anorg. Chem.* 49: 311. 1900. CAMPBELL, W. and MATTHEWS, J. A. *J. Am. Chem. Soc.* 24: 253. 1902. LORENZ, R. and PLUMBRIDGE, D. *Z. anorg. u. allgem. Chem.* 83: 243. 1913. SULLY, A. H., HARDY, H. K., and HEAL, T. J. *J. Inst. Metals*, 76: 269. 1949.

4. LORENZ, R. and ERBE, F. *Z. anorg. Chem.* 183:328. 1929.
5. LUTZ, B. C. and WOOD, J. H. *Can. J. Research, A*, 26: 145. 1948.
6. ROBERTS-AUSTEN, W. C. 4th Rept. to Alloys Research Committee, Inst. Mech. Engrs. 1897. ROSENHAIN, W. and TUCKER, P. A. *Trans. Roy. Soc. (London)*, A, 209: 89. 1908. DEGENS, P. M. *Z. anorg. Chem.* 63:207. 1909. PARRAVANO, N. and SCORTECCI, A. *Gazz. chim. ital.* 50:83. 1920. JEFFREY, F. H. *Trans. Faraday Soc.* 24:209. 1928. HONDA, K. and ABE, W. *Sci. Rept. Tohoku Imp. Univ.* 19 (1):315. 1938. STOCKDALE, D. *J. Inst. Metals*, 49:267. 1932.
7. SELTZ, H. *J. Am. Chem. Soc.* 56:307. 1934.
8. SULLY, A. H., HARDY, H. K., and HEAL, T. J. *J. Inst. Metals*, 76:269. 1949.
9. VILLELA, J. R. and BERECEKOFF, D. *Ind. Eng. Chem.* 19:1049. 1927.
10. WRIGHT, C. R. A. *Proc. Roy. Soc.* 52:14. 1892.
11. WRIGHT, C. R. A. *J. Soc. Chem. Ind.* 9:944. 1890; 11:492. 1892. PECHEUX, H. *Compt. rend.* 138:1042. 1904. GWYER, A. G. C. *Z. anorg. u. allgem. Chem.* 57:113. 1908. HANSEN, M. and BLUMENTHAL, B. *Metallwirtschaft*, 10:925. 1931. KEMPF, L. W. and VAN HORN, K. R. *Am. Inst. Mining Met. Engrs. Inst. Metals Div. Tech. Publ. No.* 990:12. 1938. CAMPBELL, A. N. and ASHLEY, R. W. *Can. J. Research, B*, 18:281. 1940.

A CONVENIENT SYNTHESIS OF DL-GLUTAMIC ACID FROM β -PROPIOLACTONE¹

BY GUY TALBOT, ROGER GAUDRY, AND LOUIS BERLINGUET

ABSTRACT

A new synthesis of DL-glutamic acid was carried out in an over-all yield of 87% from condensation between β -propiolactone and the sodium salt of diethyl acetamidomalonate, followed by acid hydrolysis. When desired, the intermediate product, the diethyl ester of N-acetyl-2-carbethoxyglutamic acid, could be isolated in a 68% yield and hydrolyzed to glutamic acid via the hydrochloride in a 95% yield.

INTRODUCTION

L-Glutamic acid is a natural α -aminodicarboxylic acid obtainable by hydrolysis of many albumins and particularly of gluten from which it was isolated for the first time (20). Numerous syntheses of racemic glutamic acid have been published since and according to the methods of preparation, they can be divided into three main groups: (1) Syntheses involving a reduction step on either α -oximinoglutamic acid, α -diazoglutamic acid, or α -oxoglutamic acid and their esters (23, 13, 7, 3, 12, 10, 21, 15). (2) The Strecker reaction performed on β -aldehydopropionic acid (9, 2). (3) Condensation of diethyl malonate derivatives with various compounds (8, 4, 19, 14, 22, 1, 6). Another method was recently published by Paris *et al.* (18) starting from γ -butyrolactone.

Of these preparations, few are of practical interest. The best ones involve condensation of a malonic acid derivative with methyl acrylate (14, 22) or acrylonitrile (1, 6).

We have investigated the preparation of DL-glutamic acid from the commercially available β -propiolactone (11) and diethyl acetamidomalonate. The chemistry of β -lactones has been recently reviewed by Zaugg (24). According to the general expectations, whenever β -propiolactone reacts with a compound MX in the ionized form, the cleavage should occur at the alkyl-oxygen bond.

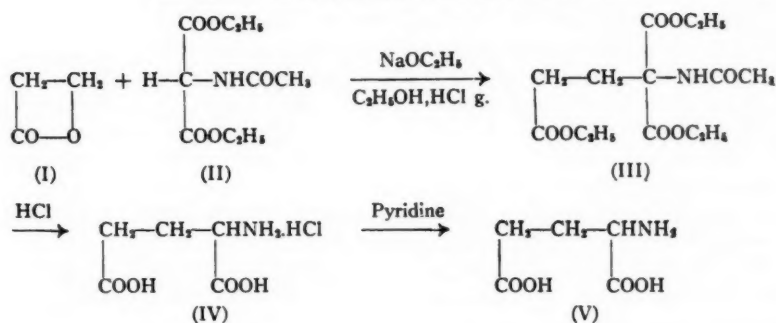
Advantage was taken of that property and β -propiolactone (I) was condensed at 0° C. with the sodium salt of diethyl acetamidomalonate (II) in absolute ethanol.

The one-step reaction including condensation of (I) with (II) and immediate hydrolysis, without isolation of any intermediate, gave an 87% yield of glutamic acid (V).

The intermediate compound, the diethyl ester of N-acetyl-2-carbethoxyglutamic acid (III), has been isolated in a 68% yield and transformed to glutamic acid hydrochloride (IV) in a 95% yield upon acid hydrolysis. The alcoholic solution of the above hydrochloride, treated with pyridine, gave a quantitative yield of DL-glutamic acid (V).

¹Manuscript received June 20, 1958.

Contribution from the Department of Biochemistry, Faculty of Medicine, Laval University, Quebec City. Paper presented before the Division of Chemistry at the 23rd Meeting of L'Association canadienne-française pour l'avancement des sciences (A.C.F.A.S.), Ottawa, November 5th, 1955.



The β -propiolactone condensation has also been successfully tried with ethyl acetamidocyano-acetate and at different temperatures varying between 0° and 78° C. The composition of the hydrolyzates was qualitatively analyzed by paper chromatography and also, which is much better, by paper electrophoresis. The best conditions found were those already described above for the condensation at 0° C. between β -propiolactone (I) and diethyl acetamidomalonate (II).

It is of interest to note that the diethyl N-acetyl-2-carbethoxyglutamate (III), isolated in the course of the reaction, had a melting point of $66-67^\circ$, after several recrystallizations, instead of $81-82.5^\circ$ as first described by Morrison (16). However, as shown in the experimental part, our sample was submitted to various analyses and proved to have the exact structure.²

EXPERIMENTAL¹

N-Acetyl-2-carbethoxyglutamic Acid Diethyl Ester (III)

In an Erlenmeyer flask fitted with a Y glass adapter and a calcium chloride tube is placed 50 ml. of absolute ethanol. Metallic sodium (1.2 gm., 0.057 mole) is dissolved in it, followed by diethyl acetamidomalonate (II) (10.85 gm., 0.05 mole). The mixture is stirred at room temperature for 30 min. and then cooled to -10° C. in a salt-ice bath. β -Propiolactone (I) (5.0 gm., 0.069 mole) is added in small portions at such a rate that the temperature of the reactants does not rise above 0° C., the addition requiring about 30 min. The mixture is then allowed to stand for 12 hr. during which time the ice is allowed to melt. Anhydrous hydrogen chloride is bubbled in the solution to ensure complete esterification. The mixture is then evaporated to dryness *in vacuo* and the residue extracted with ether. Petroleum ether is added to the concentrated ethereal solution which is then placed in the cold. The precipitate recrystallizes either from ether-petroleum ether or an alcohol-ligroin mixture. Yield, 10.8 gm. (68%); m.p. $66-67^\circ$. (Lit.: m.p. $81-82.5^\circ$ (16).) Anal. Calc. for $\text{C}_{14}\text{H}_{23}\text{O}_7\text{N}$: N, 4.41. Found: N, 4.44.

¹After this manuscript had been submitted for publication, we learned (17) that Dr. G. H. Cocolas has identified the product m.p. $81-82.5^\circ$ as being in fact 5,5-dicarbethoxy-2-pyrrolidone, which by acid hydrolysis gives glutamic acid.

²Melting points are uncorrected.

Titration of that product with 0.1 *N* sodium hydroxide showed the complete absence of a free acid group whereas its saponification equivalent was near the theoretical value, therefore proving the presence of three ester groups.

The *N*-acetyl-2-carbethoxyglutamic acid diethyl ester (III) has been found by Morrison (17) to give crystals melting at 82–83° and occasionally at 88–89°. A crude sample, kindly supplied by Dr. Morrison, was recrystallized from ethanol-ligroin to give a first crop of crystals melting at 66–67° with no depression of the m.p. upon admixture with our preparation of m.p. 66–67°. A second crop m.p. 81–82° was also obtained.

When both samples were hydrolyzed and submitted to paper electrophoresis, they gave spots identical with authentic glutamic acid and no trace of glycine, therefore excluding any possibility of contamination by unreacted diethyl acetamidomalonate (II).

Glutamic Acid Hydrochloride (IV)

N-Acetyl-2-carbethoxyglutamic acid diethyl ester (III) (5.0 gm., 0.0158 mole) was heated under reflux for five hours in 100 ml. of dilute hydrochloric acid (1:1). The solution was evaporated to dryness *in vacuo* and the residue recrystallized from alcohol-ether. Yield, 2.75 gm. (95%); m.p. 190°. (Lit.: m.p. 192–193° (9).) Anal. Calc. for $C_8H_9O_4N \cdot HCl$: Cl, 19.3; N, 7.63. Found: Cl, 19.0; N, 7.62.

Glutamic Acid (V)

Glutamic acid hydrochloride (IV) (1.0 gm., 0.005 mole) was dissolved in hot ethanol and one equivalent of pyridine added, causing an immediate separation of the free amino acid. Yield, 0.8 gm. (100%); m.p. 190°. (Lit.: m.p. 198° (23).) Anal. Calc. for $C_5H_9O_4N$: N, 9.52. Found: N, 9.46.

The benzoyl derivative, recrystallized from ether-ligroin, melted at 150°. (Lit.: m.p. 152° (5).) Anal. Calc. for $C_{12}H_{13}O_5N$: N, 5.57. Found: N, 5.55.

Glutamic Acid (V) in a One-step Reaction from β -Propiolactone (I)

The condensation in absolute ethanol at 0° C. between β -propiolactone (I) (5.0 gm., 0.069 mole) and sodium salt of diethyl acetamidomalonate (II) (10.85 gm., 0.05 mole) was carried out as described above for the preparation of *N*-acetyl-2-carbethoxyglutamic acid diethyl ester (III). When the mixture had reached room temperature, after a 12 hr. stirring, it was poured into water containing one equivalent of hydrochloric acid and evaporated to dryness *in vacuo*. The residue was dried by distilling benzene-ethanol from it, followed by ether extraction and evaporation of the solvent. The oily residue was heated under reflux for five hours in 200 ml. of hydrochloric acid (1:1) and evaporated to dryness *in vacuo*. The residue was dissolved in hot ethanol and pyridine (one equivalent) added. The glutamic acid, which crystallized in the cold, was collected. Yield, 6.4 gm. (87%); m.p. 190°. (Lit.: m.p. 198° (23).) Anal. Calc. for $C_5H_9O_4N$: N, 9.52. Found: N, 9.43.

ACKNOWLEDGMENTS

The authors are indebted to the National Research Council of Canada for Research Fellowships awarded to one of them (G.T.).

REFERENCES

1. ALBERTSON, N. F. and ARCHER, S. J. Am. Chem. Soc. 67: 2043. 1945.
2. ANATOL, J. Compt. rend. 232: 536. 1951.
3. CHILES, H. M. and NOYES, W. A. J. Am. Chem. Soc. 44: 1798. 1922.
4. DUNN, M. S., SMART, B. W., REDEMANN, C. E., and BROWN, K. E. J. Biol. Chem. 94: 599. 1931-1932.
5. FISCHER, E. Ber. 32: 2451. 1899.
6. GALAT, A. J. Am. Chem. Soc. 69: 965. 1947.
7. HAMLIN, K. E. and HARTUNG, W. H. J. Biol. Chem. 145: 349. 1942.
8. KARRER, P., ESCHER, K., and WIDMER, R. Helv. Chim. Acta, 9: 301. 1926.
9. KEIMATSU, S. and SUGASAWA, S. J. Pharm. Soc. Japan, 531: 369. 1925.
10. KNOOP, F. and OESTERLIN, H. Hoppe-Seyler's Z. physiol. Chem. 148: 294. 1925.
11. KÜNG, F. E. U.S. Patent No. 2,356,459. Chem. Abstr. 39: 88. 1945.
12. LEVENE, P. A. and MIKESKA, L. A. J. Biol. Chem. 55: 795. 1923.
13. McILWAIN, H. and RICHARDSON, G. M. Biochem. J. 33: 44. 1939.
14. MARVEL, C. S. and STODDARD, M. P. J. Org. Chem. 3: 198. 1938.
15. MENTZER, C. and BILLET, D. Compt. rend. 232: 2104. 1951.
16. MORRISON, D. C. J. Am. Chem. Soc. 77: 6072. 1955.
17. MORRISON, D. C. Private communications. April 27 and July 25, 1956.
18. PARIS, G., GAUDRY, R., and BERLINGUET, L. Can. J. Chem. 33: 1724. 1955.
19. REDEMANN, C. E. and DUNN, M. S. J. Biol. Chem. 130: 341. 1939.
20. RITTHAUSEN, F. J. prakt. Chem. 99: 6454. 1866.
21. SHEMIN, D. and HERBST, R. J. Am. Chem. Soc. 60: 1954. 1938.
22. SNYDER, H. R., SHEKLETON, J. F., and LEWIS, C. D. J. Am. Chem. Soc. 67: 310. 1945.
23. WOLFF, L. Ann. 260: 79. 1890.
24. ZAUGG, H. E. *In* Organic reactions. Vol. 8. Edited by R. Adams. John Wiley & Sons, Inc., New York. 1954. p. 305.

BASIC ESTERS OF SUBSTITUTED PYRIMIDINE-4-CARBOXYLIC ACIDS¹

BY GORDON A. GRANT, CARL VON SEEMANN,
AND STANLEY O. WINTHROP

ABSTRACT

A number of β -dialkylaminoethyl esters of 2,5-disubstituted pyrimidine-4-carboxylic acids have been synthesized and characterized as their hydrochlorides and in some cases as their methobromide and methiodide salts. Mucochloric acid has been condensed with *S*-methylisothiuronium sulphate to give 2-methylthio-5-chloropyrimidine-4-carboxylic acid, and the corresponding 5-bromo- acid has been converted to the 5-amino- acid.

INTRODUCTION

In the course of some investigations on new antispasmodic and antisecretory agents carried out in this laboratory, our attention was drawn to the possibilities offered by certain 2,5-disubstituted pyrimidine-4-carboxylic acids. 2-Methyl-5-chloro- and 2-methyl-5-bromo-pyrimidine-4-carboxylic acids have been described by Buděšínský (1), and 2-methylthio-5-bromo-pyrimidine-4-carboxylic acid by McOmie and White (2).

The corresponding 2-methylthio-5-chloropyrimidine-4-carboxylic acid was prepared by condensing mucochloric acid with *S*-methylisothiuronium sulphate, using triethylamine as condensing agent. This acid could not be converted to the corresponding 5-amino- acid by heating with concentrated ammonia at 100° for two hours; on the other hand, the corresponding 5-bromo- acid gave a good yield of the 5-amino- acid when subjected to the same procedure.

For the preparation of the basic esters, the above acids were converted to their respective acid chlorides by means of thionyl chloride. No attempt at purification was made and the crude acid chlorides were condensed with two equivalents of the respective basic alcohol in benzene. The basic esters were either isolated as oils or converted directly from their benzene solutions to hydrochlorides or quaternary ammonium salts, listed in Table I. Attempts to prepare basic esters of 2-methylthio-5-aminopyrimidine-4-carboxylic acid were not successful.

Some of the compounds listed in Table I were screened by our Pharmacology Department and were found to be moderately active antispasmodics.

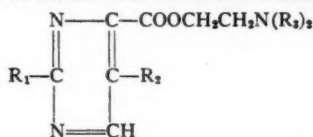
EXPERIMENTAL

2-Methylthio-5-chloropyrimidine-4-carboxylic Acid

This acid was prepared by the condensation of *S*-methylisothiuronium sulphate with mucochloric acid according to the procedure of McOmie and White (2) for the analogous 5-bromo- compound. One recrystallization from

¹Manuscript received March 23, 1956.

Contribution from Research Laboratories, Ayerst, McKenna & Harrison Limited, Montreal, Quebec.

TABLE I
 BASIC ESTERS OF SUBSTITUTED PYRIMIDINE-4-CARBOXYLIC ACIDS


R ₁	R ₂	R ₃	Salt	Recrystal. solv.	M.p., ° C.	Formula	Nitrogen, %	
							Calc.	Found
CH ₃ S	Br	Isopropyl	HCl	a	135-136	C ₁₄ H ₂₀ O ₂ N ₂ SClBr	10.17	10.01, 9.97
CH ₃ S	Cl	Isopropyl	HCl	a	145-147 (decomp.)	C ₁₄ H ₂₀ O ₂ N ₂ SCl ₂	11.40	11.21, 11.21
CH ₃	Cl	Isopropyl	HCl	a	155 (decomp.)	C ₁₄ H ₂₀ O ₂ N ₂ Cl ₂	12.50	12.68, 12.37
CH ₃	Br	Isopropyl	HCl	a	144-145 (decomp.)	C ₁₄ H ₂₀ O ₂ N ₂ ClBr	11.02	10.69, 11.08
CH ₃ S	Cl	Ethyl	HCl	b	183 (decomp.)	C ₁₄ H ₁₈ O ₂ N ₂ SCl ₂	12.30	11.90, 12.06
CH ₃ S	Cl	Ethyl	CH ₃ Br	b	159-160	C ₁₄ H ₁₈ O ₂ N ₂ SClBr	10.52	10.28, 10.28
CH ₃ S	Cl	Ethyl	CH ₃ I	c	153-154 (decomp.)	C ₁₄ H ₁₈ O ₂ N ₂ SCl ₂	9.44	9.58, 9.40
CH ₃ S	Cl	Methyl	HCl	b	185-186 (decomp.)	C ₁₄ H ₁₆ O ₂ N ₂ SCl ₂	13.45	13.56, 13.15
CH ₃ S	Cl	Methyl	CH ₃ Br	b	203-204 (decomp.)	C ₁₄ H ₁₆ O ₂ N ₂ SClBr	11.33	11.53, 11.67
CH ₃ S	Cl	Methyl	CH ₃ I	b	198 (decomp.)	C ₁₄ H ₁₆ O ₂ N ₂ SCl ₂	10.05	9.49, 9.76

NOTE: a—from benzene-acetone; b—from methanol-ether; c—from methanol-acetone-ether.

aqueous ethanol with decolorizing carbon gave yellow platelets, m.p. 169-170° C. Calculated for C₆H₆N₂ClSO₂: C, 35.22; H, 2.46; Cl, 17.33%. Found: C, 35.36, 35.83; H, 2.32, 2.71; Cl, 16.87, 17.12%.

2-Methylthio-5-aminopyrimidine-4-carboxylic Acid

2-Methylthio-5-bromopyrimidine-4-carboxylic acid was treated with concentrated ammonium hydroxide according to the procedure described by Buděšinský (1), for the preparation of the analogous 2-methyl-5-amino compound. The product, 2-methylthio-5-aminopyrimidine-4-carboxylic acid, on recrystallization from water, gave long yellow needles, m.p. 190-191.5° C. (decomp.). Calculated for C₆H₇N₃O₂S: C, 38.91; H, 3.81; N, 22.69%. Found: C, 39.37; H, 4.04; N, 22.35%.

β-Diethylaminoethyl-2-methylthio-5-chloropyrimidine-4-carboxylate

Five grams of 2-methylthio-5-chloropyrimidine-4-carboxylic acid was refluxed with 12 ml. thionyl chloride until completely dissolved (four and one-half hours). Excess thionyl chloride was removed under reduced pressure, five successive 10 ml. portions of anhydrous benzene being added to the residue. The resulting oil was considered to be sufficiently pure 2-methylthio-5-chloropyrimidine-4-carboxylic acid chloride to be used as such in the subsequent esterification.

The acid chloride was dissolved in 25 ml. anhydrous benzene, and freshly distilled β-diethylaminoethanol (5.73 gm., 2 moles per mole of acid), dissolved in 25 ml. benzene, was added slowly with stirring under anhydrous conditions. The initially vigorous reaction was completed by refluxing for five hours and the mixture was then allowed to cool to room temperature overnight.

β-Diethylaminoethanol hydrochloride (3.70 gm., 98.5% of theory) was separated as a by-product by filtration, and the benzene filtrates were washed with eight 50 ml. portions of water to pH 8.1 and dried with anhydrous

sodium sulphate. Evaporation of the solvent yielded 6.3 gm. (85% of theory) β -diethylaminoethyl-2-methylthio-5-chloropyrimidine-4-carboxylate, a brown oil which could not be brought to crystallization (the corresponding β -dimethylaminoethyl ester crystallized spontaneously, m.p. 120–121° C.).

The above basic ester (3:15 gm.) was dissolved in 25 ml. anhydrous ether and an equimolecular amount (0.38 gm.) of dry hydrogen chloride in ether solution was added. The resulting gummy precipitate was repeatedly washed with ether, dried *in vacuo*, dissolved in 20 ml. hot methanol, treated with a little decolorizing carbon, filtered, and crystallized by addition of 75 ml. ether to the filtrate, giving the crude hydrochloride, m.p. 176–177° C. (decomp.), recrystallized from methanol–ether to yield 91% of theory of the pure compound, m.p. 183° C. (decomp.).

Further samples of the basic ester were treated in ether solution with large excesses of methyl bromide or methyl iodide, keeping the mixture at 60° for four days followed by several days at room temperature. The precipitates were purified as above by dissolving in methanol, treating with decolorizing carbon, and crystallizing by addition of ether. The methobromide was thus obtained with m.p. 159–160° C. and the methiodide with m.p. 153–154° C.

ACKNOWLEDGMENTS

The authors would like to thank Dr. C. I. Chappel for the pharmacological screening and Mr. W. J. Turnbull for the microanalytical data.

REFERENCES

1. BUDĚŠÍNSKÝ, 2. Collection Czechoslov. Chem. Commun. 14: 223. 1949.
2. McOMIE, J. F. W. and WHITE, I. M. J. Chem. Soc. 3129. 1953.

LIGHT ABSORPTION STUDIES

PART V. THE RELATION OF MESOMERIC EFFECTS AND ULTRAVIOLET LIGHT ABSORPTION SPECTRA¹

By W. F. FORBES AND AUDREY S. RALPH

ABSTRACT

A method for the determination of *mesomeric* effects from ultraviolet light absorption data is critically discussed. For halogen-substituted compounds, the method gives an order of *mesomeric* effects different from that which is usually accepted for the halogens.

INTRODUCTION

It was noted in Part II (16) of this series that the spectra of *para*-substituted benzoic acids may be related to the *mesomeric* but not to the *inductive* effect of the substituent group. It was shown in particular that both wavelength displacements towards longer wavelengths and intensities of absorption (ϵ) for the halogen-substituted compounds were in the order $-I > -Br > -Cl > -F$.

Electronic spectra, like other physical properties, would be expected to require consideration primarily of the ground states of molecules; these will determine the excited states, and the main difference between the ground and excited states will be that the proportion of contributing forms will vary. Thus the electron-displacement effects which we chiefly have to take into account will be the *inductive* and the *mesomeric* (or resonance) effect. We use these terms to indicate the different types of electron displacements and the terms do not necessarily correspond to the usage with which they have been associated in other fields of study (cf. discussion section). We propose to designate as *inductive* effects, electronic interactions which are proportional to the electronegativities of the atoms concerned, and which decrease with the distance between the two interacting centers. By the *mesomeric* effect (or resonance effect) we shall designate electronic interactions which give rise to what has been termed resonance forms. The latter, therefore, would be equal, for example, for *ortho*- and *para*-methylacetophenones, since the contributing resonance structures are generally assumed to be similar. Both *inductive* and *mesomeric* effects will consequently affect both ground and electronic excited states, and it is the purpose of this paper to present a self-consistent picture of the changes observed in halogen-substituted benzenes.

Normally, a shift to longer wavelength accompanied by increased intensity of absorption represents a "closing-up" of electronic levels of the ground and excited states and thus a decrease in transition energy. Since the excited states have been shown (cf. 21) to be mainly dipolar, these dipolar forms will contribute more to the excited than to the ground states. This "closing-up" of the energy levels therefore represents a more ready formation of excited states. Hence, the data show that the dipolar states are attained more easily in the

¹Manuscript received April 27, 1958.

Contribution of the Memorial University of Newfoundland, St. John's, Newfoundland.

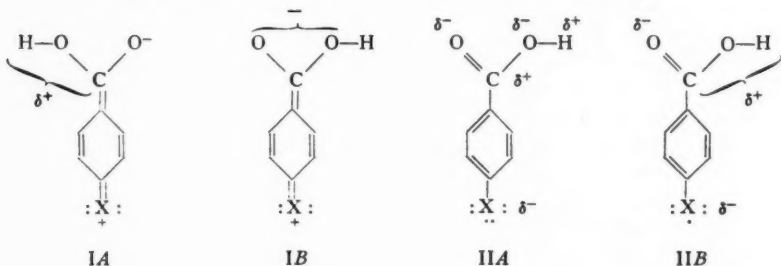
order $-I > -Br > -Cl > -F$, that is the potential energy of the excited states is lowered in the order $-I > -Br > -Cl > -F$. Since it is conclusively established that *inductive* effects are in the order $-F > -Cl > -Br > -I$ (20, 23, and references cited therein), which would indicate the reverse order of the observed effects, one is led to the conclusion that the *mesomeric* effect may account for the observed data. This supposes the *mesomeric* effect to be in the order $-I > -Br > -Cl > -F$, again the reverse of the accepted order (20), but the evidence for the *mesomeric* effects being in the order $-F > -Cl > -Br > -I$ appears to be far less conclusive than the evidence for the *inductive* effects.

Further, *inductive* effects, which are generally supposed to decrease rapidly as the distance between the two chromophores increases, would not be the same in the *ortho*- and *para*-positions. Yet spectral data indicate (13) that in the absence of steric effects, spectra obtained from *ortho*- and *para*-substituted compounds are similar.

This then points to conjugation, or resonance, effects and in particular to the *mesomeric* effect as the explanation of the observed changes. The present communication examines some of the implications in assuming the spectral changes to be due to the *mesomeric* effect, this being in the order of $-I > -Br > -Cl > -F$.

ULTRAVIOLET ABSORPTION SPECTRA

The B-band of halogen-substituted benzoic acids in the ultraviolet region may be correlated with transitions involving mainly dipolar excited states. These may be crudely represented by structures of type I (illustrating *mesomeric* effects) and by structures of secondary importance (type II; illustrating *inductive* effects, that is involving electrostatic influences of the valency electrons of the halogen atom only).



The values for the *mesomeric* effects which may be thus obtained for halogens and other atoms or groups can then be directly compared with the accepted values, as established by the evidence of dipole moments and chemical equilibria.

By using *para*-disubstituted compounds, not only are *inductive* effects minimized but steric effects may be neglected as a first approximation. There is some evidence for second-order effects under the latter heading (15), since

minor steric effects probably operate even in *para*-disubstituted compounds, because of the adjoining hydrogen atoms. Under the heading of *inductive* effects also, a large number of second-order effects suggest themselves, for example, *inductive* effects of the halogen atom directly on the carboxyl-group or intermolecular *inductive* effects. However, it has already been shown that *inductive* effects generally must be small; this was deduced from the similarity of *ortho*- and *para*-disubstituted benzene derivatives, in the absence of steric effects (cf. Table I of Part III (13)). This therefore leads to the conclusion that most of these second-order *inductive* effects similarly play only a minor part in determining transition energies.

Another argument against the predominance of *inductive* effects, even in the spectra of *meta*-disubstituted compounds, is provided by the relevant data of benzoic acids and acetanilides (16). It is found that in the *meta*-substituted compound, where the *mesomeric* effect by definition is small, the spectrum generally resembles that of the parent compound. Consequently, if the *inductive* effect is of little importance in determining the transition energies of *meta*-compounds, it seems reasonable to suppose it to be even less for the corresponding *para*-isomers.

A further reason why induced polarization may be regarded as small is that in fluoro-substituted compounds, where the *inductive* effect should be greatest, hardly any change is observed by comparison with the parent compound (see Table II). This argument is strengthened by the fact that any steric effect of the fluorine atom is small and thus second-order steric factors cannot readily be postulated to oppose any *inductive* effects.

It is of interest to note at this stage that similar relationships, namely resemblances between *ortho*- and *para*-disubstituted benzene derivatives, are not observed for dissociation constants. Thus while it may now be taken as established that the B-band of *para*-halogen substituted compounds is determined predominantly by the *mesomeric* effect, a similar relationship does not follow for the other physical properties under consideration.

The relevant spectra in absolute ethanol are collected in Table I. The $\Delta\lambda$ values, where $\Delta\lambda = \lambda_2 - \lambda_1$, and λ_2 and λ_1 represent the locations of maximal absorption of the main absorption bands of *para*-halogen substituted and parent compounds respectively, are shown in Table II.

TABLE I
MAXIMA ($M\mu$) OF B-BANDS OF COMPOUNDS $p\text{-R.C}_6\text{H}_4\text{X}$

R	X =									
	H		F		Cl		Br		I	
	λ	ϵ	λ	ϵ	λ	ϵ	λ	ϵ	λ	ϵ
—COOH (16)	227	11,000	228	11,000	234	15,000	238.5	16,000	252	17,000
—H (4, 11)	203.5	7,400	204	6,200	210	7,500	210	8,600	226	13,000
—NHCOCH ₃ (16)	242	14,500	240	13,000	249	18,000	252	18,500	254	23,000
—N(Me) ₂ (24)	250	13,600	247	12,300	259	17,000	260	19,600	—	—
—COCH ₃ (15)	240	12,500	242	11,500	249	16,000	253	16,000	262	16,000
—CHO (15)	244	13,000	245	12,000	254	15,000	257	16,000	—	—

TABLE II
 $\Delta\lambda$ VALUES IN $M\mu$ FOR *para*-HALOGEN SUBSTITUTED COMPOUNDS
 DESCRIBED IN TABLE I

R	X =			
	F	Cl	Br	I
—COOH	1	7	11.5	25
—H	0.5	6.5	6.5	22.5
—NHCOCH ₃	—2	7	10	12
—N(Me) ₂	—3	9	10	—
—COCH ₃	2	9	13	22
—CHO	1	10	13	—

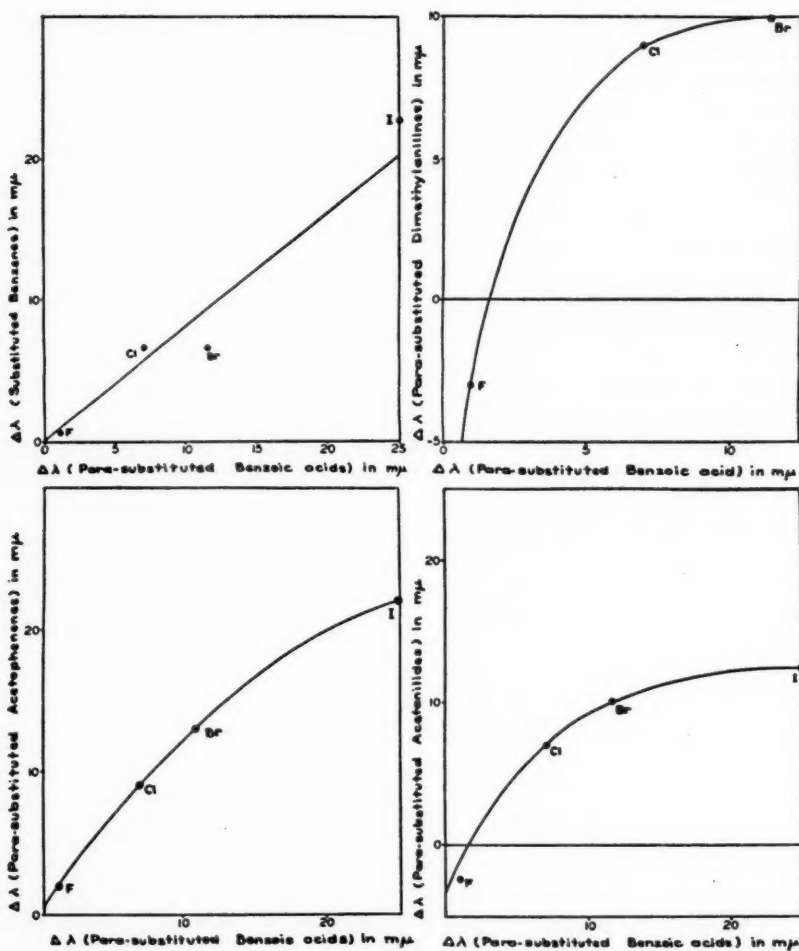


FIG. 1.

The $\Delta\lambda$ values for substituted benzenes, *para*-substituted acetophenones, *para*-substituted acetanilides, and *para*-substituted N,N-dimethylanilines are also compared with the $\Delta\lambda$ values obtained for the corresponding benzoic acids in Fig. 1.

Fig. 1 and Table II show that *mesomeric* effects are of approximately the same significance in halogen-substituted benzenes and in *para*-halogen substituted benzoic acids, acetophenones, and benzaldehydes. The slopes of the approximately straight lines thus obtained are about 45° , indicating equal displacements for the above-mentioned compounds due to *mesomeric* effects. The corresponding acetanilides and N,N-dimethylanilines, compared with benzoic acids, generally suggest slopes initially greater than 45° , but flattening out considerably towards the larger iodine atom (see Fig. 1).

A tentative interpretation of these observations may now be made. The *mesomeric* effect is caused in benzoic acids, benzaldehydes, and acetophenones primarily by the halogen atom; in the presence of a nitrogen atom, because of its unshared electrons additional conjugation enhances the congestion of electrons in the *para*-positions and this causes:

(I) A greater *mesomeric* interaction, since the effect is now able to operate more extensively (cf. also the different *mesomeric* moments obtained from dipole moment data (2)).

(II) An increase of second-order steric effects, due to interaction of the halogen atom with the now increased electron density. This becomes appreciable with the bulky iodine atom and may explain the anomalously low value for *p*-iodo-N,N-dimethylaniline.

It may be noted that in Table II and Fig. 1, wavelength changes rather than changes in the observed intensities have been chosen as the measure of electrical effects. Although both give the correct order, since the increased *mesomeric* effect also gives rise to increased transition probability, wavelength changes are more conveniently converted into energy values. Further there is evidence (cf. 12, 13, 14) that values of transition probabilities as measured by the absorption intensity (ϵ) are more susceptible to small steric effects, and other second-order interactions.

Another recent interesting example has been provided by the spectra of α' -halogen-substituted 4-methoxy-4'-methyldiphenyls (see Table III).

TABLE III
MAXIMA ($m\mu$) OF B-BANDS OF COMPOUNDS $p\text{-MeO.C}_6\text{H}_4\text{.C}_6\text{H}_4\text{.CH}_2\text{X}$
ACCORDING TO BURAWOY AND SPINNER (8), AND $\Delta\lambda$ VALUES FOR
THESE AND *para*-SUBSTITUTED BENZOIC ACIDS

X	λ	ϵ	$\Delta\lambda$	$\Delta\lambda$ (Benzoic acids)
H	260	23,600	0	0
Cl	271	23,000	11	7
Br	277	23,500	17	11.5
I	291	23,500	31	25

Although Burawoy and Spinner (8) explain the spectral changes by the "polarizability" of substituents, the spectra of these diphenyls also fit in well with our assumption. The $\Delta\lambda$ changes of the diphenyls are proportional to other $\Delta\lambda$ changes already described and hence to the proposed *mesomeric* effects. This example also emphasizes the advantages of considering wavelength changes rather than absorption intensities, since here the intensities are fairly close together.

The example finally reinforces the assumed steric hindrance of the iodine atom since the iodine atom in α' -iodo-4-methoxy-4'-methyldiphenyl is separated by a methylene group from the phenyl group, consequently causing considerably less steric interaction. In accordance with our hypothesis, the steric effect associated with high electron densities around the halogen atom is no longer observed, and the $\Delta\lambda$ value for the iodo-compound concurs with the expected value.

DISCUSSION

Both dipole moment and acid dissociation data have been extensively used to obtain values for the *mesomeric* effect of the halogen atoms (1, 2, 3, 17, 18, 19, 20, 26, 27). From both these methods it is difficult to obtain consistent results for the *mesomeric* effect and this may be ascribed primarily to the difficulty of obtaining a suitable reference compound (both dipole moment data and dissociation constant data are determined by ground states which unlike electronic spectra cannot be adequately described in terms of *mesomeric* and steric effects alone). Secondly, solvent effects play a large part in both methods, and this type of interaction does not appear to have been fully elucidated. These difficulties become appreciable on closer examination (such an examination has been carried out, but has been excluded from this paper for the sake of brevity), and it may be concluded that dipole moment data and acid dissociation data provide a less satisfactory method than ultraviolet absorption data for determining values of *mesomeric* effects.

An indication in favor of our argument may, however, be obtained from the graphs (see Fig. 2), which show reasonable agreement between the changes due to *mesomeric* effects obtained from acidity constant data (cf. 20) and those from light absorption data.

On plotting $\Delta\lambda$ values against values of the acidity constants, similar curves are obtained, namely, initially almost straight lines with a distinct "bending" or "flattening-out" towards the iodine value. This "flattening-out" has been ascribed previously to second-order steric factors and an analogous interpretation is proposed for the effect in this instance. This would suggest that acidity constants are more susceptible to steric effects than are light absorption spectra, an observation which will be referred to again (see below).

Also noteworthy is the consideration that reaction rate constants are less likely to yield accurate values of *mesomeric* effects, since the interaction of two or more molecules will introduce additional variables. For example, since the orienting influence of a group in chemical substitution may depend on polarizability factors called into operation upon the approach of a reactive

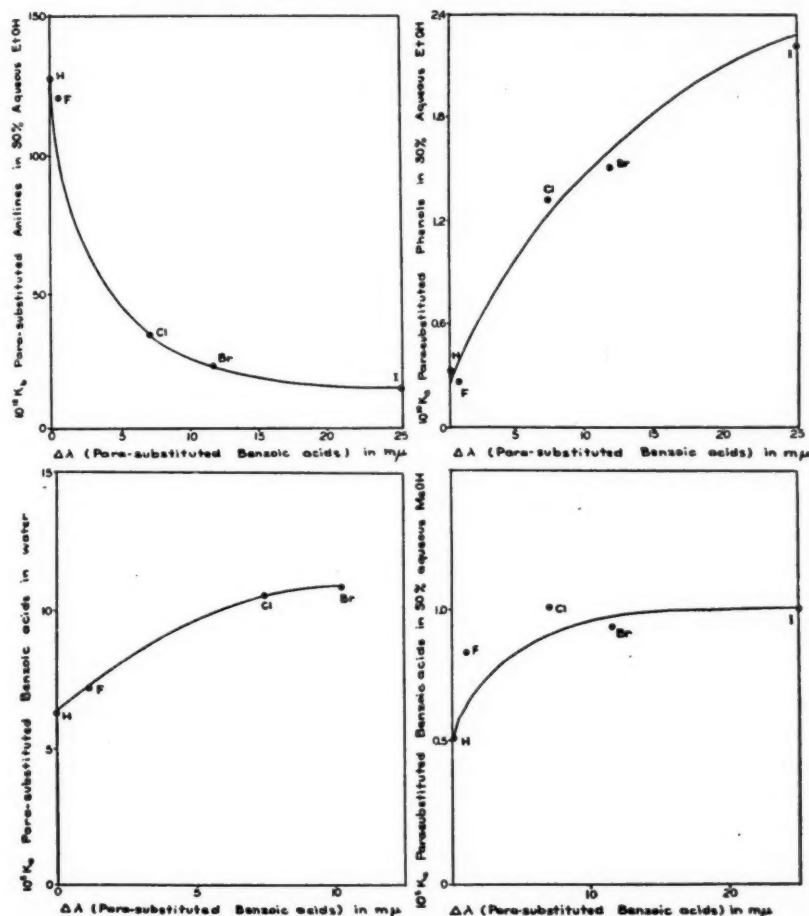


FIG. 2.

center, there is no assurance that the result is a measure of the electronic situation in the "resting molecule", as normally measured in dilute solution spectra. Nevertheless, the following conclusions seem to emerge from the data presented so far:

1. Information indicating the existence and relative magnitude of *mesomeric* effects can be obtained from reaction rates, dipole moment data, equilibrium constants, light absorption data, and other physical constants. Whether the *mesomeric* effect involves a disturbance of electrons from one atom to another, as has been proposed in the classical conception of mesomerism, or merely an *inductive* electron displacement, as has been suggested by Burawoy and others (cf. 7, 8, 22, 25), perhaps cannot be decided conclusively. If, however,

the latter hypothesis is so formulated as to suggest a decreased interaction as the distance between the chromophores increases—and so predict a dissimilarity in *ortho*- and *para*-substituted compounds—it must be deemed the less satisfactory explanation of the observed phenomena. Some recent theoretical examinations on spectral properties of alkyl-substituted compounds also suggest that energy shifts resulting from *inductive* effects *alone* will be positive, thus leading to hypsochromic shifts (9, 10). Therefore it may be concluded that normally whenever an over-all bathochromic shift occurs, the bathochromic shift due to the *mesomeric* effect must be of larger magnitude than any *inductive* effect.

2. It seems an unjustified assumption to associate the *mesomeric* effect in different compounds with one and the same dipolar excited state. For example, while one particular dipolar excited state, such as *IA*, may well be associated with the *mesomeric* effect in certain compounds, other dipolar structures, such as *IB*, may become more important on introducing other substituents. This lack of uniformity is illustrated by a recently described effect in the spectra of substituted benzaldehydes and acetophenones. There, the *para*-methyl group reduces steric interaction in 2,4,6-trimethylbenzaldehyde and 2,4-dimethylacetophenone, but increases it in 2,4,6-trimethylacetophenone (5). This phenomenon was ascribed to additional conjugation, *either* overcoming *or* further enhancing steric interactions already present. This explanation may incidentally be used to relate two other phenomena previously referred to in this paper. First, it was noted that slight steric interactions, of the type postulated in chemical equilibria, do not show up as well in light absorption properties (see Fig. 2). This may be because light absorption properties involve, to a larger extent, excited states in which the slight steric hindrance is more readily overcome (see also Fig. 3). Secondly, it was observed that a fluorine-substituted compound, with respect to the parent compound, may cause a slight negative wavelength shift (see Table II). This negative shift may now be tentatively explained by saying that the halogen atom cannot always immediately exert its *mesomeric* effect, if the latter is small. This tendency would again be more pronounced in excited states and may result in, at first, a positive energy displacement (hypsochromic shift), until the positive *mesomeric* effect becomes sufficiently large to lower again the potential energy of the excited state (or in other words, until the more usual electronic excited state again predominates).

3. The relative importance of *mesomeric* effects appears to be quite different, in properties like dipole moment and acidity constant data on the one hand, and in light absorption properties on the other. The chief difference between the two sets of properties, from our point of view, appears to be that only light absorption data involve transitions to excited states, which are largely dipolar in character. Because of the nature of these excited states, one would expect them to be more susceptible to *mesomeric* effects. Consequently, the apparent preponderance of *mesomeric* effects in light absorption data of the halogens—as evidenced from the observed wavelength changes in conjunction with the proposed order of *mesomeric* effects, and from the identity of some *ortho*- and *para*-isomers—is perhaps not surprising.

It may therefore be postulated that *mesomeric* interaction in ultraviolet light absorption is only of secondary importance in ground states and that the potential energy levels of ground states for the *para*-halogen substituted compounds are roughly equal (cf. dipole moment data and dissociation constants). In excited states *mesomeric* effects will predominate, and it is suggested that the representation of the transitions involved is approximately as shown in Fig. 3.

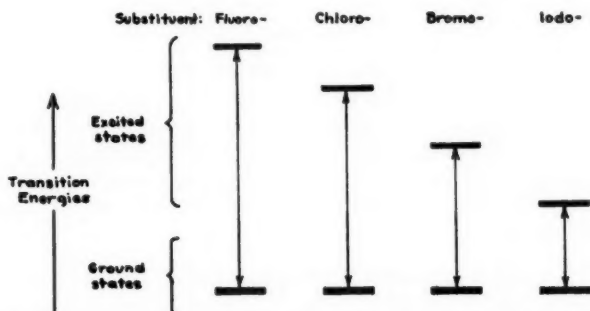


FIG. 3. Schematic representation of transitions in *para*-halogen benzoic acids after Braude and Waight (6):

Fig. 3 illustrates why the *mesomeric* effect is readily identified in light absorption data, and why it is much less easily identified from dipole moment data and acid dissociation data.

4. Although it is questionable how a knowledge acquired about *mesomeric* effects in the excited state is applicable to ground states and vice versa, a simple semiquantitative interpretation of *mesomeric* effects in the excited state is attempted. Thus it may be hoped that when the percentage of dipolar forms in the excited and ground states have been calculated, it will be possible to obtain measures of the *mesomeric* effects in various ground states.

In the meantime, the wavelength changes for halogen-substituted benzenes and *para*-halogen substituted benzoic acids have been used to evaluate the approximate energy gains associated with *mesomeric* effects in these compounds. These values are recorded in Table IV. It may be noted that on the

TABLE IV
APPROXIMATE POTENTIAL ENERGY GAINS (IN KCAL./MOLE) IN THE
PHOTO-EXCITED STATE OF HALOGEN-SUBSTITUTED BENZENES AND
BENZOIC ACIDS DUE TO MESOMERIC EFFECTS

Substituent	Wavelength changes in $m\mu$ (see Table II)		Approx. energy gain (in kcal./mole)
	Benzenes	Benzoic acids	
-F	1	0.5	0.5
-Cl	7	6.5	4
-Br	11.5	6.5	5
-I	25	22.5	13

basis of very simplified calculations the change in dipole moments from fluoro- to iodo-benzenes due to *mesomeric* effects, according to the values reported by Groves and Sugden (18, the latest available gas-phase values), amounts to an energy change of only approximately 3 kcal./mole. This, as expected, is much less than the value obtained from Table IV (approximately 13 kcal./mole), and confirms the hypothesis that *mesomeric* interactions in ultraviolet absorption spectra mainly affect the electronic excited states.

EXPERIMENTAL

Except for minor deviations in procedure, the compounds, the spectral properties of which were not previously known, were prepared by standard methods as described in the literature. Purification was effected by distillation under vacuum and was deemed adequate when redistillation resulted in no further measurable change in the absorption spectrum.

The spectra were determined on a Unicam SP 500 spectrophotometer using standard methods.

ACKNOWLEDGMENTS

The authors gratefully acknowledge a research grant from the National Research Council of Canada and a research fellowship (to A.S.R.) sponsored jointly by the following organizations: The Geological Survey of Newfoundland (Department of Mines and Resources), the Newfoundland and Labrador Corporation, and the British Newfoundland Corporation.

REFERENCES

1. AUDSLEY, A. and GOSS, F. R. *J. Chem. Soc.* 497. 1942.
2. BENNETT, G. M. and GLASSTONE, S. *Proc. Roy. Soc. (London)*, A, 145: 71. 1934.
3. BETTMAN, B., BRANCH, G. E. K., and YABROFF, D. L. *J. Am. Chem. Soc.* 56: 1865. 1934.
4. BOWDEN, K. and BRAUDE, E. A. *J. Chem. Soc.* 1068. 1952.
5. BRAUDE, E. A. and SONDHEIMER, F. *J. Chem. Soc.* 3754. 1955.
6. BRAUDE, E. A. and WRIGHT, E. S. *Progress in stereochemistry. Edited by W. Klyne. Butterworth Scientific Publications, London.* 1954. p. 143.
7. BURAWOY, A. and SPINNER, E. *J. Chem. Soc.* 2085. 1955.
8. BURAWOY, A. and SPINNER, E. *J. Chem. Soc.* 2557. 1955.
9. COULSON, C. A. *Proc. Phys. Soc., A*, 65: 933. 1952.
10. CRAWFORD, V. A. *J. Chem. Soc.* 2061. 1953.
11. DOUB, L. and VANDENBELT, J. M. *J. Am. Chem. Soc.* 69: 2714. 1947.
12. FORBES, W. F. and MUELLER, W. A. *Can. J. Chem.* 33: 1145. 1955.
13. FORBES, W. F. and MUELLER, W. A. *Can. J. Chem.* 34: 1340. 1956.
14. FORBES, W. F. and MUELLER, W. A. *Can. J. Chem.* 34: 1347. 1956.
15. FORBES, W. F., MUELLER, W. A., and RALPH, A. S. Unpublished information.
16. FORBES, W. F. and SHERATTE, M. B. *Can. J. Chem.* 33: 1829. 1955.
17. GROVES, L. G. and SUGDEN, S. *J. Chem. Soc.* 971. 1935.
18. GROVES, L. G. and SUGDEN, S. *J. Chem. Soc.* 1992. 1937.
19. INGOLD, C. K. *Rec. trav. chim.* 48: 797. 1929.
20. INGOLD, C. K. *Structure and mechanism in organic chemistry. Cornell Univ. Press, Ithaca, N.Y.* 1953.
21. MULLIKEN, R. S. *J. Chem. Phys.* 7: 121. 1939.
22. PARR, R. G. and PARISER, R. *J. Chem. Phys.* 23: 711. 1955.
23. REMICK, A. E. *Electronic interpretations of organic chemistry. John Wiley & Sons, Inc., New York.* 1950.
24. REMINGTON, W. R. *J. Am. Chem. Soc.* 67: 1838. 1945.
25. SCHUBERT, W. M. and SWEENEY, W. A. *J. Org. Chem.* 21: 119. 1956.
26. SUTTON, L. E. *Proc. Roy. Soc. (London)*, A, 133: 668. 1931.
27. WATSON, H. B. *Modern theories of organic chemistry. Oxford University Press, London.* 1949.

THE REACTIONS OF ACTIVE NITROGEN WITH METHANE AND ETHANE¹

BY P. A. GARTAGANIS AND C. A. WINKLER

ABSTRACT

Reinvestigation of the active nitrogen-methane reaction in the temperature range 45° to 500°C. has confirmed hydrogen cyanide as the only product, other than hydrogen, formed in measurable amounts. An "induction" effect in the hydrogen cyanide production was observed with increase of methane flow rate. This induction decreased with increase of temperature and was shown to be due to concomitant hydrogen atom reactions, since it could be eliminated by addition of hydrogen atoms to the reaction mixture. Reinvestigation of the active nitrogen-ethane reaction over the temperature range -100° to 475°C. also confirmed hydrogen cyanide to be the only measurable product, other than hydrogen, of that reaction. There was some indication that an induction effect was present with ethane, as with methane, and it may be concluded tentatively that both reactions are carried substantially by hydrogen atom reactions.

INTRODUCTION

In a previous study in this laboratory (7), it was observed that the Arrhenius plot for the reaction of active nitrogen with neopentane showed a marked change of slope, indicative of two activation energies in the range of temperatures used. While there was some reason to believe that this behavior might be due to two reactive species in active nitrogen, one of which is almost certainly atomic nitrogen (4, 5), there remained the possibilities that it resulted from concomitant hydrogen atom reactions or from different rates of attack by a single species in active nitrogen at the primary and quaternary carbon atoms in the neopentane molecule. Since methane and ethane are incapable of suffering such different modes of attack, the reactions of active nitrogen with these two hydrocarbons have been reinvestigated over a wider range of conditions than those used previously (3), in an effort to examine further the possible significance of the two activation energies observed with neopentane.

EXPERIMENTAL

The investigations were made with conventional fast-flow techniques. In many experiments with methane, hydrogen atoms were introduced simultaneously with nitrogen atoms. The arrangement for doing this is illustrated in Fig. 1, which, with the accompanying legend, serves also to indicate all the essential details of the apparatus currently used in this laboratory for studies on active nitrogen reactions. When necessary, the reaction vessel was surrounded by an electrically heated furnace molded from asbestos or by a plastic vessel to contain an appropriate refrigerant.

The nitrogen discharge tube was operated by a 110 v.-5000 v. transformer which fed through a diode rectifier (Raytheon, 866-A-GAA) and a 2000 ohm resistance into two condensers in parallel (each 4 μ f., 6000 v., Aerovox No. 3).

¹Manuscript received June 22, 1958.

Contribution from the Physical Chemistry Laboratory of McGill University, Montreal, Quebec, with financial assistance from the National Research Council of Canada.

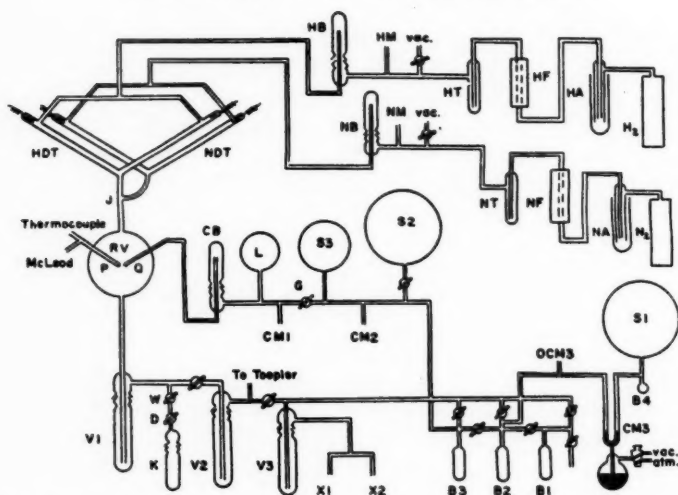


Fig. 1. Diagram of apparatus.

HA, NA: Manostats to control hydrogen and nitrogen inlet pressures. HF, NF: Furnaces filled with copper turnings at 450°C. to remove oxygen from the hydrogen and nitrogen streams. HT, NT: Liquid nitrogen traps to remove water and CO₂ from the hydrogen and nitrogen. HM, NM: Manometers to measure stream pressures. HB, NB: Calibrated capillary flow meters for hydrogen and nitrogen. HDT, NDT: Hydrogen and nitrogen discharge tubes with aluminum electrodes. J: Connecting tube, 20 cm. long, 1.8 cm. diam. RV: Reaction vessel (300 cc.), "poisoned" with phosphoric acid. P: Thermocouple. B1, B2, B3: Bulbs for condensed hydrocarbon. S1: Hydrocarbon storage vessel (5 liters). S2, S3: Calibrated hydrocarbon storage vessels (1100 cc. and 400 cc. respectively). CM1, CM2, CM3: Manometers to measure pressures in hydrocarbon storage vessels. G: Scratched stopcock to maintain constant pressure of hydrocarbon in ballast volume, L. CB: Calibrated flow meter for hydrocarbon. Q: Hydrocarbon jet. V1, V2, V3: Liquid nitrogen product traps. K: Absorber (to contain appropriate solution). X1, X2: Two Cenco "Megavac" pumps (or a single "Hypervac" pump).

These discharged across the discharge tube four to six times per second, depending on the operating pressure. The hydrogen discharge tube circuit was similar, but a variable transformer was inserted in the 110 v. line to permit controlled variation of the discharge frequency in the hydrogen discharge tube.

Hydrogen cyanide was estimated quantitatively by condensing it over frozen potassium hydroxide in the absorber, K, followed by titration of the cyanide with standard silver nitrate after the contents of the absorber had been allowed to come to room temperature.

RESULTS

Methane

Only about 1% of the methane reacted at 45°C., (comparable with the possible amount of impurities present), but significant reaction occurred above 280°C. At 358°C. and 450°C., the reaction showed a striking feature hitherto unobserved in active nitrogen reactions. The yield of hydrogen cyanide was low at low flow rates of methane, but increased rather rapidly as the

methane flow was increased. At sufficiently high flow rates, the HCN yield became constant at a given temperature, presumably after all the available active nitrogen was consumed. Typical of the results that were obtained in numerous experiments are those shown in Fig. 2. For convenience, the acceleration in hydrogen cyanide production with increased methane flow rate will be designated as an "induction", but it should be realized that it is not an induction period in the usual sense since it is not a function of time but of concentration.

Hydrogen cyanide was the only product of the reaction obtained in measurable quantities over the range of temperatures used. No cyanogen, ammonia, or hydrazine could be detected by usual analytical methods, and the mass spectrometer failed to show more than possible traces of substances that might have been C_2 and C_3 hydrocarbons or cyanogen.

It was suspected that the induction in the reaction might be caused by fast reaction of active nitrogen with methyl radicals derived from attack of methane by atomic hydrogen produced in the initial reaction with active nitrogen. The reaction of methane with active nitrogen in the presence of added molecular and atomic hydrogen was therefore studied in some detail. A large number of experiments were made, the results of which may be summarized briefly to illustrate the behavior observed.

In preliminary experiments in which molecular hydrogen was added to the active nitrogen stream before it entered the reaction vessel, pronounced induction remained. This was also true at temperatures up to $330^\circ C$. when a relatively low concentration of atomic hydrogen was added, (low voltage across HDT, Fig. 1), although at higher temperatures ($513^\circ C$.) this low H atom concentration did cause almost complete disappearance of the induction.

Complete elimination of the induction was achieved with a higher concentration of H-atoms, the total pressure of hydrogen being greater than that of nitrogen. However, the maximal hydrogen cyanide yield was now quite low. Experiments were then made to determine whether the absence of the induction could be maintained without sacrificing the hydrogen cyanide yield. This was finally accomplished by suitable adjustment of the relative concentrations of atomic hydrogen and active nitrogen admitted to the reaction vessel. A final series of experiments was then made at $480^\circ C$., with all conditions rigorously controlled, to confirm that the behavior indicated by the many previous experiments could be associated with the operating conditions used, and especially that elimination of the induction was possible for different levels of hydrogen cyanide yield. The primary of the hydrogen discharge circuit was set first at 50 v., then at 100 v., and the hydrogen cyanide yields determined at different methane flow rates in the presence of molecular and atomic hydrogen with the nitrogen pressure greater than and less than that of hydrogen. The results are shown in Fig. 3.

When molecular hydrogen was present at a pressure *lower* than the pressure of nitrogen, some induction could be observed, but when atomic hydrogen was introduced under otherwise similar conditions the induction was eliminated for a relatively high yield of hydrogen cyanide. When the pressure of hydrogen was *greater* than that of nitrogen, no induction was observed under any of the

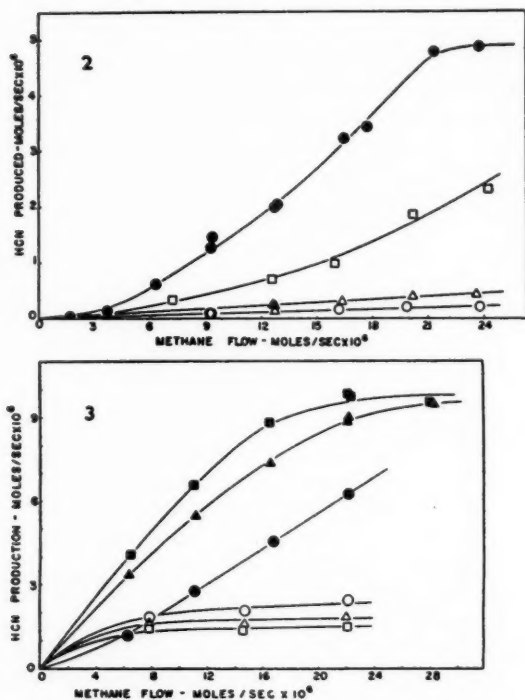


FIG. 2. Relation between hydrogen cyanide production and methane flow rate. Temperature, °C.: \circ 45 ± 3 , \triangle 280 ± 2 , \square 358 ± 5 , \bullet 441 ± 6 .

FIG. 3. Hydrogen cyanide production as a function of (a) methane flow rate, (b) voltage in the primary circuit of the hydrogen discharge tube, and (c) relative pressures of nitrogen and hydrogen in the reactions methane-active nitrogen, and methane-active nitrogen-hydrogen (molecular or atomic).

Temperature, 480°C.

Pressure:

Voltage in primary of
hydrogen discharge
circuit:

N₂ high, H₂ low
 \bullet No discharge
 \blacktriangle 50 v.
 \blacksquare 100 v.

N₂ low, H₂ high
 \circ No discharge
 \triangle 50 v.
 \square 100 v.

operating conditions, and the yield of hydrogen cyanide was quite low. Elimination of the induction in the presence of molecular hydrogen, i.e. without the hydrogen discharge in operation, was immediately traced to back diffusion of hydrogen into the nitrogen discharge tube under the pressure differential that prevailed. The characteristic reddish color of the hydrogen discharge was observed near the base of the nitrogen discharge tube, and undoubtedly enough hydrogen atoms were produced to eliminate the induction. It might be noted that the order of the curves in Fig. 3 was reversed when the relative pressures of nitrogen and hydrogen were reversed. Also, substitution of helium for hydrogen, under comparable conditions, had no effect on the induction, i.e. there was no effect of merely increasing the total pressure in the system.

Ethane

Regardless of ethane flow rate or temperature, hydrogen cyanide was the only gaseous product obtained in measurable amounts from this reaction. No cyanogen, ammonia, or hydrazine was detected chemically or mass spectrometrically. At temperatures below room temperature, small amounts of a dark brown polymer were deposited in the reaction vessel and the main trap.

The relation between hydrogen cyanide production and ethane flow rate over the temperature range $-100^{\circ}\text{C}.$ to $475^{\circ}\text{C}.$ is shown in Fig. 4. For the data recorded in Fig. 4A, no attention was given to the temperature of the

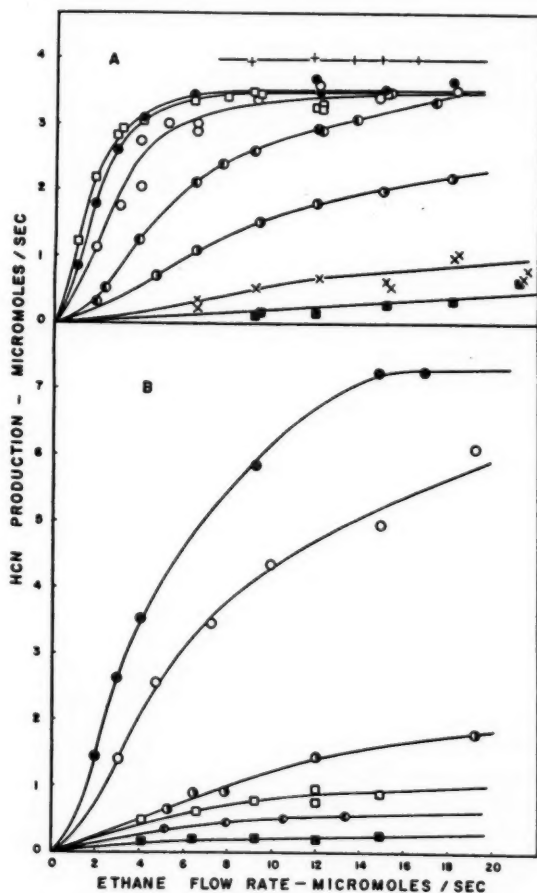


FIG. 4. Relation between hydrogen cyanide production and ethane flow rate.

Temperature, $^{\circ}\text{C}.$:

A: \blacksquare -100 , \times -50 , \odot 55 , \bullet 175 , \circ 298 , \bullet 400 , \square 475 , (+ Ethylene at 300°C)

B: \blacksquare -50 , \bullet 3 , \square 50 , \bullet 122 , \circ 253 , \bullet 404 .

tube that connected the reaction vessel to the discharge tube. For the data of Fig. 4B, however, the lower half of this connecting tube was surrounded by appropriate refrigerant for the low temperature experiments; also, for these experiments, a new discharge tube and reaction vessel were used, and the active nitrogen concentration, estimated by reaction with ethylene (2, 6, 8), was about twice that in the experiments which yielded the data of Fig. 4A.

DISCUSSION

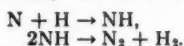
Methane

In the earlier investigation of the reaction of methane with active nitrogen (3), it was concluded that the production of hydrogen atoms in the initial attack on the methane molecule probably had little influence on the yield of hydrogen cyanide. However, the earlier experiments were made for the most part in the neighborhood of 400°C., and with a limited range of methane flow rates. The results of the present study leave little doubt that the reaction is, in fact, carried to a considerable extent by hydrogen atoms, probably by the following sequence of reactions:



There is little doubt that reaction [3] occurs with a low activation energy (1) and is very fast. Hence, as the methane flow rate is increased and reaction [2] increases in significance relative to recombination of hydrogen atoms, the hydrogen cyanide yield might be expected to show the induction effect observed. Addition of hydrogen atoms should, of course, eliminate the induction by accentuating the contribution of reaction [3] at all flow rates.

The reversal in the order of the curves in Fig. 3, and the drastic change in hydrogen cyanide yield that may be caused by addition of hydrogen atoms, suggest that hydrogen atoms may deactivate active nitrogen, possibly by



Owing to the induction effect, no reliable estimate of the activation energy of the methane-active nitrogen reaction was possible, but calculations (3) confined to low flow rates of methane, where secondary reactions are presumably minimal, gave an activation energy of about 13 kcal. and a steric factor of about 10^{-2} (cf. $E = 11$ kcal., $P = 5 \times 10^{-3}$ from Ref. 3). In these calculations, the concentration of active nitrogen was assumed to be given by the maximum yield of hydrogen cyanide obtained in the reaction with ethylene (2, 6, 8). In view of its complicating features, the reaction of methane with active nitrogen would appear to give no information about the possible presence of two active species in active nitrogen.

Ethane

It is, perhaps, impossible to state categorically whether an induction effect is present or absent in the ethane-active nitrogen reaction. While a small

induction has been drawn into some of the curves of Fig. 4, the magnitude of the effect is of the same order as the experimental error in determining the HCN yields from different experiments. (No attempt was made to establish the presence or absence of an induction by addition of hydrogen atoms, as in the experiments with methane, since such experiments are much more difficult and capable of less precision than those with a single discharge tube.) Since utmost care was taken with the experiments, it seems likely that an unequivocal result may not be possible with the present method of studying the reaction.

If second order rate constants are calculated for the different temperatures (2), and the Arrhenius lines plotted, the results of Fig. 4 lead, in both cases, to activation energies of approximately 2.7 and 6 kcal. in the temperature ranges -100°C. to about 150°C. , and 150°C. to 475°C. , respectively. The corresponding steric factors are of the order 10^{-4} and 10^{-2} .

The two activation energies may be attributed either to concomitant hydrogen atom reactions or to the presence of more than one chemically active species in active nitrogen. Of the two explanations, the first is probably to be preferred in view of the demonstrated effect of hydrogen atoms in the methane reaction.

REFERENCES

1. ARMSTRONG, D. A. and WINKLER, C. A. *Can. J. Chem.* 33: 1649. 1955.
2. BACK, R. A. and WINKLER, C. A. *Can. J. Chem.* 32: 718. 1954.
3. BLADES, H. and WINKLER, C. A. *Can. J. Chem.* 29: 1022. 1951.
4. EVANS, H. G. V., FREEMAN, G. R., and WINKLER, C. A. *Can. J. Chem.* 34: 1271. 1936.
5. EVANS, H. G. V. and WINKLER, C. A. *Can. J. Chem.* 34: 1217. 1956.
6. ONYSZCHUK, M., BREITMAN, L., and WINKLER, C. A. *Can. J. Chem.* 32: 351. 1954.
7. ONYSZCHUK, M. and WINKLER, C. A. *J. Phys. Chem.* 59: 368. 1955.
8. VERSTEEG, J. and WINKLER, C. A. *Can. J. Chem.* 31: 129. 1953.

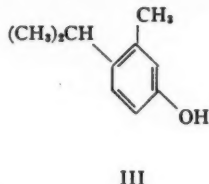
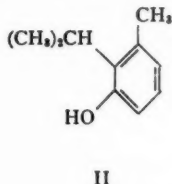
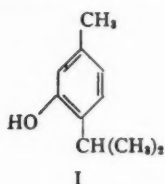
THE SYNTHESIS OF TWO ISOMERIC THYMOLS¹

By R. A. B. BANNARD AND L. C. LEITCH

ABSTRACT

2-Isopropyl-3-methylphenol has been synthesized and found to be identical with the isopropyl-3-methylphenol of m.p. 69° C. obtained from the isopropylation of *m*-cresol. 6-Isopropyl-3-methoxytoluene has been synthesized and found to be identical with the methyl ether of the isopropyl-3-methylphenol of m.p. 112° C., also obtained from the isopropylation of *m*-cresol.

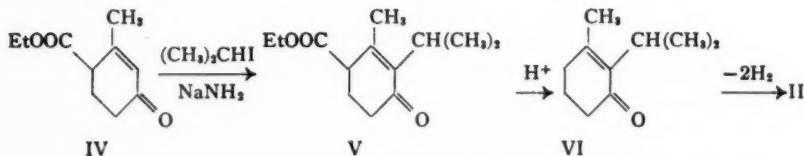
The alkylation of *m*-cresol with isopropyl alcohol in the presence of sulphuric acid reported by Chichibabine (4) and earlier workers gives, in addition to thymol (I), two isomers melting at 69° and 112° C. which were assigned the structures II and III respectively. On the basis of the orienting influences in



m-cresol and melting points, these formulae were probably correct. It seemed desirable, however, to confirm these structures either by degradation to known compounds or by independent synthesis.

The first course was not successful. All attempts to determine the location of the isopropyl group in II and III by oxidation of the methyl ethers to methoxyphthalic acids failed. The compounds were apparently completely oxidized by potassium permanganate as copious amounts of carbon dioxide were evolved on acidifying the reaction mixture and no organic compound could be isolated.

Alternatively, 2-isopropyl-3-methylphenol (II) was synthesized by the following reactions:



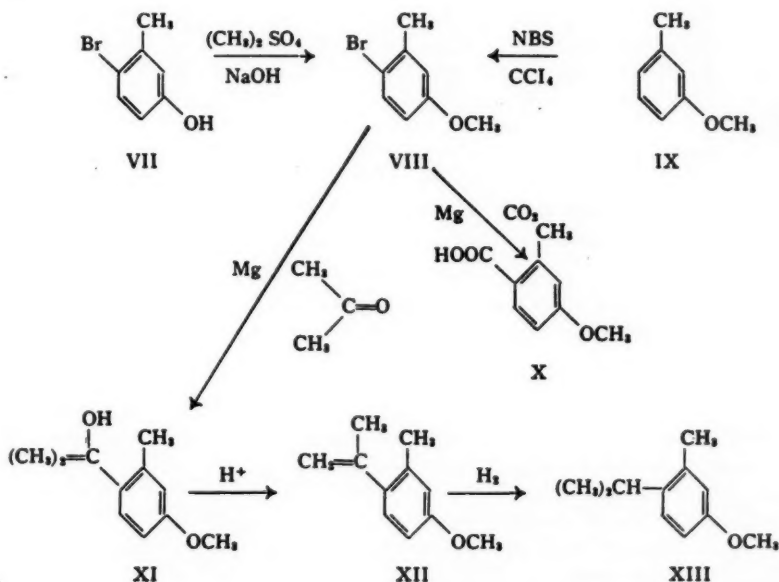
3-Methyl-4-carbethoxy-2-cyclohexene-1-one (IV), referred to as Hagemann's ester in the literature, was prepared from acetoacetic ester and trioxymethylene as described by Rouault and Smith (14). The sodio derivative of IV was

¹Manuscript received June 7, 1956.

Contribution from the Division of Pure Chemistry, National Research Council, Ottawa, Canada, and Defence Research Chemical Laboratories, Ottawa, Canada. Issued as N.R.C. No. 4071 and D.R.C.L. Report No. 217.

prepared from sodamide in liquid ammonia and alkylated therein with isopropyl iodide to 2-isopropyl-3-methyl-4-carbethoxy-2-cyclohexene-1-one (V) by the procedure of Horning, Horning, and Platt (10). Hydrolysis and decarboxylation of V as described by Horning, Denekas, and Field (9) gave 2-isopropyl-3-methyl-2-cyclohexene-1-one (VI). The semicarbazone of the ketone melted at 165–6° C. as reported by Dieckmann (7). Dehydrogenation of the ketone in mesitylene with palladized carbon according to the directions of Horning, Horning, and Walker (11) gave a small yield of a phenol, m.p. 68.5 to 69.5° C. Admixture of this compound with the isomer, m.p. 69–70° C., isolated from the isopropylation of *m*-cresol caused no depression in melting point. The infrared spectra of the two compounds were likewise identical. The structure II assigned to this isomer of thymol is therefore correct.

6-Isopropyl-3-methoxytoluene was in turn synthesized by the following sequence of reactions:



6-Bromo-3-methoxytoluene (VIII) was prepared in two ways: (a) by methylation of 3-methyl-4-bromophenol (VII) as described by Darzens and Levy (5); (b) by bromination of 3-methoxytoluene (IX) with N-bromosuccinimide by the procedure of Bannard and Latremouille (1). The orientation of the bromine atom in VIII upon which rests subsequent proof of the structure III was proved by Darzens and Levy (5) by converting the halide to 2-methyl-4-methoxybenzoic acid (X) via the Grignard reagent. The compounds obtained by the two routes were identical as shown by a comparison of their boiling points and refractive indices. Buu-Hoi (3) and Quelet and Paty (13) assigned

the same structure without proof to VIII prepared by bromination of 3-methoxytoluene (IX) with N-bromosuccinimide and bromine respectively.

The Grignard reagent prepared from 6-bromo-3-methoxytoluene (VIII) did not react with isopropyl bromide to give the expected 6-isopropyl-3-methoxytoluene. The result was surprising in view of the successful preparation of 6-*tert*-butyl-3-methoxytoluene from *tert*-butyl bromide and the same Grignard by Darzens and Levy (6). On treatment with acetone, however, the Grignard reagent gave a 45% yield of 2-(2-methyl-4-methoxyphenyl)-propanol-2 (XI) together with 38% of 6-isopropenyl-3-methoxytoluene (XII). The latter was undoubtedly formed by dehydration of the carbinol (XI) under the influence of iodine used to initiate the reaction. A similar instance has been reported recently by Edwards and Cashaw (8). 6-Isopropenyl-3-methoxytoluene was also obtained in 80% yield by dehydration of the carbinol (XI) with dilute sulphuric acid.

Hydrogenation of 6-isopropenyl-3-methoxytoluene (XII) with Adam's catalyst gave 92% of 6-isopropyl-3-methoxytoluene (XIII). Finally, methylation of the thymol isomer III yielded a product which has the same boiling point, refractive index, and infrared absorption spectrum as XIII. It must therefore be concluded that the isomer of m.p. 112° C. is 3-methyl-4-isopropylphenol.

EXPERIMENTAL*

A. Synthesis of 2-Isopropyl-3-methylphenol

3-Methyl-4-carbethoxy-2-cyclohexene-1-one (IV)

The ketoester was prepared in 40% yield by the directions of Rouault and Smith (14). After a small low-boiling fraction was collected, the pure ester distilled at 105–107° at 2 mm., n_D^{20} 1.4860.

2-Isopropyl-3-methyl-4-carbethoxy-2-cyclohexene-1-one (V)

For the alkylation of the ester IV the following modification of the method of Horning, Horning, and Platt (10) was used. The ketoester IV (25.7 gm., 0.14 mole) was added dropwise from a separatory funnel to sodamide prepared from 4.4 gm. of sodium and 125 ml. of liquid ammonia. The ammonia was allowed to evaporate during stirring and addition of 50 ml. of dry toluene. Isopropyl iodide (27.0 gm., 0.17 mole) was now added and the reaction mixture heated just below refluxing overnight. It was treated with a little ethanol and then poured into water. The toluene layer was washed with water and then dried over a small quantity of anhydrous calcium chloride. Most of the toluene was removed under 50 mm. pressure. The ester was then fractionated under 3 mm. in a small Vigreux column with total condensation – partial take-off still head. The main fraction of alkylated ketoester was collected between 115° and 119° C. at 3 mm. Yield: 15.0 gm. (60%), n_D^{20} 1.4868.

The semicarbazone separated from a solution of 1 gm. each of the ketoester, semicarbazide hydrochloride, and sodium acetate in dilute ethanol after it had been left to stand for a day. After one recrystallization from dilute ethanol–

*All melting points are uncorrected.

water the semicarbazone melted at 203–204° C. Calc. for $C_{14}H_{23}N_3O_2$: C, 59.75%; H, 8.24%; N, 14.94%. Found: C, 60.21%; H, 8.36%; N, 15.13%.

2-Isopropyl-3-methyl-2-cyclohexene-1-one (VI)

The ketoester V (14.0 gm.) was hydrolyzed and decarboxylated by treating it successively with alcoholic sodium hydroxide and sulphuric acid as reported by Horning, Denekas, and Field (9). Fractional distillation of the ketone after it had been washed and dried in ether gave 6.7 gm. of product, b.p. 94–97° C. at 14 mm., n_D^{20} 1.4888. The semicarbazone prepared as described above melted at 165–166° C. after one recrystallization from ethanol–water. Dieckmann (7) gives 167–168° C. as the melting point of the semicarbazone.

2-Isopropyl-3-methylphenol (II)

The dehydrogenation of VI was carried out as described by Horning, Horning, and Walker (11) except that the palladium adsorbed on carbon was prepared from palladium chloride (1.0 gm.), carbon black (10.0 gm.), and formaldehyde (12). Five grams of 2-isopropyl-3-methyl-2-cyclohexene-1-one (VI) was heated under reflux for two hours with 1.5 gm. of the dehydrogenation catalyst in 20 ml. of mesitylene. The supernatant liquid was decanted and extracted with 5% aqueous sodium hydroxide. On acidification of the aqueous extract a small amount of oily material which crystallized on being cooled and stirred was precipitated. It was taken up in pentane and crystallized therefrom on slow evaporation. The crystals melted at 68–69.5° C. The melting point was unchanged by admixture with the isomer of m.p. 69° isolated from the isopropylation of *m*-cresol.

B. Synthesis of 6-Isopropyl-3-methoxytoluene

3-Methoxytoluene (IX)

3-Methoxytoluene (IX) was prepared by the method of Ullmann and Uzbachian (15). Yield 70.0%, b.p. 61–63° C. at 10 mm., n_D^{20} 1.5123. The infrared spectrum of this substance was identical with that reported by Barnes *et al.* (2).

3-Methyl-4-bromophenol (VII)

3-Methyl-4-bromophenol (VII) was obtained in approximately 50% yield by the method of von Walther and Zipper (16). It melted at 62.5–63.5° C.; von Walther and Zipper (16) report m.p. 62° C.; Darzens and Levy (5), 63° C.

6-Bromo-3-methoxytoluene (VIII)

(a) *From 3-methyl-4-bromophenol (VII).*—3-Methyl-4-bromophenol (VII) (32.8 gm., 0.175 mole) was dissolved in 15% sodium hydroxide (40 cc.) in a 150 cc. beaker equipped with a teflon-covered magnetic stirring bar, thermometer, and burette. The stirred solution was treated at 40° C. with dimethyl sulphate (45.0 gm., 0.357 mole) in one portion. The temperature rose rapidly to 87° C., and the solution turned acidic, became turbid, and separated into two layers. The mixture was treated with small portions of 15% sodium hydroxide (approximately 3 cc. per addition) until no further acidic reaction was evident

(10 min., 36.5 cc.). Stirring was continued for a further 40 min. by which time the temperature had fallen to 35° C. The oily layer was taken up in ether (50 cc.), the aqueous phase extracted with ether (4×50 cc.), and the combined extracts dried over anhydrous magnesium sulphate (25 gm.). The ether solution was decanted, the ether removed by evaporation on the steam bath, and the residue distilled *in vacuo* yielding 18.1 gm. (51.4%) of 6-bromo-3-methoxytoluene (VIII) as a pale yellow oil, b.p. 104.5–106° C. at 10 mm., n_D^{20} 1.5609. (Quelet and Paty (13) report b.p. 111–112° C. at 15 mm., n_D^{20} 1.5593; Darzens and Levy (5) report b.p. 112° C. at 14 mm.) 4,6-Dibromo-3-methoxytoluene, 6.8 gm., m.p. 74–75° C., was obtained as by-product (Quelet and Paty (13) report m.p. 77° C.) together with 6.4 gm. of 3-methoxytoluene (IX).

(b) *From 3-methoxytoluene (IX).*—3-Methoxytoluene (IX) (61.0 gm., 0.500 mole) and carbon tetrachloride (80 cc.) were mixed in a 300-cc. round-bottomed flask and N-bromosuccinimide (89.0 gm., 0.500 mole) added in small portions. No evolution of heat occurred. The flask was fitted with a reflux condenser equipped with a calcium chloride guard-tube and the mixture heated by means of a "glascol" heating mantle. As soon as the solvent began to boil, a vigorous reaction occurred, making it necessary to replace the heating mantle by a cold water bath. After the initial vigorous reaction subsided, the mixture was heated under brisk reflux for six hours. The mixture was allowed to stand overnight and the precipitated succinimide removed by suction filtration and washed with carbon tetrachloride (3×20 cc.). The filtrate was concentrated by distillation at atmospheric pressure and the residue fractionated *in vacuo* yielding 89.0 gm. (88.1%) of 6-bromo-3-methoxytoluene (VIII) as a colorless oil, b.p. 104–105.5° C. at 10 mm., n_D^{20} 1.5610.

2-(2-Methyl-4-methoxyphenyl)-propanol-2 (XI)

A Grignard reagent was prepared in a conventional nitrogen-swept Grignard apparatus by addition of 6-bromo-3-methoxytoluene (VIII) (44.2 gm., 0.220 mole) in anhydrous ether (75 cc.) over a period of 3.5 hr. to magnesium turnings (4.86 gm., 0.200 gm-atom) covered with anhydrous ether (20 cc.) after the reaction had been initiated by addition of a small portion of the halide together with a crystal of iodine. The light brown reagent was heated under reflux for a further hour, then treated with a solution of acetone (11.6 gm., 0.200 mole) in anhydrous ether (15 cc.) over a period of 30 min. The reaction was exothermic and reflux was controlled by the rate of addition. Twenty minutes after the addition had been in progress the clear light brown solution deposited a pale yellow complex to form a very viscous mixture which became more fluid again by the time addition was complete. The mixture was heated under reflux for 15 min., allowed to stand overnight under nitrogen, and hydrolyzed by addition of saturated ammonium chloride solution (30 cc.) over a period of 30 min. The pale yellow solution was separated from the granular colorless solid by filtration and the latter washed with anhydrous ether (4×50 cc.). The combined filtrate and washings were dried over anhydrous magnesium sulphate (15 gm.). The ether solution was decanted and the drying agent washed with anhydrous ether (4×50 cc.). The ether was re-

moved by heating on the steam bath and the residue was distilled *in vacuo* yielding 28.4 gm. of a mixture of oil and crystals, b.p. 100–130° C. at 10 mm. Separation of the crystals by filtration and further purification by recrystallization from 60–70° petroleum ether gave 16.2 gm. (45.0%) of 2-(2-methyl-4-methoxyphenyl)-propanol-2 (XI), m.p. 66–67° C. Calc. for $C_{11}H_{16}O_2$: C, 73.30; H, 8.95%. Found: C, 73.73; H, 9.03%. The infrared spectrum of this substance showed strong hydroxyl absorption at 3.0 μ .

The residual oil, 12.2 gm. (38.0%), n_D^{25} 1.5237, b.p. 99–102° C. at 11 mm., was subsequently identified as 6-isopropenyl-3-methoxytoluene (XII).

6-Isopropenyl-3-methoxytoluene (XII)

2-(2-Methyl-4-methoxyphenyl)-propanol-2 (XI) (5.40 gm., 0.0300 mole) and 90% sulphuric acid (10 cc.) were placed in a 35-cc. round-bottomed flask equipped with a teflon-covered magnetic stirring bar and reflux condenser. The mixture was heated under reflux with stirring for six hours, cooled, and extracted with peroxide-free ether (4×10 cc.). The ether extract was washed with 5% sodium bicarbonate solution (10 cc.), then with water (2×10 cc.), and dried over anhydrous magnesium sulphate (5 gm.). The ether solution was decanted and the desiccant washed with anhydrous ether (4×10 cc.). The solutions were combined and concentrated by distillation on the steam bath. The residue was transferred to a 10-cc. pear-shaped modified Claisen flask and distilled *in vacuo* yielding 3.92 gm. (80.8%) of 6-isopropenyl-3-methoxytoluene (XII) as a colorless oil, b.p. 94.5° C. at 9 mm., n_D^{25} 1.5243. Calc. for $C_{11}H_{14}O$: C, 81.45; H, 8.70%. Found: C, 81.27; H, 8.83%. The infrared spectrum of this substance showed strong terminal methylene group absorption at 11.1 μ which disappeared on hydrogenation.

6-Isopropyl-3-methoxytoluene (XIII)

(a) *From 6-isopropenyl-3-methoxytoluene (XII).*—6-Isopropenyl-3-methoxytoluene (XII) (5.45 gm., 0.0336 mole) was placed in the reaction flask of a hydrogenator together with Adams' Catalyst (0.200 gm.) and absolute ethanol (100 cc.) and hydrogenated at atmospheric pressure. The reaction was complete in 13 min. The mixture was filtered to remove the catalyst, and the ethanol removed from the filtrate by distillation *in vacuo*. The residue was dissolved in anhydrous ether (50 cc.) and dried overnight over anhydrous magnesium sulphate (3 gm.). The orange solution was decanted and the desiccant washed with anhydrous ether (4×10 cc.). The combined ether solutions were evaporated on the steam bath, transferred to a 10-cc. pear-shaped modified Claisen flask, and distilled *in vacuo* yielding 5.09 gm. (92.3%) of colorless to amber colored oil, b.p. 98° C. at 9 mm., n_D^{25} 1.5081.

(b) *From 3-methyl-4-isopropylphenol (III).*—3-Methyl-4-isopropylphenol (III) (15.0 gm., 0.100 mole), m.p. 112–113° C., obtained from the isopropylation of *m*-cresol (4) was dissolved in 15% sodium hydroxide solution (25 cc.) in a 100-cc. beaker equipped with a teflon-covered magnetic stirring bar, burette, and thermometer. The stirred solution was treated at 40° C. with dimethyl sulphate (25.2 gm., 0.200 mole) added in one portion. The tempera-

ture rose rapidly to 82° C. and the solution became acidic and turbid and then separated into two layers. The mixture was treated with small portions (approximately 3 cc. per addition) of 15% sodium hydroxide until no further acidic reaction was evident (11 min., 18 cc.). The mixture was stirred for a further 30 min., transferred to a separatory funnel containing peroxide-free ether (25 cc.), and the ether layer separated. The aqueous phase was extracted with ether (3×25 cc.) and the combined ether solutions dried over magnesium sulphate (10 gm.). The ether solution was decanted, the desiccant washed with anhydrous ether (4×10 cc.), and the ether removed by evaporation on the steam bath. The residue was transferred to a 25-cc. pear-shaped modified Claisen flask and distilled *in vacuo* yielding 14.9 gm. (90.7%) of 6-isopropyl-3-methoxytoluene (XII) as a colorless oil, b.p. 98° C. at 9 mm., n_D^{25} 1.5083. Calc. for $C_{11}H_{16}O$: C, 80.46; H, 9.82%. Found: C, 80.56%; H, 9.90%. The infrared spectra of the 6-isopropyl-3-methoxytoluene (XIII) from 6-isopropenyl-3-methoxytoluene (XII) and from the isopropyl-3-methylphenol of m.p. 112–113° C. were measured as liquid films and found to be identical.

ACKNOWLEDGMENTS

The authors wish to thank Dr. S. F. MacDonald of the Division of Pure Chemistry for the use of his hydrogenation apparatus, and Dr. C. E. Hubley of Defence Research Chemical Laboratories for the infrared spectral analysis.

REFERENCES

1. BANNARD, R. A. B. and LATREMOUILLE, G. Can. J. Chem. 31: 469. 1953.
2. BARNES, R. B., GORE, R. C., LIDDEL, V., and WILLIAMS, Van. Z. Infrared spectroscopy. Reinhold Publishing Corporation, New York. 1944. p. 67.
3. BUU-HOI, Ng. PH. Ann. 556: 1. 1944.
4. CHICHIBABINE, A. E. and BARKOVSKY, C. Ann. chim. (Paris), 17: 316. 1942.
5. DARZENS, G. and LEVY, M. Compt. rend. 193: 292. 1931.
6. DARZENS, G. and LEVY, M. Compt. rend. 193: 321. 1931.
7. DIECKMANN, W. Ber. 45: 2697. 1913.
8. EDWARDS, J. D. and CASHAW, J. L. J. Org. Chem. 20: 847. 1955.
9. HORNING, E. C., DENEKAS, M. O., and FIELD, R. E. Org. Syntheses, 27: 24. 1947.
10. HORNING, E. C., HORNING, M. G., and PLATT, E. J. J. Am. Chem. Soc. 71: 1773. 1949.
11. HORNING, E. C., HORNING, M. G., and WALKER, G. N. J. Am. Chem. Soc. 71: 169. 1949.
12. MOZINGO, R. Org. Syntheses 26: 77, Method B. 1946.
13. QUELET, R. and PATY, M. Procès-verbaux séances soc. sci. phys. et nat. Bordeaux, 19. 1944–45.
14. ROUAULT, G. F. and SMITH, L. I. J. Am. Chem. Soc. 65: 631. 1943.
15. ULLMANN, F. and UZBACHIAN, J. B. Ber. 36: 1804. 1903.
16. VON WALTHER, R. F. and ZIPPER, W. J. prakt. Chem. [2], 91: 376. 1915.

ETHYLENE DIAMINE TETRAACETIC ACID AND CITRIC ACID AS ELUANTS IN ION EXCHANGE SEPARATION OF RARE EARTHS¹

BY F. W. CORNISH,² G. PHILLIPS, AND A. THOMAS

ABSTRACT

Studies of the distribution of rare earths between the cation exchange resin Zeokarb 225 and solutions of ethylene diamine tetraacetic acid (EDTA) show the existence of large separation factors between members of this series. However, column experiments show that the separation is poorer than with citric acid, probably because of a slow process occurring in the solution. The variation of column efficiency with distribution coefficient has been examined. Elution of europium with citric acid appears to be diffusion controlled, while that with EDTA is not. Further experiments with strontium indicate that its elution with both EDTA and citric acid is diffusion controlled. The results are in general agreement with Glueckauf's equation relating column variables with the height equivalent to a theoretical plate. Column irregularities appear to account for the very low diffusion constants calculated from this relation.

INTRODUCTION

Ordinary cation exchange resins are sufficiently selective to allow the separation of two cations possessing somewhat different ionic potentials by successive equilibration with a third ion. In the case of ions of the same charge and almost identical radii, e.g. the rare earths, the differences are so small that an almost impossibly large number of equilibrations would be required for complete separation. The effective selectivity can be increased by using complexing agents; in this way the ion which is least adsorbed by the resin undergoes the greatest complexing in the aqueous phase. Much of the selectivity under these conditions can be attributed to the complexing agents, making their choice of considerable importance. In the absence of any theory regarding the selection of such reagents it was thought that a very strongly complexing species might be expected to exaggerate the slight differences of basicity which exist between members of the rare-earth series. The distribution of rare earths between solutions of ethylene diamine tetraacetic acid (EDTA) and the cation exchanger Zeokarb 225 was therefore investigated.

The chromatographic technique employed in ion exchange separations depends on the quantities to be separated and the purity required. Large quantities are best separated by 'break through' or band displacement techniques. Several papers describing this approach using solutions of complexones have been published (4). Such methods always lead to overlapping of the bands, only a part of any one species being obtained 100% pure. Nevertheless tens or hundreds of grams can be adequately handled. Small quantities, of the order of a few milligrams, are best separated by the band elution technique, which under the correct conditions can lead to virtually total recovery of completely pure materials. The elution of traces of rare earths and strontium

¹Manuscript received May 9, 1958.

Contribution from the Chemistry Division, Atomic Energy Research Establishment, Harwell, England.

²Present address: Research Chemistry Branch, Atomic Energy of Canada Limited, Chalk River, Ontario.

by solutions of citrate and EDTA is examined in the present work in terms of the column variables.

The distribution coefficient (K_d) between solution and resin is given by (12)

$$[1] \quad K_d = \frac{(\text{quantity adsorbed on resin})(\text{volume of solution})}{(\text{quantity in solution})(\text{mass of resin})}$$

When the amount of solute adsorbed by the resin is less than about 2% of the resin capacity K_d is almost independent of solute concentration. Under these conditions the material is eluted from a column in an almost symmetrical peak (approximately a normal error curve, Fig. 1). Tompkins and Mayer

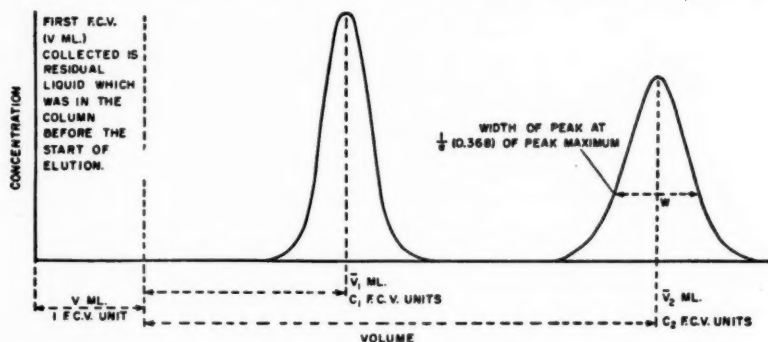


FIG. 1. Illustration of notation.

(13) have shown that the number of free column volumes of eluant required to elute the maximum of a peak is given by

$$[2] \quad C = \bar{v}/v = K_d(\text{mass of resin in column})/v$$

where \bar{v} has the significance shown in Fig. 1. The free column volume, v , is the total volume of the resin bed, v_T , less the volume of the resin. The bed distribution coefficient (K_b) is defined as

$$[3] \quad K_b = \frac{(\text{amount of solute adsorbed per ml. of bed})}{(\text{amount of solute per ml. of solution})}$$

This is identical with the D used by Kraus and Moore (8) and the K_d used by Glueckauf (5, 6). It can be shown that $K_b = fC$ where f is the fractional bed void, i.e. $f = v/v_T$. The degree of separation of two solutes by elution depends on the separation between peak maxima; a measure of this is given by the ratio of volumes required to elute each peak maximum, i.e. \bar{v}_2/\bar{v}_1 in Fig. 1. From above $\bar{v}_2/\bar{v}_1 = C_2/C_1 = K_{d_2}/K_{d_1} = K_{b_2}/K_{b_1}$, the separation factor, α ; this can be determined from equilibrium studies and is highly dependent on the complexing agent employed.

The degree of separation also depends on the widths of the eluted peaks. The physical parameters of the column system, e.g. flow rate and particle

size, usually exert more control on the width of the peak than does the complexing agent. In the present work the number of theoretical plates associated with an elution is derived from (5, 6)

$$[4] \quad N = 8(v + \bar{v})^2/w^2$$

where w is the width of the eluted peak at $1/e$ (0.368) of its maximum height in the same units as v and \bar{v} . The efficiency of a column elution can be measured in terms of the theoretical plates, for a greater number of equilibrium stages yields narrower peaks and therefore less overlapping.

EXPERIMENTAL

Equilibrium Distribution Experiments

These experiments were carried out by equilibrating known weights of resin with known volumes of solution containing 0.005 M EDTA, 0.14 M acetic acid, and a small amount of radioactive rare earth. Measurement of the radioactivity in the solution before and after equilibration furnished the data to calculate K_d from equation [1].

The resin, Zeokarb 225 (about 8% cross linked), a high capacity sulphonic acid type, was dry sieved 240–300 B.S.S. mesh. After 'fines' were removed by decantation it was washed several times with 3 M HCl and 3 M NH_4Cl solutions. A stock of this resin in the H^+ form was air dried and kept in a tightly stoppered bottle. By drying to constant weight at 105°C. it was found that the weight of air-dried resin was 1.51 times the weight of oven-dried resin.

Most of the radioactive tracers were obtained by thermal neutron irradiation of 'Specpure' rare-earth oxides; earlier experiments had shown the amount of contaminating activities to be negligible. The Ce^{144} was obtained from fission products. Experiments with dysprosium were performed with inactive material; the required concentrations were determined by a comparative radioactivation procedure involving the counting of solutions containing the 2.32 hr. Dy^{165} . The rare earths were stored as chlorides in dilute HCl solution.

Since EDTA is only slightly soluble at hydrogen ion concentrations required for reasonable K_d 's, acetic acid was added to provide greater buffering capacity. This is of considerable importance if attempts are made to separate all the rare earths by eluting with solutions of progressively higher pH values. A stock solution was prepared by dissolving a weighed quantity of EDTA in boiling water with the minimum of concentrated ammonia, diluting to the required volume, adding glacial acetic acid, and adjusting the pH with concentrated ammonia. Free EDTA slowly crystallizes from this solution at $\text{pH} < 2.94$. In order to preclude the presence of Cl^- ions (and hence associated NH_4^+ ions) the following procedure was adopted. The rare earth was adsorbed onto a small column of Zeokarb in the NH_4^+ form. After it had been washed with water it was eluted from the column with stock EDTA at pH 5. This eluate was mixed with stock EDTA at pH 3.5 to yield a rare-earth concentration of about 10^{-7} to 10^{-5} M . The pH was finally adjusted to between 4.5 and

5.0 with concentrated ammonia. Various known weights of air-dried resin (0.5 to 1.5 gm.) in the H^+ form were shaken with 15 ml. aliquots of this solution for 48 hr. This had been found to be ample time for equilibrium to be attained. The EDTA - rare earth stock and the final equilibrated solutions were analyzed by evaporating known weights on aluminum trays and β - γ counting with an end-window Geiger counter. Corrections for decay, dead time, and background were made where necessary. Measurements of pH were made with a 'Cambridge' bench type glass electrode assembly calibrated at pH 4.00 with 0.05 *M* potassium hydrogen phthalate. All experiments were carried out at room temperature.

The results for neodymium, typical of those for other rare earths, are shown in Table I. K_d values calculated from equation [1] on the basis of oven-dried

TABLE I
DISTRIBUTION OF NEODYMIUM BETWEEN 0.005 *M* EDTA PLUS 0.14 *M* ACETATE AND ZEOKARB 225 AS A FUNCTION OF pH AT 23°C.
Initial volume of solution = 15.0 ml.
Initial activity of stock solution = 3778 counts/min./gm.
Initial concentration of neodymium = 9×10^{-8} *M*

Weight of air-dried resin, gm.	Equilibrated solution		K_d	Corrected K_d
	counts/min./gm.	pH		
0.505	3910	4.33	0	0
0.533	3810	4.31	0	0
0.584	3940	4.28	0	0
0.613	3821	4.24	0	0
0.612	3800	4.24	0	0
0.679	3844	4.18	0	0
0.766	3636	4.11	1.1	1.9
0.805	3526	4.08	2.0	2.8
0.823	3386	4.05	3.2	3.9
0.860	3224	4.02	4.5	5.3
0.937	2776	3.94	8.7	9.5
1.003	1990	3.86	20.2	21
1.096	1230	3.74	42.6	45
1.159	588	3.63	105	108
1.291	198	3.48	322	324

resin are given in column 4. Above pH 4.11 the concentration of rare earth in solution after equilibration (counts/min./gm.) is slightly larger than for the original stock. If it is assumed that this occurs because of absorption of pure water by the originally air-dried resin, then it can be calculated that 1 gm. of air-dried resin absorbs about 0.5 gm. of water. Hence, a 'true' value for the volume of solution and a 'true' initial concentration can be obtained for each experiment. K_d 's calculated from equation [1] using these 'true' values and weights of oven-dried resin are given in column 5. All the results are summarized in Fig. 2; rare earths not examined are represented by broken lines.

Column Experiments

Elutions were carried out at room temperature and at 80°C. from columns of Zeokarb 225 using both EDTA and citric acid solutions. At room temperature europium and strontium were eluted separately; at 80°C. a mixture of

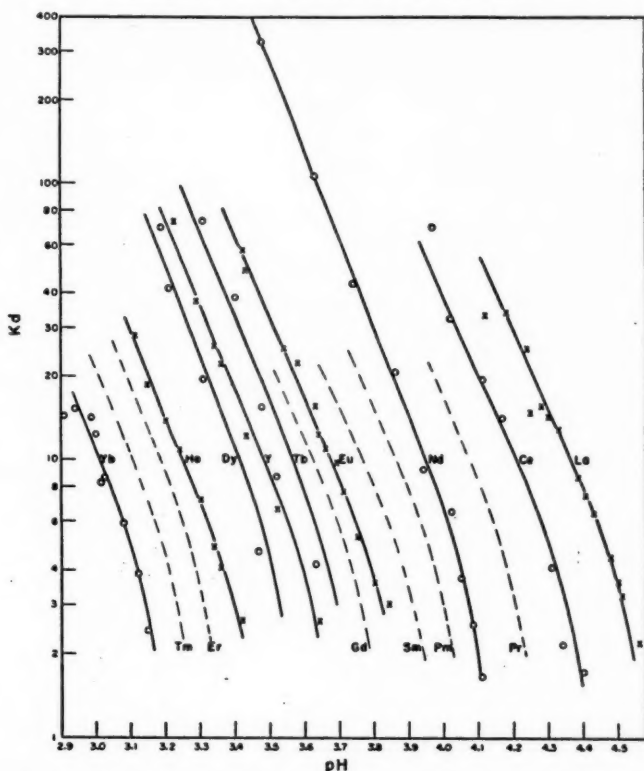


FIG. 2. Variation of distribution coefficient of rare earths between 0.005 *M* EDTA+0.14 *M* acetate and Zeokarb 225 as a function of pH.

lanthanum, cerium, and praseodymium was separated. In all cases β - γ active tracers were used and elutions were followed by measuring the radioactivity.

The Zeokarb 225 was wet-sieved in the NH_4^+ form to give a fraction which passed through a 300 B.S.S. sieve. The largest particles were selected from this fraction by repeated decantation, only those settling through 1 ft. of water in 40 min. being collected. Since 300 mesh corresponds to a particle radius of 0.0027 cm. the particles selected by decantation were estimated to have a mean radius of 0.0019 cm. This material was washed several times with 5 *M* HCl, then with slightly alkaline ammonium citrate solution, and finally with distilled water. The same batch of resin was used in all experiments.

Experiments at 80° were performed with a column 124 cm. \times 0.23 sq. cm. supported on a small pad of cotton wool. The temperature was maintained by refluxing alcohol in a surrounding jacket. A 6-ft. head of eluant was necessary to attain a flow rate of 0.069 ml./min. The effluent was passed through a short length of capillary tubing to a 2.5 cm. diameter planar spiral of thin-walled glass of internal diameter about 0.08 cm. and total volume 0.4 ml. This spiral

was held between two thin end-window Geiger tubes connected in parallel and mounted in a lead castle. Pulses from the Geiger tubes were fed to a ratemeter with a time constant of 10 sec. whose output was recorded continuously as a function of time.

Columns 40 cm. \times 1.0 sq. cm. were used for experiments at room temperature. The resin bed rested on a small pad of cotton wool nestling in the join of the glass tube with a 2 in. piece of capillary tubing. Solutions were fed in from a one liter separating funnel, and heads of between 6 in. and 5 ft. provided the different flow rates used.

All columns were packed by pouring an aqueous slurry of the resin into the column tubes which were already half full of water. The resin was allowed to settle freely, while the tubes were gently tapped at frequent intervals to assist close packing.

Before an experiment was begun the column was washed with the eluant until the pH of effluent and eluant were identical. It was then washed with water. Two separate portions of resin were removed from the top of the column, each having a settled volume of 0.5 ml. The active material was adsorbed onto one of these portions from dilute acid solution. It was then washed with a 0.5 *M* solution of ammonium chloride having a pH such that any resin in equilibrium with it would have the same $[\overline{NH}_4^+]/[H^+]$ ratio as would resin in equilibrium with the eluant. (This ammonium chloride solution was obtained by passing a 0.5 *M* solution of ammonium chloride through a separate bed of resin which had been exhaustively washed with the eluant.) The resin bearing the tracer was washed with water and then gently slurried on top of the column and allowed to settle, the original resin-water interface at the top of the column having first been made horizontal. The other 0.5 ml. portion of resin was carefully slurried on top, thus providing a protective layer over the tracer-carrying resin. After the water above the resin level had been removed the eluant was very carefully introduced to start the elution.

The position and nature of the eluted bands were obtained (a) at 80°C. by monitoring the spiral as described above, (b) at room temperature by using the spiral and by collecting each drop on a separate aluminum tray, evaporating to dryness, and counting each tray with a Geiger counter. Both methods gave the same result for the number of theoretical plates associated with any one elution. The free column volumes, *v*, were measured by determining the volumes of water required to wash through a small amount of the β - γ active I^{131} as iodide ion.

The activity in the eluant versus volume (or time) followed bell-shaped, symmetrical curves in the case of elutions with citrate and for elution of strontium with EDTA. Elution of rare earths with EDTA led to bell-shaped peaks which were relatively flatter and always had a drawn-out tail. This tail was much less pronounced at 80°C. Separations of Pr, Ce, and La at 80°C. are shown in Fig. 3. Results of other elutions are summarized in terms of theoretical plates, this number being calculated from equation [4].

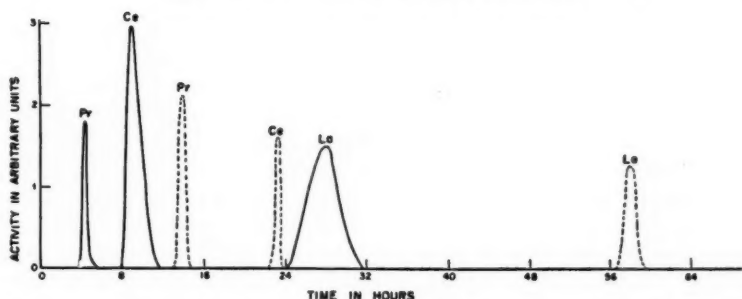


FIG. 3. Elution of 10^{-4} gm. cerium, 10^{-4} gm. praseodymium, and 10^{-6} gm. lanthanum from a column of Zeokarb 225 (particle radius = 0.0019 cm.), length 124 cm., area 0.23 sq. cm. at a flow rate of 0.069 ml./min. at 80°C . —0.005 *M* EDTA + 0.14 *M* acetate, pH 4.26; ----5% citrate, pH 3.65.

DISCUSSION

Fig. 2 shows the range of pH values over which EDTA solutions could be useful in cation exchange elution. Since the principal complexing species (10) over this range is H_2Y^{2-} (where H_4Y = EDTA) the equilibria involved are probably



where R denotes an equivalent of resin anion and M^{3+} denotes the trivalent rare-earth ion. An accurate analysis of the results in terms of these equilibria is not possible owing to the large increase of ammonium ion concentration (and hence ionic strength) with pH. This accounts for the slightly non-linear nature of the curves in Fig. 2. By using calculated activity coefficients for the aqueous components and assuming that the activity coefficient of the metal ion on the resin is a constant, the results have been compared with predictions from equations [5] and [6]. If the number of H^+ ions involved in equation [5] is used as a parameter the data for each rare earth can be fitted by using values of this parameter between the extremes of 1.7 (Nd) and 2.4 (Ho). Since the complexing of rare earths by EDTA in this pH region is known to involve the liberation of two hydrogen ions (15) the above equations appear to offer a reasonable explanation of the observed distributions. The sequence of curves (Fig. 2) follows the sequence of atomic numbers. The quasi rare earth yttrium behaves with an apparent atomic number of 65.5. This is in accord with known complexity constants (15), although Vickery (14) places yttrium between dysprosium and erbium. Comparison of values of $\alpha (=K_a/K_{a_1})$ for any two rare earths with similar data for the citrate-Dowex 50 system (12) shows that a greater separation factor is to be expected in one equilibrium stage by using EDTA. Thus, in Fig. 3 the ratios of times to reach peak maxima for any pair of rare earths are higher for the elution with complexone than for the corresponding citrate separation. Data presented

by Mayer and Freiling (9) also show that EDTA offers greater separation factors than citric, lactic, and glycollic acids.

The number of theoretical plates is a measure of the effective number of equilibrium stages brought about by the non-equilibrium process of elution. The number of plates, and hence the degree of separation, is therefore controlled by the extent of equilibration in any section of the column. Earlier work has shown that the speed of ion exchange reactions is limited by diffusion of the participating species and not by the actual ion exchange process (1). The extent of equilibration in any horizontal slice of the column will therefore depend on the time spent by the solute in the slice. This time is directly related to K_b and the flow rate. At constant flow rate the number of plates should increase with K_b and tend to a limiting value at high K_b . This qualitative conclusion is borne out by the Sr-citrate, Sr-EDTA, and Eu-citrate experiments (Fig. 4). For such diffusion controlled elutions Glueckauf (5) has developed the following theoretical relation:

$$[7] \quad HETP = 1.64r + \frac{K_b}{(K_b + f)^2} \frac{0.142r^2\bar{F}}{D_s} + \left(\frac{K_b}{K_b + f} \right)^2 \frac{0.266r^2\bar{F}}{(1 + 70r\bar{F})D_L}$$

where $HETP \equiv$ height equivalent to a theoretical plate = length of column/ N , r = particle radius, \bar{F} = linear flow rate (ml. sq. cm./sec.), f = fractional bed void. The first term represents the theoretical minimum of the $HETP$ and arises from the finite size of the resin particles. The other terms represent contributions due to (a) diffusion within the resin particle (diffusion constant D_s) and (b) diffusion through the immobile liquid film pictured as surrounding each resin particle (diffusion constant D_L). For low values of K_b diffusion through the resin accounts for the greater part of the diffusion contribution to the $HETP$. The opposite is true for high values of K_b . The full lines in Fig. 4 were calculated from equation [7] using the following values of D_s and D_L (in $\text{cm.}^2 \text{sec.}^{-1}$).

	D_s	D_L
Europium (citrate elution)	1.7×10^{-8}	1.7×10^{-7}
Strontium (both citrate and EDTA elution)	2.7×10^{-8}	4.4×10^{-7}

In the present experiment ($70r\bar{F}) \ll 1$ so that with both K_b and r constant $HETP$ is a linear function of \bar{F} (Fig. 5). The slopes of these lines from the experimental points (0.23 ($K_b = 3$) and 0.37 min.^{-2} ($K_b = 0.6$)) are in good agreement with those calculated from equation [7] using the values of D_s and D_L given above (0.21 and $0.37 \text{ cm.}^{-2} \text{min.}^{-1}$ respectively). Further, the intercept at $\bar{F} = 0$ is close to $1.64r$ as required by equation [7]. However, despite this apparent agreement the diffusion constants are much smaller than might be expected. Thus Boyd and Soldano (3) find a diffusion constant of $2.2 \times 10^{-7} \text{ cm.}^2 \text{sec.}^{-1}$ for $\text{La}^{3+}\text{-Na}^+$ exchange in an 8% cross-linked sulphonic acid resin at 25°C. ; D_s for the Eu-citrate experiments, in which D_s refers to $\text{Eu}^{3+}\text{-NH}_4^+$ exchange in the resin, is 10-fold smaller. Again D_L might be

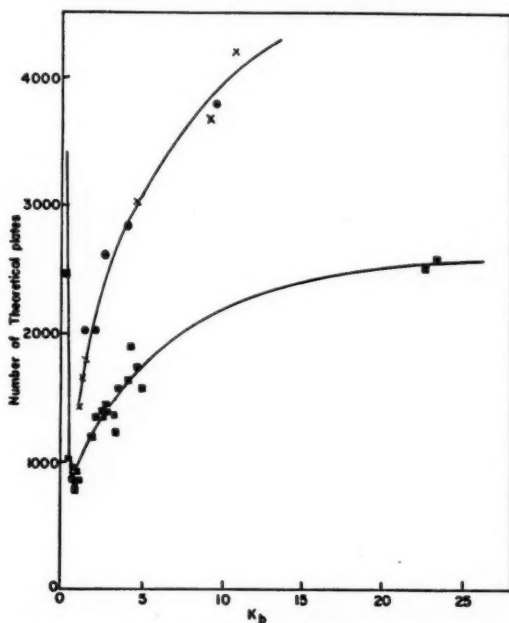


FIG. 4. Variation of number of theoretical plates with K_b using a column of Zeokarb 225 (particle radius = 0.0019 cm.), length 37 cm., area 1.0 sq. cm. at a flow rate of 0.10 ml./min. at room temperature. X elution of 10^{-4} gm. strontium with 0.10 M EDTA + 0.5 M acetate; ● elution of 10^{-4} strontium with 5% citrate; ■ elution of 0.015 mgm. of europium with 5% citrate.

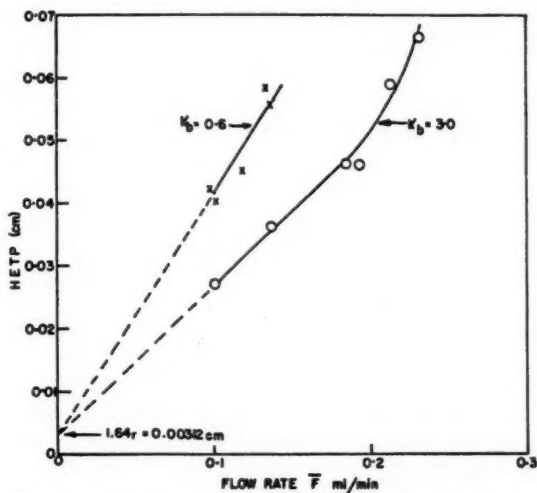


FIG. 5. Variation of HETP with flow rate for elution of 10^{-4} gm. of europium from a column of Zeokarb 225 (particle radius 0.0019 cm.), length 37 cm., area 1.0 sq. cm. with 5% citrate at room temperature.

expected to be about one third of the diffusion constants for the simple hydrated ions at infinite dilution because (a) the diffusing species are probably complexes, and (b) the ionic strength is high. On this basis we predict for the europium experiments $D_L \sim 2 \times 10^{-6}$, and for the strontium experiments $D_L \sim 3 \times 10^{-6}$ cm.² sec.⁻¹. These higher values of the diffusion parameters can be incorporated into equation [7] by assuming the first term to be too small. This is not unreasonable since this term must allow for any disturbances due to channelling, turbulence, as well as finite particle size (2). It should be pointed out that for the present experimental conditions the diffusional terms contribute considerably less to the *HETP* than the 'imperfections' term, which up to $\bar{F} \sim 0.2$ cm. min.⁻¹ must have the form "constant + $\phi \bar{F}$ " where ϕ is a function of K_b and r .

An interesting feature arises when K_b is very small. For $K_b < 0.3$ the apparent number of plates increases rapidly becoming, ideally, (length of column)/1.64 r at $K_b = 0$. This rise is 'false' in that very little interaction with the resin occurs; on the other hand it expresses the fact that the peak is very narrow. If the equation $N = 8\bar{v}(\bar{v}+v)/w^2$ were to be used (11), N would continue falling as K_b decreased from 0.3 becoming $N = 0$ at $K_b = 0$. While this would express the idea that the number of 'true' theoretical plates (i.e. equilibrations with the resin) is very small the use of such low values of N in cross-contamination calculations would lead to erroneously high results.

The decision to buffer the EDTA solutions with 0.42 *M* acetate was based on the results shown in Fig. 6. Despite this buffering, elution of europium with EDTA at room temperature invariably resulted in a small number of theoretical plates. The form of the variation of N with K_b at different EDTA concentrations is surprising (Fig. 7). The peak at $K_b = 1.3$ for 0.0125 *M* EDTA was reproducible although the precision in any single experiment was low. From these results it appears that the peak in the N versus K_b curve may move to a lower K_b with decreasing EDTA concentration. Low values for N were persistently obtained when eluting lutecium and when various concentrations of ammonium chloride were present in the eluting agent. It should be emphasized that these experiments involved the calculation of N from quite asymmetrical elution curves. Nevertheless the absence of a smooth variation of N with K_b suggests that diffusion is not the controlling feature. It seems possible that some slow chemical step occurs in the solution phase. This is supported by the observed slow exchange of ferric ions with the ferric-EDTA complex in aqueous solution (7). It was found that equilibrium was approached more slowly in the Eu-EDTA system than with Sr-EDTA, Sr-citrate, and Eu-citrate. The peak in the N versus K_b curve may perhaps be attributed to some fortunate combination of the rate determining factors. The number of theoretical plates would still be expected to increase with temperature. At 80°C. the rare earth-EDTA peaks are nearly symmetrical (Fig. 3) but the number of theoretical plates is still below that of corresponding citrate elutions (Table II). The calculated cross contamination (6) between lanthanum and cerium in Fig. 3 is slightly greater for EDTA than for citrate elution. It appears therefore that EDTA is somewhat inferior to citrate for the separation of traces of rare earths by ion exchange elution.

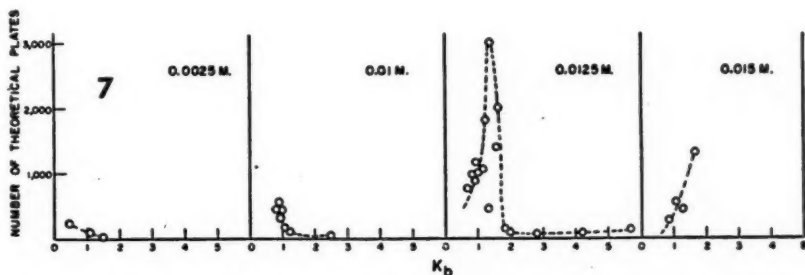
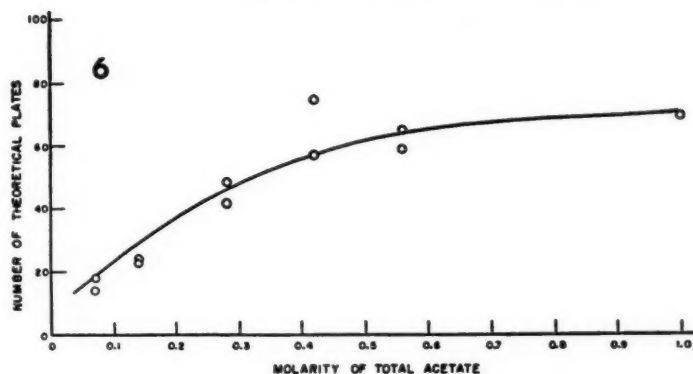


FIG. 6. Variation of number of theoretical plates with concentration of total acetate for elution of 10^{-8} gm. of europium from a column of Zeokarb 225 (particle radius 0.0019 cm.), length 40 cm., area 0.9 sq. cm. at a flow rate 0.10 ml./min. at room temperature with 0.005 *M* EDTA plus the concentration of total acetate shown.

FIG. 7. Variation of number of theoretical plates with EDTA concentration for elution of 10^{-8} gm. europium from a column of Zeokarb 225 (particle radius 0.0019 cm.), length 40 cm., area 0.9 sq. cm. at a flow rate of 0.10 ml./min., with 0.42 *M* total acetate plus the concentration of EDTA shown.

TABLE II

ELUTION OF TRACES OF Pr, Ce, AND La FROM COLUMN OF ZEOKARB 225 (PARTICLE RADIUS = 0.0019 CM.), LENGTH 124 CM., AREA 0.23 SQ. CM., WITH EITHER 5% CITRATE OR 0.005 *M* EDTA PLUS 0.42 *M* ACETATE, FLOW RATE 0.3 ML./SQ. CM./MIN. AT 80°C.

Solution	Pr		Ce		La		Ratio of K_b 's	
	K_b	<i>N</i>	K_b	<i>N</i>	K_b	<i>N</i>	Ce/Pr	La/Ce
EDTA pH 4.26	0.45	609	0.90	945	2.7	1270	2.0	3.2
EDTA pH 4.28	0.36	1005	0.85	410	3.2	470	2.4	3.8
Citrate pH 3.65	1.43	4750	2.7	7100	4.3	9550	1.9	2.7
Citrate pH 3.65	1.27	5520	—	—	6.3	6000	—	—

ACKNOWLEDGMENTS

The authors wish to thank Mr. A. A. Smales for many helpful discussions and the Director, A.E.R.E., for permission to publish this work.

REFERENCES

1. BOYD, G. E., ADAMSON, A. W., and MYERS, L. S., JR. *J. Am. Chem. Soc.* 69: 2836. 1947.
2. BOYD, G. E., MYERS, L. S., JR., and ADAMSON, A. W. *J. Am. Chem. Soc.* 69: 2849. 1947.
3. BOYD, G. E. and SOLDANO, B. A. *J. Am. Chem. Soc.* 75: 6091. 1953.
4. FITCH, F. T. and RUSSELL, D. S. *Can. J. Chem.* 29: 363. 1951. LORIER, L. and CARMINATI, D. *Compt. rend.* 237: 1328. 1953. SPEDDING, F. H. and POWELL, J. E. *J. Am. Chem. Soc.* 76: 2557. 1954. VICKERY, R. C. *J. Chem. Soc.* 4357. 1952.
5. GLUECKAUF, E. Declassified Rept. C/R 1356. 1954. U.K. Atomic Energy Research Establishment.
6. GLUECKAUF, E. *Trans. Faraday Soc.* 51: 34. 1955.
7. JONES, S. S. and LONG, F. A. *J. Phys. Chem.* 56: 25. 1952.
8. KRAUS, K. A. and MOORE, G. E. *J. Am. Chem. Soc.* 73: 9. 1951.
9. MAYER, S. W. and FREILING, E. C. *J. Am. Chem. Soc.* 75: 5647. 1953.
10. SCHWARZENBACH, G. and ACKERMAN, H. *Helv. Chim. Acta*, 30: 1798. 1947.
11. TOMPKINS, E. R. *J. Chem. Educ.* 26: 92. 1949.
12. TOMPKINS, E. R. and MAYER, S. W. *J. Am. Chem. Soc.* 69: 2859. 1947.
13. TOMPKINS, E. R. and MAYER, S. W. *J. Am. Chem. Soc.* 69: 2866. 1947.
14. VICKERY, R. C. *J. Chem. Soc.* 1895. 1952.
15. WHEELWRIGHT, E. J., SPEDDING, F. H., and SCHWARZENBACH, G. *J. Am. Chem. Soc.* 75: 4196. 1953.

THE SURFACE ENERGIES OF AMORPHOUS SILICA AND HYDROUS AMORPHOUS SILICA¹

BY STEPHEN BRUNAUER, D. L. KANTRO, AND C. H. WEISE

ABSTRACT

The total surface energies (or, more strictly, surface enthalpies) of amorphous silica and hydrous amorphous silica were determined by measuring the heats of solution in a mixture of nitric acid and hydrofluoric acid of samples having differing specific surface areas and bound water contents, and by measuring the surface areas by the B.E.T. method, using nitrogen as adsorbate. The molecular area of nitrogen was taken to be 16.2 \AA^2 at 77.3°K . The surface energy of amorphous silica of zero water content (or the energy of the pure siloxane surface) at 23°C . was found to be $259 \pm 3 \text{ ergs/cm}^2$. The heat of hydration by liquid water of the siloxane surface to silanol surface at 23°C . was found to be $258.6 \pm 13.0 \text{ cal./gm. of water}$. From these two values, with the added assumption that the molecular area of bound water was 25 \AA^2 , the surface energy of hydrous amorphous silica with a completely hydrated surface (or the energy of pure silanol surface) at 23°C . was calculated to be $129 \pm 8 \text{ ergs/cm}^2$. This value is only slightly greater than the surface energy of liquid water. Surface area determinations were also made by water vapor adsorption at 25°C . The packing of physically adsorbed water appeared to be determined by the geometry of the surface. The cross-sectional area of the adsorbed water molecule was found to be 12.5 \AA^2 . The density of amorphous anhydrous silica was 2.28 to 2.29 gm./cc . Silica particles having an average dimension of 37 \AA were dehydrated at lower temperatures and sintered at lower temperatures than particles having an average dimension of 64 \AA .

INTRODUCTION

The investigations described in this paper were preceded by an attempt to determine the surface energies of calcium silicate hydrates. The calcium silicate hydrates obtained in the hydration of tricalcium silicate, β -dicalcium silicate, and portland cements are colloids; consequently, the specific surface areas and surface energies of the hydrates play vital roles in determining many of their important structural characteristics. Powers and Brownyard (16) demonstrated highly significant correlations between the specific surface areas of hardened portland cement pastes and strength, shrinking and swelling, permeability to water, and freezing of water and thawing of ice in the pores. Until recently, no work has been done on the surface energies of the colloids constituting the most important parts of hydrated calcium silicates and portland cements. This is not surprising, because very little work has been done on the surface energies of solids, in general.

The first experiments on the surface energies of alwillite and tobermorite, the calcium silicate hydrates obtained in the hydration of tricalcium silicate at room temperature (2), revealed the complexity of the system and the difficulty of the problem. It appeared desirable, therefore, to investigate the surface energies of simpler, closely related compounds, such as calcium oxide, calcium hydroxide, amorphous silica, and hydrous amorphous silica. The results on the first two compounds were reported before (4); those on the last two are reported here.

¹Manuscript received June 6, 1956.

Contribution from the Portland Cement Association, Research and Development Laboratories, Chicago, Illinois.

There is no experimental value in the literature for the surface energy of any of the crystalline varieties of silica. Several theoretical calculations were made for quartz, which were listed by Axelsson and Piret (1). The surface energy values ranged from 510 to 2300 ergs/cm.²; Axelsson and Piret adopted the value of 980 ergs/cm.²

Shartsis and Spinner (17) determined the surface tensions of molten alkali silicates and, by extrapolating to zero alkali content, they concluded that the surface tension of vitreous silica at 1300°C. was of the order of 300 dynes/cm. Noting that the temperature coefficient of the surface tension had been found to be small, Iler and Yates (11) estimated the surface energy of vitreous silica at room temperature to be 275 ± 25 ergs/cm.²

In the present investigations, the surface energies (or, more strictly, surface enthalpies) of amorphous silica and hydrous amorphous silica were determined by measuring the heats of solution of samples having differing surface areas and bound water contents, and by measuring the surface areas by nitrogen adsorption.

EXPERIMENTAL

Materials

The materials used were Mallinckrodt's Acid Silicic S. L. (standard luminescent) and Mallinckrodt's Acid Silicic Special Bulky. The laboratory designations were A-33 and A-41, respectively. Both materials are precipitated silica gels of high purity, with the following specifications: heavy metals (as lead), 0.0005% max.; alkali salts (as sulphates), 0.10% max.; sulphate, 0.01% max.; chloride, 0.01% max.; and iron, 0.001% max. Partly because the silica samples were better than 99.9% pure (except for water), and partly because both types of silica contained about the same kinds and amounts of impurities, the heats of solution were not corrected for impurities.

Preparation of Batches

Preliminary drying was done by evacuating at 25°C. until the water vapor pressure of the hydrous silica was equal to that of ice at -78°C. (0.5μ of mercury). The apparatus used was described by Copeland and Hayes (7). The batches thus obtained were designated A-33-1 and A-41-1. Samples with lower water contents were prepared by vacuum drying at higher temperatures. A two-stage mercury diffusion pump was used, backed by a Welch "Duoseal" pump. The pressure was less than 10^{-6} mm. of mercury. The temperature was raised very slowly to avoid blowing the finely divided material into the vacuum line. The drying schedules are shown in Table I.

Preparation of Samples

After the batch was prepared, it was transferred under vacuum into a controlled-atmosphere cabinet. Air was forced into the cabinet so as to maintain a slightly higher than atmospheric pressure. The air was first passed through four drying towers: one containing soda lime, the three others anhydrous (anhydrous magnesium perchlorate). Air was then admitted to the evacuated tube containing the batch; and the batch was quickly distributed

TABLE I
DRYING SCHEDULES OF SILICA BATCHES

Batch designation	Drying temperature, °C.	Heating time to reach drying temperature, hr.	Drying temperature maintained, hr.
A-33-1	25	—	—
A-33-13	150	28	76
A-33-10	180	31	88
A-33-12	205	28	64
A-33-2	210	8	64
A-41-1	25	—	—
A-41-2	180	27	40
A-41-3	240	6	72

among four weighing bottles. The silica in each bottle was divided in the following manner: first, a 0.5 gm. sample was taken for ignition loss, then three samples (0.7, 1.0, and 1.3 gm.) for the calorimetric work, than a 1.0 gm. sample for surface area measurement or X-ray diffraction, and finally a 0.5 gm. sample for ignition loss. (The weights are approximate.) The container of each sample was covered, and each crucible and weighing bottle was placed in a separate weighing bottle. The cover of the outer weighing bottle was grease-sealed. The 24 samples were kept in ascarite-anhydron desiccators until used. Immediately before use, each sample was taken out of the outer container and weighed in the inner container without removing its cover.

The samples were exposed to the atmosphere only while they were being dropped into the calorimeter, which period averaged 15 sec. for the A-33 and 27 sec. for the A-41 samples. Experiments, similar to those described in an earlier paper (4), were performed to ascertain the amount of moisture picked up during this time. The average pickup was 0.2 mgm./gm. of silica; thus, the error introduced by this factor was found negligible.

Measurements

1. The heats of solution were determined by a calorimeter that was a modification of the one used by Verbeck and Foster (19). The changes, as well as the experimental procedure, were described before (5). The acid mixture used was 8 ml. of 49.4% hydrofluoric acid with sufficient 2 *N* nitric acid added to make the total weight 420 gm. Each sample dissolved in less than three minutes. The solutions appeared to be clear for the 0.7 and 1.0 gm. samples, and slightly cloudy for the 1.3 gm. samples.

2. The specific surface areas of the eight batches of silica were determined by the B.E.T. method (3) using nitrogen at liquid nitrogen temperature as the adsorbate. Samples of the three A-41 batches showed a rather unusual behavior. As the sample was sealed to the adsorption line, a small amount of water condensed on the inner wall of the sample tube. The sample was then evacuated for several hours at 10^{-6} mm. of mercury pressure, nevertheless the nitrogen surface area measured was only about one-third of its expected value. The equilibration was very slow. Evacuation for 16 hr. at 10^{-6} mm. pressure increased the speed of equilibration and raised the surface area to

about two-thirds of its expected value. Gentle heating with a small, smoky gas flame for about three minutes presumably removed all the adsorbed water, because thereafter the equilibration was fast and the surface area rose to its expected value. No such difficulty was encountered with samples of the A-33 batches. Shorter or longer evacuation, heating or no heating, resulted in quick equilibration and the same nitrogen surface area.

3. The specific surface areas of two batches of silica, A-33-1 and A-41-1, were determined also by water vapor adsorption, using a gravimetric method. Four relative pressures were used, produced in vacuum desiccators at 23.8°C. by means of saturated solutions of $\text{NaOH} \cdot \text{H}_2\text{O}$, $\text{LiCl} \cdot \text{H}_2\text{O}$, $\text{KC}_2\text{H}_3\text{O}_2 \cdot 1.5\text{H}_2\text{O}$, and $\text{MgCl}_2 \cdot 6\text{H}_2\text{O}$. The relative pressures of these hydrates at 25°C. are 0.0703, 0.1105, 0.2245, and 0.3300, respectively (18). Even though the relative humidities of the hydrates change with temperature (21), the changes are so slight that they do not affect the B.E.T plots; consequently, in the calculations the 25°C. values were used. A sample of each silica, in a small Erlenmeyer flask, was placed in each desiccator; the desiccators were then evacuated, and allowed to stand in a constant temperature room at $23.8 \pm 0.6^\circ\text{C}$. Periodic weighings showed that equilibrium was attained in less than two weeks.

4. Density determinations were made by water displacement in Welds type pycnometers. X-ray diffraction patterns were obtained by means of the equipment described before (2). Ignitions were carried out in platinum crucibles in a muffle furnace at 1050°C .

RESULTS

The heats of solution of the five batches of the A-33 and of the three batches of the A-41 series at different stages of dehydration and at different weights are given in Table II. The weights in the table are not the actual sample weights but the weights of silica in the samples; the heats of solution are, likewise, reported per gm. of silica, rather than per gm. of sample. The heats of solution were different at different weights, indicating relatively large concentration effects.

The specific surface areas obtained by nitrogen adsorption are shown in Table III. The molecular area of nitrogen was assumed to be 16.2 \AA^2 (4). The average values of the surface areas were 701.1, 709.7, 714.2, 666.2, and 665.9 $\text{meters}^2/\text{gm.}$ of silica for A-33-1, A-33-13, A-33-10, A-33-12, and A-33-2, respectively; the A-41 samples had almost identical surface areas, with an average of $382.1 \text{ meters}^2/\text{gm.}$

The ignition losses of the eight sets of samples are also shown in Table III. Since analyses performed on several samples indicated no carbon dioxide, the entire ignition loss was attributed to water. The average values of the ignition losses were 0.0686, 0.0631, 0.0569, 0.0515, and 0.470 gm./gm. of silica for A-33-1, A-33-13, A-33-10, A-33-12, and A-33-2, respectively; and 0.0500, 0.0471, and 0.0428 gm./gm. of silica for A-41-1, A-41-2, and A-41-3, respectively.

The total water contents of silica batches A-33-1 and A-41-1 at four relative pressures are shown in Table IV.

TABLE II

HEATS OF SOLUTION OF MALLINCKRODT'S S. L. GRADE SILICA AND SPECIAL BULKY SILICA

Sample	Weight, gm. of silica	Heat of solution, cal./gm. of silica	Sample	Weight, gm. of silica	Heat of solution, cal./gm. of silica
S.L. grade silica			Special Bulky silica		
A-33-1	0.6815	605.91	A-41-1	0.5975	590.49
	0.7004	607.07		0.6227	591.05
	0.7006	607.20		0.7227	593.30
	0.9261	604.52		0.7423	588.76
	0.9557	603.28		0.9043	590.57
	1.0063	602.80		0.9261	593.75
	1.2250	600.73		0.9559	590.39
	1.2485	600.18		0.9699	587.18
A-33-2	0.6638	609.09	A-41-2	1.2181	585.46
	0.6654	610.20		1.2200	588.13
	0.6915	608.86		1.2449	587.63
	0.9484	608.72		1.2563	587.96
	0.9526	608.66		0.6493	594.90
	0.9542	606.47		0.6625	595.19
	0.9948	606.57		0.6725	591.07
	1.2349	604.77		0.7438	592.43
A-33-10	1.2384	606.77	A-41-3	0.9158	590.25
	0.6541	608.63		0.9603	589.92
	0.6574	608.85		0.9648	588.25
	0.6755	611.45		1.0054	591.07
	0.6809	612.16		1.2396	588.17
	0.9592	607.41		1.2488	587.85
	0.9735	606.79		1.2522	585.71
	0.9791	608.51		1.2951	588.46
A-33-12	0.9843	607.96	A-41-3	0.6748	593.93
	1.2282	606.24		0.6930	595.88
	1.2625	604.99		0.7310	591.07
	1.3010	603.35		0.9515	590.84
	0.6589	609.86		0.9572	592.85
	0.6689	607.94		0.9929	592.72
	0.7399	608.31		1.0232	589.22
	0.9417	607.82		1.2540	586.98
A-33-13	0.9720	603.99		1.2881	585.43
	0.9818	606.26		1.3044	588.25
	1.2433	603.15			
	1.3023	604.17			
	1.3192	602.45			
	0.6662	609.35			
	0.6738	608.38			
	0.6823	608.37			
	0.6836	607.22			
	0.6976	607.23			
	0.9484	606.57			
	0.9506	606.43			
	0.9536	607.42			
	0.9771	605.57			
	0.9790	605.79			
	1.2302	604.34			
	1.2321	603.34			
	1.2517	602.65			

TABLE III
 SPECIFIC SURFACE AREAS AND IGNITION LOSSES

Sample	Area, m. ² /gm. of silica	Ignition loss, gm./gm. of silica
A-33-1	694.3, 701.6, 707.4	0.0682, 0.0686, 0.0687, 0.0688
A-33-2	654.3, 677.5	0.0452, 0.0471, 0.0471, 0.0486
A-33-10	709.5, 714.0, 719.2	0.0560, 0.0562, 0.0566, 0.0567, 0.0574, 0.0577, 0.0580
A-33-12	664.5, 667.9	0.0505, 0.0506, 0.0512, 0.0517, 0.0523, 0.0526
A-33-13	709.1, 709.6, 710.5	0.0616, 0.0619, 0.0620, 0.0621, 0.0622, 0.0630, 0.0632, 0.0633, 0.0634, 0.0637, 0.0640, 0.0640, 0.0640, 0.0647
A-41-1	382.5	0.0489, 0.0497, 0.0499, 0.0500, 0.0500, 0.0502, 0.0502, 0.0511
A-41-2	381.6	0.0461, 0.0465, 0.0466, 0.0474, 0.0476, 0.0486
A-41-3	382.3	0.0417, 0.0421, 0.0430, 0.0430, 0.0432, 0.0438

 TABLE IV
 VARIATION OF TOTAL WATER CONTENT WITH RELATIVE
 PRESSURE AT 23.8°C.

Relative pressure	Total water content, gm./gm. of silica	
	A-33-1	A-41-1
0.0703	0.1352	0.1074
0.1105	0.1601	0.1212
0.2245	0.2159	0.1479
0.3300	0.2558	0.1633

DISCUSSION

Analysis of Data

If all A-33 samples had identical body structures, it follows that for any sample dissolved in the calorimeter

$$[1] \quad H_{ijk} + w_j h - A_j \epsilon_s = H_k,$$

where H_{ijk} is the heat of solution in cal./gm. of silica of the i th sample of the j th batch, having weight k ;

w_j is the average bound water content of the j th batch in gm./gm. of silica;

h is the average heat of hydration of the oxide surface (siloxane) to the hydroxylic surface (silanol) (12) in cal./gm. of water;

A_j is the average specific surface area of the j th batch in meters²/gm. of silica;

ϵ_s is the average surface energy (or surface enthalpy) of the siloxane surface in cal./meters²;

and H_k is the heat of solution in cal./gm. of silica of a sample of weight k with zero bound water content and zero surface.

A least squares analysis of the data was made by the method of Deming (8). This method enables one to take into account the errors in all measured quantities. Dr. Paul Seligmann of this laboratory derived the equations for the evaluation of the weighted means and standard errors of h , ϵ_s , $H_{0.7}$, $H_{1.0}$, and $H_{1.3}$. The derivation required considerable statistical skill, and the evaluations involved hundreds of operations. The results are shown in Table V, Columns 2 and 3.

TABLE V
RESULTS OF LEAST SQUARES ANALYSIS

	A-33 data alone (5 sets)		A-33 and A-41 data (8 sets)	
	Weighted mean	Standard error	Weighted mean	Standard error
$H_{0.7}$ (cal./gm. of silica)	580.6	1.6	580.2	0.5
$H_{1.0}$ (cal./gm. of silica)	578.1	1.6	578.0	0.5
$H_{1.3}$ (cal./gm. of silica)	575.3	1.6	575.3	0.5
h (cal./gm. of water)	278.3	7.6	258.6	13.0
ϵ_s (cal./meters ²)	0.0634	0.0027	0.0618	0.0007

If it is assumed that the A-41 batches had the same body structures as the A-33 batches (in other words, if the A-41 batches differed from the A-33 batches *only* in bound water content and specific surface area), the three sets of data obtained for A-41 can be combined with the five sets of data obtained for A-33, and the five parameters can be evaluated from the eight sets of data with the help of Dr. Seligmann's equations. The results are shown in Table V, Columns 4 and 5.

1. Comparison of the zero bound water and zero surface heat values in Columns 2 and 4 shows that least squares analysis of the five sets of data obtained for the A-33 samples alone gave results that were practically identical with those obtained from analysis of all eight sets of data. (The A-41 data could not be analyzed alone in a similar manner because all samples had the same specific surface areas.) The close similarities between the five-set and the eight-set heats of solution indicate strongly that the body structures of A-33 and A-41 were practically identical.

2. Because the body structures of A-33 and A-41 were found to be practically identical, it is a legitimate procedure to evaluate ϵ_s and h from the combined data obtained for all eight batches. That a more accurate value can be obtained for ϵ_s by such a combination is clear from the following considerations. The difference between the specific surface areas of the high and low surface A-33 batches was about 40 meters²/gm. but the difference between the specific surface areas of the A-33 and A-41 batches was about 300 meters²/gm. Since the error in the surface area determination is about the same for each batch, the error in the differences between surface areas is much smaller on a percentage basis for the eight-set data than for the five-set data. Table V

shows that the standard error of ϵ_s is four times as large for the latter as for the former. This indicates that the eight-set values give better estimates of the parameters than the five-set values.

The eight-set value of ϵ_s in Table V is 0.0618 cal./meter², with a standard error of ± 0.0007 cal./meter². Thus, *the surface energy of amorphous silica of zero water content—or the energy of the pure siloxane surface—at 23°C. is 259 ± 3 ergs/cm.²* This is an average surface energy, and the surface may possess some sites of higher and lower energy than the average. There was some indication, however, that the silica surfaces were more uniform than those ordinarily encountered in adsorbents. The B.E.T. plots of adsorption isotherms usually deviate from linearity below a relative pressure of 0.05, which is attributed to adsorption on high energy sites at low pressures. The B.E.T. plots of the nitrogen adsorption isotherms for A-33 and A-41 remained linear down to the lowest relative pressures measured in these experiments, about 0.005. Perhaps such uniformity of surface is less surprising in an amorphous substance than it would be in a crystalline adsorbent, since different exposed crystal faces, as well as edges and corners, are bound to introduce heterogeneity.

The surface energy of 259 ergs/cm.² is based on the assumption that the molecular area of nitrogen is 16.2 Å². If Livingston's (15) value of 15.4 Å² were used, the surface energy would be 5% larger. The standard error of ± 3 ergs/cm.² does not include the uncertainty in the molecular area of nitrogen.

As stated in the introduction, the surface energy of vitreous silica, estimated by Iler and Yates (11) from the data of Shartsis and Spinner (17), was 275 ± 25 ergs/cm.² This value agrees with that reported here within 16 ergs/cm.²

3. The eight-set value of h in Table V is 258.6 cal./gm. of water, with a standard error of ± 13.0 cal./gm. Thus, *the heat of hydration by liquid water of the siloxane surface to silanol surface, or the heat of chemisorption of liquid water on the siloxane surface, at 23°C. is 4660 ± 230 cal./mole of water.* This is an average heat of hydration; but, as pointed out before, the siloxane surface was probably rather uniform.

4. The energy of the silanol surface can be calculated from ϵ_s and h , provided the area occupied by a water molecule on the surface is known. Iler (13) showed that the area to be assigned to an SiOH group on the surface of amorphous silica of specific gravity 2.20 is close to 12.5 Å². Since the chemisorption of a water molecule results in two SiOH groups (12), the area assignable to a water molecule is 25.0 Å². On the basis of this area, the heat of hydration of the siloxane surface to silanol at 23°C. amounts to 130 ± 7 ergs/cm.² and *the average surface energy of hydrous amorphous silica with a completely hydrated surface—or the energy of the pure silanol surface—at 23°C. is 129 ± 8 ergs/cm.²* The standard error does not include the uncertainty in the molecular area of water.

It is worth noting that the total energy of the silanol surface is only slightly higher than the total surface energy of liquid water, which is 118.5 ergs/cm.² at 25°C. (10). This was predicted by Iler (11). Hydrous silica and liquid water are amorphous substances, and the chemical compositions of their surfaces

should show considerable similarities if, as the presently accepted model postulates, the hydroxyl groups in the silanol surface are on top, and the silicon atoms are below the hydroxyl groups (13). The present results support this model. If the silicon atoms were on top, or even on the same level with the hydroxyl groups, it would be difficult to understand the close similarity between the surface energies of water and hydrous silica.

The total energy of the hydrated surface of amorphous silica is probably lower than that of most solids. The surface free energy is bound to be even lower. Thus, the tendency to pass from smaller to larger particles is relatively small, which may explain many of the unusual colloidal properties of hydrous amorphous silica (11).

Another fact worth noting is that the difference between the energies of the siloxane and the silanol surface, 130 ergs/cm.², is the same as the difference between the surface energies of calcium oxide and calcium hydroxide, reported in an earlier paper (4). This may be just a coincidence, but there seems to be at least an indication here that the hydration of the surface involves a conversion of the surface oxide ions into surface hydroxyl ions both in calcium oxide and in silica and, further, that both in calcium oxide and in silica, the oxide ions are on top and the positive ions below. Thus, the facts noted in this and the previous paragraph tend to confirm Weyl's hypothesis (22) as to the structures of ionic surfaces.

Identity of Body Structures

1. The differences between the heats of solution of A-33 and A-41 samples could be ascribed to differences between surface properties (surface water content, specific surface area) only if the body structures of A-33 and A-41 were identical. In an earlier paper (4), strong evidence was cited for the identities of the body structures of high and low surface calcium oxide and calcium hydroxide on the basis of X-ray diffraction measurements (precision determination of lattice parameters, line broadening). It was impossible to do this for the silica samples, because the diffraction pattern of each sample consisted of a single very wide band only, with a broad maximum at $d = 3.95$ Å. The samples also showed pronounced low angle scattering. A radial distribution analysis, such as that carried out by Warren (20), could have supplied useful indications as to the identity of the body structures of A-33 and A-41, but the appropriate equipment was not available.

2. In order to show some independent evidence regarding the body structures, density measurements were performed on several batches of A-33 and A-41. It soon appeared that a thorough investigation of the density would be a research problem comparable in extent to that described in this paper. Because of this, only some tentative results can be reported here.

If the density is plotted against the fraction of the surface covered with bound water, and the data are extrapolated to zero surface covering, the density values obtained are

$$d_{A-33} = 2.28 \pm 0.01 \text{ gm./cc. and } d_{A-41} = 2.29 \pm 0.01 \text{ gm./cc.}$$

at 26°C. If the density of packing of the silicon atoms in the surface is slightly lower than that in the body, d_{A-41} should be somewhat larger than d_{A-33} , since A-33 has a much larger specific surface area than A-41.

3. The decisive evidence regarding the identity of the body structures of A-33 and A-41 was found in the zero bound water and zero surface heats of solution shown in Table V for the five-set data and the eight-set data. The significance of the close agreement between the heat values will be more apparent after the following considerations. The density difference between A-33 and A-41 is not significant statistically; nevertheless, the 0.44% difference between the densities may be real. If the energy content per gm. of the body of amorphous silica is inversely proportional to r^3 , where r is the average distance between silicon atoms, a 0.44% change in density would cause a change of 2.5 cal./gm. of silica in the heat of solution. The average difference between the five-set and eight-set heat values in Table V is less than 0.2 cal./gm. of silica. Thus, the close agreement between the heat values indicates close similarity between the body structures. If the density difference between A-33 and A-41 is real, it is caused by a difference between the densities of packing of atoms in the surface and in the body, as was pointed out in the previous section.

Bound Water Content

1. The value of h , 258.6 cal./gm. of water, represents the heat of hydration of the siloxane surface correctly only if there was no physically adsorbed water in the A-33 and A-41 samples. If one takes Iler's value of 25 Å² for the molecular area of bound water, the nitrogen surface area of A-33 indicates that the amount of bound water at complete coverage would be 0.084 gm./gm. of silica. Greenberg (9) determined the amount of bound water in Mallinckrodt's S. L. grade silica at complete coverage of the surface in three different ways and obtained the values 0.090, 0.083, and 0.079 gm./gm. of silica. A-33-1, equilibrated at 25°C. and a vapor pressure of 0.5 μ of mercury, contained 0.0686 gm. of water of silica, and all other batches of A-33 contained less water. It seems, therefore, that the A-33 samples contained only bound water, and the surfaces of the samples were only partly covered with bound water.

2. It is more difficult to show the same for A-41. Greenberg's values for the bound water content of Mallinckrodt's Special Bulky silica, determined in three different ways, were 0.071, 0.066, and 0.049 gm./gm. of silica; but the nitrogen surface area of A-41 combined with Iler's molecular area for water indicates only 0.046 gm. of bound water per gm. of silica at complete coverage. The water values for A-41-1, A-41-2, and A-41-3 were 0.0500, 0.0471, and 0.0428 gm./gm. of silica, respectively; which would correspond to 109.3, 103.0, and 93.6% coverage.

These results can be explained by assuming that the excess water in A-41-1 and A-41-2 was physically adsorbed water and not bound water. This hypothesis was tested by using the $H_{0.7}$, $H_{1.0}$, $H_{1.3}$, and ϵ_s values of Table V, and calculating h for each of the three batches of A-41 from the experimental

results. The value of h was found to be almost exactly the same for all three batches. This means either that all three batches contained only bound water, or that the average heat of adsorption of water physically adsorbed on the *most active* fraction of the silanol surface was approximately equal to the average heat of hydration of the *entire* siloxane surface. Both alternatives are reasonable, and no decisive evidence exists at present that would enable one to make a clean-cut choice.

The second alternative is favored by the present investigators, because the first one is out of line with the accepted views on the mechanism of hydration of the siloxane surface. The average area per silicon atom on the surface of amorphous silica is 12.5 \AA^2 , and it is generally accepted that a water molecule produces two surface SiOH groups. However, if all the water in batch A-41-1 was bound water, the molecular area of chemisorbed water was not 25 \AA^2 , but 22.9 \AA^2 . This would mean that there were more hydroxyl groups on the surface than Si atoms.

Of course, the above argument is not decisive; it is possible that the area to be assigned to a water molecule was 22.9 \AA^2 . In that case, ϵ_s and h in Table V would remain unaffected, but the surface energy of the fully hydrated surface would become 117 ergs/cm^2 , instead of 129 ergs/cm^2 .

3. If it is assumed that the ultimate silica particles are equal spheres, the nitrogen surface areas of A-33 and A-41 correspond to particle diameters of about 37 and 64 \AA , respectively. Batches A-33-1 and A-41-1 were dried to a near-equilibrium state at 25°C . and a water vapor pressure of 5×10^{-4} mm. of mercury. It is interesting to note that at this vapor pressure the surface hydrate was perfectly stable on the larger particles; the surface of A-41-1 was completely covered with bound water. On the other hand, the surface hydrate on the smaller particles partly decomposed; the surface of A-33-1 was only about 80% covered with bound water. These examples illustrate the effect of particle dimension or the curvature of the surface on the stability of the surface film. The effect of size or curvature upon the stability of the silica particles themselves is illustrated by the fact that A-33 began to sinter at 200°C ., whereas A-41 showed no sintering at 300°C .

Physical Adsorption of Water

The determination of the specific surface areas of A-33-1 and A-41-1 by the B.E.T. method using water vapor at 23.8°C . as the adsorbate encountered two difficulties: (a) distinguishing between bound water and physically adsorbed water, and (b) uncertainty in the molecular area of physically adsorbed water.

1. The energy of interaction between a polar molecule and an ionic surface is much greater than that between a nonpolar molecule and an ionic surface. For example, Chessick, Zettlemoyer, Healey, and Young (6) showed that the net heat of physical adsorption of an alcohol on a rutile (TiO_2) surface was 361 ergs/cm^2 , whereas that of a hydrocarbon was 92 ergs/cm^2 . The difference was almost entirely due to the energy of interaction between the dipole of the adsorbate and the electrostatic field of the surface. Because of the high energy

of interaction between water and an ionic surface, it is difficult to make a clean-cut separation between physically and chemically adsorbed water.

2. The structure of the underlying surface has little effect on the packing of physically adsorbed nitrogen; consequently, it is possible to assign a single value to the molecular area of nitrogen that is valid, to a good approximation, for any adsorbent. This is not true of physically adsorbed water. The ions of the adsorbent surface orient the dipole of the water molecule, and the packing of the adsorbed molecules is influenced by the structure of the underlying surface. An example of this is found in some experiments of Jura (14), who determined the specific surface areas of five ionic adsorbents by means of the B.E.T. method, using nitrogen and water vapor as adsorbates. If it is assumed that the molecular area of nitrogen was the same on all five adsorbents, then the molecular area of water varied over a range of 35%, from the highest to the lowest value.

It is especially interesting to note the results for quartz among Jura's five adsorbents. On the basis of the customary 16.2 \AA^2 for the molecular area of nitrogen, the molecular area of physically adsorbed water on the quartz surface was 11.3 \AA^2 . If the average distance between silicon atoms on the surface of quartz is the same as in the body of the crystal, the average area assignable to a silicon atom on the quartz surface is 11.24 \AA^2 . This indicates that the number of silicon atoms on the surface determines the packing of physically adsorbed water molecules. If the same is true for amorphous silica, the molecular area of physically adsorbed water molecules on the surfaces of A-33 and A-41 was 12.5 \AA^2 .

3. The total water isotherms of A-33-1 and A-41-1 at 23.8°C . were determined in the relative pressure range 0.07 to 0.33. The results were shown in Table IV. If one assumes a certain value for bound water, and further assumes that the bound water content did not vary in the relative pressure range investigated, subtracting the assumed value from the total water gives the amount of physically adsorbed water. A B.E.T. plot of the physical adsorption isotherm, combined with a molecular area of 12.5 \AA^2 , then gives the specific surface area of the adsorbent. The variation of the specific surface area with assumed bound water content is shown in Fig. 1.

The bound water content of A-33-1 was 0.0686 gm./gm. of silica at the beginning of the experiment. If no hydration of the surface occurred in the course of the experiment, the surface area measured by water adsorption was 658 meters²/gm., as Fig. 1 shows. Iler stated that the siloxane surface "hydrates scarcely at all at a relative humidity of, say, 40 or 50%." The maximum relative humidity used in these experiments was 33%, and the results confirm Iler's statement. The surface area of 658 meters²/gm. is 6% smaller than the value obtained by nitrogen adsorption. Any appreciable hydration of the surface in the course of the adsorption experiments would make the discrepancy greater.

The water content of A-41-1 was 0.0500 gm./gm. of silica at the start, but it is possible that a part of this was adsorbed water, as discussed before. The nitrogen area indicated a bound water content of 0.0460 gm./gm. of

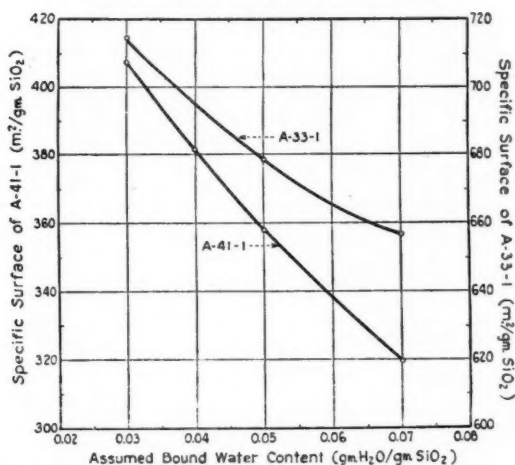


FIG. 1. Variation of specific surface area with assumed bound water content.

SiO₂ at complete coverage. According to Fig. 1, the values of 0.0460 and 0.0500 gm. of water per gm. of silica correspond to surface areas of 367.5 and 358.5 meters²/gm. respectively. The former is 4%, the latter 6%, smaller than the nitrogen adsorption area.

Thus, the surface areas obtained by water vapor adsorption were about 4 to 6% smaller than the nitrogen areas. It is possible that 16.2 Å² is too large for the molecular area of nitrogen. Livingston (15) favors the value of 15.4 Å², which is 5% smaller than the one used here. It is also possible that 12.5 Å² is too small for the molecular area of water. Livingston calculated the molecular area of water from the two-dimensional van der Waals constant *b*, and obtained 13.1 Å², which is 5% larger than the value used here. Obviously, it is also possible that the molecular area of nitrogen was somewhat too large and the water area somewhat too small, the two errors adding up to about 5%. Adequate data are lacking between these alternatives, but the good agreement between the surface area values obtained by nitrogen and water adsorption is gratifying.

The value of the *c* constant (3) of the B.E.T. equation was 9 for A-33-1 and 23 for A-41-1, indicating a stronger binding of physically adsorbed water to the surface of the latter. Since the surface of A-41-1 was a pure silanol surface, whereas the surface of A-33-1 was a mixed silanol-siloxane surface, the implication is that the heat of adsorption of water on the silanol surface is greater than on the siloxane surface. This is in agreement with certain experiments reported by Iler (12), indicating that the siloxane surface is somewhat hydrophobic.

ACKNOWLEDGMENT

We are greatly indebted to Dr. Paul Seligmann for deriving the complicated statistical equations used in the evaluation of the results.

REFERENCES

1. AXELSON, J. W. and PIRET, E. L. *Ind. Eng. Chem.* 42: 665. 1950.
2. BRUNAUER, S., COPELAND, L. E., and BRAGG, R. H. *J. Phys. Chem.* 60: 112, 116. 1950.
3. BRUNAUER, S., EMMETT, P. H., and TELLER, E. *J. Am. Chem. Soc.* 60: 309. 1938.
4. BRUNAUER, S., KANTRO, D. L., and WEISE, C. H. *Can. J. Chem.* 34: 729. 1956.
5. BRUNAUER, S., KANTRO, D. L., and WEISE, C. H. *J. Phys. Chem.* 60: 771. 1956.
6. CHESSICK, J. J., ZETTMLOYER, A. C., HEALEY, F. H., and YOUNG, G. J. *Can. J. Chem.* 33: 251. 1955.
7. COPELAND, L. E. and HAYES, J. C. *ASTM Bull. No.* 194: 70. Dec. 1953.
8. DEMING, W. E. *Statistical adjustment of data.* John Wiley & Sons, Inc., New York. 1953. Parameters were estimated by the method of Chap. IV, pp. 49-58; standard errors of the estimates were obtained by the method of Chap. IX, pp. 167-168.
9. GREENBERG, S. A. *J. Phys. Chem.* 60: 325. 1956.
10. HARKINS, W. D. and JURA, G. *J. Am. Chem. Soc.* 66: 1362. 1944.
11. ILER, R. K. *The colloid chemistry of silica and silicates.* Cornell Univ. Press, Ithaca, N.Y. 1955, p. 10.
12. ILER, R. K. *The colloid chemistry of silica and silicates.* Cornell Univ. Press, Ithaca, N.Y. 1955, p. 234.
13. ILER, R. K. *The colloid chemistry of silica and silicates.* Cornell Univ. Press, Ithaca, N.Y. 1955, pp. 242-243.
14. JURA, G. *In The physical chemistry of surface films.* By W. D. Harkins. Reinhold Publishing Corporation, New York. 1952, p. 235.
15. LIVINGSTON, H. K. *J. Colloid Sci.* 4: 447. 1949.
16. POWERS, T. C. and BROWNARD, T. L. *J. Am. Concrete Inst.* Oct. 1946-April 1947. *Proc.* (43). 1947. Portland Cement Assoc. Research Dept. Bull. 22.
17. SHARTSIS, L. and SPINNER, S. *J. Research Natl. Bur. Standards*, 46: 385. 1951.
18. STOKES, R. H. and ROBINSON, R. A. *Ind. Eng. Chem.* 41: 2013. 1949.
19. VERBECK, G. J. and FOSTER, C. W. *Proc. Am. Soc. Testing Materials*, 50: 1235. 1950.
20. WARREN, B. E. *J. Appl. Phys.* 8: 645. 1937.
21. WECHSLER, A. and HASEGAWA, S. *J. Research Natl. Bur. Standards*, 53: 19. 1954.
22. WEYL, W. A. *A new approach to surface chemistry and to heterogeneous catalysis.* Mineral Inds. Exp. Sta. Bull. No. 57.

NOTES

A NOTE ON THE TEMPERATURE DEPENDENCE OF THE ELECTRICAL RESISTANCE OF SALT SOLUTIONS ADSORBED IN POROUS GLASS¹

BY MAX HUBER² AND E. A. FLOOD

INTRODUCTION

It has been shown that the flow of liquids through "Vycor" glass is roughly inversely proportional to the liquid viscosity (5). The temperature variations of the specific electrical resistances of some dilute salt solutions, e.g. NaCl, follow quite closely the temperature variation of the viscosity of water (4, 6, 7). If such solutions are adsorbed as a whole without causing marked concentration gradients, specific resistances of the adsorbed solutions should give rough measures of adsorbate mobilities and the temperature coefficients of these resistances should afford some measure of the "viscosity" activation energies.

Accordingly we have carried out some exploratory measurements of the specific electrical resistances, at various temperatures, of 0.1 *N* solutions of NaCl and of KCl when contained (adsorbed) within the micropore system of Vycor glass.

Our results indicate little "selective" adsorption of these salts.

The true specific resistances of the solutions depend on the pore structures. Assuming a pore structure consisting of three mutually perpendicular non-intersecting straight uniform capillaries, the specific resistances of the solutions were found to be about three times that of the bulk solutions. This is consistent with a pore structure consisting of relatively large islands interconnected by narrow necks. This latter structure is consistent with the method of manufacture of these porous glasses (5).

The temperature coefficients of the specific resistances of the NaCl and KCl solutions are somewhat greater than those of the bulk solutions.

It is concluded that the viscosities of adsorbed 0.1 *N* NaCl and 0.1 *N* KCl solutions are of the same order as those of the bulk solutions.

This work is part of a general investigation concerning the flow of adsorbed fluids. We have described the flow of adsorbed gases through the micropore systems of activated carbons as a laminar viscous flow of liquid films of adsorbate (2). It has been shown that the temperature coefficient of the viscosity of adsorbed water is somewhat greater than that of water in bulk. This has been attributed to surface forces and is consistent with a surface potential of the order of 2-5 kcal. per mole adsorbed (3). This order of surface potential is consistent with the temperature coefficients of the resistances reported below.

¹Issued as N.R.C. No. 4048.

²National Research Council Postdoctorate Fellow, 1953-1955.

EXPERIMENTAL

1. Materials

Porous glass (Vycor No. 7930) tubes were obtained from the Corning Glass Works. It was stated that the Vycor had the following properties:

Apparent density	1.45
Void space per cc.	0.34
Average pore diameter	40 Å
Surface area B.E.T. N ₂	120 meters ² /gm.
NH ₃	204 meters ² /gm.

The KCl and NaCl used were Merck's reagent grade.

The conductance of the distilled water used in the experiments and for the making of the solutions varied from about 2 to $5 \times 10^{-6} \Omega^{-1}$.

2. Electrical Apparatus and Procedures

Fig. 1 illustrates the apparatus used for measurement of the resistance of the walls of the Vycor test tubes, the micropores of which contained the solutions. Alternating current was supplied from a Hewlett and Packard (Model 205 AG) 1000 c.p.s. 15 w. generator, impedance adjustable between 50 and 5000 Ω . The voltage drops across the porous glass and a standard resistance box (Leeds and Northrup 4749) were measured by means of a Hewlett and Packard Decibel-Voltmeter (Model 400 c). The precision of readings was of the order of 1%. The measurements were always reproducible within the precision of instruments.

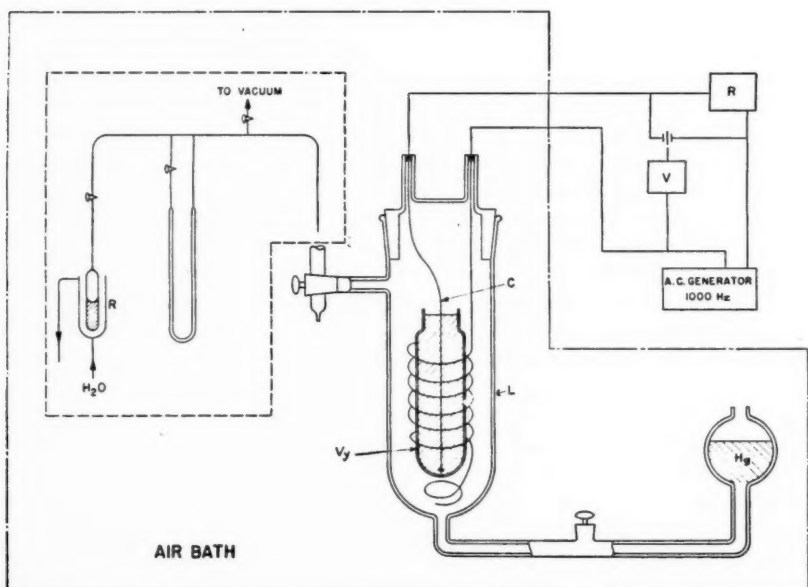


FIG. 1.

The Vycor tubes, V_y (Fig. 1), were test-tube shaped but with somewhat restricted necks. The necks were fired and practically non-porous.

A test tube after immersion for 8–10 days in the appropriate solution was wiped once with adsorbent paper (Kleenex) to remove excess liquid, placed in the copper helix holder, filled with mercury, and quickly placed in the tube L . The Vycor tube (V_y) was held in place in the outer tube L by means of the stout copper wires (C) which also served as electrical leads. Mercury was then allowed to rise from the reservoir (Hg) until above the Vycor tube after which it was lowered to 2 mm. below the edge of the Vycor tube. The tube was then evacuated and opened to the water vapor system where any desired humidity could be maintained. The outer mercury level would be lowered during equilibrations at various relative humidities. In general, it was found that the resistance of the glass between the two volumes of mercury was independent of the mercury pressure, the resistance being the same in vacuum and at 760 mm.

Two distinctly different types of measurement were made: (a) resistances of the salt solutions contained in the micropore system between the two volumes of mercury where the temperature of the mercury and salt solution was varied and (b) resistances at 35.3°C. of salt and water contained in the micropore system where the water content varied as the water equilibrium pressure was varied. Resistances at various temperatures showed little or no drift with time. Usually within five minutes after raising or lowering the temperature, the resistances became constant within the experimental error.

RESULTS

Preliminary experiments with fragments of one of these Vycor tubes indicated the following:

When dried at 130°C. for 15 hr. the weights were readily reproducible within 1%.

Water adsorption isotherms were essentially similar to those reported in the literature (1) and by the manufacturers although the quantity taken up at saturation varied from 0.22 to 0.24 gm. per gm. saturation which is somewhat less than usually found, namely 0.25 gm. per gm.

When red and blue litmus papers were laid on the wet Vycor tube no change in color could be detected after 15 min. However, when the tubes were immersed in 10% NaCl and similarly tested a faint acid reaction could be detected.

The specific resistance of the Vycor tubes as supplied when saturated with water was of the order of $1.5 \times 10^4 \Omega$ while after continued washing and immersion in distilled water the resistance was of the order of $8 \times 10^4 \Omega$. Evidently, the Vycor contains traces of electrolyte difficult to remove.

When Vycor fragments were immersed in salt solutions for 8 to 10 days, removed, wiped, and dried first in a desiccator and subsequently in vacuum at 130°C., the gains in weight corresponded closely to the filling of the void space with the salt solution in which they were immersed. For saturated KCl solutions the gains corresponded to slightly more than that corresponding

to the saturated solution, while in the case of 10% NaCl solution the mean values corresponded to about 9% NaCl. Accordingly, it was judged that within the experimental error there was little or no selective adsorption and it is assumed that when the Vycor tubes are immersed in 0.1 *N* solutions of KCl and NaCl for 8 to 10 days the concentrations in the micropore system are close to 0.1 *N*.

The relation between the specific resistance of the solution within the micropore system and the measured resistance of the Vycor tube will depend upon the structure of micropore system as well as upon the dimensions of the tube. The mean wall thickness of the tubes (Nos. 1, 2, and 3) was between 0.12 and 0.13 cm. and the area of the porous part of the tube 37.0 cm. Accordingly, if ρ is the specific resistance of the solution, then the measured resistance, *R*, will be given by

$$R = \rho(0.125/37) \cdot F$$

where *F* is a factor depending on the micropore structure and the void volume, per cc. of glass, which we take as 0.34. If all of the pores are perpendicular to the axis of the tube and perfectly straight and uniform in cross section, $F = 1/0.34$. If only one-third of the pores are parallel with current, the remaining two-thirds not being interconnected and being perpendicular to the current direction, then $F = 3/0.34$. If the pores are intersecting, *F* will lie between these figures. If the micropore system is an interstitial type structure consisting of "islands" interconnected by necks, the factor can vary from something less than 3/0.34 to very large values, depending on the degree of isolation.

We have used the factor 3/0.34 in calculating specific resistances of the solutions, i.e., specific resistance = measured resistance \times 34. In Fig. 2 the specific resistances of 0.1 *N* KCl solution (tube No. 3) and 0.1 *N* NaCl solution (tube No. 2) are plotted as functions of temperature. The I.C.T. values multiplied by suitable factors (KCl \times 3.37, NaCl \times 2.44) are plotted for comparison. A single point for 0.1 *N* KCl tube No. 1 is included. Evidently *F* is of the order of three, which suggests an interstitial structure where the "necks" are of the order of one-sixth of the diameters of the islands.

The measured resistances *R*, in ohms, of tube No. 1, which was immersed in 0.1 *N* KCl and then dried as above and equilibrated to various relative humidities, are presented in Table I.

TABLE I
ELECTRICAL RESISTANCE OF VYCOR TUBE NO. 1 (EXPOSED
TO 0.1 *N* KCl) DURING ADSORPTION AND DESORPTION OF
WATER (35.3°C.)

p/p_s	<i>R</i> (Ω)	p/p_s	<i>R</i> (Ω)	p/p_s	<i>R</i> (Ω)
0.000	—	0.713	108	0.670	100
0.110	630,000	0.892	5.9	0.387	8670
0.388	9180	1.000	5.5	0.352	15,300
0.552	1150	0.756	21.7	0.000	1,500,000

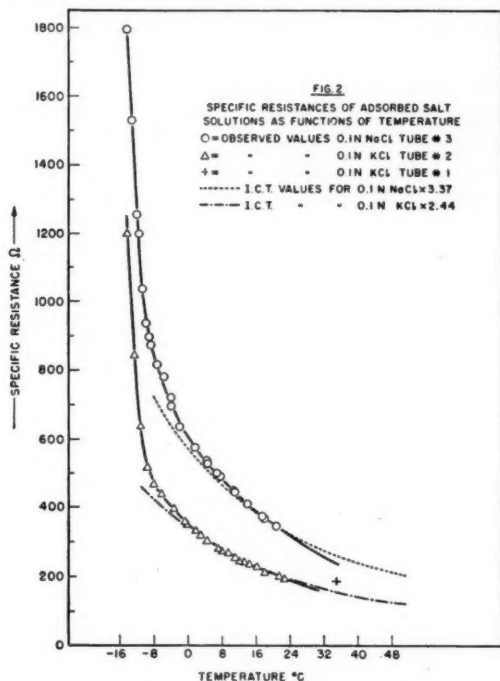


FIG. 2.

1. AMBERG, C. H. and MCINTOSH, R. *Can. J. Chem.* 30: 1012. 1952.
2. FLOOD, E. A., TOMLINSON, R. H., and LEGER, A. *Can. J. Chem.* 30: 389. 1952.
3. HUBER, M. E., FLOOD, E. A., and HEYDING, R. D. *In press.*
4. KRAUS, C. A. *The properties of electrically conducting systems.* Am. Chem. Soc. Monograph No. 7. Reinhold Publishing Corporation, New York. 1922.
5. NORDBURG, M. E. *J. Am. Ceram. Soc.* 27: 299. 1944.
6. ROBINSON, R. A. and STOKES, R. H. *Electrolyte solutions.* Butterworth Scientific Publications, London. 1955.
7. SHEMLIT, L. W., DAVIES, J. A., and GORDON, A. R. *J. Chem. Phys.* 16: 340. 1948.

RECEIVED JUNE 15, 1956.

DIVISION OF PURE CHEMISTRY,
NATIONAL RESEARCH COUNCIL OF CANADA,
OTTAWA, CANADA.

THE PURITY OF SMALL SODIUM CHLORIDE PARTICLES PREPARED BY ELECTROSTATIC PRECIPITATION¹

BY F. VAN ZEGGEREN,² H. P. SCHREIBER,³ AND G. C. BENSON

Recently Benson and Benson (2) have attempted to determine the surface enthalpy of crystalline sodium chloride by measuring heats of solution of samples having different specific surface areas. The fine salt used in these

¹Issued as N.R.C. No. 4047.

²N.R.L. Postdoctorate Fellow, 1955-.

³N.R.L. Postdoctorate Fellow, 1953-55. Present address: Central Research Laboratories, Canadian Industries Limited, McMasterville, Quebec.

experiments was made by electrostatic precipitation of a sodium chloride smoke. Essentially the same method of preparation has been employed by a number of other workers (6, 3, 11, 7).

In the course of the surface enthalpy study the following indications of impurities in the fine salt were noted:

(i) Some samples had a definite bluish hue and when dissolved in water gave alkaline solutions. Patterson, Morrison, and Thompson (7) have also reported obtaining a pH value as high as 9 under similar circumstances.

(ii) Other material which did not give any marked increase in pH nevertheless led to anomalous heats of solution. Thus finely divided salt, which had been thermally sintered to very small surface, apparently had a lower enthalpy than pure bulk crystals. Aqueous solutions of this material gave a positive diphenylbenzidine spot test (4) indicating the presence of nitrate or nitrite impurities.

The blue color and alkaline pH undoubtedly result from the presence of excess sodium in the fine material. The existence of blue salt in nature is well known (5) and recently Scott, Smith, and Thompson (8) have studied the absorption spectrum of salt which was colored blue artificially by a colloidal dispersion of sodium.

Since the occurrence of sodium nitrate impurity in fine sodium chloride prepared by electrostatic precipitation has not been considered by previous users of the method, the purpose of the present note is to give some indication of the extent of this contamination in salt samples prepared under various control conditions. This information should be of value in selecting operating conditions to minimize the content of this impurity.

EXPERIMENTAL

The apparatus used for the production of a sodium chloride smoke was essentially the same as that described by Thompson, Rose, and Morrison (10). A stream of carrier gas at room temperature and at a flow rate of 3.7 cu. ft./min. was obtained by heating liquefied gases. Three different nitrogen-oxygen mixtures were employed for this purpose. These were liquid air and liquid nitrogen produced in the Division of Pure Chemistry, N.R.C., and another grade of liquid nitrogen obtained from Linde Air Products Co., which contained approximately 18%, 2%, and 0.05% oxygen respectively.

The precipitator was a cylindrical Pyrex tube 40 cm. long and 6.5 cm. in diameter on the outside of which was wrapped a layer of brass shim. Alternating current voltages from 6 to 15 kv. (60 cycles/sec.) were applied between this layer and an axial 20 gauge platinum wire. The molten salt was maintained manually at an approximate temperature of 900° C. The temperature in the precipitator was about 40° C.

Samples of sodium chloride smoke were precipitated at various voltages using carrier gases of different oxygen content. X-ray diffraction examination confirmed the presence of sodium nitrate impurity in a number of these. The nitrate content of some of the samples was determined quantitatively by the ferrous sulphate titration method (9). In later work estimation of nitrate

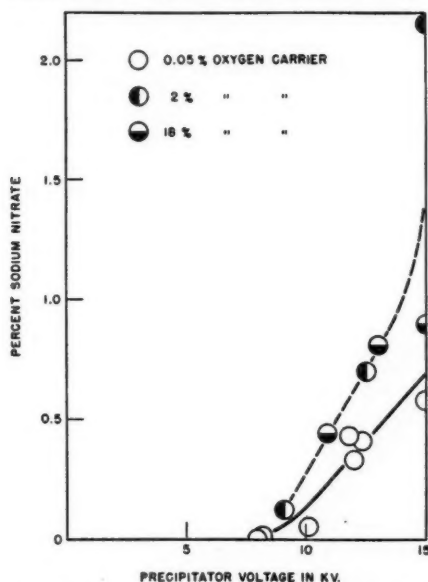


FIG. 1. Variation of nitrate content with precipitator voltage for different percentages of oxygen in the carrier gas.

based on the reaction with brucine (1) and using a photoelectric colorimeter was found to be more convenient.

Data derived from these analyses are illustrated in Fig. 1 where the per cent sodium nitrate content is plotted against the precipitator voltage for runs with the 18%, 2%, and 0.05% oxygen carrier gases. These results are only semiquantitative in nature since duplicate runs sometimes showed considerable variation in the nitrate content. In such cases an average value has been plotted in Fig. 1. It seems probable that this lack of reproducibility stems from variations in the detailed geometry of the discharge in the precipitator from run to run. Within the reproducibility of the experiments there is no significant difference between the results obtained with the 18% and 2% carrier gases and only one curve has been drawn through these data. The curve for the 0.05% case, however, is quite definitely lower. For both curves the nitrate content increases with precipitator voltage and in some cases the nitrate content may be as high as 1 to 2%.

Since samples prepared at high voltages usually showed traces of color as well, the possibility of a correlation between nitrate content and pH of an aqueous solution of the sample was examined. For this purpose the pH of 0.05 *N* solutions of some of the fine salt samples in boiled conductivity water was measured with a Beckman glass electrode meter. In plotting the results shown in Fig. 2 the pH of a similarly prepared 0.05 *N* solution of reagent grade sodium chloride has been adopted as a zero. Thus ΔpH is defined by

$$\Delta\text{pH} = \text{pH (fine salt solution)} - \text{pH (reagent salt solution)}.$$

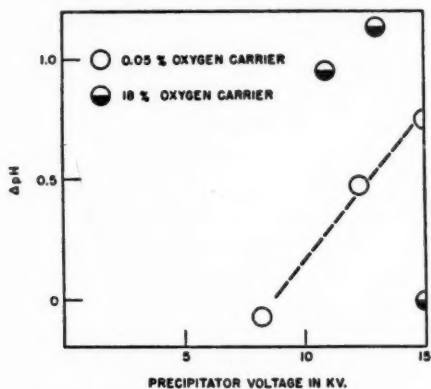


FIG. 2. Variation of ΔpH with precipitator voltage for different percentages of oxygen in the carrier gas.

For the 0.05% oxygen carrier ΔpH increases approximately linearly with precipitator voltage and hence in view of the data of Fig. 1, a fairly linear relation exists between ΔpH and nitrate content. However, when the oxygen content of the carrier is increased the use of pH alone as a criterion of purity becomes unsatisfactory. This is illustrated by the three points in Fig. 2 for the 18% oxygen carrier. In this case the ΔpH falls off at high voltages. The result plotted at 15 kv. is the average of +0.02, -0.08, and +0.03 obtained in three independent runs. Apparently when there is a high content of oxygen in the carrier gas the nitrate formation may be sufficient to annihilate the free sodium produced in the discharge process. Around 15 kv. and under the control conditions used in the present work this process reduces the ΔpH to zero. However this may not be the case at still higher voltages or under different control conditions. No attempt has been made to investigate this mechanism in detail since our primary interest is in the production of pure samples.

DISCUSSION

From the data presented in Figs. 1 and 2 it is evident that the precipitation voltage and oxygen content of the carrier gas should both be as low as possible. The minimum voltage at which any significant collection of salt can be obtained is 6 to 7 kv. and about 8 kv. gives a reasonable collection efficiency. Samples with areas 20-30 square meters/gm. have been prepared at this voltage under the present conditions of flow and temperature.* It is difficult to obtain large flow rates of very pure nitrogen and the 0.05% oxygen content gas used in the present work seems to be the best available under the present circumstances. If this is used as carrier with a precipitator voltage of 8 kv. the nitrate content should be less than 0.05%. As a further check several samples of salt prepared under these conditions were sintered thermally to have areas near zero and the heats of solution determined as in Reference 2.

*By varying the flow rate up to 6 cu. ft./min. specific areas as high as 60 square meters/gm. have been obtained. Changes in flow rate do not appear to influence the purity of the product markedly.

Without exception the enthalpies of the samples were greater than that of pure bulk salt and the differences, which were only a few calories/mole, could be accounted for by the remaining surface enthalpy of the sintered material which still had a small non-zero area.

A rough calculation shows that a nitrate content of about 0.3% would explain the intercept of -5.4 cal./mole reported in Reference 2. Since the carrier gas used in that work contained 2% oxygen and the operating voltage was about 10 kv. this estimate is quite in accord with the present findings.

The effect of this impurity on the surface enthalpy (i.e. the slope of the line in Reference 2) is difficult to estimate because of uncertainties in the energetics involved when a chloride ion is replaced by a nitrate ion and also because of lack of information about the distribution of nitrate ions in the lattice. In all probability the nitrate is formed at the surface of the particles while they are in the precipitator. If it is assumed that diffusion into the bulk of the crystal is relatively slow and that the particles are uniform cubes the percentage P of surface molecules which are sodium nitrate is given approximately by the formula

$$P = 1200(x/A)$$

where A is the area in square meters/gm. and x the weight per cent of sodium nitrate in the whole sample (x assumed small compared to 100%). Thus for material of area 30 square meters/gm. and containing 0.3% sodium nitrate, as high as 12% of the surface molecules might be sodium nitrate. In such a case some effect on the surface properties and in particular on the surface enthalpy is quite conceivable. However, any definite conclusion must await the results of the experimental redetermination of the surface enthalpy of sodium chloride now in progress.

ACKNOWLEDGMENTS

In conclusion, we wish to thank Mr. D. S. Russell of the Analytical Laboratory of the Division of Applied Chemistry, N.R.C., for performing the nitrate analyses by the ferrous sulphate method, and Dr. L. D. Calvert of the Metallurgical Chemistry Section of the Division of Applied Chemistry, N.R.C., for carrying out the X-ray diffraction examination.

1. A. S.T.M. Standards, Pt. 7. American Society for Testing Materials, Baltimore. 1955. p. 1419.
2. BENSON, G. C. and BENSON, G. W. *Can. J. Chem.* 33: 232. 1955.
3. CRAIG, A. and MCINTOSH, R. *Can. J. Chem.* 30: 448. 1952.
4. FEIGL, F. Spot tests. Vol. I. 4th ed. Elsevier Press, Inc., N.Y. 1954. p. 299.
5. GMELINS HANDBUCH DER ANORG. CHEM. Teil 21. Verlag Chemie, Berlin. 1928. p. 329.
6. KEENAN, A. G. and HOLMES, J. M. *J. Phys. Chem.* 53: 1309. 1949.
7. PATTERSON, D., MORRISON, J. A., and THOMPSON, F. W. *Can. J. Chem.* 33: 240. 1955.
8. SCOTT, A. B., SMITH, W. A., and THOMPSON, M. A. *J. Phys. Chem.* 57: 757. 1953.
9. SNELL, F. D. and BIFFEN, F. M. Commercial methods of analysis. McGraw-Hill Book Company, Inc., New York. 1944. p. 152.
10. THOMPSON, F. W., ROSE, G. S., and MORRISON, J. A. *J. Sci. Instr.* 32: 325. 1955.
11. YOUNG, D. M. and MORRISON, J. A. *J. Sci. Instr.* 31: 90. 1954.

RECEIVED JUNE 12, 1956.
DIVISION OF PURE CHEMISTRY,
NATIONAL RESEARCH COUNCIL,
OTTAWA, CANADA.

THERMODYNAMIC PROPERTIES OF BENZOIC ACID¹BY R. GOTON² AND E. WHALLEY

The thermodynamic properties of benzoic acid were required in connection with its synthesis from benzene and carbon dioxide under high pressure. Accurate measurements of the heat of combustion and of the heat capacity have been made since the last reported thermodynamic study of Parks and Huffman (5), and we have recalculated these properties.

The heat capacity between 14° and 410° K. has been measured with considerable care on exceptionally pure samples by Ginnings and Furukawa (3). Their measurements appear to be much more accurate than previous ones (1) and were used exclusively. Likewise the heat of combustion when each of the gases involved is at its standard state (benzoic acid being at one atmosphere pressure) was determined very accurately by Jessup (4) and his value of $26,428.4 \pm 2.6$ int. j. gm.⁻¹ at 25° C., confirmed by Prozen and Rossini (7), is adopted.³ The following conversion factors were used:

$$1 \text{ int. joule} = 1.000165 \text{ abs. joule}$$

and

$$1 \text{ abs. joule} = 0.239006 \text{ defined calorie.}$$

From the heat of combustion and the heats of formation of carbon dioxide (6) and water (8), we calculated the standard heat of formation of benzoic acid at 25° C. (298.15° K.), at the saturation pressure.⁴ We found

$$(\Delta H_f^\circ)_{298.15} = -384,140 \pm 290 \text{ abs. j. mole}^{-1}.$$

The error involved in this quantity is twice the estimated standard error (9) calculated from measurements of each compound, applying the root-mean-square rule.

The heat capacity data of Ginnings and Furukawa are given at 5° intervals. The entropy was obtained at different temperatures by integrating C_p/T vs. T using Simpson's one-third rule. From the enthalpy function ($H_T^\circ - H_0^\circ$) and the entropy, the free energy function ($F_T^\circ - H_0^\circ$) was obtained. Dimensionless values of these quantities are given in Table I. (T_0 is the ice point temperature.) The accuracy is of the same order as that of the original heat capacity measurements. The precision between 60° and 395° K. is within 0.2%. Above 395° K. the results are less reliable (0.3%), benzoic acid being liquid (m.p. 395.52° K.) and possibly reacting with the containers. Between 60° and 14° K. the accuracy decreases to 1% because of uncertainties in the temperature measurements. In Table I, values at 298.15° K. and 395.52° K. were obtained by a graphical method. In Table II we give the conversion factors for different units. The molecular weight of benzoic acid has been taken as 122.12.

The standard heat of formation at 0° K. calculated from that at 298.15° K.,

¹Issued as N.R.C. No. 4065.

²National Research Council of Canada Postdoctorate Fellow 1955-56.

³A recent determination of the heat of combustion of benzoic acid (Coops, J., Adriaanse, N., and van Nes, K. *Rec. trav. chim.* 75: 287, 1956) agrees very well with previous measurements.

⁴The enthalpy difference between saturated pressure and one atmosphere is negligible.

TABLE I

$T, ^\circ\text{K.}$	$\frac{(H_T^\circ - H_0^\circ)}{RT_0}$	$\frac{S^\circ}{R}$	$-\frac{(F_T^\circ - H_0^\circ)}{RT}$	$-\frac{(\Delta F_f^\circ)}{RT}$
100	1.544	7.503	3.285	405.2
150	3.160	10.74	4.986	252.5
200	5.202	14.26	6.154	175.6
220	6.146	14.76	7.135	153.0
240	7.165	16.31	8.154	135.7
260	8.264	17.89	9.207	121.3
280	9.442	18.68	9.467	108.3
298.15	10.58	20.15	10.45	99.77
300	10.70	20.26	10.52	98.92
310	11.36	20.85	10.84	93.74
320	12.04	21.44	11.16	88.42
330	12.74	22.03	11.48	83.15
340	13.46	22.62	11.80	79.88
350	14.21	23.20	12.15	76.30
360	14.97	23.79	12.43	73.38
370	15.75	24.67	13.04	69.27
380	16.56	25.55	13.65	65.76
390	17.38	26.43	14.05	62.20
395.52	17.85	26.46	14.13	61.75
395.52*	25.78	31.93	14.13	61.75
400*	26.27	32.79	14.84	60.20
410*	27.40	33.55	15.31	57.45

*Values at these temperatures are for the liquid.

TABLE II

To convert tabulated value of	To	Having the dimensions indicated below	Multiply by
$\frac{S^\circ/R}{-(F_T^\circ - H_0^\circ)/RT}$	$\frac{S^\circ}{-(F_T^\circ - H_0^\circ)/T}$	cal. deg. ⁻¹ mole ⁻¹ cal. gm. ⁻¹ deg. ⁻¹ abs. j. gm. ⁻¹ deg. ⁻¹	1.9871 0.016272 0.068083
$\frac{-(\Delta F_f^\circ)_T/RT}{(H_T^\circ - H_0^\circ)/RT_0}$	$\frac{-(\Delta F^\circ)_T/T}{(H_T^\circ - H_0^\circ)}$	B.t.u. (lb. mole) ⁻¹ deg. ⁻¹ B.t.u. lb. ⁻¹ deg. ⁻¹	1.9858 0.016261
		cal. mole ⁻¹ cal. gm. ⁻¹ j. gm. ⁻¹ B.t.u. (lb. mole) ⁻¹ B.t.u. lb. ⁻¹	542.80 4.4448 18.597 976.38 7.9953

and the enthalpy function for benzoic acid, graphite (2), oxygen, and hydrogen (10), is

$$(\Delta H_f^\circ)_0 = -366,761 \pm 310 \text{ abs. j. mole}^{-1}.$$

In the last column of Table I we give some values of the free energy of formation of benzoic acid, calculated from the free energy functions of the elements (References 2 and 10).

1. ANDREWS, D. H., LYNN, G., and JOHNSON, J. J. Am. Chem. Soc. 48:1274. 1926.
2. PARKS, G. S., HUFFMAN, H., and BARMORE, M. J. Am. Chem. Soc. 55:2733. 1933.
3. DE SORBO, W. and TYLER, W. W. J. Chem. Phys. 21:1660. 1953.
4. GINNINGS, D. C. and FURUKAWA, G. T. J. Am. Chem. Soc. 75:522. 1953.
4. JESSUP, R. S. J. Research NBS, 29:247. 1942.

5. PARKS, G. S. and HUFFMAN, H. Free energies of some organic compounds. Monogr. Ser. No. 60. The Chemical Catalog Co., Inc., New York. 1932.
6. PROZEN, E. J., JESSUP, R. S., and ROSSINI, F. D. J. Research NBS, 33(6): 447. 1944.
7. PROZEN, E. J. and ROSSINI, F. D. J. Research NBS, 33(6): 439. 1944.
8. ROSSINI, F. D. J. Research NBS, 22: 407. 1939.
9. ROSSINI, F. D. and DEMING, W. E. J. Wash. Acad. Sci. 29(10): 416. 1939. ROSSINI, F. D. Experimental thermochemistry. Interscience Publishers, Inc., New York. 1956. p. 308.
10. TABLES OF THERMAL PROPERTIES OF GASES. U.S. Natl. Bur. Standards, Circ. 564. 1955.

RECEIVED JUNE 21, 1956.
DIVISION OF APPLIED CHEMISTRY,
NATIONAL RESEARCH COUNCIL OF CANADA,
OTTAWA, CANADA.

SEPARATION OF HIGH SPECIFIC ACTIVITY Na^{22} FROM IRRADIATED ALUMINUM¹

BY N. HOLLBACH² AND L. YAFFE

Na^{22} , a positron emitter with a half-life of 2.6 years, is very useful as a tracer. It is however difficult to obtain in high specific activity. We have separated a high specific activity source and are reporting the method because of the general interest in this radionuclide.

Na^{22} may be produced in a cyclotron by the reaction $^{13}\text{Al}^{27}(p, 3p3n)^{11}\text{Na}^{22}$ (3). Preparation of a solution of high specific activity necessitates the separation of sodium from macro amounts of aluminum without the addition of a "carrier". This ruled out methods involving precipitation of the sodium. Precipitation of the aluminum was also ruled out because of excessive losses due to Na^{22} adsorption. The sinter-leach method (1) was not used because of the low yields suspected (4). The two methods remaining were (a) vacuum distillation and (b) ion exchange separation. The ion exchange method was chosen because of the relative speed, simplicity, and the quantitative nature of the separation.

In a study of the chemical composition of coal ash by Ellington and Stanley (2), a neutral solution of sodium and aluminum was adsorbed on a cation exchange resin. Elution with 0.4 *N* HCl caused the sodium to appear in the effluent while the aluminum remained adsorbed on the column. A variation of this method was adopted.

The irradiated 'spec-pure' aluminum was dissolved in a minimum amount of a mixture of concentrated hydrochloric acid and hydrogen peroxide which was gently warmed to hasten solution. The solution was evaporated until precipitation just commenced. The solution was cooled, diluted to 20 ml. with water triply-distilled from a quartz still, and concentrated ammonia added dropwise until the aluminum hydroxide precipitate persisted after 30 sec. of stirring. The precipitate was redissolved with a minimum of hydrochloric acid which had been diluted with the triply-distilled water, and the solution was adsorbed on an Amberlite IR-120 cation exchange resin. The column dimensions were 2.5 cm.² × 30 cm. and a flow rate of 8 ml./min. was used.

¹With financial assistance from the National Research Council and the Atomic Energy Control Board.

²Holder of a Russell J. Eddy Award of the Chemical Institute of Canada, 1955.

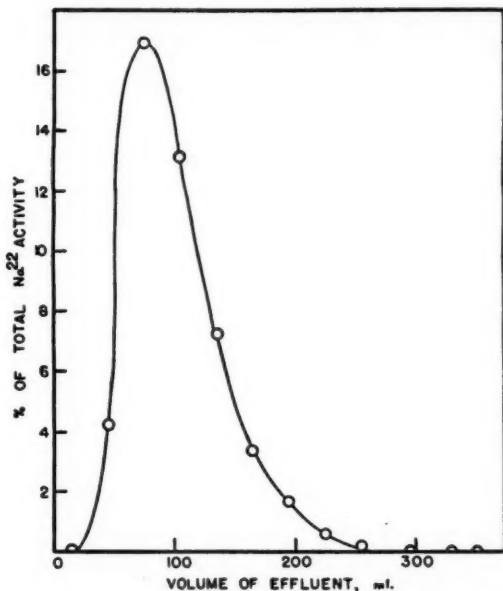


FIG. 1. Separation of Na^{22} from aluminum using Amberlite IR-120.

The sodium was eluted from the resin with 0.4 *N* hydrochloric acid. The first 270 ml. contained 100% of the sodium and the results are shown in Fig. 1. The solution was evaporated to about 1 ml. and again passed through the regenerated resin. The resulting solution was evaporated to dryness. The residue (~10 mgm.) contained organic matter from the resin, ammonium chloride, and a small amount of hydrated aluminum oxide. The residue was treated with concentrated nitric acid and taken to dryness several times to destroy organic matter, converted to the chloride, and heated strongly to volatilize ammonium chloride. The residue (aluminum oxide) was leached with cold water. The centrifugate from five washings contained 99.8% of the original Na^{22} activity and was radiochemically pure.

The specific activity of an evaporated sample of the solution was of the order of 0.1 microcurie per microgram and could obviously be increased.

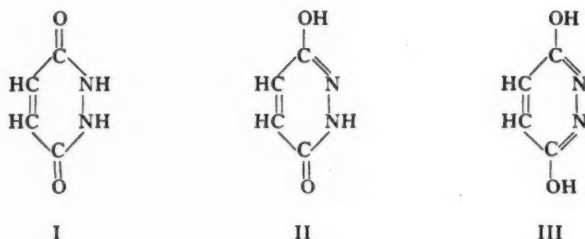
1. ARCHIBALD, A. K. and McLEOD, M. E. *Anal. Chem.* 24: 222. 1950.
2. ELLINGTON, F. and STANLEY, L. *Analyst*, 80: 313. 1955.
3. HINTZ, N. M. and RAMSEY, N. F. *Phys. Rev.* 88: 19. 1952.
4. PLUMB, R. C. and SILVERMAN, R. H. *Nucleonics*, 12(12): 29. 1954.

RECEIVED JUNE 1, 1956.
RADIOCHEMISTRY LABORATORY,
DEPARTMENT OF CHEMISTRY,
MCGILL UNIVERSITY,
MONTREAL, QUEBEC.

**THE STRUCTURE OF MALEIC HYDRAZIDE AS INFERRED FROM THE
ULTRAVIOLET SPECTRA OF ITS METHYL DERIVATIVES¹**

By D. M. MILLER AND ROBERT W. WHITE

Maleic hydrazide (MH) exhibits acidic properties and has been shown to have a single pK_a of 5.65 (4). It has also been shown (4) to have two spectra, one at low pH (A) and one at high pH (B). There are three possible tautomeric forms for MH:



so that spectrum A may be assigned to structure I, II, or III while the ionized form of II or III may account for the B spectrum. Arndt, Loewe, and Ergener (1), however, have shown that structure III is unlikely since the reaction of O-methyl maleic hydrazide (IV) with an excess of diazomethane gave the O,N-dimethyl maleic hydrazide (V) but no O,O'-dimethyl (VI) product. A study of the ultraviolet spectra of several methyl derivatives of MH has been undertaken in this laboratory to gain information about the various possible structural forms, and the results are given here.

The methyl derivatives investigated and the methods of their synthesis are as follows:

- 6-methoxy-3(2H)pyridazinone (IV),
- 6-methoxy-2-methyl-3(2H)pyridazinone (V),
- 3,6-dimethoxypyridazine (VI),
- 6-hydroxy-2-methyl-3(2H)pyridazinone (VII),
- 1,2-dimethyl-3,6(1H,2H)pyridazinedione (VIII).

Compound IV was obtained in low yield by the reaction of methyl iodide on the silver salt of MH (5); V, VII, and VIII were all prepared according to the methods of Eichenberger, Staehle, and Druey (3); and VI was made according to the directions of Druey, Meier, and Eichenberger (2).

Technical maleic hydrazide obtained from Naugatuck Chemicals, Elmira, Ontario, was twice recrystallized from water giving a crystalline product melting at 296° C.

The ultraviolet spectra reproduced in Fig. 1 were obtained on a Beckman

¹Contribution No. 80, Science Service Laboratory, London, Ontario.

Model DK-1 recording spectrophotometer and were made on solutions of concentration $5 \times 10^{-3} M$ at two pH's for each compound as follows:

A—0.1 *N* HCl,

B— $\text{Na}_4\text{P}_2\text{O}_7$ buffer at pH 8.40.

The two spectra for IV, V, and VIII were found to coincide while separate spectra were found for the others. The similarity between the spectra of MH and VII is obvious. For the sake of comparison each of the other spectra has superimposed on it (as a broken line) that spectrum of MH most closely resembling it.

Titration curves of aqueous solutions of each of the compounds were obtained. The only methyl derivatives showing inflection points were VII for which a pK_a of 5.65 was found (identical to that of MH), and VI for which a pK_b of 12.0 was found.

The dimethyl derivatives, VIII, V, and VI, have configurations similar to structures I, II, and III respectively, while of the monomethyl derivatives, VII may have configuration I or II and IV, II or III. Comparing now spectrum A for unionized MH with the other spectra in Fig. 1 it can be seen

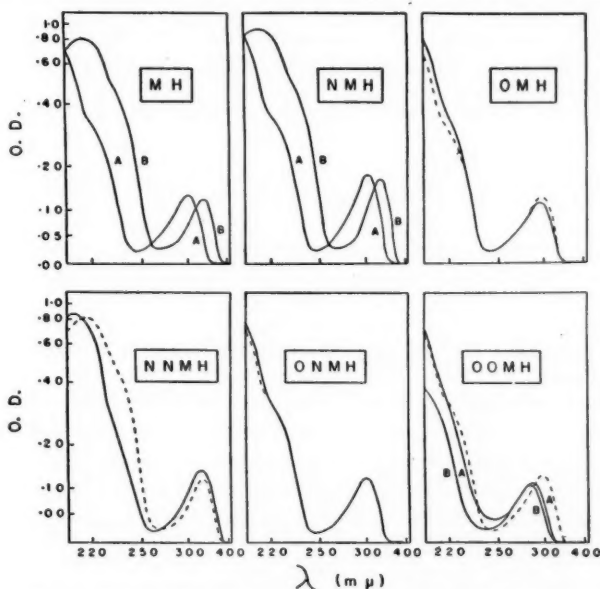


FIG. 1. Ultraviolet spectra of MH and its methyl derivatives. NMH, VII; OMH, IV; NNMH, VIII; ONMH, V; OOMH, VI.

that it is similar only to the spectra of IV, V, and VII, the compounds capable of existing in form II. On the other hand, spectrum B for the ionized form of MH shows a similarity only to that of VII, the one derivative capable of ionizing as an acid.

The similarity between the ultraviolet spectra, pK_a values, and chemical reactivities of MH and VII could only arise from a similarity in structure. This fact added to the other evidence presented here leads to the conclusion that MH exists as structure II, i.e. 6-hydroxy-3(2H)pyridazinone.

We wish to thank Dr. F. Arndt for his useful suggestions concerning the synthesis of IV and Dr. J. Druey for a sample of this compound, also Dr. G. D. Thorn for helpful discussion and Mr. B. Huston for technical assistance.

1. ARNDT, F., LOEWE, L., and ERGENER, L. *Rev. fac. sci. univ. Istanbul, A*, 13: 103. 1948.
2. DRUEY, J., MEIER, K., and EICHENBERGER, K. *Helv. Chim. Acta*, 37: 121. 1954.
3. EICHENBERGER, K., STAEHEIM, A., and DRUEY, J. *Helv. Chim. Acta*, 37: 837. 1954.
4. MILLER, D. M. *Can. J. Chem.* 33: 1806. 1955.
5. Unpublished results. See also Ref. 1 for an alternative method.

RECEIVED JUNE 25, 1956.
CANADA DEPARTMENT OF AGRICULTURE,
SCIENCE SERVICE LABORATORY,
UNIVERSITY SUB POST OFFICE,
LONDON, ONTARIO.

THE RELATION BETWEEN ACTIVATION ENERGY OF THE VISCOSITY AND HEAT OF VAPORIZATION FOR MOLTEN SALTS¹

BY F. VAN ZEGGEREN²

The temperature dependence of the viscosity of a liquid is expressed in the formula

$$\eta = B \exp(E_{v1s}/RT)$$

where η is the viscosity, E_{v1s} the so-called activation energy of the viscosity, B a constant, and R and T have their usual significance. This formula can be derived theoretically by applying the theory of absolute reaction rates to the problem of viscosity (4).

Since in viscous flow holes have to be available of the size of the atom or molecule in the activated state, i.e. on top of the barrier which corresponds with E_{v1s} , and the work necessary to form a hole of molecular size in the liquid is the energy of vaporization ΔE_{vap} , E_{v1s} must be a fraction of ΔE_{vap} . For a large number of liquids the ratio $\Delta E_{vap}/E_{v1s}$ has been determined, and the important conclusion is that

$$C = \Delta E_{vap}/E_{v1s}$$

is a constant for all "normal" liquids. The value of the constant C is 3.5 ± 0.5 .

For liquids such as molten metals this ratio of the heat of vaporization to the activation energy of the viscous flow has also been determined (3), but much too large values have been found, viz. varying between 8 and 25 or more.

¹Issued as N.R.C. No. 4073.

²National Research Council Postdoctorate Fellow 1955-.

However, Ewell and Eyring (3) showed that this can be accounted for by the difference in mechanism between the two processes: vaporization and viscous flow. In vaporization the neutral metal atoms are the units which contribute to ΔE_{vap} , whereas in viscous flow the energy barrier E_{vis} corresponds with the metal ions, stripped of their conductance electron (s). The barrier is not influenced by the moving electrons. In correcting their ratio values with a factor that takes this difference into account, they obtained for the quantity

$$C = \frac{\Delta E_{\text{vap}}}{E_{\text{vis}}} \times \frac{\text{vol. of ion}}{\text{vol. of atom}}$$

or

$$C = \frac{\Delta E_{\text{vap}}}{E_{\text{vis}}} \times \frac{(r_{\text{ion}})^3}{(r_{\text{atom}})^3}$$

a constant value, which is the same as found for the normal liquids, viz. 3.5 ± 0.7 .

It seemed interesting to investigate if an analogous relation holds for the molten salts.

For a large number of molten salts the relationship between viscosity (or fluidity) and the number of holes in the melt is supported by the fact that for these salts the relation of Batschinski

$$\eta = a/(V - V_s)$$

is valid, as is the case for normal liquids (1). In this formula η is the viscosity, V and V_s are the molar volumes of liquid and unexpanded solid respectively, and a is a constant. Thus the hole theory of liquids can also be applied in this case. Indeed, Bloom and Heymann (2) were able to show that the relation $\eta = B \exp(E_{\text{vis}}/RT)$ also holds for fused salts.

Assuming that the molecule is the unit that evaporates, and that both positive and negative ions have to cross the energy barrier for the viscous flow, the correction factor would be

$$[\frac{4}{3}\pi(r_+)^3 + \frac{4}{3}\pi(r_-)^3]/V_{\text{mol}}$$

where r_+ and r_- are the radii of positive and negative ions respectively, and V_{mol} is the volume of the molecule. Thus:

$$C = \frac{\Delta E_{\text{vap}}}{E_{\text{vis}}} \times \frac{\frac{4}{3}\pi(r_+^3 + r_-^3)}{V_{\text{mol}}}$$

E_{vis} has been determined for a few salts by Bloom and Heymann (2), ΔE_{vap} for these compounds is given by Herz (5). In Table I values of ΔE_{vap} , E_{vis} , $\frac{4}{3}\pi(r_+^3 + r_-^3)$, V_{mol} , and C are tabulated for a number of alkali halides. Bloom and Heymann expressed some doubt about the value for E_{vis} of LiBr and indeed for this salt an extremely high value for C is found. Nevertheless, taking this value into account, it can be said that C is a constant, with an average value of $3.1 (\pm 0.5)$, which proves that a molten salt can be considered as a normal liquid in the same sense as, for example, a molten metal.

TABLE I

Salt	ΔE_{vap} in kcal./mole	E_{vis} in kcal./mole	$^{1/2}\pi(r_+^2 + r_-^2)$ in \AA^2	V_{mol} in \AA^3	C
LiCl	37.7	8.8	25.8	34.0	3.3
NaCl	44.4	9.4	28.5	44.8	3.0
KCl	40.4	7.8	34.7	62.4	2.9
LiBr	35.7	6.0(?)	32.1	41.6	4.6
NaBr	38.6	10.6	34.8	53.3	2.4
KBr	38.4	7.9	41.0	71.9	2.8
NaI	39.0	7.4	46.5	67.9	3.6
KI	37.2	9.2	52.7	88.0	2.4

ACKNOWLEDGMENT

The author wishes to thank Dr. G. C. Benson for his interest in this work.

1. VAN AUBEL, E. *Bull. classe sci. Acad. roy. Belg.* 12(5):374. 1926.
2. BLOOM, H. and HEYMANN, E. *Proc. Roy. Soc. A*, 188:392. 1947.
3. EWELL, R. H. and EYRING, H. *J. Chem. Phys.* 5:726. 1937.
4. GLASSTONE, S., LAIDLER, K. J., and EYRING, H. *The theory of rate processes.* McGraw-Hill Book Company, Inc., New York. 1941. p. 477.
5. HERZ, W. *Z. anorg. u. allgem. Chem.* 179:277. 1929.

RECEIVED JUNE 25, 1956.
DIVISION OF PURE CHEMISTRY,
NATIONAL RESEARCH COUNCIL,
OTTAWA, CANADA.

NUCLEAR MAGNETIC RESONANCE STUDY OF PHASE TRANSITIONS IN ANHYDROUS SODIUM STEARATE

BY R. F. GRANT,¹ N. HEDGECOCK,² AND B. A. DUNELL¹

The investigation of mesomorphic phase transitions in sodium stearate has been made by a number of workers using several techniques. Puddington and his co-workers (2, 5, 8, 9, 10) have studied the variation of viscosity, density, and light transmission with temperature, and R. and M. Vold with their co-workers (11, 12, 13, 14, 15) have studied the density, heat capacity, and electrical conductivity of sodium stearate and observed phase transitions optically using the "hot wire" technique. Table I lists the main phase transitions that have been observed in anhydrous sodium stearate and shows the range of temperatures within which each transition has been reported.

Interpretation of the molecular mechanisms of these transitions has been assisted by X-ray diffraction studies on sodium stearate (3, 4, 7). It is considered that each transition represents a change in the degree of freedom of rotational motion of the hydrocarbon part of the molecule or a change in the ability of the polar end to reorient, the low temperature transitions being associated with rearrangement of the hydrocarbon chains, and the high

¹Chemistry Department, University of British Columbia.

²Physics Department, University of British Columbia. Present address: Physics Department, McMaster University, Hamilton, Ontario.

TABLE I
PHASE TRANSITIONS IN ANHYDROUS SODIUM STEARATE

Transition	Range of reported temperatures, ° C.	References
Genotypical point	65-70	9, 13
Curd to supercurd	89-93	11, 14
Supercurd to subwaxy	110-117	9, 13
Subwaxy to waxy	125-135	2, 10, 13, 14
Waxy to superwaxy	165-168	2, 11, 12
Superwaxy to subneat	189-209	10, 11, 12, 13
Subneat to neat	226-262	10, 11, 12, 13, 15
Melting point	278-290	8, 12, 15

temperature transitions being associated with reorientation of the polar ends of the molecules. Investigation of line width in nuclear magnetic resonance studies gives an indication of the extent of molecular rotation and reorientation in the solid state (1). A study has been started, therefore, of the nuclear magnetic resonance spectrum of sodium stearate over a range of temperatures within which phase changes are observed.

The sodium stearate used in this investigation was prepared from Eastman Kodak white label stearic acid by two methods, following the procedure of Stainsby, Farnand, and Puddington (10). In one procedure, stearic acid dissolved in hot 95% ethanol was titrated with a saturated 95% ethanol solution of sodium hydroxide to two or three drops beyond a phenolphthalein end point, and in the other, stearic acid dissolved in hot absolute ethanol was titrated just beyond a phenolphthalein end point with a 3% solution of sodium ethoxide in absolute ethanol. In both cases the indicator was used externally. The dried sodium stearate crystals, sealed in melting point tubes, became translucent at 130° C. and became transparent and showed a meniscus at 262° C., in agreement with the behavior reported by M. and R. Vold (11, 13). The sodium stearate samples used in the experiments were melted in sample bulbs under vacuum. Dry nitrogen was then introduced into the vacuum system and the sample bulb sealed off and detached from the vacuum system.

The sample and nuclear magnetic resonance spectrometer probe were immersed in a thermostat which consisted of a dewar vessel filled with nujol heated by an immersion knife-heater. The magnet and recording apparatus used were those described by Waterman and Volkoff in a recent paper (16). The remainder of the spectrometer was an adaptation of one described by Gutowsky, Meyer, and McClure (6). Line width was taken as the separation in gauss of the points of maximum slope on the absorption signal, and was measured in an experiment in which the sodium stearate sample was heated slowly to the required temperature and maintained at that temperature for 30 min. before the absorption signal was recorded.

In Fig. 1, the line width is plotted as a function of temperature for the two samples of sodium stearate prepared in the two ways described above. No distinction in behavior was observable for the two samples. The line width vs. temperature curve shows three discontinuities between 20° C. and 200° C.

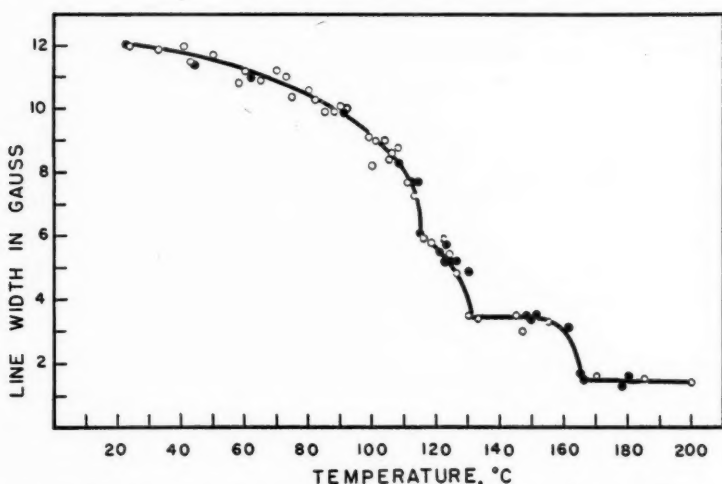


FIG. 1. Variation of line width with temperature for sodium stearate. Open circles: Sample prepared by neutralization of stearic acid with sodium hydroxide. Filled circles: Sample prepared by neutralization of stearic acid with sodium ethoxide.

These correspond to observed transitions at 114° C., 130° C., and 165° C., although it may reasonably be claimed that the presence of a transition at 114° C. is not unequivocally shown by these results. Comparison of our observed transition temperatures with some of those of other workers is shown in Table II. A satisfactory discussion of the significance of these results in

TABLE II
COMPARISON OF TRANSITION TEMPERATURES OBSERVED IN THIS
WORK WITH THOSE OBSERVED BY OTHER METHODS

Transition	Method and temperature				
	Calorimeter (13)	Hot wire (11)	Dilatometer (12)	Light transmission (2)	N.M.R.* this work
Supercurd to subwaxy	114	—	117	—	114
Subwaxy to waxy	134	132	132	132	130
Waxy to superwaxy	—	167	—	165	165

*Nuclear magnetic resonance.

terms of molecular motion requires the calculation of the second moments of the line shapes. The absorption signals from which these results are taken have not proved satisfactory for this purpose since they were obtained primarily to measure line width. Work is in progress, however, to determine the second moments of the line shapes for sodium stearate and other fatty acid salts.

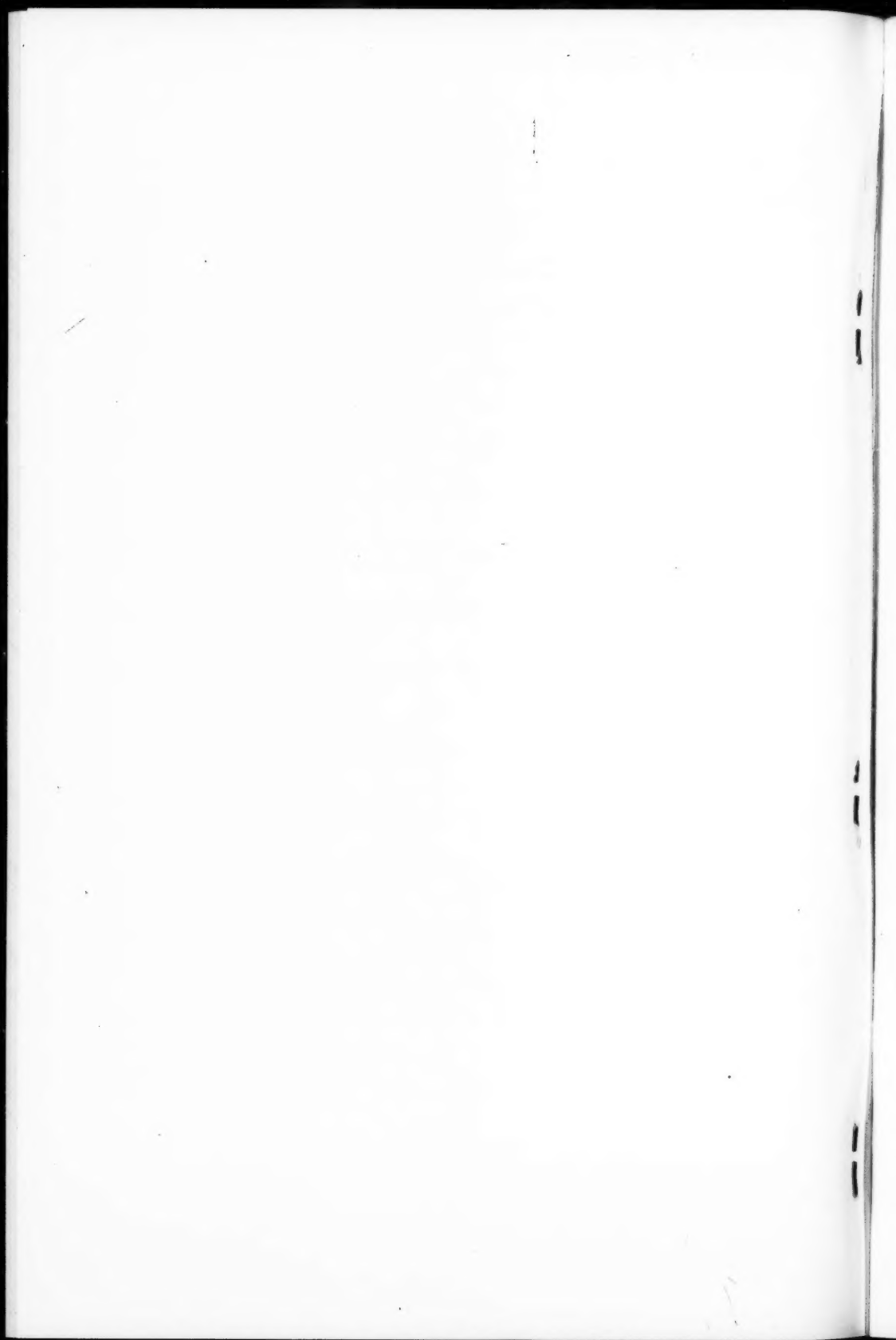
We are indebted to Drs. G. M. Volkoff and G. M. Shrum of the Physics Department of this university for their co-operation in making the facilities

of their department available to us for doing these experiments. We also wish to thank the National Research Council of Canada for Grant G. 304 which has made this work possible.

1. ANDREW, E. R. Nuclear magnetic resonance. Cambridge University Press, London. 1955.
2. BENTON, D. P., HOWE, P. G., and PUDDINGTON, I. E. Can. J. Chem. 33:1384. 1955.
3. DE BRETTEVILLE, A. and MCBAIN, J. W. J. Chem. Phys. 11: 426. 1943.
4. BUEGER, M. J., SMITH, L. B., DE BRETTEVILLE, A., and RYER, F. V. Proc. Natl. Acad. Sci. U.S. 28: 526. 1942.
5. GALLAY, W. and PUDDINGTON, I. E. Can. J. Research, B, 21: 202. 1943.
6. GUTOWSKY, H., MEYER, L., and MCCLURE, R. Rev. Sci. Instr. 24: 644. 1953.
7. MCBAIN, J. W., BOLDUAN, O., and ROSS, S. J. Am. Chem. Soc. 65: 1873. 1943.
8. POWELL, B. D. and PUDDINGTON, I. E. Can. J. Chem. 31: 828. 1953.
9. SOUTHAM, F. W. and PUDDINGTON, I. E. Can. J. Research, B, 25: 125. 1947.
10. STAINSBY, G., FARNAND, R., and PUDDINGTON, I. E. Can. J. Chem. 29: 838. 1951.
11. VOLD, M. J. J. Am. Chem. Soc. 63: 160. 1941.
12. VOLD, M. J., MACOMBER, M., and VOLD, R. D. J. Am. Chem. Soc. 63: 168. 1941.
13. VOLD, R. D. J. Am. Chem. Soc. 63: 2915. 1941.
14. VOLD, R. D. J. Phys. Chem. 49: 315. 1945.
15. VOLD, R. D. and HELDMAN, M. J. J. Phys. & Colloid Chem. 52: 148. 1948.
16. WATERMAN, H. H. and VOLKOFF, G. M. Can. J. Phys. 33: 156. 1955.

RECEIVED JUNE 18, 1956.

DEPARTMENTS OF CHEMISTRY AND PHYSICS,
UNIVERSITY OF BRITISH COLUMBIA,
VANCOUVER, BRITISH COLUMBIA.



CANADIAN JOURNAL OF CHEMISTRY

Notes to Contributors

Manuscripts

(i) **General.** Manuscripts, in English or French, should be typewritten, double spaced, on paper $8\frac{1}{2} \times 11$ in. The original and one copy are to be submitted. Tables and captions for the figures should be placed at the end of the manuscript. Every sheet of the manuscript should be numbered.

Style, arrangement, spelling, and abbreviations should conform to the usage of this journal. Names of all simple compounds, rather than their formulas, should be used in the text. Greek letters or unusual signs should be written plainly or explained by marginal notes. Superscripts and subscripts must be legible and carefully placed.

Manuscripts and illustrations should be carefully checked before they are submitted. Authors will be charged for unnecessary deviations from the usual format and for changes made in the proof that are considered excessive or unnecessary.

(ii) **Abstract.** An abstract of not more than about 200 words, indicating the scope of the work and the principal findings, is required, except in Notes.

(iii) **References.** References should be listed alphabetically by authors' names, numbered, and typed after the text. The form of the citations should be that used in this journal; in references to papers in periodicals, titles should not be given and only initial page numbers are required. The names of periodicals should be abbreviated in the form given in the most recent *List of Periodicals Abstracted by Chemical Abstracts*. All citations should be checked with the original articles and each one referred to in the text by the key number.

(iv) **Tables.** Tables should be numbered in roman numerals and each table referred to in the text. Titles should always be given but should be brief; column headings should be brief and descriptive matter in the tables confined to a minimum. Vertical rules should be used only when they are essential. Numerous small tables should be avoided.

Illustrations

(i) **General.** All figures (including each figure of the plates) should be numbered consecutively from 1 up, in arabic numerals, and each figure referred to in the text. The author's name, title of the paper, and figure number should be written in the lower left corner of the sheets on which the illustrations appear. Captions should not be written on the illustrations (see Manuscripts (i)).

(ii) **Line Drawings.** Drawings should be carefully made with India ink on white drawing paper, blue tracing linen, or co-ordinate paper ruled in blue only; any co-ordinate lines that are to appear in the reproduction should be ruled in black ink. Paper ruled in green, yellow, or red should not be used unless it is desired to have all the co-ordinate lines show. All lines should be of sufficient thickness to reproduce well. Decimal points, periods, and stippled dots should be solid black circles large enough to be reduced if necessary. Letters and numerals should be neatly made, preferably with a stencil (do NOT use typewriting) and be of such size that the smallest lettering will be not less than 1 mm. high when reproduced in a cut 3 in. wide.

Many drawings are made too large; originals should not be more than 2 or 3 times the size of the desired reproduction. In large drawings or groups of drawings the ratio of height to width should conform to that of a journal page but the height should be adjusted to make allowance for the caption.

The original drawings and one set of clear copies (e.g. small photographs) are to be submitted.

(iii) **Photographs.** Prints should be made on glossy paper, with strong contrasts. They should be trimmed so that essential features only are shown and mounted carefully, with rubber cement, on white cardboard with no space or only a very small space (less than 1 mm.) between them. In mounting, full use of the space available should be made (to reduce the number of cuts required) and the ratio of height to width should correspond to that of a journal page ($4\frac{1}{2} \times 7\frac{1}{4}$ in.); however, allowance must be made for the captions. Photographs or groups of photographs should not be more than 2 or 3 times the size of the desired reproduction.

Photographs are to be submitted in duplicate; if they are to be reproduced in groups one set should be mounted, the duplicate set unmounted.

Reprints

A total of 50 reprints of each paper, without covers, are supplied free. Additional reprints, with or without covers, may be purchased.

Charges for reprints are based on the number of printed pages, which may be calculated approximately by multiplying by 0.6 the number of manuscript pages (double-spaced typewritten sheets, $8\frac{1}{2} \times 11$ in.) and including the space occupied by illustrations. An additional charge is made for illustrations that appear as coated inserts. The cost per page is given on the reprint requisition which accompanies the galley.

Any reprints required in addition to those requested on the author's reprint requisition form must be ordered officially as soon as the paper has been accepted for publication.

Contents

	Page
Preparative Partition Chromatography of Carbohydrates on Celite Columns— <i>R. U. Lemieux, C. T. Bishop, and G. E. Pelletier</i>	1365
Effects of Complexing on the Homogeneous Reduction of Mercuric Salts in Aqueous Solution by Molecular Hydrogen— <i>G. J. Korinek and J. Halpern</i>	1372
The Infrared Absorption Spectra of Deuterated Esters. I. Methyl Acetate— <i>B. Nolin and R. Norman Jones</i>	1382
The Infrared Absorption Spectra of Deuterated Esters. II. Ethyl Acetate— <i>B. Nolin and R. Norman Jones</i>	1392
The System $\text{LiNO}_3\text{--C}_2\text{H}_5\text{OH--H}_2\text{O}$ at 25°C.— <i>A. N. Campbell and E. M. Kartzmark</i>	1405
Diphenylcyanamide Derivatives. III. 2-Thiopseudoureas— <i>Ronald E. Beals and William H. Brown</i>	1408
Periodate-Permanganate Oxidations. V. Oxidation of Lipids in Media Containing Organic Solvents— <i>E. von Rudloff</i>	1413
Kinetics of the Oxidation of Uranium(IV) by Molecular Oxygen in Aqueous Perchloric Acid Solution— <i>J. Halpern and J. G. Smith</i>	1419
The Systems Aluminum-Tin and Aluminum-Lead-Tin— <i>A. N. Campbell and R. Kartzmark</i>	1428
A Convenient Synthesis of DL-Glutamic Acid from β -Propiolactone— <i>Guy Talbot, Roger Gaudry, and Louis Berlinguet</i>	1440
Basic Esters of Substituted Pyrimidine-4-carboxylic Acids— <i>Gordon A. Grant, Carl von Seemann, and Stanley O. Winthrop</i>	1444
Light Absorption Studies. Part V. The Relation of Mesomeric Effects and Ultraviolet Light Absorption Spectra— <i>W. F. Forbes and Audrey S. Ralph</i>	1447
The Reactions of Active Nitrogen with Methane and Ethane— <i>P. A. Gartaganis and C. A. Winkler</i>	1457
The Synthesis of Two Isomeric Thymols— <i>R. A. B. Bannard and L. C. Leitch</i>	1464
Ethylene Diamine Tetraacetic Acid and Citric Acid as Eluants in Ion Exchange Separation of Rare Earths— <i>F. W. Cornish, G. Phillips, and A. Thomas</i>	1471
The Surface Energies of Amorphous Silica and Hydrated Amorphous Silica— <i>Stephen Brunauer, D. L. Kantro, and C. H. Weise</i>	1483
Notes:	
A Note on the Temperature Dependence of the Electrical Resistance of Salt Solutions Adsorbed in Porous Glass— <i>Max Huber and E. A. Flood</i>	1497
The Purity of Small Sodium Chloride Particles Prepared by Electrostatic Precipitation— <i>F. van Zeggeren, H. P. Schreiber, and G. C. Benson</i>	1501
Thermodynamic Properties of Benzoic Acid— <i>R. Goton and E. Whalley</i>	1506
Separation of High Specific Activity Na^{22} from Irradiated Aluminum— <i>N. Hollbach and L. Yaffe</i>	1508
The Structure of Maleic Hydrazide as Inferred from the Ultraviolet Spectra of Its Methyl Derivatives— <i>D. M. Miller and Robert W. White</i>	1510
The Relation between Activation Energy of the Viscosity and Heat of Vaporization for Molten Salts— <i>F. van Zeggeren</i>	1512
Nuclear Magnetic Resonance Study of Phase Transitions in Anhydrous Sodium Stearate— <i>R. F. Grant, N. Hedgecock, and B. A. Dunell</i>	1514

